INVESTIGATION OF ENERGY CONSERVATION IN CLASSIC BUILDINGS WITH PCM MULTI-LAYER WALLS

By

Ronny Stanley Achaku, (CEng. IMECHE)

A thesis submitted in partial fulfilment of the requirement of the University of Hertfordshire for the degree of

Doctor of Engineering

University of Hertfordshire School of Physics, Engineering, and Computer Science

October 2024

Author's declaration

I declare that the work in this dissertation was carried out in accordance with the requirements of the University's Regulations and Code of Practice for Research Degree Programmes and that it has not been submitted for any other academic award. Except where indicated by the specific reference in the text, the work is the candidate's work. Any views expressed in the dissertation are those of the author.

Ronny Stanley Achaku Reg no. 06132459

Dehau.

Acknowledgement

I want to express my deepest gratitude to those who have supported and encouraged me throughout this PhD journey.

First and foremost, I thank the Almighty God for His guidance, strength, and blessings that have sustained me through this challenging yet fulfilling endeavour.

My deepest appreciation goes to my beloved wife, Shamim Senoga Achaku, and our wonderful children, Rosh and Martha Achaku. Your unwavering love, patience, and encouragement have been my constant source of strength. I also extend my heartfelt gratitude to my mother, Suzan Namubiru, for her endless support and prayers. Additionally, I am thankful to our church for standing with me in prayer and offering spiritual support that has been invaluable.

I am immensely grateful to the School of Physics, Engineering, and Computer Science at the University of Hertfordshire for their invaluable support and provision of experimental materials essential for my research. A special thanks to my supervisors, Prof. Yong Chen of the University of Hertfordshire and Dr. Li Liang of Brunel University. Your relentless efforts, insightful guidance, and intellectual contributions were the driving force behind this project.

I am also thankful to Mr. Alex Kingstrom, the laboratory head, and his dedicated team for their assistance and collaboration, which were crucial to the successful completion of my experiments. I am also grateful to the University security officers, who always provided assistance at short notice and ensured a safe place to conduct the studies.

My heartfelt thanks go to my workplace managers, Ian Gibson and Martin Coulbeck of MITIE Technical Services at GlaxoSmithKline plc (GSK), Ware Hertfordshire. Your immense support, understanding of my needs, and flexibility in my work schedule gave me the best opportunities to complete this research.

To all who have contributed to this journey, mentioned and unmentioned, your support and encouragement have been invaluable. This thesis would not have been possible without you.

SYNOPSIS

Integrating Phase Change Materials (PCMs) into building envelopes presents a viable strategy for enhancing energy efficiency, stabilising indoor temperatures, and reducing carbon emissions, particularly in historical and modern structures. This study explores the effectiveness of PCM integration in various building types, including Victorian-era and hospital buildings in cold climates and modern office buildings with double-glazed windows. The primary aim was to investigate how PCM could reduce heating and cooling demands, contributing to global sustainability goals such as the European Union's climate-neutral strategy by 2050.

Prototypes replicating the wall structures of these buildings were constructed for an experimental investigation, and PCM of RT28HC, with a melting point of 27°C, was integrated into the walls. Through a combination of experimental testing and dynamic simulations conducted using TRNSYS, the study identified that the optimal PCM placement within these walls occurred between 341 mm and 356 mm from the external wall surface. This positioning allowed the PCM to fully activate at its phase change temperature, reducing heat transfer and maintaining stable internal wall surface temperatures. In modern office buildings with double-glazed windows, this configuration resulted in 34% to 37% savings in heating and cooling energy consumption while maintaining a Predicted Mean Vote (PMV) of 0.21 and a Predicted Percentage of Dissatisfied (PPD) of 6.0%, ensuring optimal thermal comfort for occupants.

In Victorian-era hospital buildings with thick multi-layered walls, placing the PCM at the optimal depth led to a 5.3% to 6.2% reduction in energy consumption. The experimental results further indicated that this PCM placement expanded the indoor temperature range by up to 7.9°C and mitigated peak temperature fluctuations by 1.74°C to 2.0°C, significantly improving indoor comfort. However, PCM layers positioned near the outer wall in cold climates often failed to reach the necessary phase change temperatures, reducing their effectiveness.

The study also validated a critical model that described heat transfer across multi-layered PCM walls with integrated windows using an exponentially decaying function combined with a sinusoidal component, accurately reflecting the PCM's phase change behaviour. The

comparison between experimental and simulation results confirmed the reliability of the models, with Mean Absolute Percentage Error (MAPE) values below 20% and Root Mean Square Error (RMSE) values ranging from 10.41 to 16.44, indicating high accuracy in predicting PCM performance.

These findings have underscored the practical benefits of PCM integration in enhancing energy efficiency, stabilising indoor temperatures, and improving thermal comfort, particularly in heritage buildings and modern office constructions. The validated simulation models have provided a robust framework for optimising PCM placement in building designs, supporting energy conservation and aligning with global environmental targets. Future research should explore long-term PCM performance across different climates and investigate synergies with other sustainable building technologies.

List of abbreviations

A&E Accident and Emergency

ADJ_CEILING Adjacent Ceiling

ADJ_WALL Adjacent Wall

AHU Air Handling Unit

BEMS Building Energy Management System

CHP Combined Heat and Power

CHW Chilled Water

CO₂ Carbon dioxide

DESNZ Department for Energy Security and Net Zero

EC Energy Centre

EMS Energy Management Systems

EPC Energy Performance Certificate

EU European Union

EXT External Temperature

EXT_ROOF External Roof

EXT_WALL External Wall

EXT_WINDOW External Window

HVAC Heating Ventilation and Air Conditioning

LCA Life Cycle Assessment

LHS Latent Heat Storage

LTHW Low Temperature Hot Water

MAE Mean Absolute Error

MAPE Mean Absolute Percentage Error

mPCM Macroencapsulated Phase Change Material

NHS National Health Service

ODE Ordinary Differential Equation

PCH Phase Change Hysteresis

PCM Phase Change Material

PMV Predicted Mean Vote

PPD Predicted Percentage of Dissatisfied

RSME Root Mean Square Error

SDC Differential Scanning Calorimeters

TES Thermal Energy Storage
Tmax Maximum Temperature
Tmin Minimum Temperature

TOP Operative Room Temperature

TPCM PCM Temperature

TRNSYS Transient System Simulation

Troom Room Temperature

List of definitions

Ambient Temperature The overall surrounding outdoor (environment) temperature.

Indoor Temperature The air temperature inside a building or room, typically measured to

assess thermal comfort.

External Temperature The temperature on the external surfaces of the walls which may differ

from outdoor air temperature due to solar radiation or heat transfer.

MAE A statistical measure of prediction accuracy, calculated as the average

absolute difference between observed and predicted values.

MAPE A measure of prediction accuracy expressed as a percentage, calculated

by averaging the absolute percentage differences between observed and

predicted values.

Operative Temperature A weighted average of air temperature and mean radiant temperature,

used to assess perceived thermal comfort.

Outdoor Temperature The air temperature outside a building influenced by weather and

environmental conditions.

PMV A scale that predicts a group of people's average thermal sensation vote,

ranging from -3 (cold) to +3 (hot).

PPD A metric indicating the percentage of people likely to feel dissatisfied

with the thermal environment.

RMSE A statistical measure of prediction accuracy, calculated as the square

root of the average squared differences between observed and predicted

values.

Thermal Comfort A condition of mind that expresses satisfaction with the thermal

environment, typically influenced by air temperature, humidity, radiant

temperature, and air movement.

Table of Contents

Author's de	eclaration statement	i
Acknowled	lgement	ii
SYNOPSIS	S	iii
List of Abb	previations	v
List of Def	initions	vii
Ū	ıres	
List of Tab	les	xvi
CHAPTER	1: INTRODUCTION	1
	ackground and Importance of the Field	
	ecessity of the Research	
	•	
	im and Objectives	
	oject Plan	
1.5 Pr	rogram of Work to Accomplish the Project Objectives	7
1.6 Sc	cope and Limitations	9
1.7 St	ructure of the Thesis	10
CHAPTER	2: LITERATURE REVIEW	12
2.1 O	verview of Energy Conservation Strategies in Buildings	16
2.1.1	Integrated Energy Conservation Strategies in Building Design	17
2.2 Ph	nase Change Materials (PCMs): Properties and Applications	19
2.2.1	Introduction to Phase Change Materials (PCMs)	19
2.2.2	Classification of Phase Change Materials	20
2.2.3	Desirable Properties of Phase Change Materials	23
2.3 PC	CM Applications in Engineering and Construction Materials	23
2.3.1	Phase Change Material Wallboards	25
2.3.2	Phase Change Material Positioning in the Multi-layer Wallboard	30
2.3.3	Heat Transfer Techniques of Phase Change Materials	37
234	Energy Simulation	38

	2.3	.5	Thermal Hysteresis	40
	2.3	.6	Environmental Conditions and Temperature Operating Range	42
	2.3	.7	Ventilation and Infiltration Rates	43
	2.3	.8	Insights from Literature: Case Studies on PCM Integration in Retrofitting	44
2	4	Sur	nmary	46
СН	APT	ER	3: METHODOLOGY	48
3	.1	Intr	oduction	48
3	3.2	Res	search Design	48
3	3.3	The	eoretical and Numerical Background	49
	3.3	.1	Key Principles of Heat Transfer	49
	3.3	.2	Analytical Models and Governing Equations	50
	3.3	.3	General Formulation of Phase Change Problems	51
	3.3	.4	Numerical Methods and Governing Equations in TRNSYS	54
	3.3	.5	Numerical Models: Discrete Forms and Solution Schemes	54
	3.3	.6	Governing Equations in TRNSYS	56
	3.3	.7	Assumptions	57
3	.4	Sin	nulation Framework	58
	3.4	.1	Numerical Methods in TRNSYS	59
	3.4	.2	Validation of Simulation Software and Methods	60
	3.4	.3	Validation of the Numerical Method Approach	62
	3.4	.4	Software Selection and Simulation Tool	62
	3.4	.5	TRNSYS and Associated Simulation Tool for Modelling	64
	3.4	.6	TRNSYS Kennel for Wall Configuration with and without PCM	67
3	5.5	Exp	perimental Method	71
	3.5		Building Models and Configurations	
	3.5	.2	Selection of Phase Change Material (PCM) and Properties	
	3.5	.3	Standardised Wall Model for PCM Integration in Heritage and Contempora	
			Buildings	77

3.6.1 Data Collection Methods 78 3.6.2 Data Analysis Techniques 78 3.7 Project and Building Description 79 3.7.1 Challenges and Opportunities for Hospital Energy Efficiency: A Focus on Chase Farm Hospital 81 3.8 Research Questions/Hypotheses 82 3.9 Ethical Considerations 84 3.10 Summary 84 CHAPTER 4: SIMULATION FRAMEWORK AND RESULTS OF PCM INTEGRATION IN MULTI-LAYER WALLS 85 4.1 Introduction: Simulation for Thermal Performance Analysis 85 4.2 Building Model Description 85 4.3 Simulation Results 90 4.3.1 Introduction to Simulation Results: Overview of Thermal Performance and Energy Efficiency 90 4.3.2 Baseline Simulation Results 91 4.3.3 Simulation Results: Wall Integrated with PCM but Without a Window 96 4.3.4 Simulation Results: PCM Integration in a Wall with a Window 102 4.3.5 PCM in Full-Building 110 4.4 Summary 117 CHAPTER 5: EXPERIMENTAL ANALYSIS OF PCM INTEGRATION IN MULTI-LAYER WALLS 119	3.6		Dat	a Collection and Analysis Techniques	77
3.7 Project and Building Description	3	.6.	1	Data Collection Methods	78
3.7.1 Challenges and Opportunities for Hospital Energy Efficiency: A Focus on Chase Farm Hospital 81 3.8 Research Questions/Hypotheses 82 3.9 Ethical Considerations 84 3.10 Summary 84 CHAPTER 4: SIMULATION FRAMEWORK AND RESULTS OF PCM INTEGRATION IN MULTI-LAYER WALLS 85 4.1 Introduction: Simulation for Thermal Performance Analysis 85 4.2 Building Model Description 85 4.3 Simulation Results 90 4.3.1 Introduction to Simulation Results: Overview of Thermal Performance and Energy Efficiency 90 4.3.2 Baseline Simulation Results 91 4.3.3 Simulation Results: Wall Integrated with PCM but Without a Window 96 4.3.4 Simulation Results: PCM Integration in a Wall with a Window 102 4.3.5 PCM in Full-Building 110 4.4 Summary 117 CHAPTER 5: EXPERIMENTAL ANALYSIS OF PCM INTEGRATION IN MULTI-LAYER WALLS 119 5.1 Introduction 119 5.2 Experimental Procedure 119 5.3 PCM Wall without Window 121 5.3.1 <td>3</td> <td>.6.</td> <td>2</td> <td>Data Analysis Techniques</td> <td> 78</td>	3	.6.	2	Data Analysis Techniques	78
Chase Farm Hospital 81 3.8 Research Questions/Hypotheses 82 3.9 Ethical Considerations 84 3.10 Summary 84 CHAPTER 4: SIMULATION FRAMEWORK AND RESULTS OF PCM INTEGRATION IN MULTI-LAYER WALLS 85 4.1 Introduction: Simulation for Thermal Performance Analysis 85 4.2 Building Model Description 85 4.3 Simulation Results 90 4.3.1 Introduction to Simulation Results: Overview of Thermal Performance and Energy Efficiency 90 4.3.2 Baseline Simulation Results 91 4.3.3 Simulation Results: Wall Integrated with PCM but Without a Window 96 4.3.4 Simulation Results: PCM Integration in a Wall with a Window 102 4.3.5 PCM in Full-Building 110 4.4 Summary 117 CHAPTER 5: EXPERIMENTAL ANALYSIS OF PCM INTEGRATION IN MULTI-LAYER WALLS 119 5.1 Introduction 119 5.2 Experimental Procedure 119 5.3 PCM Wall without Window 121 5.3.1 Experimental Setup 121	3.7		Pro	ject and Building Description	79
3.8 Research Questions/Hypotheses 82 3.9 Ethical Considerations 84 3.10 Summary 84 CHAPTER 4: SIMULATION FRAMEWORK AND RESULTS OF PCM INTEGRATION IN MULTI-LAYER WALLS 85 4.1 Introduction: Simulation for Thermal Performance Analysis 85 4.2 Building Model Description 85 4.3 Simulation Results 90 4.3.1 Introduction to Simulation Results: Overview of Thermal Performance and Energy Efficiency 90 4.3.2 Baseline Simulation Results 91 4.3.3 Simulation Results: Wall Integrated with PCM but Without a Window 96 4.3.4 Simulation Results: PCM Integration in a Wall with a Window 102 4.3.5 PCM in Full-Building 110 4.4 Summary 117 CHAPTER 5: EXPERIMENTAL ANALYSIS OF PCM INTEGRATION IN MULTI-LAYER WALLS 119 5.1 Introduction 119 5.2 Experimental Procedure 119 5.3 PCM Wall without Window 121 5.3.1 Experimental Setup 121	3	.7.	1	Challenges and Opportunities for Hospital Energy Efficiency: A Focus on	
3.9 Ethical Considerations .84 3.10 Summary .84 CHAPTER 4: SIMULATION FRAMEWORK AND RESULTS OF PCM INTEGRATION IN MULTI-LAYER WALLS .85 4.1 Introduction: Simulation for Thermal Performance Analysis .85 4.2 Building Model Description .85 4.3 Simulation Results .90 4.3.1 Introduction to Simulation Results: Overview of Thermal Performance and Energy Efficiency .90 4.3.2 Baseline Simulation Results .91 4.3.3 Simulation Results: Wall Integrated with PCM but Without a Window .96 4.3.4 Simulation Results: PCM Integration in a Wall with a Window .102 4.3.5 PCM in Full-Building .110 4.4 Summary .117 CHAPTER 5: EXPERIMENTAL ANALYSIS OF PCM INTEGRATION IN MULTI-LAYER WALLS .119 5.1 Introduction .119 5.2 Experimental Procedure .119 5.3 PCM Wall without Window .121 5.3.1 Experimental Setup .121				Chase Farm Hospital	81
3.10 Summary	3.8		Res	earch Questions/Hypotheses	82
CHAPTER 4: SIMULATION FRAMEWORK AND RESULTS OF PCM INTEGRATION IN MULTI-LAYER WALLS	3.9		Eth	ical Considerations	84
IN MULTI-LAYER WALLS	3.10	0	Sun	nmary	84
4.1 Introduction: Simulation for Thermal Performance Analysis	CHAI	PT]	ER 4	4: SIMULATION FRAMEWORK AND RESULTS OF PCM INTEGRATION	NC
4.2 Building Model Description 85 4.3 Simulation Results 90 4.3.1 Introduction to Simulation Results: Overview of Thermal Performance and Energy Efficiency 90 4.3.2 Baseline Simulation Results 91 4.3.3 Simulation Results: Wall Integrated with PCM but Without a Window 96 4.3.4 Simulation Results: PCM Integration in a Wall with a Window 102 4.3.5 PCM in Full-Building 110 4.4 Summary 117 CHAPTER 5: EXPERIMENTAL ANALYSIS OF PCM INTEGRATION IN MULTI- LAYER WALLS 119 5.1 Introduction 119 5.2 Experimental Procedure 119 5.3 PCM Wall without Window 121 5.3.1 Experimental Setup 121				IN MULTI-LAYER WALLS	85
4.3 Simulation Results	4.1		Intr	oduction: Simulation for Thermal Performance Analysis	85
4.3.1 Introduction to Simulation Results: Overview of Thermal Performance and Energy Efficiency	4.2		Bui	lding Model Description	85
Energy Efficiency	4.3		Sim	nulation Results	90
4.3.2 Baseline Simulation Results	4	.3.	1	Introduction to Simulation Results: Overview of Thermal Performance and	
4.3.3 Simulation Results: Wall Integrated with PCM but Without a Window				Energy Efficiency	90
4.3.4 Simulation Results: PCM Integration in a Wall with a Window 102 4.3.5 PCM in Full-Building 110 4.4 Summary 117 CHAPTER 5: EXPERIMENTAL ANALYSIS OF PCM INTEGRATION IN MULTI- LAYER WALLS 119 5.1 Introduction 119 5.2 Experimental Procedure 119 5.3 PCM Wall without Window 121 5.3.1 Experimental Setup 121	4	.3.	2	Baseline Simulation Results	91
4.3.5 PCM in Full-Building	4	.3.	3	Simulation Results: Wall Integrated with PCM but Without a Window	96
4.4 Summary	4	.3.	4	Simulation Results: PCM Integration in a Wall with a Window	102
CHAPTER 5: EXPERIMENTAL ANALYSIS OF PCM INTEGRATION IN MULTI- LAYER WALLS	4	.3.	5	PCM in Full-Building	110
LAYER WALLS	4.4		Sun	nmary	.117
5.1Introduction1195.2Experimental Procedure1195.3PCM Wall without Window1215.3.1Experimental Setup121	CHAI	PT]	ER 5	5: EXPERIMENTAL ANALYSIS OF PCM INTEGRATION IN MULTI-	
5.2 Experimental Procedure1195.3 PCM Wall without Window1215.3.1 Experimental Setup121				LAYER WALLS	.119
5.3 PCM Wall without Window	5.1		Intr	oduction	.119
5.3.1 Experimental Setup	5.2		Exp	perimental Procedure	.119
	5.3		PCI	M Wall without Window	.121
	5	.3.	1	Experimental Setup	121
		2	2		

	5.3	5.3	Experimental Results from PCM Wall with no Window	126
	5.4	PC	M Wall with a Window	133
	5.4	.1	Experimental Setup	133
	5.4	.2	Experimental Description	133
	5.4	3	Experimental Results from PCM Wall with Window	136
	5.5	Ex	perimental Construction Challenges and Their Impact on PCM Wall	
		Per	formance	149
	5.6	Sui	nmary	150
C	СНАРТ	ΓER	6: DISCUSSION	153
	6.1	Int	oduction	153
	6.2	An	Analysis of Thermal Performance	153
	6.3	Per	formance Metrics	155
	6.3	.1	Error Metrics for Validation	155
	6.3	5.2	Thermal Comfort Indices	156
	6.3	3.3	An Analysis of Inside Wall Surface Temperature	158
	6.3	.4	Energy Consumption Analysis	161
	6.3	5.5	Cost-Benefit Analysis of PCM Integration RT28HC	168
	6.3	.6	Predicted Mean Vote (PMV) and Predicted Percentage of Dissatisfied	
			(PPD)	169
	6.3	5.7	Implications for Building Design and Energy Efficiency	172
	6.4	Imj	portance of PCM Location for Heat Transfer Efficiency and Thermal	
		Co	mfort	174
	6.5	Co	ntributions to the Field	175
	6.6	Lir	nitations of the Study	177
	6.7	Sui	nmary	181
C	НАРТ	ΓER	7: CONCLUSIONS AND RECOMMENDATIONS	183
	7.1	Co	nclusions	184
	7 1	1	Impacts of PCM on Ruilding Walls	18/

7.1	1.2	Impacts on Classic Buildings and Modern Office Buildings	185
7.2	1.3	PCM Location and Moisture Management in Multi-Layer Walls	186
7.2	Re	ecommendations for Practice and Policy	.187
7.3	Re	eflections and Overall Assessment of the Research Project	.187
7.4	Re	ecommendations and Suggestions for Future Research	.189
7.5	Pu	blications	.189
REFE	REN	CES.	.191
PROJE	ECT 1	RISK MANAGEMENT	.215
APPEN	NDIX	Κ	.218

List of Figures

Figure 1-1. Project flow chart
Figure 2-1. Latent heat and Sensible heat of fusion
Figure 2-2. PCM classification
Figure 2-3. (a) Layout of the sample without PCM, (b) with PCM in position 1, (c) with
PCM in position 2, (d) with PCM in position 3, and (e) with PCM in position 4 30
Figure 2-4. Differential scanning calorimetry, DSC, curve, (a) Ideal phase change transition
and (b) Practical phase change transition
Figure 3-1. Flow chart showing link/relationship between Equations (3-4) to (3-15) 55
Figure 3-2 TRNSYS simulation components system layout without PCM
Figure 3-3. TRNSYS simulation components system layout showing macro and exploded
PCM integration for five thermal zones
Figure 3-4. Schematic of wall layers representation with PCM at different positions, x, from
the external wall surface
Figure 3-5. Schematic wall and glass window representation with PCM at different
positions, x, from the external wall surface.
Figure 3-6. PCM Manufacturer's specifications. (a) PCM packaging, (b) PCM Enthalpy Vs
temperature curve
Figure 3-7. CHASE FARM HOSPITAL (Enfield, North London, UK) project 80
Figure 4-1: Trnsys3d building model for simulation
Figure 4-2: Daily Building Occupancy Schedule
Figure 4-3. 48-hour inside temperature profile (Baseline model)
Figure 4-4. Room operative temperature (Baseline model)
Figure 4-5. Heat energy transfer rate (Baseline model)
Figure 4-6. PMV and PPD values (Baseline model)
Figure 4-7. Simulated inside surface room temperature (wall without window) with PCM at
various positions
Figure 4-8. Simulated room operative temperature (wall without window) with PCM at
various positions
Figure 4-9. Heat energy demand with PCM at various positions
Figure 4-10. PMV and PPD values with PCM at various positions

Figure 4-11. Simulated inside room temperature (wall with window) with PCM at various	
positions 10	2
Figure 4-12. Simulated operative room temperature (wall with window) with PCM at	
various positions	4
Figure 4-13. (a) – (c) Heat energy transfer rate with PCM at various positions 10	6
Figure 4-14. PMV and PPD values with PCM at various positions	9
Figure 4-15. Full-building 48-hour temperature profile with optimal PCM position 11	0
Figure 4-16. 12-month full-building simulated operative room temperature with PCM at	
various positions	1
Figure 4-17. 12-month full-building heating and cooling profile for various PCM positions	
	3
Figure 4-18. Full-building simulation results: (a) PMV and, (b) PPD for various PCM	
positions 11	6
Figure 5-1. The prototype wall construction and assembly	2
Figure 5-2. (a) Dimensions of the prototype. (b) Heater placed inside the prototype 12	2
Figure 5-3. Schematic and boundary conditions in the multi-layer wall with PCM 12	3
Figure 5-4. Wall configuration without window at various PCM positions	5
Figure 5-5. In situ calibration of thermocouples	6
Figure 5-6. PCM temperature variation with PCM positions (measured from the wall out-	
surface)	7
Figure 5-7. Temperature distribution against various PCM positions	7
Figure 5-8. Variation of inner wall surface temperatures with PCM position	8
Figure 5-9. Temperature distribution across the wall thickness against PCM position 13	1
Figure 5-10. Variation of PCM position on heat transfer across the wall	2
Figure 5-11. PCM Prototype wall integrated with a double-glazed window	4
Figure 5-12. Wall configuration with window at various PCM positions	6
Figure 5-13. Variation of PCM temperature across different PCM positions	7
Figure 5-14. PCM and temperature variations for various PCM positions with various	
external conditions 13	8
Figure 5-15. (a)-(i) Temperature distribution across various PCM configurations. (j)	
Temperature gradient with various PCM positions	1
Figure 5-16. Effects of PCM positions: (a). Layered wall construction, (b) Heat transfer rate	;
versus wall PCM position across the wall	4
Figure 5-17 Energy consumption for various PCM positions	7

Figure 6-1. Inside wall temperature versus variation with PCM positions	. 153
Figure 6-2. Comparison of simulated energy consumption vs. 2019 measured data	. 161
Figure 6-3. PPD and PMV values versus various PCM positions of a wall with a window	v 170
Figure 6-4 PPD and PMV values for various PCM positions of a wall no window	. 171
Appendix 1. Lower Ground Floor Plan (Zone LG)	. 219
Appendix 2. Ground Floor Plan (Zone G)	. 220
Appendix 3. First Floor Plan (Zone 1)	. 221
Appendix 4. Second Floor Plan (Zone 2)	. 222
Appendix 5. Third Floor Plan (Zone 3)	. 223
Appendix 6. Fourth Flow Plan (Zone 4)	. 224
Appendix 7. The hospital Brick block work plan as constructed	. 225
Appendix 8. Rubitherm quotation for RT28HC	. 226
Appendix 9. Sample Picolog data for wall with PCM activated (28°C) at the position of	344
mm	. 227
Appendix 10. PCM RT28HC data sheet	. 228
Appendix 11. Travis Perkins Material quote	. 229

List of Tables

Table 1-1. Project Overview
Table 2-1. Summary of Advantages and Disadvantages of Phase Change Material 22
Table 2-2. Phase Change Material Desirable Properties
Table 2-3. Summary of Key Research Findings on PCM Integration in Building
Applications for Energy Efficiency and Thermal Comfort
Table 2-4 The Effects of Phase Change Material Position and Thickness Inside the Multi-
layer Wall on Heat Transfer
Table 2-5. Comparison of Different Thermal Conductivity Enhancement Method 37
Table 3-1. Thermophysical Properties of the Different Layers of the Wall Construction 74
Table 3-2. PCM properties
Table 4-1. EXT_WALL "Construction Type" Manager
Table 4-2 Ceiling Layout
Table 4-3. Main TRNBuild Outputs Used in the Project
Table 4-4. Comparison of Full Building Simulation Monthly and Annual Energy Demand
for Various PCM Positions against 2019 Measured Data (MJ)
Table 5-1. Thermophysical Properties of the Different Layers of the Wall Construction 125
Table 5-2. Standard Deviation of Recorded Temperatures Across Wall Layers and Room
Tuble 5 2. Standard Deviation of Recorded Temperatures 7xcross wan Eagers and Room
Conditions
Conditions 128
Conditions 128 Table 5-3. The Window Properties 134
Table 5-3. The Window Properties
Conditions
Table 5-3. The Window Properties

CHAPTER 1: INTRODUCTION

1.1 Background and Importance of the Field

The building sector is a significant contributor to global energy consumption, accounting for nearly 40% of total energy use and one-third of greenhouse gas emissions worldwide [1, 2]. This trend has been driven by the rapid population growth and rising living standards, which have increased energy demand in buildings over recent decades [3]. As a result, the sector faces growing pressure to reduce its reliance on fossil fuels, which remain the primary energy source. Without stringent measures, such as enforcing minimum performance standards and building energy codes, this reliance is likely to continue, complicating efforts to achieve Net Zero Emissions by 2050 [4, 5].

The finite nature of fossil fuel reserves, coupled with escalating concerns about greenhouse gas emissions, underscores the urgent need to prioritise efficient energy utilisation in the building sector [6, 7, 8]. Recognising this, the Department for Energy Security and Net Zero (DESNZ) in the United Kingdom (UK) has set out a mission to seize the energy efficiency opportunity [9]. The DESNZ policy is designed to maximise the benefits of existing regulations and realise the broader potential of energy efficiency across the UK economy. This strategy aims to connect knowledge and technologies to finance, support innovation in energy efficiency, and harness the power of improved energy use information.

Within this context, an integration of phase change materials (PCMs) into building designs as wallboards offers a promising approach to enhancing energy efficiency, particularly in historical buildings and modern office structures [10]. PCMs have the potential to stabilise indoor temperatures by absorbing and releasing heat during phase transitions, thus reducing the need for mechanical heating and cooling systems. This technology is especially relevant for classic Victorian-era buildings, where maintaining architectural integrity is crucial, and for modern office buildings with cavity walls with integrated windows, where energy efficiency must be balanced with design and functionality [11].

However, optimising the application of PCMs presents unique challenges, particularly in cold climates with high heating demands [12]. Understanding the optimal positioning of PCMs within building envelopes is essential to achieving significant energy savings while preserving

buildings' historical and aesthetic value. This study explores the integration of PCMs in both Victorian-era buildings and modern office buildings, aiming to determine the most effective PCM placement strategies that enhance energy efficiency, reduce peak energy loads, and improve thermal comfort. The findings of this study contribute to the broader goal of harmonising heritage conservation with modern environmental stewardship, aligning with the EU's climate-neutral objectives by 2050.

1.2 Necessity of the Research

With their unique architectural and historical significance, Victorian-era, hospital and modern office buildings face significant challenges in enhancing energy efficiency while maintaining their essential functions. Victorian buildings require solutions that respect their historical integrity, while hospital buildings, which are energy-intensive consumers due to their 24/7 operations and strict environmental controls, demand innovative approaches to reduce operational costs without compromising patient care and safety. Similarly, modern office buildings, particularly those with cavity walls and integrated windows, must balance energy efficiency with design aesthetics and functionality.

An integration of PCMs within building envelopes offers a promising approach to improving thermal performance and reducing energy consumption across these diverse building types. However, the specific application and effectiveness of PCMs, particularly in Victorian-era buildings, modern hospitals and office buildings with advanced architectural features, remain underexplored. This research aims to tackle these challenges by investigating the use of PCMs in multi-layer walls across these contexts. The study aims to develop practical solutions that reduce energy consumption while preserving the architectural integrity of historic buildings and meeting the operational demands of modern healthcare and office environments. Through a combination of simulation and experimental approaches, this study will validate the effectiveness of PCM applications, offering insights for optimising building designs in historical and contemporary settings, all while considering the material properties relevant to local construction practices.

The motivation for this research arises from the growing need to enhance energy efficiency in diverse building types while preserving architectural integrity, particularly in historic buildings. Although PCMs have shown the potential in improving energy efficiency through

heat absorption and release during temperature fluctuations, a significant gap exists in understanding their effectiveness when integrated into real-world buildings. Current research lacks comprehensive studies that address whether PCM integration can substantially reduce the energy demands, particularly air conditioning needs, in buildings constructed from traditional materials with properties similar to those found in Victorian-era structures and other heritage buildings.

Additionally, the research on the application of PCMs in modern buildings is limited, such as hospitals and offices, with cavity walls integrated with double-glazed windows. These environments present complex energy demands, requiring optimisation of PCM placement to balance thermal performance with aesthetic and functional design considerations. Despite the promise of PCMs, a conclusive analysis of their potential for energy cost reduction and concrete strategies for their implementation in varied building contexts remain underexplored.

Furthermore, the literature lacks sufficient focus on the fire retardation, potential toxicity and health hazards associated with PCM materials, raising concerns about their safe application in real-world settings. The cladding on buildings following the Grenfell Fire incident of 14th June 2017 [13], also highlights the need to carry out detailed research on PCMs fire retardation properties. However, this aspect falls outside the scope of this study.

Given these knowledge gaps, this study is significant as it investigates the energy-saving potential of PCMs in both historic and contemporary buildings. By optimising PCM integration in different building types, including Victorian-era buildings, modern hospitals, and office buildings, this study seeks to develop strategies that contribute to global sustainability targets such as the UK's Department for Energy Security and Net Zero (DESNZ) goals, which aim for Net Zero Emissions by 2050. This study's findings will provide valuable insights for reducing operational energy costs, improving thermal performance, and supporting sustainable building practices across various architectural contexts.

In summary, from the existing literature, the following knowledge gaps were identified: i) there is a gap in understanding whether PCMs could reduce the air conditioning demands of buildings constructed with materials possessing properties similar to those used in traditional

building practices; ii) conclusive energy cost reduction analysis and reduction strategies are not addressed.

1.3 Aim and Objectives

Aim

The primary aim of this study is to investigate the effectiveness of PCMs in enhancing energy efficiency in different building types, including Victorian-era buildings, modern hospital buildings, and contemporary office buildings with cavity walls and integrated double-glazed glass windows. Specifically, this study aims to contribute to the broader goal of reducing energy costs and aligning with global sustainability targets, such as the UK Department for Energy Security and Net Zero (DESNZ) and the Europe 2030 targets, which support the transition towards Net Zero Emissions by 2050.

Objectives

- i. To reduce the energy cost of CHASE FARM Hospital's main building by a considerable percentage through the application of PCMs
 - Investigate how PCM integration can significantly lower the operational energy costs in a hospital setting, aligning with energy efficiency strategies and sustainability goals.
- ii. To evaluate the thermal performance and energy-saving potential of PCM multi-layer walls in Victorian-era buildings
 - Assess how PCM integration can reduce energy consumption while preserving these buildings' architectural and historical integrity.
- iii. To study the optimisation and impact of PCM-enhanced cavity walls with integrated windows in modern hospital and office buildings
 - Explore how PCM configuration inside walls and integrating other parameters, such as windows, affect energy consumption and how PCM can achieve aesthetic and functional design goals while improving thermal performance in these building types.
- iv. To conduct a series of lab tests to evaluate the simulation results and validate PCM performance

- Perform experimental investigations to validate simulation outcomes, ensuring the reliability of PCM applications in real-world settings.
- v. To provide practical guidelines and design recommendations for incorporating PCM-drywalls in building upgrades/refurbishments or new construction
 - Develop strategies for optimising PCM use in hospital buildings, Victorian-era structures, and modern offices to achieve energy efficiency and sustainability.
- vi. To align the study's findings with the UK DESNZ and the Europe 2030 targets
 - Contribute to the broader understanding of PCM applications in diverse architectural contexts, supporting the global effort to reduce greenhouse emissions and promote sustainable development.

These objectives aim to bridge the gap between historic preservation, modern design demands, and sustainable energy practices. It is intended to offer solutions that can be applied across various building types to achieve significant energy cost reductions and align with long-term environmental goals.

1.4 Project Plan

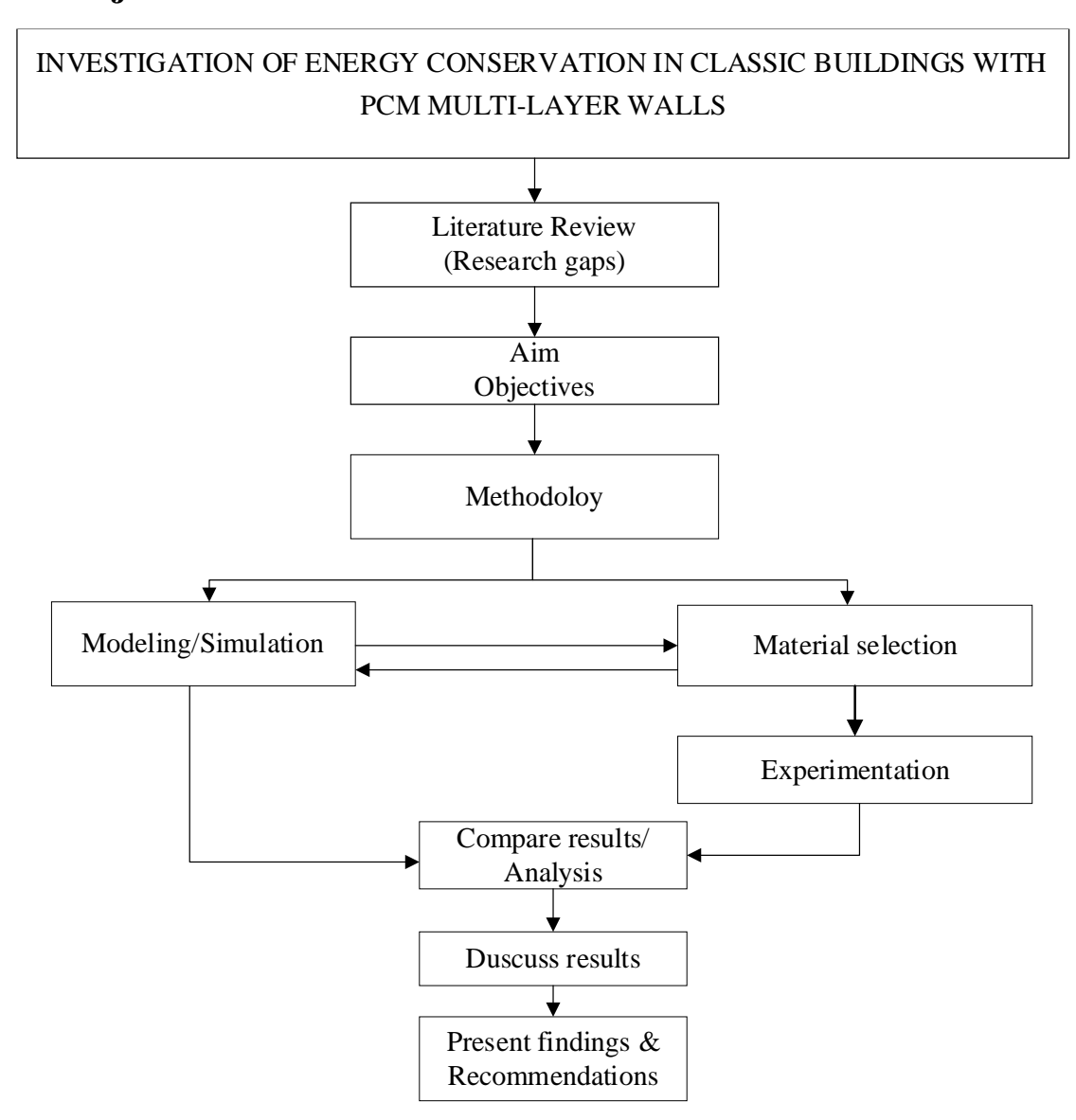


Figure 1-1. Project flow chart

The flowchart in Figure 1-1 outlines the research process for this study. It starts with a literature review to identify knowledge gap(s), followed by defining the aim, objectives and methodology. This leads to parallel streams of modelling/simulation and material selection, which feed into experimentation. The results are then compared, analysed, and discussed, and the final findings are presented.

1.5 Program of Work to Accomplish the Project Objectives

To investigate the effects of PCM configuration inside walls on energy consumption, a mathematical model was formulated, with necessary assumptions and boundary conditions established. Simulations were then conducted for wall configurations both without PCM and with PCM wallboards placed at different distances from the outer wall surface. The TRNSYS simulation software, licensed to the University of Hertfordshire, was used to generate a numerical model and simulate heat transfer to the room. A prototype wall was also constructed for experimental validation, and the simulation results were compared to the experimental data for energy consumption.

The study further explored the impact of windows by integrating a double-glazed glass window into the wall layers. Room temperature measurements were taken for different PCM configurations, and energy calculations were compared with simulation results to assess accuracy.

A series of laboratory tests were conducted to validate the simulation findings. Thermal testing equipment was designed to assess heat storage, and a heat source was provided to trigger the PCM phase change. Temperature measurements of the wall layers were recorded over 48-hour intervals, and these were used to evaluate the correlation between simulation and experimental results.

To assess comfort levels, the Predicted Mean Vote (PMV) and Predicted Percentage of Dissatisfied (PPD) indices were calculated for different PCM configurations using the Fanger comfort model. These results were compared to simulation outcomes to understand the impact of PCM on occupant comfort in various building spaces. Finally, recommendations were provided for incorporating PCM in drywalls for energy-efficient upgrades or new construction projects based on the overall findings.

Table 1-1. Project Overview

Task Name	Start Date	End Date
CHAPTER 1: INTRODUCTION		
Background	01/10/19	31/10/19
Necessity of PCM integration (Project justification)	01/11/19	20/11/19
Aim and Objectives	21/11/19	29/11/19
CHAPTER 2: LITERATURE REVIEW		
Critical review of available literature	29/11/19	20/05/20
Thermal energy storage systems and classification	01/06/20	30/06/20
PCM wallboards and engineering applications	01/07/20	31/07/20
CHAPTER 3: METHODOLOGY		
Review of Numerical models	30/07/20	15/05/20
Review of Analytical models	15/05/20	15/05/20
Initial registration	25/05/20	29/05/20
8months initial registration (First assessment)	30/01/20	30/06/20
The description of the wallboard model	06/01/20	06/07/20
Investigate the effects of wall configuration on energy consumption	06/07/20	01/09/21
CHAPTER 4: SIMULATION		
Without PCM wallboard simulation	01/09/21	30/09/22
With PCM wallboard simulation	30/09/22	09/12/22
36months preparations & progression assessment	09/12/22	30/11/23
CHAPTER 5: EXPERIMENTAL WORK		
Conduct laboratory tests to validate simulation results and discussion	12/12/23	28/01/24
Conduct laboratory tests with PCM and measure room temperatures	01/03/24	30/03/24
Experiment with the window effect: a wall with a glass window	01/04/24	30/05/24
CHAPTER 6: DISCUSSION		
Perform thermal performance analyses	30/05/24	30/06/24
Compare Simulation and Experimental results	30/06/24	30/07/24
CHAPTER 7: CONCLUSIONS AND RECOMMENDATIONS		
Conclusions and Recommendations	01/07/24	30/09/24
Conference presentation, Journal and Thesis (write-up) - submission	01/07/24	30/09/24

Table 1-1, shows the Project overview with the following key milestones:

- Oct 2019 Sep 2021: Initial chapters and project planning, including a detailed review of literature and methodology.
- Sep 2021 Nov 2023: Intensive simulation work and progression assessments.
- Dec 2023 May 2024: Conduct laboratory experiments to validate the simulations, including the effects of PCM and Windows.

- Jun 2024 - Sep 2024: Write journal papers, prepare for conferences and finalise the thesis.

1.6 Scope and Limitations

Scope

This study investigated the integration of PCMs into building envelopes to enhance energy efficiency across different building types, specifically Victorian-era buildings and contemporary office buildings with cavity walls and integrated windows. The research covered both simulation and experimental approaches to validate the effectiveness of PCM applications.

i. Building Types

The study examined two distinct building types: historical Victorian-era buildings and hospital or office buildings with cavity walls with integrated double-glazed glass windows, providing a comprehensive analysis of PCM effectiveness in diverse architectural contexts.

ii. Materials

The study emphasises buildings constructed with materials whose properties are characteristic of local construction practices, assessing the compatibility and performance of PCMs in these contextually relevant constructions.

iii. Methodology

The research employed a combination of simulation and experimental methods to analyse the thermal performance, energy consumption, and optimal positioning of PCMs within multilayer walls. This dual approach ensured robust validation of the findings.

iv. Geographical Focus

While the study drew on examples from the UK, particularly the CHASE FARM Hospital and Victorian-era buildings, the findings aimed to offer broader applications and insights that could be adapted to other regions with similar building types and climates.

v. Practical guidelines

The study provides practical guidelines for architects, engineers, and building managers, facilitating the effective incorporation of PCMs in new constructions and retrofitting projects.

Limitations

Despite its comprehensive approach, the study has several limitations:

i. Applicability

The findings from the specific building types and materials studied may not directly apply to all building contexts, particularly those with significantly different architectural designs, materials, or climate conditions.

ii. Material Specificity

The study focused on buildings constructed with local materials, which may limit the generalisability of the findings to buildings made from different materials. The performance of PCMs in walls made from other materials may vary.

iii. Simulation Constraints

While simulations provide valuable insights, they are based on certain assumptions and ideal conditions that may not fully capture the complexities of real-world environments. Experimental validation helps bridge this gap, but the results are still subject to the limitations of the specific cases studied.

iv. Experimental Limitations

The experimental investigation was conducted on a sample wall/prototype, which may not capture all the variables and complexities of full-scale building applications. Additionally, experimental results were influenced by the specific conditions and settings in which they were conducted.

v. Climate conditions

The study primarily focused on the UK climate, which may not fully account for the performance of PCMs in significantly different climate zones, where temperature fluctuations and other environmental factors may affect PCM behaviour differently.

vi. Time and Resource Constraints

The scope of the study was limited by time and resource availability, which may restrict the extent of the experimental investigations, and the number of case studies analysed.

These limitations should be considered when interpreting and applying the study's findings to broader contexts. Further research is recommended to explore the application of PCMs in other building types, materials, and climates to expand the understanding of their potential benefits and limitations.

1.7 Structure of the Thesis

This thesis consists of seven chapters, each focusing on a distinct aspect of the research. Chapter 1 introduces the background, problem statement, research objectives, significance of the study, and scope and limitations. An extensive literature analysis in Chapter 2 provides existing literature, identifies key studies and research gaps, and presents the theoretical framework that underpins the study. Chapter 3 outlines the methodology, covering both the simulation and experimental approaches used in investigating PCM integration. Chapter 4 presents the simulation results, while Chapter 5 details the experimental work, including setup, procedures, and outcomes. Chapter 6 combines and discusses the simulation and experimental findings, validating the results and exploring their implications for energy-efficient building designs. The final chapter, Chapter 7, is a detailed summary that provides the key findings, conclusions, and recommendations, offering insights for future research and practical applications. The thesis concludes with references and appendices containing supplementary materials.

CHAPTER 2: LITERATURE REVIEW

The building sector is responsible for a significant portion of global energy consumption, accounting for 40% of energy usage, and a major contributor to greenhouse gas emissions, representing nearly one-third of the global total [14, 15]. In recent decades, energy demand in this sector has surged, driven by population growth and increasing living standards [16, 17]. This trend suggests that, unless stringent measures such as minimum performance standards and energy codes are enforced, the sector will continue to rely on fossil fuels, making it difficult to align with Net Zero Emissions goals by 2050 [18]. The urgency to prioritise efficient energy utilisation is further driven by finite fossil fuel reserves and rising concerns about greenhouse gas emissions [19, 20, 21].

Research into innovative technologies, particularly thermal energy storage (TES) systems, offers pathways to reduce reliance on fossil fuels and improve energy efficiency. TES systems can augment energy conversion and optimise the use of various heat sources [22, 23]. Energy can be stored as sensible heat, latent heat through Phase Change Materials (PCMs), or via chemical reactions [24, 25]. PCMs are particularly effective because they absorb and release substantial energy during phase transitions, operating as latent heat storage units [26, 27, 28]. These materials can stabilise indoor temperatures by absorbing excess heat during warm periods and releasing it when temperatures drop, thus reducing the demand for heating and cooling [29].

Several studies have highlighted the significant potential of PCMs for enhancing energy efficiency across diverse climates. For instance, one study reported a maximum 12.9% reduction in annual energy demand with PCM integration across 13 global climate zones [30], but it only addressed future climate scenarios, limiting its immediate applicability. Another study into the Trombe wall enhanced with PCMs achieved a 36% reduction in energy consumption in hot climates [31], though the focus on a single building element restricts broader applicability. A comprehensive investigation into the influence of repositioning, thermo-physical properties, and thickness of PCM relative to the wall thickness identified the mid-wall position as the most efficient for PCM integration in thermal storage walls [32], but the analysis was limited to five locations in Serbia, making it less applicable to different climates. Further research evaluated the energy flexibility and saving potential of PCM-

integrated walls under different precooling strategies and showed that a 1 cm layer of RT-27 PCM reduced heat ingress by 12.06% in summer, although doubling the PCM thickness did not proportionally increase energy savings [33], indicating a need for better optimisation strategies. Another in-depth study has also shown that optimising PCM placement and precooling strategies increased the energy flexibility index by 69.7% and reduced electricity costs by 51% for a 1.3 % reduced load [34], but these findings require validation in diverse building types and climates.

Additionally, research on PCM in a Mediterranean climate showed up to 73.81% and 76.46% energy demand reduction under optimal conditions of PCM application in simple wall and double wall buildings, respectively [35]; however, the focus on Mediterranean climates and generic building types, along with the omission of dynamic factors like occupant behaviour, necessitates further research. An experimental evaluation of macroencapsulated PCM in tropical climates demonstrated significant reductions in thermal amplitude (40.67%-59.79%), peak temperature (7.19%-9.18%), and cooling load (38.76%), with a time delay of 60-120 minutes [36], but was limited to cubicle structures, lacking exploration of diverse building types. Also, an investigation of the thermal and energy performance of a PCM-integrated midrise apartment building across 15 climatic zones and 60 cities using EnergyPlus software demonstrated energy savings of up to 32.2% [37], though it lacked analysis of diverse building types and real-world dynamic factors.

While PCM applications have been extensively studied in warmer climates, there remains a substantial opportunity to explore their applications in colder regions where heating challenges are more pronounced [38, 39]. For instance, one study demonstrates the effectiveness of PCM-integrated thermal storage systems in reducing temperature swings (up to 10°C) and heating requirements (up to 17%) in solaria within cold climates, with phase change temperatures ranging from 18-24°C [40]. However, the study's narrow focuses on a specific building type, limited climate scope, minimal cooling performance analysis, and lack of investigation into long-term PCM behaviour and real-world conditions, highlight the need for further research.

Colder regions, particularly European countries, renowned for their Victorian architecture, face high energy costs due to outdated building designs that lack modern energy efficiency standards [41, 42]. Although PCMs can stabilise indoor temperatures and reduce energy

consumption in such climates, most research has not thoroughly explored their use in regions with long, harsh winters. This lack of focus on cold climates means that the specific challenges of maintaining heat during prolonged periods of cold are underexplored [43]. This gap is critical, as improving energy efficiency in colder climates can have significant economic benefits.

Victorian-era buildings, along with other historical structures in European countries, are often valued for their unique architectural features and cultural significance [44]. However, upgrading these buildings to meet modern energy efficiency standards poses a significant challenge due to the need to preserve their aesthetic and structural integrity [41, 45]. This highlights a gap between heritage preservation practices and environmental sustainability [46]. PCM technology, with its ability to store and release heat, offers the potential to stabilise indoor temperatures and reduce reliance on continuous heating and cooling for these buildings [41, 42]. This presents significant opportunities for energy savings and decreased use of traditional heating methods [31, 47, 48]. As the construction sector increasingly emphasises sustainability, the adoption of PCM walls aligns with market demands and EU 2050 long-term strategies, potentially making these buildings eligible for incentives [49].

Heritage buildings, especially in the UK, where they represent 20% of the building stock, present a unique opportunity for PCM technology to play a role in energy reduction while preserving historical value [50]. However, much of the existing research has overlooked the specific requirements for heritage buildings with thick, multi-layered walls typical of Victorian-era structures. Similarly, many studies also fail to account for the soft retrofit approaches needed to preserve architectural integrity while upgrading energy systems [49, 51, 52]. Research has highlighted the importance of monitoring and simulation models for adapting historic buildings to modern energy efficiency and climate resilience standards [53], yet detailed exploration of advanced technologies like PCM remains limited. While energy retrofitting in historic buildings is recognised as complex, involving the balance of energy efficiency, occupant needs, and economic considerations, few studies explore the integration of modern retrofitting technologies specifically designed for heritage structures [54, 55]. Research on climate change's impact on historic buildings revealed that energy consumption for preservation often exceeds that for human comfort, though it mainly focuses on HVAC systems and overlooks the role of advanced energy-saving technologies like PCM [56].

Further criticism can be drawn from the fact that research on PCM integration has often focused on systems deemed impractical or too costly for cold climates [57, 58]. The materials and methods suggested [24, 59, 60, 61], are often unsuitable for the local building materials traditionally used in heritage structures, which tend to be significantly thicker and have more complex thermal properties than modern buildings. This limitation highlights a gap in the understanding of how PCMs can be adapted for use with materials that exhibit the specific thermal and structural properties common in heritage buildings. There is a need to focus on PCM integration in real-world, thick-walled, multi-layer heritage structures, testing their effectiveness in enhancing energy efficiency while preserving architectural integrity, which the study seeks to address. Additionally, existing research lacks a detailed analysis of the economic feasibility and practicality of PCM applications in heritage or cold-climate buildings. Although some studies have demonstrated the energy-saving potential of PCMs, they often ignore the long-term durability, cost-effectiveness, and ease of integration in retrofitting heritage buildings [41, 62, 63].

However, one critical area that remains underexplored is the integration of PCMs within multi-layered walls that include windows, a common feature in both modern and historic buildings. Windows account for 25% to 30% of residential heating and cooling energy consumption [64, 65], significantly complicating the thermal dynamics of buildings. While integrating PCMs with thick, multi-layered walls that incorporate windows could mitigate heat losses and gains and help stabilise indoor temperatures, limited research has examined this combined effect. For instance, a study in Mexico evaluated the thermal performance of a window shutter with PCM in both warm and cold climates, but it did not address the combined effects of PCM integration with multi-layered walls [66].

Other studies have explored PCM placement in buildings [67, 68], but few have considered the impact of windows. For example, a parametric analysis in China of innovative glazing windows with integrated solid-solid PCM and silica aerogel found an energy-saving potential of 18.22% in cold regions [14]. However, the study did not consider broader PCM applications beyond window systems. Similarly, a triple-pane glass window with a PCM frame demonstrated an energy-saving potential of 12.2%, although it could be costly to implement [69]. Altering the window cavity shape slightly reduced heat transfer, decreasing window energy loss by 20%, while replacing air with paraffin PCM in the cavity reduced heat transfer

by a factor of four [70]. However, these configurations may reduce natural light, potentially increasing the need for artificial lighting and affecting occupant comfort.

2.1 Overview of Energy Conservation Strategies in Buildings

Energy conservation in buildings is a vital component of sustainable development. It aims to reduce energy consumption, lower carbon emissions, and enhance overall energy efficiency. In the UK, these efforts are supported by the Energy Performance Certificate (EPC) system, which rates buildings based on their energy efficiency and environmental impact.

Regulatory and Policy Frameworks

Energy conservation is also guided by regulatory and policy frameworks, which promote the adoption of energy-efficient technologies like PCM technology. Such approaches include:

- i. Energy Performance Certificates (EPC): In the UK, EPCs rate buildings based on energy efficiency. Integrating PCMs can significantly improve a building's EPC rating by reducing overall energy consumption and enhancing thermal performance [71].
- ii. Building Codes and Standards: Regulations that encourage or mandate the use of energy-efficient materials and designs [72], including PCMs, in new constructions and retrofits.
- iii. Incentive Programs: Programs that provide financial incentives for adopting energy-saving technologies could be extended to support the broader adoption of PCMs in building projects.
- iv. Sustainability Certifications: Certifications like Leadership in Energy and Environment Design, LEED (US), Building Research Establishment Environment Assessment Method, BREEAM (UK), and many others are globally recognised certifications for making buildings more sustainable, high-energy performance, and efficient, where PCM integration can contribute to achieving these standards [73, 72].

The European Green Deal aims to make Europe the first climate-neutral continent by 2050, with objectives including reducing greenhouse gas emissions, decarbonising the energy sector, promoting a circular economy, preserving biodiversity, and ensuring a just transition for all [74]. This study aligns with the Green Deal's goals by exploring the integration of PCMs into building designs to enhance energy efficiency and reduce carbon emissions. By improving the thermal performance of buildings, particularly in heritage and modern

structures, the study contributes to the broader objectives of the Green Deal, supporting the transition to a sustainable and climate-resilient future.

The Department for Energy Security & Net Zero (DESNZ) is a UK government body focused on ensuring reliable energy supplies and leading the transition to net-zero carbon emissions by 2050. Its goals include enhancing energy security, promoting renewable energy, improving energy efficiency, and fostering innovation in low-carbon technologies [75]. DESNZ aims to drive green economic growth, create jobs, and position the UK as a global leader in climate action.

Integrating PCMs into building design and retrofits is a forward-looking strategy that enhances energy efficiency, contributes to improved EPC ratings, and supports the broader DESNZ goals of sustainability and climate action. As buildings increasingly adopt PCM technologies, they can achieve significant energy savings while maintaining occupant comfort and preserving environmental integrity.

2.1.1 Integrated Energy Conservation Strategies in Building Design

Achieving energy efficiency in buildings involves a combination of passive, active, and technological strategies alongside the conscious behaviour of occupants. These approaches work synergistically to reduce energy demand and enhance thermal comfort, with PCMs playing a crucial role in many of these strategies.

Passive design strategies focus on optimising a building's architectural features and materials to naturally regulate indoor temperatures, thereby naturally minimising the natural need for mechanical systems [76]. Key methods include building orientation and layout, which ensure that structures are aligned to maximise natural light while minimising heat gain or loss. This approach complements PCMs, which help stabilise temperature fluctuations by absorbing and releasing heat during phase transitions. Integrating thermal insulation, particularly with PCMs, further enhances the building's ability to maintain stable indoor temperatures [35]. Additionally, passive design incorporates natural ventilation, where buildings are structured

to promote airflow and natural cooling, with PCMs offering extra thermal regulation to maintain comfortable conditions indoors.

In contrast, active design strategies rely on mechanical systems and technologies to manage energy use efficiently. When combined with PCM-enhanced walls, high-efficiency HVAC systems reduce energy consumption by 44.16% [77], moderating temperature fluctuations to 25.52°C [78] and alleviating the load on heating and cooling systems. Similarly, smart building technologies can optimise energy consumption using automation and control systems, where PCMs act as thermal buffers, ensuring stable indoor environments [79]. The integration of renewable energy sources, such as solar panels, benefits from PCMs which help manage the intermittent nature of these energy sources by storing and releasing energy when needed [78]. When combined with PCMs' ability to regulate temperatures, efficient lighting systems further contribute to reducing overall energy consumption in building use [80].

Material and technological innovations are essential for advancing energy conservation, with PCMs at the forefront of these developments. PCMs significantly enhance the thermal performance of buildings by absorbing and releasing heat during phase transitions, which directly reduces the energy required for heating and cooling [81]. When incorporated into building envelopes, particularly in walls and ceilings, PCMs contribute to higher energy performance certificate (EPC) ratings. High-performance glazing ratings, when used in conjunction with PCMs, green roofs and walls, further improve the building's capacity to manage heat transfer, while PCM layers, when combined with green roofs and walls, provide additional insulation and energy savings, especially in regions with extreme heating or cooling demands [82, 81].

In addition to design and material strategies, behavioural and operational approaches play an important role in energy conservation. Energy Management Systems (EMS), which monitor and optimise energy use, work more effectively when combined with PCMs, as the materials provide a stable thermal environment, reducing the need for frequent heating or cooling adjustment systems [79]. Furthermore, encouraging energy-conscious behaviours among building occupants, such as maximising natural ventilation or adjusting HVAC settings based on PCM-driven thermal stability, enhances overall energy savings.

2.2 Phase Change Materials (PCMs): Properties and Applications

2.2.1 Introduction to Phase Change Materials (PCMs)

A phase change material is described as a substance characterised by a high heat of fusion that can store and release large amounts of energy on melting and solidifying at a specific temperature. Thus, when the substance changes from solid to liquid or vice versa, heat is absorbed or released, thereby classifying PCMs as Latent Heat Storage (LHS) units [83, 84].

PCMs can store or extract heat energy without substantial temperature change, and therefore, they can be applied to temperature stabilisation requirements. Hence, PCMs can store about 3 to 4 times more heat per volume than sensible heat in solids and liquids at an approximate temperature of 20 °C than sensible heat storage materials such as water, masonry and rock [85, 86, 87, 83].

Thermal Energy Storage System (TESS)

There is an increase in research on new thermal energy storage systems (TESS) that can reduce buildings' dependency on fossil fuels. The use of TESS provides a means of increasing the efficiency of energy conversion and utilisation of various available sources of heat [88]. Thermal energy can be stored using sensible heat of solids or liquids, latent heat of phase change materials (PCMs) or chemical reaction of some chemicals [84].

Sensible heat $(Q_{sensible})$ of solids or liquids is the heat released or absorbed by a substance during a temperature change. Mathematically, it is the product of a given mass (m), its specific heat (C_p) and the change in temperature (ΔT) as given in Equation (2-1) [89].

$$Q_{sensible} = m \times C_n \times \Delta T \tag{2-1}$$

Latent heat (Q_{latent}) is the amount of heat released or stored by a substance during a change of state at a constant temperature. For small volumetric changes, the latent heat can be written as [89]:

$$\Delta Q_{latent} = m \times \Delta h \tag{2-2}$$

where Δh is the change in enthalpy.

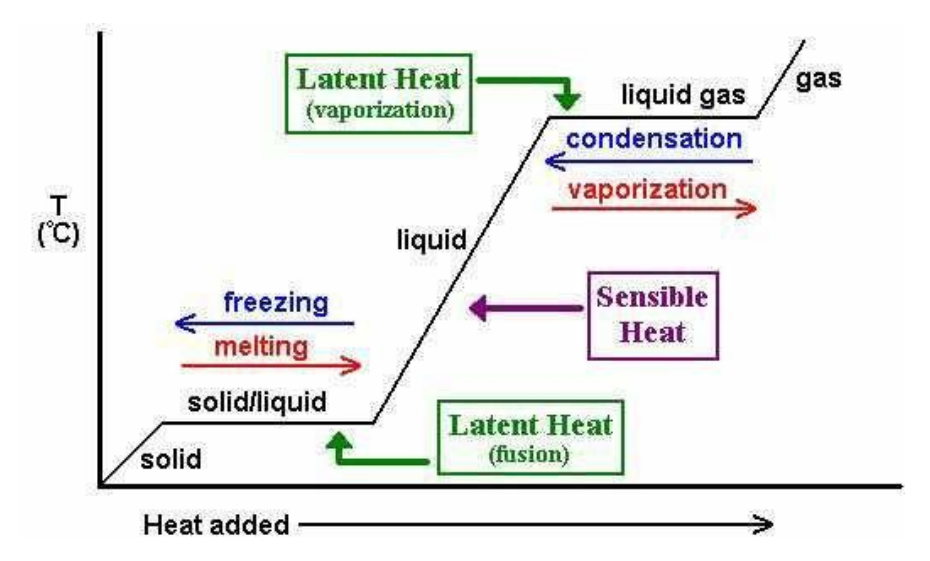


Figure 2-1. Latent heat and Sensible heat of fusion [90]

Figure 2-1 illustrates the difference between sensible and latent heat storage with temperature. Latent heat storage can occur at solid-liquid phase change and liquid-gas/vapour phase change. In the case of solid-liquid phase change material, the latent heat stored equals the enthalpy difference between the solid and the liquid phase [90].

2.2.2 Classification of Phase Change Materials

As shown in Figure 2-2 phase change materials (PCMs) can be classified as [87]: organic (paraffins and fatty acids); inorganics (salt hydrates and metallic); and eutectic (combination of organic-organic, inorganic-organic, or inorganic-inorganic materials. They can be briefly described as follows [91]:

Organic PCMs consist of two main groups: paraffin and non-paraffin. Organic PCMs have the advantage of having a good heat storage density, which is a key desirable factor in choosing and determining which PCM to be employed. They freeze or melt without supercooling, resulting in a more reliable system. The main disadvantages of organic PCMs include the high production cost and the fact that they are derived from crude oil, which is not a renewable energy resource [92]. Their extremely high flammability limits their applications in the construction industry.

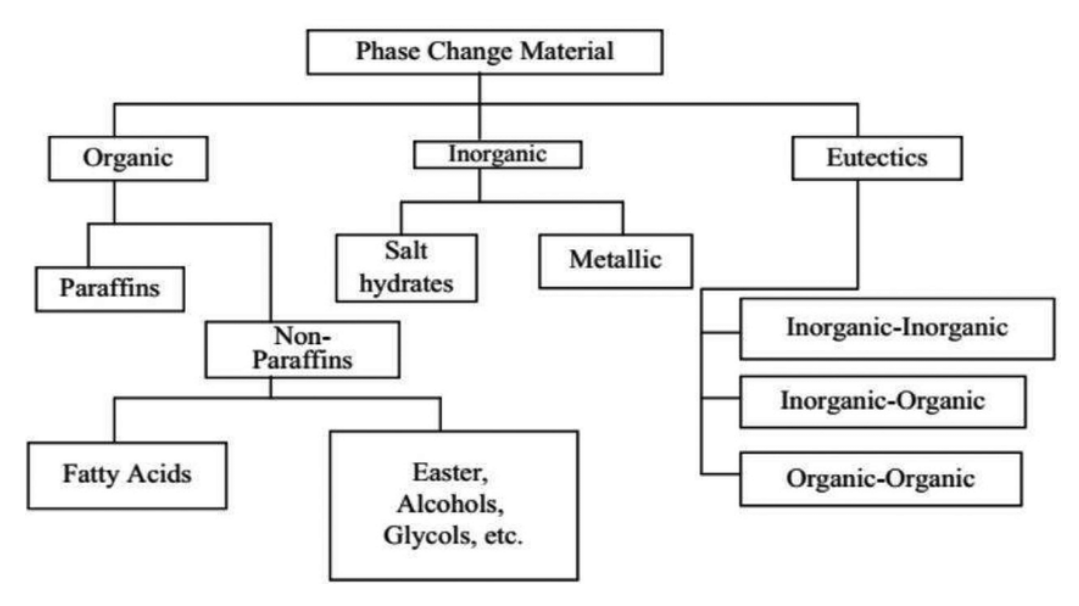


Figure 2-2. PCM classification

Inorganic PCMs are generally common salt hydrates, relatively cheap to produce, readily available, and poses a high latent heat capacity and high thermal conductivity, which is a key performance characteristic of PCMs [87]. However, inorganic PCMs are vulnerable to supercooling, a risk that could cause a system to under-perform where they are applied [93].

Fatty acid PCMs are derived from either plants or animals as hydrocarbon or carboxyl group molecules. Hence, they are environmentally friendly or non-toxic, cheap to use, and have a high latent heat capacity. However, fatty acid PCMs are poor thermal conductors and tend to be heated/cooled unevenly, which enhances only partial material changing of the state, resulting in material under-performance [93].

A Eutectic PCM compound is a homogenous mixture composed of two or more components that melt and freeze harmoniously to form a single component that may form crystals upon freezing and/or melt simultaneously without separation. Eutectics PCMs could be made as organic-organic, inorganic-inorganic or organic-inorganic mixtures, depending on the desired properties. Table 2-1, summarises the main advantages and disadvantages of the different classified PCMs.

Table 2-1: Summary of Advantages and Disadvantages of Phase Change Materials [87].

Type of PCM	Advantages	Disadvantages
	Available in a large temperature range	• Low thermal conductivity (around 0.2 W/mK)
	 Chemically inert and do not undergo phase segregation 	 Moderately flammable
	 Thermally stable for repeated freeze/melt cycles 	 Non-compatible with plastic containers
	 Low vapour pressure in the melt form and small melting heat 	
_	 Non-corrosive or mildly corrosive (fatty acids) 	
Organic	 Compatible with construction materials 	
	 Small volume change during phase transitions 	
	 Little or no super-cooling effect during freezing 	
	• Innocuous (usually non-toxic and non-irritant; non-paraffin type may	
	have various levels of toxicity)	
	• Stable below 500°C (non-paraffin type shows instability at high	
	temperatures	
	 Recyclable 	
Inorganic	High volumetric storage heat and melting heat	Super-cooling during freezing
	 High thermal conductivity (0.5 W/mK) 	 Phase segregation during transitions
	 Cheap and readily available 	 Corrosive to metals and irritant
	 Non-flammable 	 High vapour pressure
	 Compatible with plastic containers 	Low durability
	 Sharp phase change 	 Moderate chemical stability
	 Low environmental impact and potentially recyclable 	High volume change
Eutectic	Sharp melting temperature	Limited data on their thermo-physical
	 High volumetric thermal storage capability (slightly lower than organic PCMs) 	properties is available

2.2.3 Desirable Properties of Phase Change Materials

The desirable properties of phase change materials in latent heat storage systems are classified using thermodynamic, kinetic, chemical, and economic properties, as shown in Table 2-2.

Table 2-2: Phase Change Material Desirable Properties [94]

Thermodynamic	Melting temperature in the desired range
properties	 High latent heat of fusion per unit volume
	High thermal conductivity
	 High specific heat and high-density
	• Small volume changes on phase transformation and small
	vapour pressure at operating temperatures to reduce the
	containment problems
	Congruent melting
Kinetic	High nucleation rate to avoid supercooling
properties	 High rate of crystal growth to meet demands of heat
	recovery from the storage system
Chemical	Complete reversible freezing/melting cycle
properties	Chemical stability
	 No degradation after many freezing/melting cycles
	 No corrosiveness
	• Non-toxic, non-flammable, and non-explosive material
Economic	• Effective cost
properties	Large-scale availabilities

2.3 PCM Applications in Engineering and Construction Materials

Thermal energy storage application of PCMs is increasingly being integrated into buildings as a passive system for temperature stabilisation, effectively reducing the energy required for cooling [95]. PCMs are embedded in various building components such as wall and ceiling boards, Trombe walls, and under-floor heating systems, enhancing heat storage

capacity and supporting temperature regulation, thereby decreasing heating and cooling energy consumption [96]. The construction industry incorporates PCMs into a range of building materials, including concrete, plasterboard, masonry brick tiles, floors, and roofs, to enhance the thermal mass of the building and mitigate rapid temperature fluctuations within the building envelope [97].

PCM passive systems integrate PCMs into building envelopes with low thermal inertia, such as wallboards, floors, roofs, and windows. In these systems, the PCM typically melts during the daytime and solidifies at night, cooling and heating the internal environment, respectively [98]. On the other hand, an active PCM system integrates PCMs with heating or cooling systems to achieve peak load reduction and manage energy demand. A passive PCM system may sometimes fail to complete the melting-freezing cycle, necessitating an active system where sufficient heat is supplied to enable the complete cycle, thus maintaining indoor temperatures at comfortable levels [99]. This research study focuses on PCM passive systems. Furthermore, various techniques exist for integrating PCMs into building envelopes, including direct incorporation, immersion, shape-stabilised PCM, form-stable composites of PCM, and encapsulation, [96], as shown below.

Direct incorporation

This is when liquid or powdered PCM material is directly added to building materials such as gypsum wallboards, concrete, or plaster board during production. Normally, no equipment is required for this method; however, leakages and incompatibility with construction materials may pose significant problems [96].

Immersion

In this method, the building structure components, such as gypsum boards, brick, or concrete, are immersed into melted PCMs, and the PCM material is absorbed into the components' internal pores with the help of capillary attraction. However, studies have shown that this method presents leakage problems which affect long-term use [96].

Encapsulation

Encapsulation can be categorised into macro-encapsulation and microencapsulation. Macro-encapsulation is inserting or adopting a PCM in a macroscopic containment (typically 1 cm in diameter) such as tubes, pouches, spheres, panels, or other suitable containers [100].

Microencapsulation involves the encapsulation or micro-packaging technique involving the deposition of thin polymeric coatings on small particles 1-1000 µm of solids, droplets of liquids, or dispersions of solids in liquids [101]. Macro-encapsulation is a favourable solution for the thermal energy storage of buildings because the leakage problem of the PCM from the surface is contained. However, when the PCM is microencapsulated, partial phase change (melting or solidification) remains [96]. This problem is overcome by enclosing the encapsulated PCM in sheets laminated with aluminium, placed longitudinally within building walls to enhance full melting or solidification, also known as 'thermal shielding' [102].

2.3.1 Phase Change Material Wallboards

PCM wallboards are increasingly recognised as a cost-effective solution for building applications, particularly in lightweight construction, due to their ability to enhance thermal performance and reduce energy consumption [103]. Numerous studies, including numerical investigations [104, 105, 106, 94, 107, 108, 109, 110, 111, 112], experimental assessments [113, 114, 115, 116, 117], and combined numerical-experimental approaches [118, 119, 120, 121, 122, 123, 88, 124], have evaluated the performance of PCM-enhanced wallboards in various building environments. The results consistently show that PCM integration reduces energy consumption, though several key factors influence the effectiveness. These factors include PCM positioning within the wall, the type of PCM used, wall orientation, environmental conditions, outdoor solar gains, internal heat sources, surface colour of the PCM, ventilation and infiltration rates, as well as the thermo-physical properties of the PCM over the temperature range where phase change occurs and the latent heat capacity of the PCM.

In the context of this study, these findings were critical for understanding the optimal deployment of PCMs within multi-layered wall structures to maximise energy savings and thermal comfort. Table 2-3 and Table 2-4 illustrate some of the explorations of the influence of PCM thickness, positioning, and thermal properties in reducing heat transfer and improving building energy performance. Analysing various configurations of PCM walls under different conditions would provide insights into the most effective strategies for PCM integration in both modern and heritage buildings, contributing to the growing knowledge of PCM-enhanced wallboards for sustainable construction.

Table 2-3. Summary of Key Research Findings on PCM Integration in Building Applications for Energy Efficiency and Thermal Comfort

Authors	Review	Highlights	Ref.
Marani &	Integrating PCM in construction materials: Critical	PCM alter the thermal mass and thermal inertia of the building, thus enhancing	[102]
Nehdi (2019)	review	thermal energy storage.	
		• Various methods of incorporating PCM into the building to reduce leakage:	
		microencapsulation, macro-encapsulation, shape-stabilisation, and porous inclusion.	
Xie et al (2017)	A review on house design with energy saving system	• Buildings are responsible for 40% of global energy use, contributing to 30% of total [[125]
	in the UK	CO ₂ emissions. Increasing building insulation using technologies such as a PCM	
		reduces gas consumption and provides a reasonable payback period.	
Bai et al (2020)	Analytical model to study the heat storage of phase	The study was to develop a mathematical model for passive buildings, the factors [[126]
	change material envelopes in lightweight passive	affecting the heat storage process of PCM envelopes in summer, and to determine	
	buildings	efficient methods of temperature control in rooms with PCMs. This concluded that	
		the effectiveness of the PCM is limited, the average room temperature is reduced	
		via ventilation. The average room temperature is determined by coupling the	
		ambient temperature conditions and building parameters. In contrast, the amplitude	
		is determined by these two factors and the properties of the PCM used.	
Nazir et al	Recent developments in PCM for energy storage	• PCMs with higher thermal storage density lead to a reduction of storage tar [[127]
(2019)	applications: A review	size/volume with a range of flexible operating temperatures.	
		• Organic, inorganic, and eutectic PCM selection depends on kinetic, thermos-	
		dynamic properties, availability, melting point, latent heat, energy density and	
		thermal conductivity characteristics.	
Li et al (2019)	Heat reduction in buildings by embedding PCM in	PCM presence reduces temperature fluctuations and heat transfer to the room. The	[122]
	multi-walls	stored energy amount depends on the percentage of PCM in the wall	

Chandel &	Review of the current state of research on energy	• knowledge gap in research and a lack of literature on toxicity, health hazards and	[128]
Agarwal	storage, toxicity, health hazards and	fire retardation of PCM	
(2017)	commercialisation of phase-changing materials.	PCMs could cut down the air conditioning demands.	
		Conclusive energy cost reduction analysis reduction strategies are not addressed.	
Bhamare et al	The review provides a detailed classification and	• Emphasis on the future need for techniques to prepare a combination of PCM	[129]
(2019)	thorough literature on passive cooling techniques for	building materials with stability to avoid leakage, durability, hardness, and water	
	building applications.	permeability of such materials for innovative designs.	
		• Calls to evaluate capital expenditure in installing an economic system against	
		building passive cooling.	
Solgi et al	A literature review of night ventilation strategies in	• Night ventilation strategies are effective across most climate types, but optimisation	[130]
(2018)	buildings. The paper reviews subsequent key research	is required.	
	literature on night ventilation (NV) strategies. The	• Potential for utilising PCMs and lightweight thermal storage for NV systems, which	
	review identifies and classifies NV performance into	may considerably reduce the need for HVAC systems. Hence, a performance	
	three categories: climate, building and technical	analysis is required for PCM multi-wall buildings.	
	parameters.		
Mourid et al	Experimental investigations of the use of PCM in a	• 20% energy consumption reduction compared to building without PCM.	[113]
(2018)	residential room envelope with PCM placed on the		
	inner face of the walls and the ceiling were carried out		
	using full-scale cells		
Figueiredo et al	This paper investigated the optimisation process and	• 7.23% overheating reduction, representing a PCM efficiency of 35.49%.	[131]
(2017)	constructive solutions by incorporating different types	• After the optimisation process, the use of PCM in one of the rooms reduced	
	of PCM of varying melting temperatures and enthalpy,	overheating by about 34%.	
	different flow rates of natural ventilation and the	• 18 years payback time when PCM is used.	
	potential payback time of these novel solutions.		

		•	The techniques and approach of this paper outline possible applications and implications of the work to be done in this study	
Saffari et al. (2017)	Application of simulation tools such as Energy plus, TRNSYS, ESP-r for passive cooling of building was reviewed. Feasibility of PCM passive cooling for different climatic conditions was presented.	•	This study mentioned positive aspects but more sophisticated numerical methods for analysing the cooling performance of PCM-based night ventilation cooling.	[100]
Liu et al (2016)	Thermal conductivity enhancement of phase change materials for thermal storage: A review	•	Use of PCM in building applications not only improves indoor thermal comfort but also enhances energy efficiency	[132]
Lizana et al (2018)	Identification of best thermal energy storage compounds for low-to-moderate temperature storage applications in buildings	•	Highest volumetric storage capacities for best available sensible, latent, and thermochemical storage materials are 250MJ/m³, 514 MJ/m³ and 2000MJ/m³, respectively corresponding to water, barium hydroxide octahydrate, and magnesium chloride hexahydrate.	[93]
Samiev and Ibragimov (2022)	Annual thermal performance of a passive solar heating system with a Trombe wall with phase change materials		The study aimed to evaluate the potential of a passive solar heating system for a 3-room residential building in Uzbekistan with a PCM Trombe wall for hot climatic conditions. Results proved that using PCM in the Trombe wall reduced energy consumption by at least 36%.	[133]

The findings presented in the Table 2-3 align with the need to focus on optimising the integration of PCMs in building applications for energy savings and improved thermal comfort. Several studies have demonstrated the significant energy-saving potential of PCMs and their ability to reduce building temperature fluctuations. For instance, Marani and Nehdi [102] highlighted that integrating PCMs into construction materials modifies the building's thermal mass and inertia, enhancing thermal energy storage and reducing energy consumption, but did not explore how PCM integration affects thick, multi-layered walls or with window.

It has been reported that buildings contribute to 40% of global energy use and 30% of CO2 emissions [134], and that technologies like PCMs have been highlighted for their ability to reduce gas consumption, offering reasonable payback periods [125]. However, the studies often focus on modern structures, overlooking the challenges of retrofitting Victorian-era buildings, where energy efficiency improvements are needed without compromising historical integrity. Previous research has also shown that PCM integration reduces heat transfer and temperature fluctuations, with the stored energy being dependent on PCM percentage within walls [122]. Although these findings are promising, there is limited exploration of the optimal PCM layer thickness and positioning in multi-layer walls, especially in heritage buildings. While experimental studies report energy consumption reductions of up to 20% in residential buildings [113], and reductions in overheating by 7.23% to 34% with PCM optimisation [131], these studies often focus on small-scale residential models rather than complex, multi-layer wall systems in large buildings.

Simulation tools like TRNSYS have been validated as effective for assessing PCM performance in passive cooling systems across various climates [100]. However, there has been little application of these tools to historical buildings with thick, multi-layer walls. Furthermore, studies on Trombe wall systems suggest PCM use can reduce energy consumption by 36% [133]. While valuable, these studies focus narrowly on single building components, and there is need to take on a more holistic approach, examining the entire building envelope and PCM integration in walls and windows to achieve broader energy efficiency goals.

2.3.2 Phase Change Material Positioning in the Multi-layer Wallboard

A number of studies have explored PCM positioning in walls, showing how optimal placement, whether in the middle of wallboards, on the exterior, or in layered configurations, can reduce peak heat loads and significantly improve thermal performance. However, a critical analysis of these studies reveals several limitations and gaps that justify the need for further investigation, particularly in the context of Victorian-era and modern buildings with walls integrated with windows.

A systematic review of latent heat storage in building elements found that the optimal PCM position depends on both climate and application, suggesting that a double PCM layer may be required for year-round performance in some regions [135]. However, these studies did not account for the complexity of integrating PCMs into traditional or modern multi-layered walls, especially in structures with windows, which can significantly alter heat flow. For instance, an experimental study to develop a detailed mathematical model to calculate the effects of PCMs in insulation layers of lightweight walls as well as the effects of temperature, heat flux, and positioning in a typical wallboard where the PCM was inserted at different positions on the wallboards demonstrated that placing the PCM layer in the middle of a lightweight wall, as shown in Figure 2-3, can reduce peak heat load by 15% [136]. However, the study only focused on non-traditional building materials and did not replicate the thermal dynamics of Victorian-era or modern buildings with windows, which represent a significant part of the building sector.

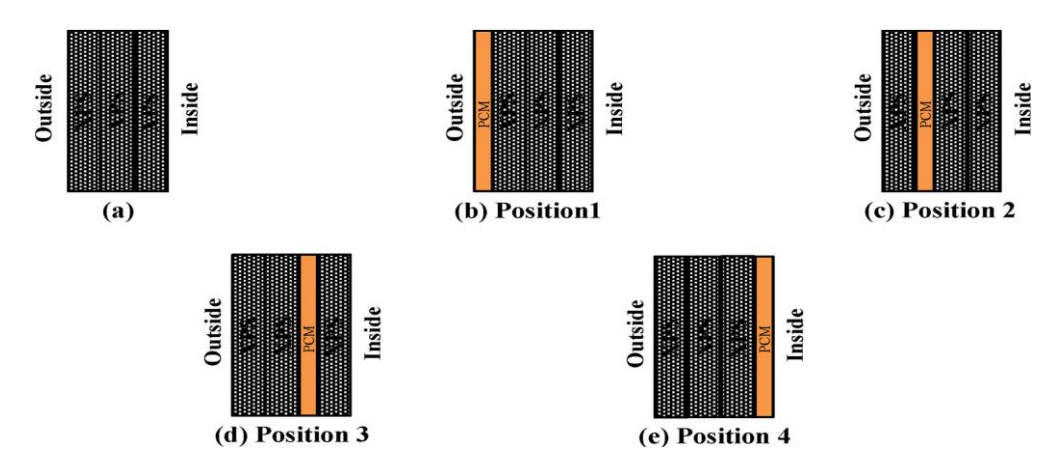


Figure 2-3. (a) Layout of the sample without PCM, (b) with PCM in position 1, (c) with PCM in position 2, (d) with PCM in position 3, and (e) with PCM in position 4 [136].

A simulation study conducted on a south-facing wall in Shanghai, China, investigated different PCM types, thicknesses, and positions, finding that the best performance was achieved with a 20mm PCM layer on the outside of the wall, resulting in a 34.9% heat transfer reduction [104]. However, this study did not address the effects of windows, which are critical for heat transfer between indoor and outdoor environments. In buildings with significant window coverage, as is typical in both Victorian-era and modern buildings, the heat link between the external environment and the indoor space complicates the effectiveness of PCM layers placed solely on the wall [137].

Another experimental study was conducted to identify the optimal PCM positioning using wood and plywood materials and found that PCM/Wood/PCM/Wood wall configuration significantly reduced surface temperature and heat flux [96]. However, the study's materials did not reflect those used in Victorian or modern buildings, which typically feature thicker, multi-layered walls made of brick or masonry, with integrated windows. The reliance on wood-based walls does not provide adequate insights into PCM performance in the more complex and thicker wall assemblies characteristic of historic and modern energy-efficient buildings.

Moreover, research on PCM bricks with embedded paraffin PCM materials demonstrated a 30% energy reduction in heat flux over a seven-day assessment period [138]. However, the high melting point of the PCM in this study (47°C) may be impractical for typical building environments, particularly in temperate regions or buildings with integrated windows, where lower melting points would be more effective for maintaining thermal comfort. Additionally, this brick-based study did not consider the interaction of PCM with windows, which plays a significant role in heat transfer. A different experimental study examining the benefits of PCM underfloor heating and PCM wallboards found that incorporating PCM into walls, ceilings, and floors can shift peak loads and generate potential energy savings [139]. This approach, while effective, implies high initial costs due to the multiple PCM layers in various building elements. The return on investment for such configurations may not be justified for Victorian-era buildings or modern buildings with integrated windows, where a more focused and cost-effective PCM solution is necessary.

A separate study has investigated a combination of passive and active PCM systems, showing that a PCM wallboard enhanced with paraffin and expanded perlite (EP) (60 wt%, 40 wt%) and prepared through a self-made vacuum absorption roller significantly improved thermal comfort and reduced energy consumption [99]. While the findings are impressive, implementing active PCM systems, such as solar thermal heating combined with PCM, appears expensive to set up and maintain. This suggests that this approach may be less practical for many buildings, especially heritage structures, where preservation of the original architecture is a priority.

These studies reveal important insights into PCM performance and underscore critical gaps. The focus on non-traditional building materials, high-cost active systems, and the lack of consideration for window-integrated walls limits the applicability of these findings to buildings with more complex architectures, such as Victorian-era structures. In these buildings, the aesthetic and historical value must be preserved while improving energy efficiency. Moreover, modern buildings with large window areas present a unique challenge for PCM integration, as windows are a significant source of heat transfer that complicates the performance of PCM-based walls.

Further research findings from the literature are presented in Table 2-4, which investigated the effects of PCM position and thickness within multi-layer walls on heat transfer. For instance, it has been reported that PCM positioned closer to the external wall surface in hot climates or during summer conditions effectively reduces heat transfer into indoor spaces [122]. Another study reported that a 20mm RT42 PCM layer on the outside of the wall reduced heat transfer by 34.9% and demonstrated that thicker PCM layers further decrease the amount of heat transferred, though with diminishing returns [104]. Although these findings directly support the study's focus on optimising PCM layer positioning for energy efficiency, they primarily focus on hot climates and basic wall configurations, which limits their applicability to more complex building structures or colder temperatures.

Moreover, other findings have also indicated that PCMs with higher melting temperatures and thermal storage capacities are more effective when placed closer to the heat source. This is particularly relevant in dynamic environments where heat gains are variable, such as in climates with high-temperature swings between day and night or between seasons [140]. For cold regions, placing PCMs closer to the indoor environment helps to stabilise internal

temperatures, a key consideration for maintaining thermal comfort in colder climates. While these findings underscore the importance of placing PCMs with higher melting temperatures closer to the heat source for optimal thermal performance, they are predominantly derived from studies focusing on dynamic environments with substantial heat fluctuations. Such conditions do not entirely represent colder climates where steady heat retention is more critical.

Some studies have also suggested that using multiple PCM layers could enhance energy storage and reduce CO2 emissions. One study showed that a dual-PCM layer design increased energy savings by up to 3.2% compared to single-layer designs and reduced CO2 emissions by up to 18.4% [141]. However, the reported benefits, such as a modest 3.2% increase in energy savings, may not justify the added complexity and cost. Additionally, previous studies lack comprehensive evaluations of dual-layer PCM performance in diverse building types or climates, highlighting the need for further research into their effectiveness, particularly in heritage and colder climate structures.

Furthermore, it has been reported that integrating dynamic insulation material systems (DIMS) with PCM layers led to significantly greater energy savings, with reductions in annual heat gain and heat loss ranging from 15-72% and 7-38%, respectively, depending on the climate and wall orientation [142]. This underscores the importance of considering both PCM and insulation materials in tandem, a concept aligned with the study's approach to enhancing building energy performance. However, these findings are highly dependent on specific climates and wall orientations, limiting their broader applicability to complex, real-world building settings.

The findings from these studies indicate the need to focus on determining the optimal PCM placement and thickness to reduce heat transfer, enhance energy savings, and maintain thermal comfort in multi-layer walls for modern and heritage buildings. By considering factors such as climate, wall orientation, and the integration of dynamic insulation, this study aims to offer a more comprehensive solution for PCM utilisation in building applications.

Table 2-4 The Effects of Phase Change Material Position and Thickness Inside the Multi-layer Wall on Heat Transfer

Author (year)	PCM parameter investigated	Findings	Ref
Wang et al	To reduce solar heat gains in summer with	• The heat transfer rate and average inner surface temperatures during	[104]
(2018)	different PCM melting temperatures, PCM	working hours are significantly reduced by applying PCM in walls.	
	thickness, PCM position and window sizes under	Heat transfer to indoor space in PCM walls decreases with increased PCM	
	changing conditions.	layer thickness.	
		• The best performance in simulated cases was achieved by using a 20mm	
		RT42 layer on the outside of the wall, which reduced heat transfer by 34.9%.	
		• Window system is a weak link between environment and indoor space.	
Faraji (2017)	Numerical study of thermal behaviour of novel	PCM/concrete wall can provide good performance	[143]
	composite PCM/concrete wall: Investigating the		
	possibility of substituting the thick and heavy		
	thermal mass external wall with a PCM/Concrete		
	wall		
Li et al (2019)	Effect of repositioning, thermo-physical	PCMs' presence generally reduces temperature fluctuations.	[122]
	properties, and thickness of PCM	• PCM type RT27 of 1 cm thickness decreased the amount of heat entering	
		the room by 12.06%	
		• Thermal conductivity is most significant in PCM selection.	
		• PCM closer to the exterior has better performance in heat transfer reduction.	
		PCMs with melting temperatures closer to room temperature are preferred	
		for PCMs with the same thermal conductivity.	

Vigna et al (2018)	Phase Change Materials in transparent Envelopes: A SWOT Analysis	 Two-fold increase in thickness of PCM leads to less than a two-fold reduction in heat transfer Analysis of different PCM glazing concepts in transparent/translucent building envelope components in multilayer façade system. The results are a series of SWOT analyses, pointing out the main strengths, weaknesses, 	[144]
		opportunities, and threats.	
Zeyad et al (2020)	Phase Change Materials and Their Optimum Position in Building Walls	A review of existing literature to examine PCMs' application in different positions within the building walls to locate the optimum position and the influential parameters. • In hot regions or during summer, PCM is required closer to the outdoor environment, and in cold regions or in winter, it is required closer to the indoor environment • reducing external heat gain, the PCMs are required in the external surface of the wall; while reducing the internal heat gain and indoor temperature fluctuation, the PCM is applied towards the internal surface of the wall • With a higher PCM's melting temperature and a higher heat of fusion, the PCM is required closer to the heat source • higher PCM quantity results in a higher thermal storage capacity • higher thermal resistance of wall materials reduces the heat and coolness transfer to PCMs, which can cause PCMs' optimum position to move outwards, closer to the heat source, or inward, closer to the conditioned indoor environment	[140]

Mukram, T, A	A review of novel methods and current	The article evaluated various models suggested by researchers for building	[145]
& Daniel, J	developments of phase change materials in the	cooling with PCMs. It was found that PCM walls can be constructed using	
(2021)	building walls for cooling applications	techniques such as adding a separate layer or inserting PCM in brick holes.	
Arici et al	Energy saving and CO2 reduction potential of	The study investigated the use of two-phase change material layers instead of	[141]
(2022)	external building walls containing two layers of	one to improve energy storage by maximising the latent heat of utilisation.	
	phase change material	Seven scenarios were considered: one or two PCM layers on the inner, outer, or	
		both sides of an external wall. Energy savings analysis was carried out using a	
		verified numerical model. Results showed the optimum PCM melting	
		temperature to be 5°C to 30°C. With two PCM layers, the energy saving due to	
		latent heat activation increased from 2.5% to 3.2%. The design also reduced the	
		CO ₂ emissions by up to 18.4% and caused wall surface temperature to reach	
		comfortable room temperature, thereby decreasing thermal loads and improving	
		thermal comfort.	
Kishore et al	Enhancing building energy performance by	An investigation comparing the use of a dynamic insulation material system	[142]
(2021)	effectively using phase change material and	(DIMS) with traditional thermal insulation (with fixed thermal resistance) that	
	dynamic insulation in walls	limits PCM utilisation restraining the energy potential of PCM-integrated	
		envelope to a small percentage. The study identified that using both PCM-	
		DIMS integrated walls provided significantly higher energy-saving potential	
		than the DIMS-only integrated wall or the PCM-only integrated wall in all	
		climates and wall orientations analysed. Depending on the climate, the PCM-	
		DIMS-integrated wall could provide as much as a 15-72% reduction in annual	
		heat gain and a 7-38% reduction in annual heat loss.	

2.3.3 Heat Transfer Techniques of Phase Change Materials

A numerical study has indicated that utilising complete reversible chemical reactions of materials, where molecular bonds are continuously broken and formed through endothermic and exothermic processes, forms the underlying heat transfer principle in thermal chemical storage applications [146]. This approach provides thermal energy storage (TES) systems with the advantages of high energy storage density, compact storage volume, and isothermal storage. However, many PCMs suffer from low thermal conductivity in both their liquid and solid phases, which limits their efficiency by slowing down the heat transfer process during the charging and discharging cycles [147]. To address this issue, several methods have been suggested to enhance heat transfer, including the use of fins, heat pipes, porous media, highly conductive additives, and micro-encapsulation of the PCM [148]. These techniques are categorised into two main approaches: extending the heat exchange area and increasing thermal conductivity. The methods of thermal conductivity enhancement, that have been suggested, are summarised in Table 2-5.

Table 2-5. Comparison of Different Thermal Conductivity Enhancement Methods [148].

Methods	Mechanisms	Limitations
Fins and extended	Increasing heat transfer area.	Increases in total weight, cost, and the
surfaces		properties of PCM are not changed.
PCM-embedded	Increasing heat transfer area,	The porous material is expensive; it
porous matrices	forming a thermal transfer	can reduce total heat storage capacity
	network, and increasing the	and increase total weight.
	thermal conductivity of PCM.	
Dispersion of highly	Increasing thermal	Sedimentation of highly conductive
conductive particles	conductivity of PCM by the	particles may appear, and these
within the PCM	particles with high thermal	particles can hardly form a heat
	conductivity.	transfer network.
PCM	Increasing heat transfer area.	Costly and will reduce the mass per
Microencapsulation		unit volume of PCM.
Multiple PCM	Increasing average	Only adapt to design conditions, and
methods	temperature difference.	may not be useful at variable working

2.3.4 Energy Simulation

Enearu, Chen & Kalyvas [149] suggested that CFD modelling and simulations were often used in systems involving materials that experienced a phase change to study and understand the behaviour and performance of these systems. Elnajjar [138] suggests that typical PCM numerical models are solved using finite difference, finite element, and finite volume, and control volume finite element methods use two approaches: effective heat capacity formulation and enthalpy formulation. The enthalpy formation approach is treated as a dependent variable in energy conservation, as shown in Equation (2-3) proposed by Saffari et al [100] to construct the 'enthalpy vs temperature' (h-T) curve of the PCM. There are reports of formulating a two-phase interface boundary known as the 'Stefan Problem'. The PCM may be treated as a pure material where the phase change occurs at a single constant temperature, or it may be treated as a mixture of different materials where the phase change takes place over a range of temperatures.

$$h(T) = C_{p,const}T + \frac{h_2 - h_1}{2} \times \left\{ 1 + \tanh\left[\frac{2\beta}{\tau}(T - T_m)\right] \right\}$$
 (2-3)

where: C_p is specific heat [kJ/Kg.K], T is temperature [K], h is specific enthalpy [kJ/kg], β is inclination [-], τ is the width of the melting zone [K], and T_m is melting temperature [K].

Mostafavi et al [94] aimed to derive and solve the governing energy conservation equations for heat transfer from a hot wall into a PCM with Cartesian fins extended into the PCM to determine the transient temperature distribution. A perturbation method-based solution for the Stefan problem with time-dependent boundary conditions was applied. The analytical model was validated by comparing it with finite-element simulations, showing that the transient and non-linear nature of heat transfer in such systems results in complex governing equations for temperature distribution. The study emphasised transitioning from a simpler linear differential equation for steady-state temperature distribution in single-phase fluids to a more complex non-linear differential equation in phase change materials. The practical outcomes revealed that fin temperature distribution and heat absorbed by the PCM are critical parameters in the optimal design of phase change energy storage systems.

Various studies have effectively used TRNSYS simulation tool in PCM-related research. For instance, a study developed and validated the Type 3258 model in TRNSYS to simulate PCM behaviour in walls, accounting for temperature-dependent properties and supercooling. By using a finite difference method combined with the enthalpy approach, the model captured transient phase

change events and handled interrupted transitions better than models based on the effective heat capacity method. The results showed that Type 3258 aligns closely with reference models, confirming it as a reliable tool for studying PCM behaviour in energy-efficient building applications [150]. Another TRNSYS-based study focused on developing and validating the Type 399 model to simulate the thermal performance of a chilled PCM ceiling system, incorporating hysteresis effects during the phase change of salt hydrate PCMs. This model was validated with real-scale office building data and exhibited high accuracy in temperature simulations with low RMSE values [106]. However, slight deviations in PCM temperature during phase change were observed, attributed to the limitations in the hysteresis model. Future work remains to optimise the system control, refining the model using additional monitoring data.

A numerical model for PCM storage tanks was also developed and implemented as a TRNSYS component. Validated against experimental data, the model was used to evaluate the PCM tank's performance in combination with other energy systems like solar energy. The results showed less than 1% error in PCM temperature predictions and highlighted the tank's effectiveness in improving heating and cooling loads by 22.5% and 18.75%, respectively, with a seasonal storage scenario reducing cooling energy by 7% [151].

Similarly, a two-dimensional heat transfer model for a PCM layer (PEPCML) was developed and integrated into TRNSYS18 as Type 207. This model was validated through scaled experiments and showed high accuracy. A case study conducted with this module explored the effects of PCM parameters like phase change temperature, latent heat, and layer thickness. The findings indicated that optimal thermal performance depended on carefully calibrating these parameters, with phase change temperature being the most critical factor. The study recommended conducting specific optimisation designs using TRNSYS for different cases, confirming the effectiveness of the tool in simulating dynamic heat transfer and optimising PCM-based building systems [152].

This body of research underscores the effectiveness of TRNSYS in accurately simulating PCM thermal behaviour across a variety of applications, from walls to ceilings and storage systems. Thus, it is a valuable tool for optimising PCM-based building energy performance. For this study, TRNSYS was chosen as the primary simulation tool due to its demonstrated effectiveness in accurately modelling complex thermal behaviours and phase change events in building systems, particularly those involving PCMs.

2.3.5 Thermal Hysteresis

Thermal hysteresis is the condition where thermal history determines the behaviour and properties of the system when properties vary in cooling and heating [153]. Several PCMs exhibit a melting range rather than a single melting temperature; as a result, the shape of the enthalpy curve as a function of temperature [H (T)] defines the material with much better accuracy or precision, as shown in Figure 2-4 [154]. As indicated by Goia et al [124], "Numerical simulations of PCM-based components are often used both for research activities and as a design tool, although present-day codes for building performance simulation (BPS) present some shortcomings that limit their reliability". Goia et al [155] have developed and validated an algorithm in EnergyPlus that has dealt with the hysteresis effect of PCMs utilising the Energy Management System (EMS). An original algorithm was developed that allows for the hysteresis phenomenon to be accounted for and applied to different versions of EnergyPlus. Furthermore, the algorithm utilised the EMS group in EnergyPlus. It permitted the execution of two 'enthalpy vs temperature' curves to correctly model both the melting and congealing processes of PCMs.

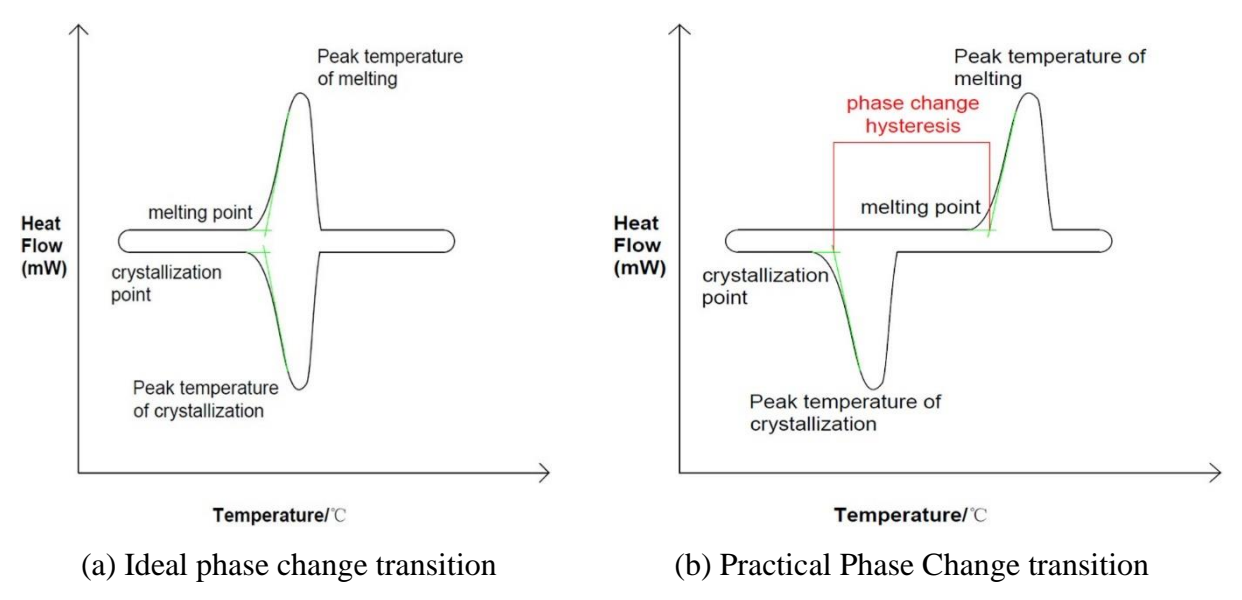


Figure 2-4. Differential scanning calorimetry, DSC, curve, (a) Ideal phase change transition and (b)

Practical phase change transition [154]

Figure 2-4(a), illustrates that the ideal phase change transition is often modelled as isothermal, where the PCM undergoes phase change at a constant temperature; this assumption is typically valid for pure PCMs. However, in practice, especially with composite PCMs, phase change hysteresis (PCH) occurs, as demonstrated in Figure 2-4(b). PCH describes the temperature delay between melting and

solidification, with the solidification temperature generally being lower than the melting temperature [154]. This delay can significantly affect the thermal performance of PCMs in real-world applications.

Although the hysteresis effect is well-recognised and has been addressed in tools like EnergyPlus through the work of Goia et al [124], for simplicity, the study assumed that the PCM undergoes a phase change at a constant temperature. While this assumption streamlines the analysis, it is acknowledged that real-world PCMs, especially composites, exhibit more complex thermal behaviour due to hysteresis. It is reasonable to consider the assumption of constant-temperature phase change in a study for a foundational understanding of PCM performance, but still, future research could incorporate more advanced algorithms, such as those developed by Goia et al [124], to account for hysteresis and further refine simulation accuracy.

Benefits of PCMs in Historical Buildings

An integration of PCMs into historical buildings could significantly improve energy efficiency. PCMs could enhance the thermal performance of these structures by absorbing and releasing heat during their phase transitions, thereby reducing temperature fluctuations. This process helps lower heating and cooling demands, which is essential for maintaining comfortable indoor environments while conserving energy. Such energy efficiency upgrades are significant for older buildings, which often grapple to meet modern standards of thermal regulation due to their original design.

In contrast to traditional insulation methods, which can compromise the aesthetic integrity of historical buildings, PCMs offer a more subtle solution. Traditional insulation may require invasive changes that alter the building's structure or appearance. In contrast, PCMs can be integrated discreetly into walls, ceilings, or floors, allowing for largely invisible energy improvements. This method preserves the building's original design and materials, aligning with conservation goals while delivering modern energy-saving benefits.

Furthermore, historic buildings, especially those constructed before modern heating and cooling technologies, often face challenges in adapting to current climate conditions. PCMs can help address this issue by enhancing the building's capacity to regulate internal temperatures, particularly in response to seasonal variations. By integrating PCMs, historical buildings can achieve a more adaptive climate control, bridging the gap between traditional architecture and the demands of contemporary living environments. This adaptation is vital to ensure that historical buildings remain functional and comfortable amidst changing climate patterns.

Integration Methods

a) Internal Wall Applications

PCMs can be applied within the internal layers of walls, where they can store and release thermal energy [112]. This method ensures the external facade remains untouched, preserving the building's exterior appearance.

b) Ceiling and Floor Integration

In addition to walls, PCMs can be integrated into ceilings and floors [156]. This application is beneficial in buildings with high ceilings, where maintaining a consistent temperature can be challenging.

c) Retrofit Solutions

PCMs can be incorporated as part of a broader retrofit strategy involving the addition of secondary layers to existing structures, such as underlays beneath floor boards or within secondary wall linings [157].

2.3.6 Environmental Conditions and Temperature Operating Range

Research findings demonstrate the significant potential of PCMs in enhancing building energy efficiency. For example, an experimental study to investigate the daily thermal characteristics of the microencapsulated phase change materials (mPCM) wallboard under different indoor boundary conditions has shown to effectively dissipate heat, with performance impacted by indoor air conditions [118]. Another study demonstrated a 34.9% reduction in heat transfer in buildings with PCM layers in south-facing walls, highlighting the importance of proper PCM placement and thickness for optimal performance [104]. Furthermore, selecting the correct PCM melting temperature based on climate can yield substantial energy savings, particularly in cooling-dominant climates, where the optimal melting temperature ranges from 20–26°C [100]. The thermal performance of PCM wallboards also varies seasonally, further emphasising the need for climate-specific solutions [129].

Despite the positive findings, challenges remain in optimising PCM placement, thickness, and melting temperature for different climates and building types. Limited research exists on PCM performance in multi-layer walls in heritage buildings, particularly in relation to modern building codes and energy efficiency targets. There is a need to address this gap by investigating the optimal PCM configuration in multi-layer walls for both modern and Victorian-era buildings.

2.3.7 Ventilation and Infiltration Rates

Paroutoglou et al [158] studied a ventilation system comprising an air handling unit, a 2-pipe active chilled beam system, and a cooling system incorporating latent heat thermal energy storage (LHTES) using PCM. The results indicated that using high-temperature cooling systems combined with renewable energy sources significantly improves energy efficiency by reducing peak loads. The study suggests that integrating PCM into air-conditioned buildings offers energy cost savings, though the payback period should be carefully evaluated against the investment. Another study found that natural ventilation combined with PCM technology enhanced energy savings in office buildings, particularly in climates with cooler nocturnal temperatures. However, in hot, arid climates, PCM alone was less effective, and the benefits of natural ventilation were similar to using ventilation alone [159]. This focus on modern office buildings may limit its applicability to heritage buildings or regions lacking nocturnal cooling. This gap needs to be addressed in the current study by investigating PCM use in contemporary and heritage buildings, considering cases where ventilation is limited or infeasible.

A separate study explored the effect of mechanical ventilation on PCM performance in external walls across Morocco's climate zones, showing that PCM23 was most effective in semi-arid climates, while PCM25 performed better in warmer climates. Increasing PCM thickness and ventilation rates led to cooling energy reductions of 19.5% to 62.9%, with thinner PCM layers and higher ventilation rates yielding optimal results [160]. However, this research did not address the optimising PCM placement and ventilation across different building types, particularly modern and heritage structures.

A study assessing ventilation strategies combined with PCM for cooling energy savings found that changeover ventilation provided the highest savings (up to 96%) in most climate zones, except humid continental climates, although the PCM utilisation remained below 50% and indicated that further optimisation was necessary [161]. While this research focused on modern buildings, it overlooked heritage buildings with restricted ventilation options.

In summary, while previous studies have effectively highlighted the benefits of combining PCMs with natural ventilation for cooling energy savings [162], most focus on modern buildings and mild climates, neglecting the complexities of heritage buildings and harsher environments. The current study seeks to fill this gap by exploring PCM integration in multi-layer walls for both modern and heritage buildings, addressing challenges related to optimising natural ventilation in diverse and

restrictive environments. This approach offers a more comprehensive understanding of PCM performance across various building types and climates.

2.3.8 Insights from Literature: Case Studies on PCM Integration in Retrofitting

Case Study 1

The study investigated the application of PCM for energy retrofitting in an archetype office building constructed in Italy between 1946 and 1970, located in the climates of Palermo and Turin. The retrofitting options considered include interventions on either the external or internal side of the walls. The study employed multi-objective optimisation analyses using a Python implementation of the NSGA-II algorithm and a building energy model developed in EnergyPlus [163].

Case Study 1 findings

The study found that retrofitting on the internal side of the external walls yielded the best energy performance at the lowest cost, with all solutions characterised by a constant low U-value, 0.15 W/(m²K). PCM1, with a lower peak melting temperature (less than 23°C), was more effective in the cooling-dominated climate of Palermo. In contrast, PCM2, with a higher peak melting temperature (greater peak melting temperature than 23°C), was better suited to the heating-dominated climate of Turin. The study also highlighted that the thermal properties of the PCM, such as peak melting temperature, latent heat of fusion, and thermal conductivity, were critical in optimising energy performance. For instance, an exploration range 0.15 to 0.9 (W/mK) ensured minimum energy needs for heating, though these were not the same for cooling. Moreover, the optimal placement of PCM layers varied depending on the retrofit approach, with significant energy savings observed under specific conditions.

Case Study 1 challenges

The study identified several challenges, including balancing energy efficiency with cost-effectiveness, as PCM solutions were not always economically feasible. Additionally, the complexity of multi-objective optimisation, particularly in achieving convergence to the true Pareto front, posed difficulties in analysing results. The trade-offs between optimisation criteria, such as energy consumption, comfort, and environmental impact, also highlighted the need for a robust post-optimisation analysis to guide informed decision-making. Furthermore, the study noted that

increasing the number of optimisation objectives complicates the computational process and analysis, making it more challenging to derive clear solutions.

Case study 2

The study investigated the impact of incorporating PCM into retrofit panels on heat transfer through the vertical walls of buildings in two cities with different climates: Ottawa and Brasilia. The research used a transient numerical heat transfer model developed in Transient System Simulation (TRNSYS) software and validated with experimental data [164].

Case study 2 findings

The study found that the optimal placement for the PCM layer is at the end of the retrofit panel, closer to the interior of the building. In Ottawa, the PCM was most effective between May and September, reducing heat loss by 13% and heat gain by 8%. In Brasilia, the PCM provided heating and cooling savings year-round, with annual heat gain and heat loss savings of 27% and 2%, respectively. An economic analysis revealed that the initial investment for PCM retrofitting in Ottawa could be repaid in 15.63 years based on local electricity prices, with a shorter payback period when accounting for inflation and comparing global energy prices.

Case Study 2 challenges

This study highlighted the need for favourable diurnal temperature swings and indoor setpoints to activate the PCM's latent heat storage effectively. Additionally, while the economic analysis showed promise, the relatively long payback period in Ottawa indicated that further research was needed to develop strategic policies that could improve the economic viability of PCM integration in retrofitting projects. The study also suggested the importance of quantifying the carbon footprint reduction associated with PCM retrofitting as a benefit for mitigating climate change.

From the above two cases, it can be seen overall that integration of PCM into historic buildings has shown promising results in several case studies, particularly in Victorian-era buildings and public heritage sites like churches and museums [45, 165]. The effectiveness of PCM retrofits largely depends on selecting suitable materials and strategically positioning them within the building envelope to maximise energy savings.

However, retrofitting heritage buildings with energy-efficient technologies like PCM presents unique challenges [166]. Due to these buildings' historical and cultural significance and non-standard

construction methods, retrofitting options are more limited than modern buildings. This necessitates a careful balance between preserving the building's integrity and achieving energy efficiency. Key considerations include the need for non-invasive methods that do not alter the building's appearance or structure, the potential impact on indoor climate control critical for preserving artefacts, and the economic viability of such retrofits. Despite these challenges, when carefully applied, PCM integration, along with other measures like draught-proofing, windows, insulation, and ventilation, can substantially reduce energy use in heritage buildings, although a one-size-fits-all approach does not exist [137]. Each retrofit must be tailored to the specific building to achieve the desired outcomes.

2.4 Summary

The critical analysis of existing studies highlights several key knowledge gaps that underscore the importance of the research. Notably, most existing studies on PCM integration have focused on buildings constructed with modern, non-traditional materials, leaving a significant gap in understanding how PCMs can perform in structures built from traditional materials with distinct thermal and structural properties, such as those found in Victorian-era buildings. This is crucial because heritage buildings, which often have thick, multi-layered walls, require energy efficiency improvements that respect their historical and architectural integrity. The study addresses this gap by investigating how PCMs can reduce air conditioning demands and energy consumption in buildings constructed with traditional, local materials. Furthermore, while many studies have explored the impact of PCM integration on energy efficiency, few have examined its effects in buildings incorporating traditional materials, such as cement, stone, brick, or lime mortar, which are typical of older constructions. These materials have distinct thermal properties that may affect the performance of PCMs differently than modern construction materials. By focusing on traditional building materials, this study provides new insights into how PCMs can improve energy efficiency in a way that aligns with the preservation of historic structures.

In addition, the complexity of multi-layered wall systems with integrated windows in traditional buildings has been largely overlooked. Most studies examining PCM integration in building envelopes have concentrated on modern buildings, ignoring the unique thermal challenges posed by older buildings. This research investigates PCM performance in both Victorian-era and modern buildings, particularly in the context of walls with integrated windows, offering a more comprehensive understanding of how PCM can mitigate energy demands and temperature fluctuations in real-world, traditionally constructed buildings.

Finally, while simulation tools like TRNSYS have been used to evaluate PCM performance in modern structures, such tools are limitedly applied to buildings made from traditional, local materials. The study employs TRNSYS to simulate PCM performance in both heritage and modern buildings and compares with experimental results, providing a robust evaluation of PCMs' energy-saving potential.

In general, the key knowledge gaps identified include the lack of research on PCM performance in buildings constructed with traditional materials exhibiting distinct thermal and structural properties and the need for an in-depth investigation of PCM integration in multi-layered wall systems with windows. The focus on these underexplored areas offers valuable insights into how PCM technology can be applied to reduce energy consumption in buildings that maintain their historical and architectural integrity.

CHAPTER 3: METHODOLOGY

3.1 Introduction

This chapter outlines the methodology employed to evaluate the integration of PCMs within building envelopes. It begins with the Research Design, detailing the approaches used to address the objectives. The Theoretical and Numerical Background introduces key principles of heat transfer and governing equations essential to the study. The Simulation Framework discusses software tools such as TRNSYS and TRNBuild, along with validation techniques to ensure accurate results.

The Experimental Methodology covers the construction of building models, PCM properties, and configurations designed to simulate heritage and modern structures. The Data Collection and Analysis Techniques section explains the methods used to gather and validate field and experimental data. Additionally, a Project and Building Description highlights case studies like Chase Farm Hospital to demonstrate practical applications. Ethical considerations are addressed to ensure transparency, and the chapter concludes with a summary of the key elements.

3.2 Research Design

Research Overview of Research Approach

The research design for this study was structured to address the identified gaps in the literature regarding the application of PCM for energy savings in historic multi-layered Victorian-era buildings, hospitals, and modern office buildings with cavity walls integrated with double-glazed glass windows. This study has employed a mixed-methods approach, combining simulation studies and experimental validation to explore the optimal positioning of PCMs within buildings systematically. This included comprehensively understanding PCM's effectiveness in enhancing energy savings and maintaining thermal comfort.

The focus was on two primary building types: Victorian-era buildings and office buildings with cavity walls and integrated windows. These were chosen to represent a range of historical and contemporary architectural styles with different energy efficiency challenges. Prototypes and simulation models were designed to represent typical structures within these categories, ensuring that the findings apply to real-world scenarios. This study sought to identify the most effective PCM configurations for enhancing energy efficiency and thermal comfort in historical and modern buildings by systematically validating the models and comparing experimental results with simulations.

The study is structured into three main phases:

i). Baseline Simulation and Experimentation

The study began with a baseline simulation and experimental investigation of a wall prototype without PCM integration. This phase was crucial for validating the simulation model and software by comparing the simulation results with experimental data. The validated model then served as the foundation for subsequent PCM integration studies.

ii). PCM Integration and Optimisation

In this phase, PCMs were integrated into the wall prototype at various positions. The objective was to experimentally determine the optimal PCM position for energy savings and thermal comfort. This was followed by simulating the same wall prototype in the software to obtain comparable results. The findings from both experimental and simulation analyses are compared to identify the optimal PCM positioning. This optimal position was then used to simulate the energy performance of the entire building, with the results compared against measured energy data from 2019.

iii). PCM Integration with Double-Glazed Window

The final phase involved constructing a wall prototype incorporating a double-glazed glass window. The study experimentally investigated various PCM positions to determine the optimal configuration for energy savings and comfort. A corresponding simulation was then performed to validate these results. The identified optimal PCM position is subsequently used to simulate the energy performance of the entire building, with the results compared against measured energy data from 2019.

3.3 Theoretical and Numerical Background

3.3.1 Key Principles of Heat Transfer

Heat transfer principles form the theoretical foundation of this study, which investigates the thermal performance of PCM-integrated multilayer walls in historic and modern buildings. The three primary modes of heat transfer; conduction, convection, and radiation [167] are critical to understanding the energy interactions within building envelopes.

a) Conduction governs heat flow through solid materials. Fourier's law of heat conduction describes this process:

$$q = -K\nabla T \tag{3-1}$$

where q is the heat transfer rate (W/m²), k is the thermal conductivity of the material (W/m.K), and ∇ T is the temperature gradient (K/m). This equation is particularly relevant for PCM layers, as their heat conduction properties influence phase change efficiency.

b) Convection addresses heat transfer between a solid surface and a moving fluid. Newton's law of cooling expresses this relationship:

$$q = h\Delta T \tag{3-2}$$

where h is the convective heat transfer coefficient (W/m².K), and ΔT is the temperature difference between the surface and fluid.

c) Radiation describes heat transfer through electromagnetic waves, often significant for external building surfaces exposed to sunlight. The Stefan-Boltzmann law quantifies radiative heat transfer:

$$q = -\sigma \epsilon (T^4 - T_{amb}^4) \tag{3-3}$$

where σ is the Stefan-Boltzmann constant (5.67×10–85.67 10^{-8} W/m².K⁴), ϵ is the emissivity of the surface, and T and T_{amb} are the surface and ambient temperatures, respectively.

The governing equations are utilised throughout the thesis to connect field (measured) data analysis, simulation, and experimentation seamlessly. In data analysis, Fourier's Law is employed to estimate heat flux using measured temperature gradients and thermal resistance values, enabling real-world performance interpretation. For simulations, TRNSYS integrates these equations as boundary conditions to model transient heat transfer and PCM behaviour effectively. In experimental work, derived equations calculate thermal resistance and heat transfer rates based on measured temperature and energy data. This integration highlights the versatility of these equations across various methodologies, ensuring consistency and reliability.

3.3.2 Analytical Models and Governing Equations

Most analytical problems with more than two phases are much more difficult to study than two-phase problems because of interactions among phases [168]. In these n-phase problems, it is difficult to describe the exact number of individual phase-change boundaries without ascertaining the number of split sub-regions [169]. The Stefan problem solves this problem by defining the temperature distribution u(x, t), where x is spatial coordinate (m), and y is phase change front (m), to generate a formulated solution for freezing/melting of a semi-infinite PCM-layer initially at a constant temperature in a homogenous phase, and constant temperature at the surface [170]. Phase change behaviour of PCMs is not an isothermal process but complex, and as such many advanced analytical

methods have been formulated. Analytical solutions have disadvantages and hence, comprehensive numerical methods were used.

Three numerical grid methods were considered for solving thermal problems involving PCMs: fixed grid, deforming grid, and hybrid grid methods. The fixed grid method, known for its versatility, convenience, adaptability, and ease of programming, was selected for this research, as supported by references [117, 171]. This method uses fixed spatial grids where boundaries are tracked by an auxiliary function, allowing effective incorporation of latent heat evolution via methods such as the enthalpy method, heat capacity method, temperature transforming model, and heat source method. All PCM algorithms in this research employed fixed grid methods, which facilitated simplicity and reliability in the modelling process. In comparison, the deforming grid method, which permits grid nodes to move along the boundary as the solution evolves (closely following Stefan's condition), and the hybrid grid method, which combines features of both fixed and deforming grids, were deemed less suitable due to the complexities they introduce. Therefore, the fixed grid approach was used for all simulations, ensuring an efficient and robust representation of PCM integration within the studied multi-layer wall structures.

3.3.3 General Formulation of Phase Change Problems

Phase change problems [149] with natural convection form a significant role in several industrial applications. For pure materials, a clear distinction between the solid and liquid phases separated by a sharp moving interface, melting occurs at isothermal temperature. However, the main challenge of phase change problems is the moving boundary where the Stefan condition must be fulfilled. For conduction-controlled heat transfer, the governing equation for solid and liquid phases to satisfy Stefan's condition [172], can be written as:

Heat transfer in the solid phase:

$$\rho \times \zeta_s \times \frac{\partial T_s}{\partial t} = \frac{\partial}{\partial r} \left(k_s \times \frac{\partial T_s}{\partial r} \right) \tag{3-4}$$

Heat transfer in the liquid phase:

$$\rho \times C_l \times \frac{\partial T_l}{\partial t} = \frac{\partial}{\partial r} \left(k_l \times \frac{\partial T_l}{\partial r} \right) \tag{3-5}$$

The Stefan condition that enforces the heat equilibrium solid-liquid interface is:

$$\frac{\partial}{\partial x} \left(k_s \times \frac{\partial T_s}{\partial x} \right) \times n - \frac{\partial}{\partial x} \left(k_l \times \frac{\partial T_l}{\partial x} \right) \times n = \rho \times L \times \nu \times n$$
(3-6)

where ρ is density, C is the specific heat capacity, k is conductivity, T is the temperature, t is time, x is space distance, L is the latent heat of fusion, v is the velocity of the interface, and n is the unit normal on the phase interface. Subscript l is liquid phase and s is solid state.

i) The Enthalpy Method

In this enthalpy method, the governing equation combines both the latent and specific heat into an enthalpy term. For conduction heat transfer problems, the governing Equations (3-4) to (3-6), can be reformulated into one equation where the latent heat is absorbed into the enthalpy term below:

$$\rho \frac{\partial h}{\partial t} = \frac{\partial}{\partial x} \left(k \frac{\partial T}{\partial x} \right) \tag{3-7}$$

Where ρ is the density, h is the latent heat, t is the time, T is the temperature and, x is the coordinate through the thickness.

ii) The Heat Capacity Method

This method engages the effect of enthalpy (sensible and latent heat) by increasing the heat capacity value during the phase change stage [119]. The apparent heat capacity, C^A , and effective heat capacity are used to liberate heat capacity. The conduction one-dimensional heat transfer equation using the apparent heat capacity can be written as:

$$\rho \times C^{A}(T) \times \frac{\partial T}{\partial t} = \frac{\partial}{\partial x} \left(k \frac{\partial T}{\partial x} \right)$$
 (3-8)

where, ρ is the density superscript A is apparent, C^A is apparent heat capacity, T is the temperature, k is the thermal conductivity of the material, and the rest of the terms are defined in Equation (3-7). The heat capacity method is popular because the temperature is the only variable to be solved in the discretised form, and the approach lies in the heat capacity approximation.

iii) The Temperature Transforming Model

The temperature-transforming method overcomes the time and spatial limitations of the heat capacity method. Still, it provides inconsistent results, especially when mass transfer through PCM is considered. Correction proposals have been put forward to improve its accuracy. Equation (3-8) is

transformed into a nonlinear equation with a single dependent variable, temperature Equations (3-9) and (3-10) [172].

$$\rho \times C_{eff}(T) \times \frac{\partial T}{\partial t} = \frac{\partial}{\partial x} \left(k \frac{\partial T}{\partial x} \right) - \rho \times \frac{\partial S}{\partial t}$$
(3-9)

where C_{eff} is the effective specific heat capacity, S is the heat source term represented by the following Equation (3-10) [173] in the governing equation.

$$S(T) = \begin{cases} C_s \times \epsilon, & T < T_{m-\epsilon} \\ \frac{C_s + C_l}{2} \times \epsilon + \frac{1}{2}, & T_{m-\epsilon} \le T \le T_{m+\epsilon} \\ C_l \times \epsilon + L, & T \ge +\epsilon \end{cases}$$
(3-10)

where \in is the half range melting temperature, m is melting, C_s , and C_l , are the specific heat capacity in solid state and liquid state, respectively. T_{m_s} is the melting temperature of PCM, L is the latent heat, and T is the temperature.

iv) The Heat Source Method

The heat source method is derived from the total enthalpy Equation (3-4) and is split into the specific heat and latent heat, but the latent heat acts as the source term in this case. Thus, the heat source equation is derived from Equation (3-4) [172] to become:

$$\rho \times C_{avg} \times \frac{\partial T}{\partial t} = \frac{\partial}{\partial x} \left(k \frac{\partial T}{\partial x} \right) - \rho \times L \times \frac{\partial f_l}{\partial t}$$
(3-11)

where: C_{avg} is the average specific heat capacity, L is the latent heat of fusion, f_l is the fluid fraction of PCM, which takes a value of 0 for solid, 1 for liquid, and any value for the range 0 to 1, representing a mushy phase. The rest of the terms are defined in Equation (3-6). The fluid fraction becomes linear in the heat source method, and the equation can be solved iteratively with temperature. The liquid fraction term can then be approximated using the equation below:

$$f_{l} = \begin{cases} 0, & T < T_{m} \\ \frac{T - T_{l}}{T_{l} - T_{s}}, & T_{m} \leq T \leq T_{m} + \Delta T \\ 1, & T \geq T_{m} + \Delta T \end{cases}$$
(3-12)

For PCM integrated wall applications, these methods are tailored to incorporate boundary conditions specific to the PCM layer, such as heat flux interactions with adjacent materials, and to simulate

transient heat transfer, reflecting real-world thermal behaviour. They are further used to evaluate energy efficiency by quantifying the heat storage and release during heating and cooling cycles. By analysing PCM performance, these methods assess its ability to regulate temperature, reduce heat transfer, and enhance energy savings. Implemented in simulation tools like TRNSYS, they provide valuable predictions of PCM behaviour under diverse operational and environmental conditions, offering practical insights for energy-efficient building designs.

3.3.4 Numerical Methods and Governing Equations in TRNSYS

TRNSYS (Transient System Simulation) tool is a versatile software environment used for simulating the transient performance of thermal and electrical energy systems, particularly in the context of building energy analysis [174]. The software uses numerical methods to solve a set of governing equations that represent the energy and mass balances within the system components over time [175]. Below is an overview of the numerical methods and governing equations used in TRNSYS.

3.3.5 Numerical Models: Discrete Forms and Solution Schemes

The finite element method, finite difference method and finite volume method are commonly used in formulations used in PCM. Numerical models overcome the problem of solving heat transfer problems with PCM wallboards algebraically because of non-linearity. Numerical solutions are solved by a finite difference method [109]. The time spatial discretisation is the form of a second-order finite difference scheme, as stated by Xie et al [109]:

$$\left. \frac{\partial^2 T}{\partial x^2} \right|_{ij} = \frac{T_{i-1}^j - 2T_i^j + T_{i+1}^j}{\Delta x^2} + 0(\Delta x^2)$$
 (3-13)

The time discretisation is a first-order backward differential equation:

$$\left. \frac{\partial H}{\partial t} \right|_{ij} = \frac{H_i^j - H_i^{j-1}}{\Delta t} + 0(\Delta t) \tag{3-14}$$

Using Equations (3-13) and (3-14), the heat transfer equation can now be expressed as:

$$\rho_i \frac{H_i^j - H_i^{j-1}}{\Delta t} = \lambda_i \frac{T_{i-1}^j - 2T_i^j + T_{i+1}^j}{\Delta x^2}$$
(3-15)

where Indexes i, i - 1 and i + 1 refer to space coordinates, j and j - 1 refer to time coordinate. The rest of the terms are defined in Equations (3-7) and (3-8).

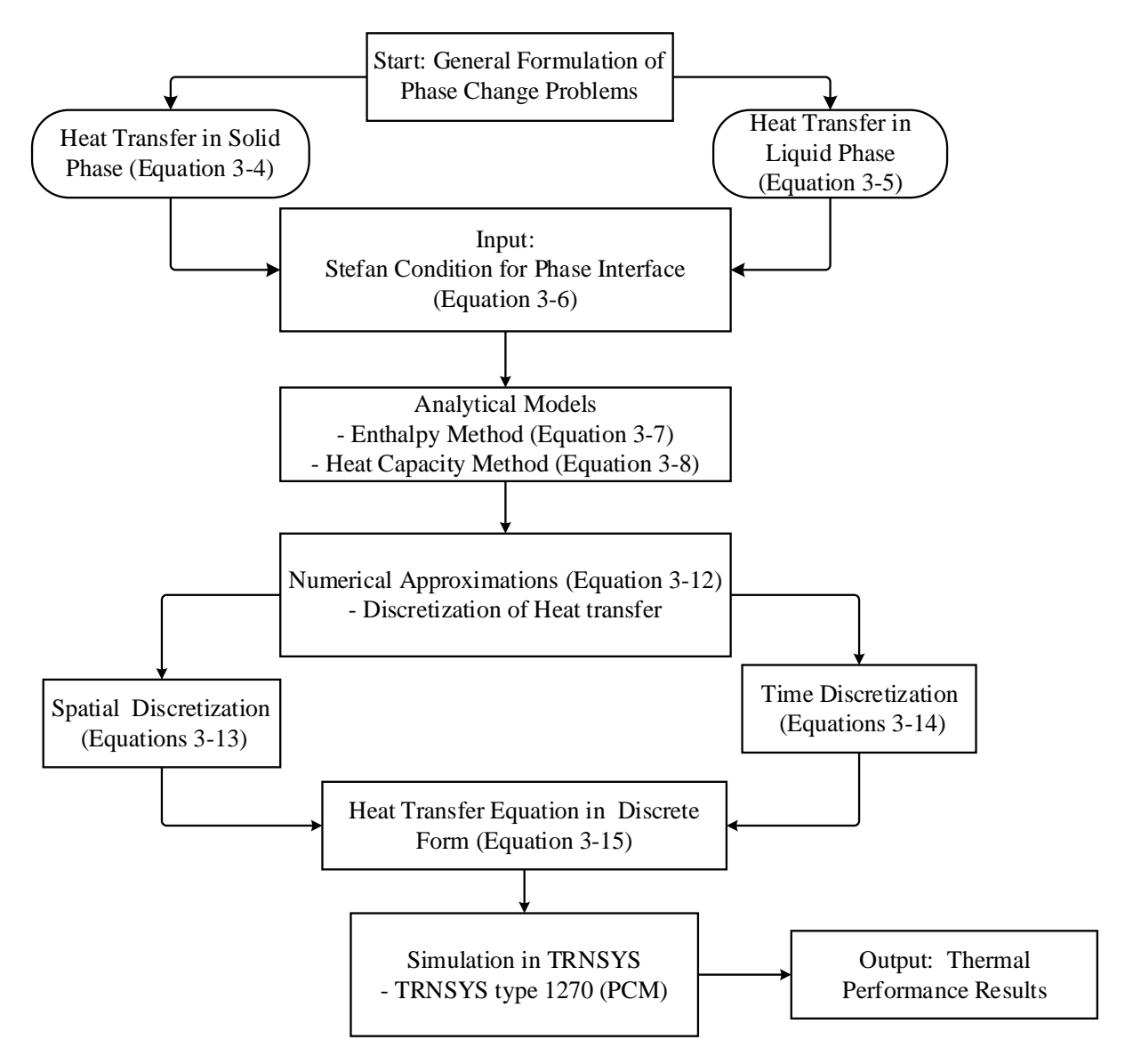


Figure 3-1. Flow chart showing link/relationship between Equations (3-4) to (3-15)

Figure 3-1 illustrates a summary of the process of modelling heat transfer in building structures incorporating PCM, leading to solutions using TRNSYS. The process begins with formulating the phase change problem, setting boundary conditions, and defining the governing heat transfer equations (Equations (3-4), (3-5), (3-6)). Analytical models such as the Enthalpy Method, Equation (3-7) and the Heat Capacity Method, Equation (3-8), are then applied. Numerical methods, including the Fixed Grid Method and Discretisation, Equations (3-13), (3-14), (3-15), Solve these equations, followed by simulation using TRNSYS, specifically Type 1270, to incorporate PCM dynamics. The Apparent Heat Capacity Method, Equation (3-8), helps determine the PCM's impact on temperature and energy efficiency. The simulation results are then analysed to assess the energy-saving potential and thermal performance benefits, demonstrating TRNSYS's effectiveness in analysing PCM-integrated building structures.

3.3.6 Governing Equations in TRNSYS

The governing equations in TRNSYS are based on fundamental principles of energy and mass conservation. These equations are applied to each component (or "Type") in the simulation, representing anything from a building wall to an HVAC system. The software's ability to handle time-dependent heat and mass transfer, coupled with its specific modelling capabilities for PCMs, makes it an ideal tool for analysing energy performance in buildings. Below are the primary governing equations used in TRNSYS:

i). Energy Balance Equation

The energy balance for a system component is governed by the first law of thermodynamics, which states that the rate of change of internal energy within a control volume is equal to the net rate of heat transfer into the system plus the net rate of work done on the system [176], as shown in Equation (3-16).

$$\frac{dU}{dt} = \dot{Q_{in}} + \dot{Q_{out}} + \dot{W_{in}} - \dot{W_{out}}$$
(3-16)

where: ${}^{dU}/{}_{dt}$ is the rate of change of internal energy, \dot{Q}_{in} and \dot{Q}_{out} are the rates of heat transfer into and out of the system, respectively. \dot{W}_{in} and \dot{W}_{out} are the rates of work done on and by the system, respectively.

ii). Heat Transfer Equation

For a solid element, such as a building wall or PCM layer, the heat transfer equation is based on Fourier's law of heat conduction, as shown in Equation (3-17).

$$q = -K\nabla T Q_{out}$$
 (3-17)

where: q is the heat flux (W/m²), K is the thermal conductivity of the material (W/m·K), ∇T is the temperature gradient within the material (K/m), and Q_{out} is the rate of heat transfer into and out of the system. The heat transfer within the material over time is governed by the heat diffusion equation (also known as the heat equation), given in Equation (3-18).

$$\rho C_p \frac{\partial T}{\partial t} = \nabla \cdot (k \nabla T) + \dot{q}_{source}$$
 (3-18)

where: ρ is the density of the material (kg/m³), C_p is the specific heat capacity at constant pressure (J/kg·K), $\frac{\partial U}{\partial t}$ is the rate of change of temperature with time (K/s), \dot{q}_{source} represents any internal heat generation (W/m³), the rest of the terms are defined in Equation (3-17).

iii). Mass Balance Equation

For components involving fluid flow, the mass balance equation ensures that mass is conserved within the system:

$$\frac{\partial m}{\partial t} = \sum \dot{m}_{in} - \sum \dot{m}_{out} \tag{3-19}$$

where: $\frac{\partial m}{\partial t}$ is the rate of change of mass within the control volume, \dot{m}_{in} and \dot{m}_{out} are the mass flow rates into and out of the system, respectively.

iv). Phase Change Modelling with PCM (Type 1270a)

The Type 1270a add-on in TRNSYS is specifically designed to model the behaviour of the PCM within building components. The energy balance equation for a PCM that accounts for the latent heat absorbed or released during the phase transition is given in Equation (3-20) [177]:

$$\frac{dU}{dt} = \dot{Q_{in}} + \dot{Q_{out}} + m. \Delta H. \frac{d\alpha}{dt}$$
(3-20)

where: m is the mass of the PCM (kg), ΔH is the latent heat of the phase change (J/kg), and α is the phase change fraction, representing the proportion of material that has undergone the phase transition. The rest of the terms are defined in Equation (3-16).

The phase change process is typically modelled as a function of temperature, with the phase change fraction α being dependent on the material's temperature relative to its melting and freezing points.

3.3.7 Assumptions

To simplify both the simulation and experimental approaches, , the following assumptions were made for the study [109]. Transient heat transfer was assumed in simulations to accurately capture PCM phase change dynamics, while one-dimensional heat transfer was analysed to reduce computational complexity. PCM and wall materials were treated as isotropic to simplify calculations, though real-world deviations are acknowledged. Additionally, radiation effects on internal wall surfaces were considered negligible, allowing the study to focus primarily on conduction and convection. These assumptions were critical in guiding the study design, ensuring a balance between accuracy and feasibility. The above assumptions can be broken down into:

- i. The wall surfaces are appropriately covered. Wall-end effects on the heat transfer are negligible.
- ii. The inner wall surface is subjected to steady free convection with a constant heat transfer coefficient ($h_i = 7.7 W/m^2 K$), and the outer wall surface is exposed to real-time solar radiation and forced convection heat transfer coefficient ($h_o = 25 W/m^2 K$).
- iii. The momentum equations used to solve the liquid phase and the energy equation for the different sections of the wall are completely solved.
- iv. PCM volumetric and thermal expansions are neglected, and three phase zones (solid, liquid, and mushy) are present.
- v. The solid-liquid interface during the phase change process of PCM (mushy zone) is a mixture of solid and liquid, a Newtonian incompressible fluid. Any resulting flow of the liquid PCM inside the PCM pack is assumed laminar and incompressible.
- vi. There is no movement of PCM when fully solidified.
- vii. The heat transfer through the wall occurred in one direction only.
- viii. No internal heat generation.
 - ix. Homogeneous materials, except for the PCM, are uniform in composition; that is to say, with small temperature variations, the thermo-physical properties of the materials and PCMs are assumed constant.
 - x. PCM had a constant specific heat in both solid and liquid states, with phase change occurring at a constant temperature.
 - xi. Thermal contact resistance between layers of materials within the wall, including the PCM layer, was negligible.
- xii. The air temperature inside the room was uniform, ignoring stratification, and radiation heat on the wall surface was identical.

3.4 Simulation Framework

The simulation method uses advanced software tools to model the building wall prototype's energy performance and thermal behaviour under different scenarios.

Baseline Simulation and Validation

The objective of this phase was to simulate the thermal performance of a wall prototype without PCM integration and validate the results against experimental data for a wall prototype without PCM. TRNSYS was used to simulate the wall's thermal behaviour, and the results were then compared with

experimental data to ensure the accuracy and reliability of the software models. The model was generated using Google SketchUp, with material properties defined in TRNBuild. The simulation environment in TRNSYS focused on studying the impact of PCM positioning and wall configurations in a multi-layered wall to understand its energy performance. Results were exported into Excel as a *.txt file for detailed analysis and compared with experimental data. This phase successfully established a validated baseline model to serve as a reference point for subsequent PCM integration studies.

PCM Integration and Positioning

The second phase aimed to simulate the thermal performance of the wall prototype with PCM integrated at various positions. An additional TRNSYS component, Type 1270a, was employed to model the PCM. Multiple configurations were tested by placing the PCM at different depths within the wall assembly to identify the optimal placement for energy savings and thermal regulation. The simulation results were validated against experimental data to confirm the best PCM positioning, ensuring the findings were both accurate and practical for real-world applications.

Full Building Simulation

In the final phase, the entire building's energy performance was simulated using the optimal PCM position identified from the wall prototype studies. The simulation results were then referenced against the 2019 measured energy consumption data to evaluate the difference between scenarios with and without PCM integration. This step provided insights into how PCM placement could enhance energy efficiency in a complete building scenario.

3.4.1 Numerical Methods in TRNSYS

a) Transient Simulation Approach

TRNSYS performs transient simulations, meaning that it models the dynamic behaviour of systems over time rather than assuming steady-state conditions. This approach is crucial for accurately capturing the time-dependent nature of energy flows and thermal responses in buildings and other systems.

b) Time-Stepping Method

TRNSYS uses a time-stepping method to solve the system's equations at discrete intervals. At each time step, the system's state is updated based on the previous state and the inputs for that interval.

The time step size can be adjusted depending on the required resolution and the dynamics of the system being modelled.

c) Numerical Integration

The software solves ordinary differential equations (ODEs) that describe energy and mass balances in the system using numerical integration methods. Most commonly used two methods in TRNSYS include:

- Euler Method: A simple, first-order method where the future value of a variable is estimated by adding the current value and the product of the derivative (rate of change) and the time step.
- Runge-Kutta Methods: Higher-order methods that improve accuracy by considering the
 derivative at multiple points within the time step. TRNSYS often uses the fourth-order RungeKutta method, which provides a good balance between accuracy and computational
 efficiency.

d) Iterative Solver

In systems with coupled components or non-linear equations, TRNSYS employs an iterative solver to achieve convergence. The solver iteratively adjusts the variables until all the governing equations are satisfied within a specified tolerance, ensuring the model's outputs are consistent and accurate.

3.4.2 Validation of Simulation Software and Methods

This section outlines the validation process for the simulation software and methodologies used in this study. Ensuring the accuracy and reliability of valid results from these tools is essential in order to guide the integration of PCMs into building designs for optimal energy efficiency and thermal comfort.

- a) Simulation Software Verification
 - i). Software Selections and Purposes

TRNSYS, TRNBuild, Google SketchUp, type 1270a add-on for PCM modelling, and Excel for data analysis were employed. These tools were chosen for their ability to accurately model dynamic behaviour, energy performance, and the integration of PCMs within building envelopes. TRNSYS is a powerful tool for simulating the transient thermal behaviour of building systems, including HVAC and renewable energy systems [174, 178]. TRNBuild is a component of TRNSYS that allows for detailed modelling of building geometry, materials, and thermal zones [179]. Google SketchUp was

utilised to create 3D models of the buildings, which were then exported to TRNBuild for thermal analysis. Type 1270a add-on for TRNSYS was specifically designed to model the behaviour of PCMs within building components, allowing for accurate simulation of phase change effects [177]. Excel was used for detailed data analysis, including statistical evaluations, regression modelling, and comparisons between simulated and experimental results.

ii). Verification process

Initial verification of the selected software tools was verified through benchmark tests, simulating standard building configurations with published outcomes. The results from the benchmark simulations were compared against documented outcomes from existing literature to validate the results accuracy. A parameter sensitivity analysis was conducted to evaluate the influence of variations in material properties and climate data on the simulation results ensuring robustness under varying conditions.

b) Methodology Validation

i). Baseline experimentation for validation

A wall prototype without PCM was constructed to serve as a baseline model for validation purposes. This prototype was designed to replicate the materials, dimensions (scaled down), and thermal properties used in the simulation models developed in TRNBuild and SketchUp. Experimental measurements of the thermal performance of the baseline wall prototype were taken in a controlled environment. The key data collected were the temperature gradients across the wall layers. The baseline wall configuration was simulated using TRNSYS and TRNBuild, and the results from these simulations were then compared with the experimental data. Any discrepancies between the simulated and experimental results were carefully analysed, and the simulation models were calibrated accordingly to enhance accuracy.

ii). Validation of PCM integration methodology

After validating the baseline model, PCMs were integrated into the wall prototype at various positions. These configurations were experimentally tested to measure thermal performance, and the same scenarios were simulated using the Type 1270a add-on in TRNSYS. The simulation models were refined using an iterative process, repeatedly comparing them with experimental results. This iterative validation has ensured that the simulation methodology accurately represented the real-world behaviour of PCMs within building envelopes.

iii). Full-Building Simulation Validation

The full-building simulation model, incorporating the optimal PCM placement, was validated by comparing its outputs against actual energy consumption data recorded for 2019. This comparison provides a critical real-world benchmark for assessing the accuracy of the simulations. The simulation

model was also validated across different seasonal conditions to ensure accuracy in predicting yearround energy performance. This seasonal or longitudinal validation has confirmed the model's reliability for comprehensive energy analysis.

iv). The validation of the simulation results

The tools employed in this study, including TRNSYS, TRNBuild, and Google SketchUp, have been widely used in previous studies, such as in the "Estimation of Cooling Load of a Residential House using TRNSYS" [180], demonstrating their reliability in the thermal performance modelling. The Type 1270a add-on, specifically used for PCM modelling in TRNSYS [181], further confirms the capability of these software applications in simulating buildings with integrated PCMs. By rigorously testing and refining these tools against experimental data and established literature, the study ensured that the results were robust, reliable, and reflective of real-world building performance. This validation process was crucial for supporting the study's findings on the optimal integration of PCMs to achieve energy savings and enhanced thermal comfort in building designs.

3.4.3 Validation of the Numerical Method Approach

The numerical method was rigorously validated to ensure accurate and reliable predictions of PCM performance in the simulation models. This validation involved comparing simulation results with experimental data [182, 183] to assess the accuracy of temperature profiles, heat flux, and energy consumption predictions. The implementation of boundary conditions, including internal and external environmental factors, was critically evaluated to ensure precision. Additionally, error metrics such as Mean Absolute Error (MAE), Root Mean Square Error (RMSE), and Mean Absolute Percentage Error (MAPE) were utilized to quantify the accuracy of the results. This comprehensive validation process established confidence in the numerical approach, enabling accurate analysis of PCM integration and reliable predictions of energy savings and thermal performance. By integrating field data, simulation outputs, and experimental results, this study provides a robust framework for optimizing PCM applications in building designs.

3.4.4 Software Selection and Simulation Tool

TRNSYS

TRNSYS was utilised for its flexibility and accuracy in modelling buildings' dynamic thermal performance [175], and under the University of Hertfordshire TRNSYS licence. TRNSYS allows for detailed customisation of building components, including PCM layers within walls, and simulates the interaction between the building envelope and the HVAC systems. TRNSYS software is a valuable

tool in component-based problems to simulate the behaviour of transient building energy systems [106]. The components may vary from heat pumps, solar collectors, and controllers to complex ones like multi-zone building components. The software is commonly used in the simulation of passive PCM systems. Conversely, when considering a chilled PCM ceiling that can operate as an active system, another heat transfer mechanism (type 399) must be implemented to combine both passive and active operation modes. However, this increases computational space and time. The literature review in Chapter 2 also identified other software tools used in whole-building simulation by the other researchers, such as EnergyPlus and ESP-r [184]:

EnergyPlus

EnergyPlus is simulation software used in energy analysis and thermal loading to model heating, cooling, lighting, and ventilation in buildings with the capability to employ variable time steps and other modular systems that can integrate heat and mass balance-based zone simulation, multizone air flow, thermal comfort, and natural ventilation [87]. The model is introduced using an implicit conduction finite-difference solution algorithm, encompassing phase-change enthalpy and temperature-dependent thermal conductivity. However, EnergyPlus was not selected as it requires larger computational space, and the University has no licence available for this study.

ESP-r

ESP-r is an advanced software tool for building energy simulation and allows for further detailed thermal and optical descriptions of buildings to be integrated with the analysis. The domain is discretised in a control volume scheme, and the conservation equations for mass, momentum, and energy are solved [100]. The software can integrate the effects of other factors such as weather, external shading, occupancy gains, HVAC systems, and many others. Like Energy Plus, ESP-r was not selected as it requires larger computational space, and no University licence was available for this study.

Star-CCM+

STAR-CCM+ is an all-in-one solution that delivers accurate and efficient multidisciplinary technologies in a single integrated user interface of the STAR-CCM+ software [185]. It is a complete multidisciplinary platform for the simulation of products and designs operating under real-world conditions. It is also a powerful, all-in-one tool that combines the following [186]: ease of use, automatic meshing, extensive modelling capabilities and powerful post-processing.

STAR-CCM+ is widely used in various fields, including aeroacoustics, fluid dynamics, heat transfer, rheology, multiphase and particle flows, solid mechanics, reacting flows, electrochemistry, and electromagnetics. These applications highlight its versatility in simulating complex physical phenomena across different engineering and scientific disciplines. The advantages and disadvantages of using STAR-CCM+ are listed below.

Advantages

- i. Hybrid structural/unstructured body-fitted grids
- ii. Complex geometries
- iii. Reasonable grid generation times
- iv. Good geometry/boundary layer definition
- v. General purpose
- vi. Improved accuracy, especially drags and pitching moments

Disadvantages

- i. No automated adaptive grid refinement
- ii. Computationally more expensive (10 hours on 16 cores)
- iii. Commercial cost

STAR-CCM+, though it has a University licence, was not selected either, as it does not appear capable of handling heat transfer problems since no review papers highlight STAR-CCM+ software as the simulation tool for PCM heat transfer problems.

3.4.5 TRNSYS and Associated Simulation Tool for Modelling

This section describes the simulation tools employed in creating the building model.

Google SketchUp

SketchUp is a 3D modelling tool that facilitates the creation of detailed geometric surface information required for advanced calculations, such as radiation analysis, in building simulations. To simplify the process of inputting geometric data into the building model, a plug-in called TRNSYS3D for SketchUp is used.

TRNSYS 3D

TRNSYS 3D is a plugin for the SketchUp tool that facilitates the modelling of multizone buildings [187]. Users can create the building geometry from scratch, specifying heat transfer surfaces and

zones and adding windows and shading surfaces. All information is saved in an *IDF file. The building geometry data can be exported into TRNBuild, eliminating the need for manual data entry. This allows users to efficiently input geometric data into energy models which simplifies the process of integrating complex building designs into simulation environments, ensuring accurate surface representation for thorough thermal and energy performance analysis.

TRNBuild

TRNBuild, the multi-zone building interface, allows users to create and edit all non-geometry information required by the TRNSYS building model, thereby dividing the building into thermal zones [174]. The TRNBuild tool enables the specification of detailed input data for multi-zone building structures, such as wall layer thickness and material properties, window optical properties, heating and cooling schedules, incorporation of ceilings and floors, heat radiation, and occupant comfort.

TRNSYS

TRNSYS models and is the simulation environment for the transient simulation of systems, including multi-zone buildings [188]. Engineers and researchers use it to validate new energy concepts, ranging from simple domestic hot water systems to the design and simulation of buildings, including control strategies, occupant behaviour, alternative energy systems (wind, solar, photovoltaic, hydrogen systems, Trombe walls, ventilated facades,), etc [175].

TRNSYS 18 simulations are constructed by connecting individual component models (Types) into a complete model [175]. Components represent any equipment or system of equations to calculate its performance, such as pumps, pipes, chillers, solar collectors, etc. The components are then connected to the TRNSYS environment. When a simulation is initiated, the TRNSYS brain or the "kerne1" determines which Types are included in the simulation by reading the input file. It checks the input file for syntax errors, and at each new time step of the simulation, the kernel calls the Types once in the order they appear in the input file. The kernel records each Type's output and sets the previous outputs as inputs to the Types as appropriate, as described by the connections indicated in the input file, then calls all the Types again. This process is repeated as necessary to complete the simulation.

The kernel compares the newly computed outputs at each simulation against the values calculated in the previous iteration. Convergence is said to be achieved if the values between the output and input values are less than the user-defined tolerance. If the output values have changed more than the tolerance allows, the kernel repeats the substitution process until the outputs converge or a user-specified iteration limit is reached. If the limit set is reached without convergence, a warning is issued by the kernel, which then proceeds to the next time step. When significant warnings are issued without resolution, an error is generated, and the simulation is terminated.

Type 1270 Component for Modelling PCM Layer in TRNSYS

According to TRNSYS Tess-Libraries [189], Type 1270 component models a PCM layer that is entirely contained within a wall or not directly adjacent to the zone air. The wall layers are modelled in TRNBuild, while the PCM layer is modelled externally. Through iterations, Type-56 reassesses and (if necessary) passes information back to the external model based on the TRNSYS kernel's inherent ability to solve such systems by successive substitution. Type1270 models a PCM located anywhere in the wall thickness of a Type-56. The model has built-in values, or the user can specify the PCM's physical properties (density, specific heat, melting temperature, freezing temperature, and latent heat of fusion). For inbuilt values within the model, the user may select a model number directly by setting a single parameter. However, Type1270 models a pure PCM. Hence, the PCM is assumed to undergo its freeze/thaw process at constant temperatures.

According to the TRNSYS TESS library [139], the PCM wall was split into two parts, each containing the standard wall layers located on one side of the PCM layer. The two walls are each set as a "Boundary wall" with the back side convection coefficient set to 0.0001 (direct contact) and the boundary temperature set to a user-defined input called T_PCM. The two walls' output "QCOMO" (NTYPE20) in TRNBuild was selected to give the energy flux that crosses each boundary wall's outside surface. Two energy inputs were taken from Type-56, and temperatures were computed for the PCM layer. The resulting temperature(s) was then passed back to the Type-56 as T_PCM input.

"In the engineering applications, the thermal contact resistance has an important effect on heat transfer design and operation of systems and devices..." [190]. "For general contact heat transfer, as long as the geometry, mechanics and boundary conditions are known, the steady thermal contact resistance of the interface will be unique, independent of theoretical prediction and experimental measurement methods..." [190]. In TRNBuild, setting the boundary wall with the back side convection coefficient to 0.0001 ensured that the surfaces were in direct contact [191].

In TESSLibs3-Mathematical Reference [177], type1270 mathematically is quite simplistic with the following assumptions:

- The specific heat of the PCM is constant in the solid state and another in the liquid state.
 Type 1270 simulates PCM behaviour assuming a constant temperature phase change method without taking into account the PCM hysteresis and variable thermal conductivity [192].
- ii). The thermal contact resistance to energy flow between the PCM layer and the standard adjacent material layers to it, is negligible.
- iii). The freezing or thawing process occurs at a constant temperature.

When the PCM material has fully frozen, the PCM temperature at the end of a time step is given by Equation (3-21):

$$T_{final} = T_{Initial} + \frac{Q_1 + Q_2}{m_{pcm}c_{p,solid}}$$
(3-21)

And when the PCM is fully thawed, the temperature at the end of a time step is given by Equation (3-22):

$$T_{final} = T_{Initial} + \frac{Q_1 + Q_2}{m_{pcm}c_{p,liquid}}$$
(3-22)

where Q_1 and Q_2 are the quantities of energy input in the PCM from the boundary wall layers, m_{pcm} is the mass of the PCM, $C_{p,solid}$, is the specific heat capacity at the solid-state of PCM and $C_{p,liquid}$, is the specific heat capacity of PCM in its liquid state. The final and initial temperature is equal when the PCM material is in the transition phase.

3.4.6 TRNSYS Kennel for Wall Configuration with and without PCM

The initial baseline simulation was performed without any PCM to determine the thermal performance of the building, and was performed under standard conditions to validate the model. Subsequent simulations with modified parameters, incorporating the PCM, were then compared against this benchmark to analyse improvements in thermal efficiency. Figure 3-2 and Figure 3-3 shows the TRNSYS simulation kennel used for a simulation without and with PCM in the wall configuration, respectively. The individual components are explained below.

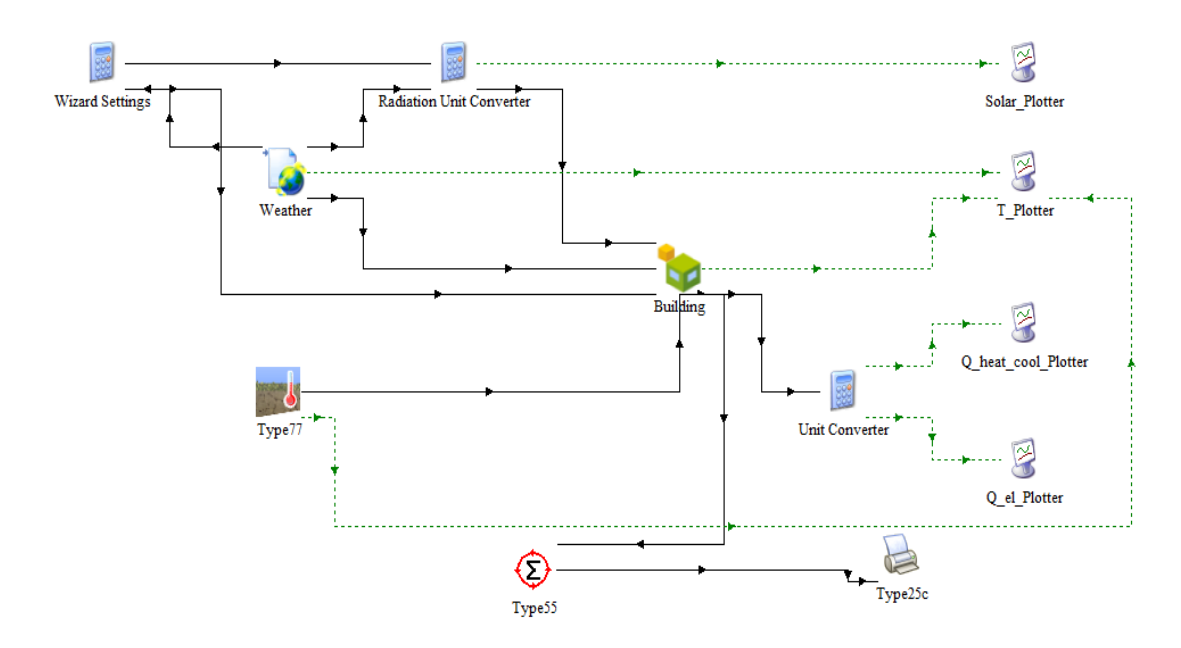


Figure 3-2 TRNSYS simulation components system layout without PCM

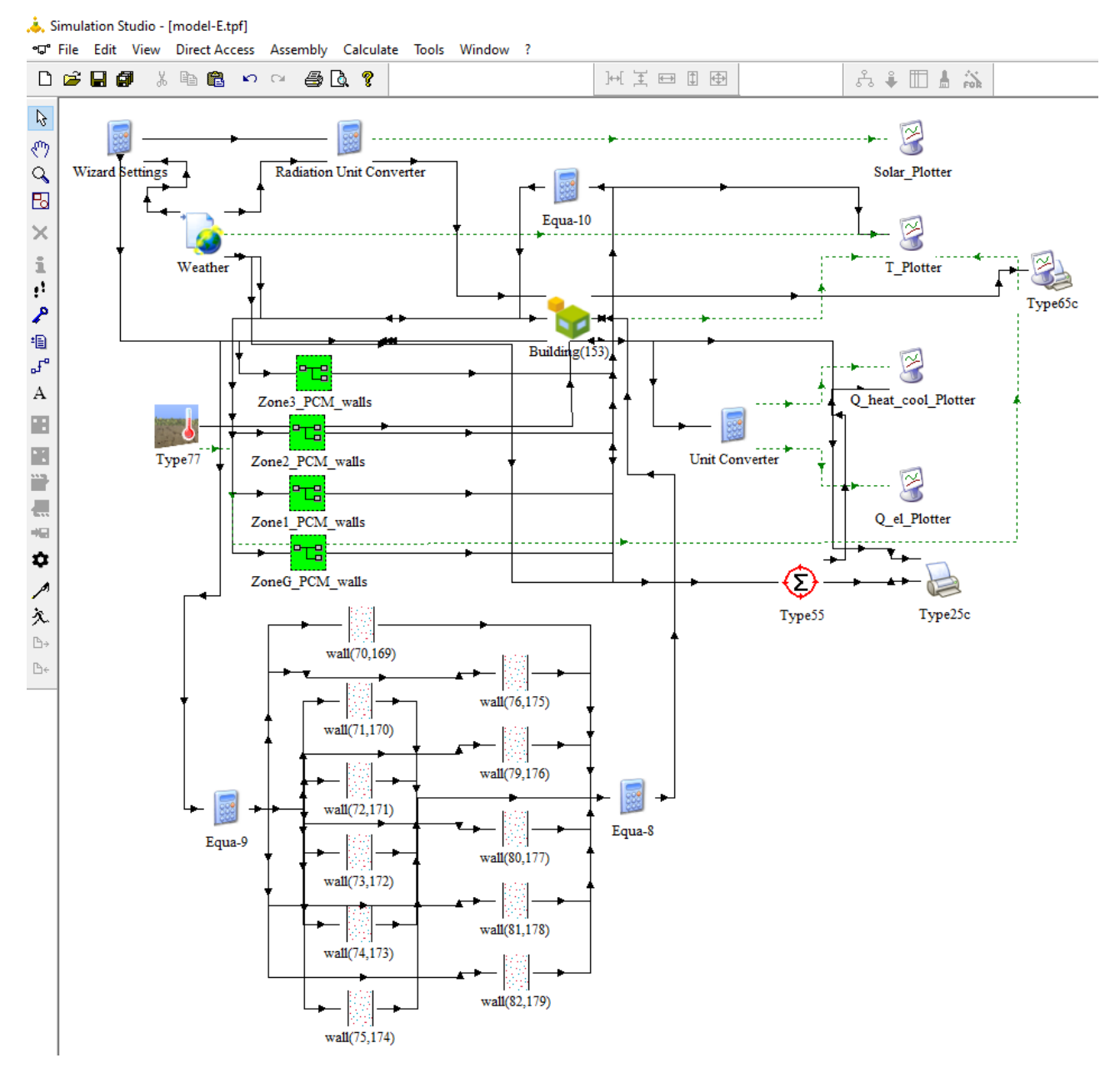


Figure 3-3. TRNSYS simulation components system layout showing macro and exploded PCM integration for five thermal zones

Figure 3-2 and Figure 3-3 show the TRNSYS simulation setup, illustrating various components, each serving a specific function, as described below:

Weather (Type 15-6)

As shown in Figure 3-2 and Figure 3-3, the weather component reads the weather data at regular intervals from the external weather data file, interpolating the data (including external temperature, solar radiation for tilted surfaces, etc) at timesteps of less than one hour and making it available to

other TRNSYS components within the simulation kennel [191]. The output from the weather data reader is the input to type-56 (the building).

Building (Type 56)

The weather data (UK London weather data in this case) is passed onto the model, Type-56 (building wall), as shown in Figure 3-2, a component that models the thermal behaviour of the building with multiple thermal zones. The building description is passed to the model as a building description file (*.b18, *.b17, *.bui) generated by the TRNBuild pre-processor program.

Type 77

This models the information about the vertical temperature distribution information of the ground given the mean ground surface temperature for the year, the amplitude of the ground surface temperature for the year, the time difference between the beginning of the calendar year and the occurrence of the minimum surface temperature, and the thermal diffusivity of the soil [177]. This information is passed to the building (Type 56) for modelling.

The Periodic Integrator Type 55

This component takes on the output from type-56 (the building) and calculates the count, mean, sample standard deviation, sum of squares, variance, minimum, time at which the minimum occurs, maximum, and time at which the maximum occurs of a series of INPUTS over a range of time periods specified by the user [191]. The component will calculate the integral of the INPUT with respect to the time of year or the sum of the INPUT over the year. It is set to start the simulation at the start of the year

- relative starting hour for input = 0
- duration for input repeat every month = -1
- cycle repeat time for input = -1
- Reset time for input = -1
- Absolute starting hour for input = 0
- Duration of simulation = 1 year (8760 hrs)

Type 65 online plotter

It is an online graphics component that displays (plots) selected system variable outputs from Type-

56 as the simulation progresses, providing variable information. The selected variables are displayed in a separate plot window on the screen. In this instance of the Type 65 online plotter, no output data file is generated.

Type 25c

This online output printer component outputs (or prints) selected system variables at specified time intervals. The output can be printed in even intervals relative to the simulation start time or absolute time. The output data is stored and accessed through the external files "**.out" extension file and can be exported to other applications like excel, for data analysis.

Equation editor (Equa)

The 'Equa' component assists in creating custom equations to calculate new values within the simulation and unit conversations. It also enables the definition of constants and conditions to manage the simulation's behaviour.

TRNSYS applications

Some of TRNSYS applications include [193]:

- Solar systems
- Low energy buildings and HVAC systems with advanced design features (natural ventilation, slab heating/cooling, double facade, etc.)
- Renewable energy systems
- Cogeneration, fuel cells
- Dynamic simulation applications

3.5 Experimental Method

The experimental method involved constructing and testing physical wall prototypes to validate simulation results and identify the optimal PCM positioning for energy savings and thermal regulation.

Baseline Experimental Investigation

The objective of the baseline experiment was to construct a wall prototype without PCM to

determine its thermal performance experimentally. The data collected from this setup was then used to validate the baseline simulation model by comparing the experimental results with the simulation outputs.

PCM Integration and Testing

In the ensuing phase, a wall prototype was constructed with PCM integrated at various positions to identify the optimal PCM placement for energy savings and indoor temperature regulation. The prototype's thermal performance was carefully monitored, focusing on indoor stability and wall layer temperatures. These results were then compared with simulation data to validate the findings and refine the PCM placement strategy.

PCM Integration with Glazed Window

To explore more realistic conditions, a wall prototype was constructed that included a double-glazed glass window along with PCM integration at different positions. This setup replicated real-world building scenarios, allowing for a comprehensive assessment of the PCM's thermal performance. The experimental results were used to validate the corresponding simulation model and determine the most effective PCM configuration. The optimal PCM placement derived from this experiment was then applied in a full-building simulation for energy analysis, with the outcomes referenced to the measured energy consumption data from 2019 to assess the benefit of PCM integration.

3.5.1 Building Models and Configurations

a) Experimental investigation of a wall prototype in Victorian-era buildings

A detailed model of a Classic Multi-Layered Victorian-era building wall was created to reflect typical construction materials. Figure 3-4, shows a schematic representation of a wall with multiple layers and integrated PCM. The PCM was placed at different positions (x) from the external wall surface to study its thermal behaviour. The wall consisted of various layers (labelled 1 to 9), including an air gap, replicating a typical building wall's structural wall. The outside surface was exposed to external conditions, and the indoor environment was maintained by a heater, simulating internal heat sources. The heat transfer coefficients $h_i = 7.7 \text{ W/m}^2\text{K}$ for the inside and $h_o = 25 \text{ W/m}^2\text{K}$ for the outside are constants representing the assumed steady-state heat exchange between the wall surfaces and their respective environments. Heat flux (q) and temperature distribution (T) were considered along the wall layers.

A data logger was connected to a computer to monitor the temperature profile across the wall in real time. This setup helped to evaluate the influence of PCM placement on thermal regulation and energy performance within the wall assembly. The large arrows in Figure 3-4 illustrate the direction of heat transfer through the wall layers.

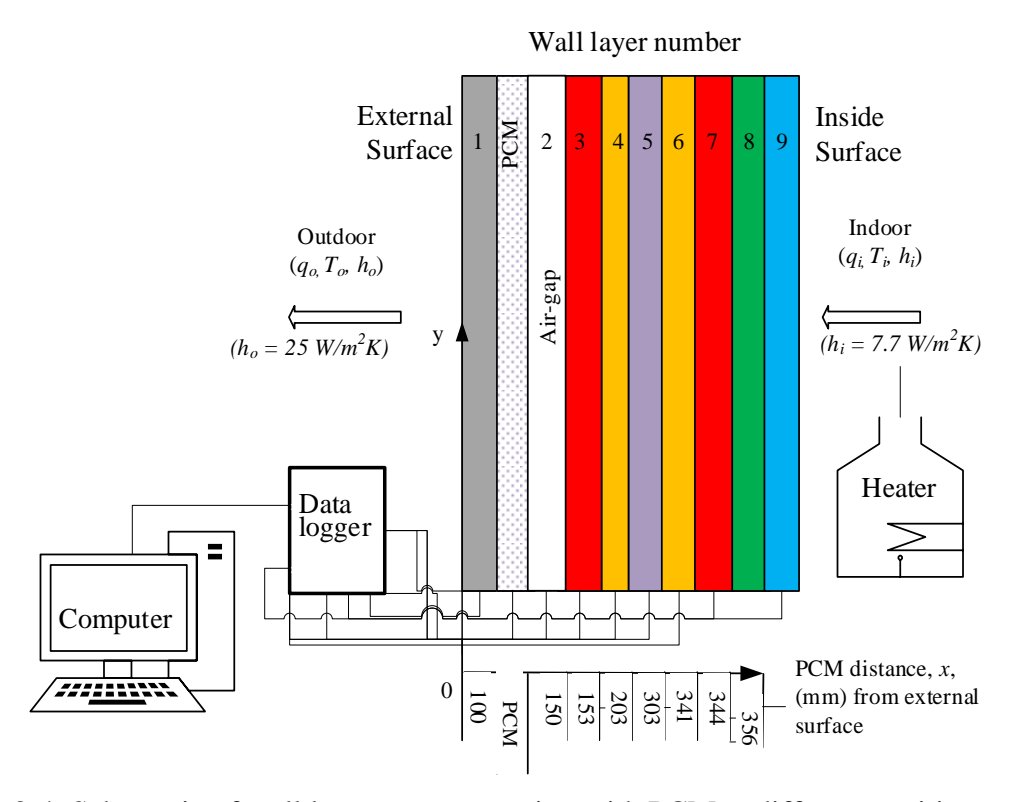


Figure 3-4. Schematic of wall layers representation with PCM at different positions, *x*, from the external wall surface.

where 1,2,3, etc, are layers:

- 1. 100mm Concrete blockwork
- 2. 50mm Air gap
- 3. 3mm Vapour barrier
- 4. 50mm Kingspan Kooltherm, K118, cavity board
- 5. 100mm Concrete blockwork
- 6. 38mm Kingspan Kooltherm, K112, cavity board
- 7. 3 mm vapour barrier
- 8. 12.5mm Fermacell gypsum fibre board
- 9. 12.5mm Fermacell gypsum fibre board

Only a portion of the wall was considered for the computation, as shown in Figure 3-4. The thickness (mm) of the different materials are given as l_1 , l_2 , ..., l_9 , q is the heat flow (W/m².K), h is the

convective heat transfer coefficient, $(W/m^2.K)$, and T is the temperature. Subscripts, o, i, represent outdoor and indoor environments. The wall layer material properties are shown in Table 3-1.

Table 3-1. Thermophysical Properties of the Different Layers of the Wall Construction

Layer	Layer name	Thickness,	Conductivity,	Resistance, R,	Density	Specific Heat
		<i>x</i> (m)	k, (W.m ⁻¹ .K ⁻¹)	$(\mathbf{W}.\mathbf{m}^{-2}.\mathbf{K}^{-1})$	(kg.m ⁻³)	$(kJ.kg^{-1}.K^{-1})$
1	Outer block	0.100	1.400	0.071	1400	1.000
2	Airgap	0.050	0.024	2.083	1.200	1.005
3	Vapour -barrier	0.003	0.200	0.015	161.1	1.200
4	Outer-Kingspan	0.050	0.021	2.381	40.00	1.400
	(K118) in studs					
5	Inner block	0.100	1.400	0.071	1400	1.000
6	Inner-Kingspan	0.038	0.021	1.810	40.00	1.400
	(K112					
7	vapour-barrier	0.003	0.200	0.015	161.1	1.200
8	Outer-Gypsum	0.125	0.170	0.740	950.0	0.840
	board					
9	Inner-Gypsum	0.125	0.170	0.740	950.0	0.840
	board					

b) Experimental investigation of a PCM wall prototype with integrated windows in modern office buildings

A detailed prototype model of an office building with a multi-layered wall integrated with a double-glazed glass window was created, reflecting typical construction materials. The model and the experimental layout included multi-layered walls with PCMs positioned at various depths to assess their impact on energy performance, as shown in Figure 3-5.

Figure 3-5, shows a schematic representation of a prototype wall integrated with a double-glazed glass window, along with PCM layer positioned at different distances (x) from the external wall surface. The wall was composed of multiple layers (labelled 1 to 9), including an air gap, replicating a typical structure of building walls. The setup included an outside surface exposed to outdoor conditions, represented by outdoor heat flux (q_o) and temperature (T_o) . The heat transfer coefficient for the outside $(h_o = 25 \text{ W/m}^2\text{K})$ and the inside $(h_i = 7.7 \text{ W/m}^2\text{K})$ were assumed constants reflecting the assumed steady-state conditions. A heater was used to simulate internal heat sources to maintain the indoor environment.

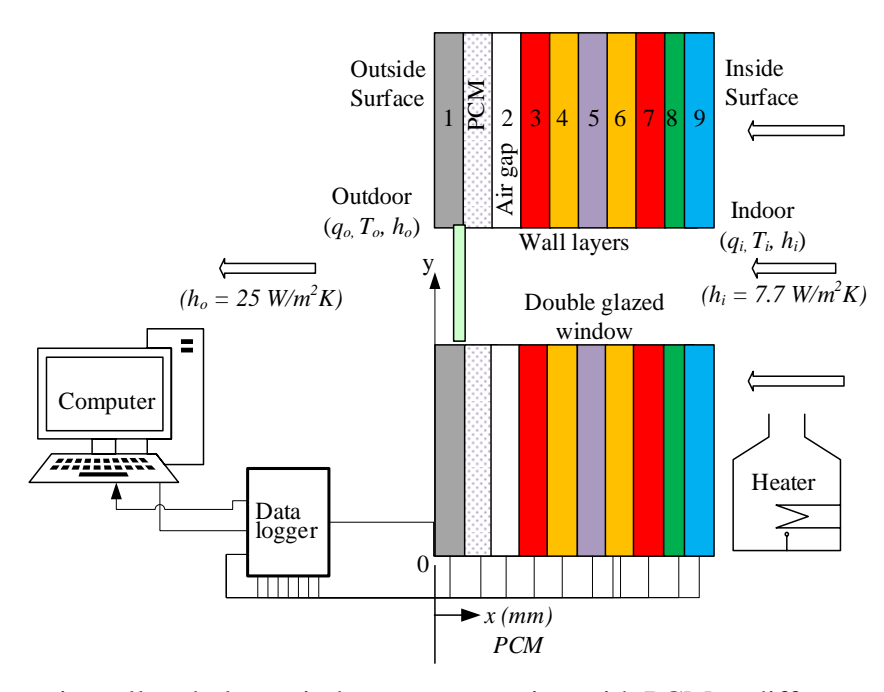


Figure 3-5. Schematic wall and glass window representation with PCM at different positions, x, from the external wall surface.

A data logger, as shown in Figure 3-5, was connected to a computer to monitor real-time temperature changes across the wall layers with PCM embedded at different positions (*x*). The large arrows in Figure 3-5 show the heat transfer direction through the wall, and including a double-glazed glass window allowed for the analysis of its impact on thermal performance. This experimental design was employed to evaluate the effects of PCM placement and the window on indoor temperature control, energy savings, and the overall thermal behaviour of the building envelope.

3.5.2 Selection of Phase Change Material (PCM) and Properties

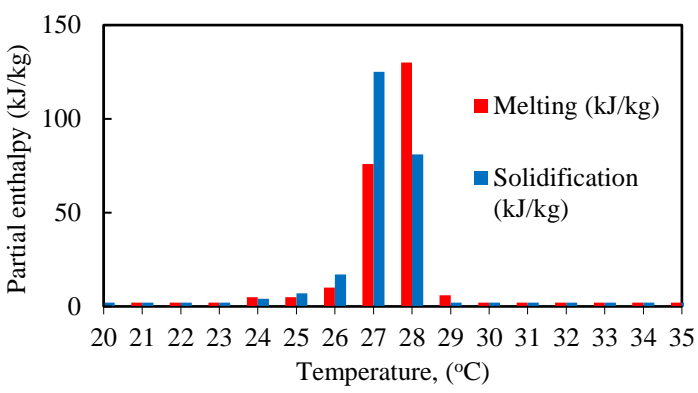
A specific type of PCM, RT28HC PCM, enclosed in macro aluminium with a thickness of 15mm and featuring a phase change temperature range from 27°C to 29°C, was selected for its high heat storage capacity.

Table 3-2. PCM properties

PCM	Thickness, (mm)	Conductivity, k (kJ/h.m.K)	Phase change temp (°C)	Density (kg/m³)	Specific Heat (kJ/kg °C)	Combined latent & sensible heat storage
						capacity (kJ/kg)
RT28HC	15	0.2	27-29	0.88(s)	2.0	250
				0.77(l)		

This paraffin-based organic PCM [83] was provided by Rubitherm Technologies [194] and was used without any modification. The specific properties of the PCM are listed in Table 3-2. The PCM and supplied manufacturer's PCM data are shown in Figure 3-6.





- (a) macro aluminium casing
- (b) RT28HC Enthalpy-temperature curve [165]

Figure 3-6. PCM Manufacturer's specifications. (a) PCM packaging, (b) PCM Enthalpy Vs temperature curve

The decision to employ RT28HC PCM with a phase change temperature of 27°C was made based on several key considerations so that made this material is more suitable for this study than lower melting point PCMs. First, RT28HC has a higher heat storage capacity, as shown in Table 3-2 critical for achieving significant energy savings in larger applications such as building retrofits. Lower melting point PCMs, commonly packaged in plastic containers and used in small applications like the food industry, were not ideal for this project due to their limited thermal capacity, packaging and availability.

Additionally, where PCM wallboards with lower phase change temperatures are available, these are notoriously susceptible to the hysteresis effect [124], which can cause inconsistent phase transitions and reduce the PCM's effectiveness. There was also a practical constraint regarding the availability of PCM wallboards in the UK. At the time of material procurement, UK-based PCM manufacturers confirmed that they do not produce PCM wallboards, and ordering such materials would have involved long lead times, potentially delaying the study. To overcome these constraints, RT28HC was considered since, it has a demonstrated strong performance in the existing literature [195, 196, 197], and was available in Europe. The PCM of RT28HC was enclosed in macro aluminium modules by the manufacturer for increased heat transfer efficiency, and therefore, these were set up as flat boards for the experimental work.

3.5.3 Standardised Wall Model for PCM Integration in Heritage and Contemporary Buildings

To validate this research's applicability to Victorian-era and modern office buildings, a standard multi-layered wall structure was developed to serve as a representative model for these distinct building types. The wall consisted of an air gap, insulation, block layers (for the baseline structure), and a PCM layer designed to replicate the retrofitted walls of historical buildings and the cavity wall systems found in contemporary office structures. For Victorian-era buildings, the model simulates scenarios where insulation or PCMs are integrated to enhance energy efficiency while maintaining the architectural integrity of the design. In contrast, for modern office buildings, especially those incorporating windows, the model reflects the use of PCMs to optimize thermal regulation during an initial construction.

The use of a unified wall structure enabled a direct analysis of PCM behaviour, including phase change temperature and heat transfer characteristics, across both contexts. This approach ensures consistency in evaluation while addressing the material and construction differences between the two building types. Victorian buildings often use solid, thick masonry walls, while modern offices typically employ lightweight, layered systems. Despite these differences, the standardised wall design captures the essential elements of PCM performance, allowing the results to be interpreted for both settings.

The findings will validate the relevance of PCM integration for retrofitted historical structures and contemporary office designs, demonstrating energy-saving potential in each application. While historical materials differ significantly from modern ones, the study's methodology ensures that the results provide transferable insights. This applicability highlights the versatility of PCM systems in improving energy efficiency and occupant comfort across diverse architectural styles. Additional clarification and detailed results are included in this thesis to illustrate the relevance of this research to both scenarios outlined in the objectives.

3.6 Data Collection and Analysis Techniques

The data collection and analysis techniques were designed to ensure the finding's accuracy, reliability, and applicability. By integrating robust data collection methods with advanced analysis techniques, valuable insights into the optimal use of PCMs in building envelopes to enhance energy efficiency and thermal comfort could be provided.

3.6.1 Data Collection Methods

Simulation data collection

Data from the TRNSYS-developed models was collected, focusing on key outputs such as inside wall surface temperature, room operative temperature, energy consumption metrics (heating and cooling loads), and thermal comfort indices, including Predicted Mean Vote (PMV) and Predicted Percentage of Dissatisfied (PPD). For each simulation scenario: baseline, PCM integration at different positions, and PCM integration with a double-glazed window, the data was logged and organised for a further analysis.

Experimental data collection

Experimental wall prototypes constructed for corresponding PCM placements were tested under controlled environmental conditions. Temperature sensors placed within the wall assembly linked to data loggers recorded real-time data on temperature variation across wall layers. The setup enabled continuous monitoring of temperature profiles, and energy usage was calculated.

Validation and cross-referencing

The data collected from the experimental prototypes was used to validate the simulation models. Comparisons between the experimental and simulated data were made to ensure the accuracy and reliability of the simulations. Any discrepancies were analysed to refine the models and improve their predictive capabilities.

3.6.2 Data Analysis Techniques

Quantitative Analysis

All sets of data collected from simulations and experiments were subjected to statistical analysis. Techniques such as Mean Absolute Error (MAE), Mean Absolute Percentage Error (MAPE), Root Mean Square Error (RMSE) and Correlation Analysis were used to identify significant trends, correlations, and the effects of PCM positioning on energy consumption and thermal comfort.

Heat transfer rates were analysed to understand the impact of PCM integration on the building envelope's thermal performance. The effectiveness of different PCM positions was evaluated by comparing the heat flux data across various wall configurations.

Energy savings were calculated by comparing the total energy consumption in the baseline scenario with that in the PCM-integrated scenarios. The percentage reduction in heating and cooling loads was determined to quantify the energy efficiency improvements.

Comparative Analysis

Two types of analyses have been conducted. Scenario comparative analysis was conducted across different PCM placements within the wall prototypes. The analysis was focused on identifying the position that provided the optimal balance between energy savings, thermal comfort, and practical implementation. Full building simulation comparison of the optimal PCM position identified from the prototype studies simulated the entire building's energy performance. The results were referenced against actual energy consumption data from 2019 to assess the effectiveness of the PCM integration in real-world conditions.

Validation and Refinement

The simulation models were refined to improve their accuracy by comparing simulated and experimental data. This iterative process ensured that the models could reliably predict the performance of PCM-integrated building envelopes under various conditions. Using the validated models, predictive equations and algorithms have been developed to guide the optimal placement of PCMs in building designs. These models considered wall thickness, climate conditions, and building type to provide tailored recommendations for PCM integration.

3.7 Project and Building Description

The redevelopment of CHASE FARM HOSPITAL (Enfield, North London, UK) was a major project, (Figure 3-7 and Appendix 1 to Appendix 7), that consisted of the construction of a five-storey new heated-ventilated and air-conditioned (HVAC) hospital building following the merger of ROYAL FREE LONDON NHS Foundation Trust with BARNET and CHASE FARM HOSPITAL NHS Trust [198]. The hospital comprises an Urgent Care Centre, Inpatient elective surgery and rehabilitation beds, a Surgical centre incorporating a four table 'Barn' operating theatre, four stand-alone operating theatres, Imaging, Diagnostics, Endoscopy, Chemotherapy and supporting facilities. As opposed to the traditional hospital design criteria, it was desired to make the building less like a hospital and more like a 'hotel' [199]. The wards are located on the top floor of the building, and every room benefits from an outward-facing view, either in the countryside or over the distant city of London.

The development sits between a new housing development and the remaining old hospital facilities. The structural building comprises a load-bearing concrete/steel skeleton and a drywall system.

The main building relies on electricity from the national grid as its primary power source. The building's central heating is provided by Low-Temperature Hot Water (LTHW), which is generated by steam boilers and a central gas-fired Combined Heat & Power (CHP) system that operates continuously and is located in the Energy Centre (EC). Plate heat exchangers achieve an LTHW operating band of 80°C flow and 55°C return through the installed flow and return pipework. Chilled Water (CHW), generated by chillers in the energy centre and LTHW, circulates through the pipework routes and 'tees-off' to serve the Air Handling Unit's (AHU) frost and heating coils, thereby supplying heated or cooled air to the occupants' space. The Combined Heat & Power (CHP) operates on gas, generating both electricity and heat for the LTHW to supplement the building's energy demand while also powering the chilled water plant, contributing to high energy costs for the building's operation. Therefore, it is necessary to develop innovative ways to reduce the hospital's energy consumption. Such innovations could include using energy-storing materials like PCMs that can store and release energy when embedded in multi-wallboards.



Figure 3-7. CHASE FARM HOSPITAL (Enfield, North London, UK) project

The installed Heating, Ventilation and Air Conditioning (HVAC) system is designed to provide thermal comfort for occupants. The HVAC system includes heating, ventilation, and cooling or air-conditioning equipment. Depending on thermal comfort demand, outdoor air is drawn into the

building and heated or cooled before it is distributed into the occupants' spaces; it is then exhausted to the external ambient air or reused in the system [200, 201]. This is achieved by LTHW and CHW generated by boilers and chillers circulating in heating and cooling coils, in which heat is exchanged. Humidity is regulated by ventilation, and dehumidification is provided by cooling air, which reduces the amount of moisture the air can hold, resulting in reduction of condensation.

3.7.1 Challenges and Opportunities for Hospital Energy Efficiency: A Focus on Chase Farm Hospital

A Building Energy Management System (BEMS) monitors, manages and controls building services and plants, ensuring it operates at maximum levels of efficiency and reliability. It does this by maintaining the optimum balance between conditions, energy use and operating requirements [202]. BEMS controls Chase Farm Hospital's HVAC from a centrally managed location, which enhances the ability to interact with and improve the quality of the data centre infrastructure. The system intelligently understands and responds to patterns of usage by fully optimising some services like lighting and will turn off in unoccupied areas [198]. The individual room temperature is pre-set and managed by this system, but occupants can change their temperature requirements, though only limited to $\pm 5^{\circ}$ C.

In the winter, when the indoor temperature is much greater than the outside temperature, heat loss tends to be from inside to the outside through the walls and windows, and vice versa in summer, when the outdoor temperature is much higher than the indoor temperature. The BEMS responds accordingly and create a demand for the LTHW or chilled water, as required. However, it is suggested that applying PCMs in the multi-wallboard could significantly reduce the demand for indoor temperature stabilisation. There is always a trade-off between efficiency improvement and cost reduction in energy conservation. Li et al [203] state that natural working carbon dioxide (CO₂, R744) has attracted the widest attention for the next-generation energy systems to tackle climate change due to its extraordinary thermophysical properties and environmental friendliness of zero, non-toxicity, and non-flammability. For most commercial buildings, targeted applications include standalone refrigeration systems, heat pumps, power generation systems, and cogeneration systems by integrating the cooling, and/or heating, and/or power subsystems to meet various demands [203].

Exploring the thermo-economic analysis is necessary to improve energy conservation and reduce the CO₂ of commercial buildings.

Therefore, there is a need for energy efficiency and/or an obligation to generate power using industrial waste heat and renewable energy [204], to save costs, especially for the struggling National Health Service (NHS). Hence, the government and the NHS continue to put considerable work into offsetting the financial gap, which calls for spending cuts. The current cuts in NHS's capital budget mean that [205];

- Hospitals no longer afford the most modern scanners and surgical equipment to treat patients who have cancer and other diseases.
- The ambulance services are breaking down after being kept in service for too long.
- Some NHS Trusts have scrapped plans to:
 - ✓ Introduce electronic scheduling of operations due to the unaffordability of technology.
 - ✓ Expand Accident and Emergency (A&E) units to cope with rising patient numbers.
 - ✓ Repair rotten windows and leaking roofs in hospital buildings, but shrink the hospital size and transfer vital services to regional referral units, leaving locals prone to fatalities in emergencies.

According to the NHS website, "The NHS' 10 Point Efficiency Plan," [206], states that "...the NHS also needs to protect and improve its estates and facilities. Facilities management has a direct bearing on patient experience, for instance, by ensuring that premises are safe, warm, and clean environments for staff and patients and by preparing high quality and nutritious hospital food...". Therefore, exploring opportunities that may help reduce energy consumption and improve patients' comfort and experience of ward space, theatres, laboratories, and other general communal areas is necessary.

3.8 Research Questions/Hypotheses

The research questions and hypotheses have been developed and are designed to guide the investigation into the application of PCMs across different building types. They aim to uncover significant findings that contribute to energy conservation and sustainable building practices. These are outlined as follows:

i. How effective is an integration of PCMs in reducing energy consumption in Victorian-era buildings while preserving their historical and architectural integrity?

Hypothesis 1:

An integration of PCMs into multi-layer walls in Victorian-era buildings significantly would reduce energy consumption without compromising the buildings' historical and architectural features.

ii. Can the application of PCMs in the cavity walls with integrated windows of modern hospitals or office buildings lead to substantial energy savings and improved thermal performance?

Hypothesis 2

PCM-enhanced cavity walls with integrated windows in modern hospital or office buildings would result in significant energy savings and enhanced thermal performance compared to conventional building designs.

iii. What will be the optimal configuration of PCM within walls and integrated windows to maximise energy efficiency in different building types?

Hypothesis 3

The optimal PCM configuration within walls and windows would vary depending on the building type, with customised configurations leading to maximised energy efficiency in historic and modern structures.

iv. How would the simulation results for PCM applications compare to experimental findings in terms of accuracy and reliability?

Hypothesis 4

The simulation results for PCM applications would be proven consistent with experimental findings, demonstrating the accuracy and reliability of simulation models in predicting real-world performance.

v. What practical guidelines can be developed to effectively incorporate PCM-drywalls in building upgrades or new constructions to align with energy efficiency targets and sustainability goals?

Hypothesis 5

Practical guidelines developed from this research would enable the effective incorporation of PCM-drywalls in various building types, supporting energy efficiency targets and sustainability goals, including those outlined in the DESNZ UK energy strategy and Europe 2050 targets.

3.9 Ethical Considerations

This study adhered to ethical standards by ensuring that all experimental procedures are conducted safely and comply with relevant building codes and regulations. Privacy and confidentiality have been maintained for any data involving real buildings or occupants. At present, there are no ethical concerns.

3.10 Summary

This chapter has detailed the research methodology for evaluating PCM integration in building envelopes. The Research Design outlined the framework, while the Theoretical and Numerical Background provided foundational heat transfer principles and governing equations. The Simulation Framework demonstrated the use of TRNSYS and TRNBuild for modeling PCM performance, complemented by robust validation methods.

The Experimental Methodology described constructing and testing scaled models, integrating PCM layers and windows to replicate real-world conditions. Data collection and analysis techniques ensured robust interpretation of results, while the Project and Building Description provided practical context. Ethical considerations emphasized transparency and reliability. This chapter establishes a rigorous framework for assessing PCM's impact on energy efficiency and thermal comfort.

CHAPTER 4: SIMULATION FRAMEWORK AND RESULTS OF PCM INTEGRATION IN MULTI-LAYER WALLS

4.1 Introduction: Simulation for Thermal Performance Analysis

This chapter presents a detailed analysis of building energy performance through simulation, focusing on integrating Phase Change Materials (PCMs) within wall assemblies. Using TRNSYS software, dynamic simulations evaluated how different PCM positions influence thermal performance, energy efficiency, and occupant comfort. Numerical methods have been employed to solve heat and mass balance equations over time, capturing the transient behaviour of heat transfer in both PCM-enhanced and non-PCM wall configurations. Key simulation parameters include internal wall surface temperature, room operative temperature, heat transfer rate, Predicted Mean Vote (PMV), and Predicted Percentage of Dissatisfied (PPD). These parameters have been analysed across different PCM placements to identify the optimal positioning for reducing energy consumption and improving indoor thermal comfort. The findings from these simulations are critical for informing future designs and applications of energy-efficient building systems, providing insights into the dynamic interaction between PCM layers and overall building thermal behaviour.

The chapter progresses from baseline simulations without PCM to increasingly complex configurations, incorporating various PCM placements and their impact on thermal metrics. The results comprehensively show how PCM influences energy demand across different seasons and room conditions. A detailed exploration of these trends, supported by data from both short-term (48-hour) and long-term (annual) simulations, is presented in the later part of the chapter.

4.2 Building Model Description

a) A typical building model

A typical building model was set up in the northern hemisphere to compute the correct azimuth angles of surface orientations and included 3D geometric surface information, which was input into the model using "TRNSYS 3D" for Google SketchUp, as shown in Figure 4-1. The interior walls comprised the six Trnsys3D zones (lower ground - LG, ground - G, first floor - Zone1, second floor - Zone2, third floor - Zone3, and fourth floor - Zone4) to simulate the dynamic energy flow [191].

Detailed floor plans are shown in Appendix 1 to Appendix 7). TRNSYS 3D surfaces are assumed to be in line of sight with all other surfaces of the zone or convex [179]. The interzonal adjacencies were also considered with mating surfaces between zones linked together. For two surfaces to match, both must have the same number of vertices and have the vertices lined up. Furthermore, construction names of the matched surfaces were changed in the software (for each corresponding surface or subsurface type) to: "ADJ_CEILING" (adjacent ceiling) and "ADJ_WALL" (adjacent wall) for construction objects of those names which appear in the current *.idf* file. The IDF file was saved by choosing Plugins -> TRNSYS 3D -> save, from the main menu within the SketchUp environment [191].

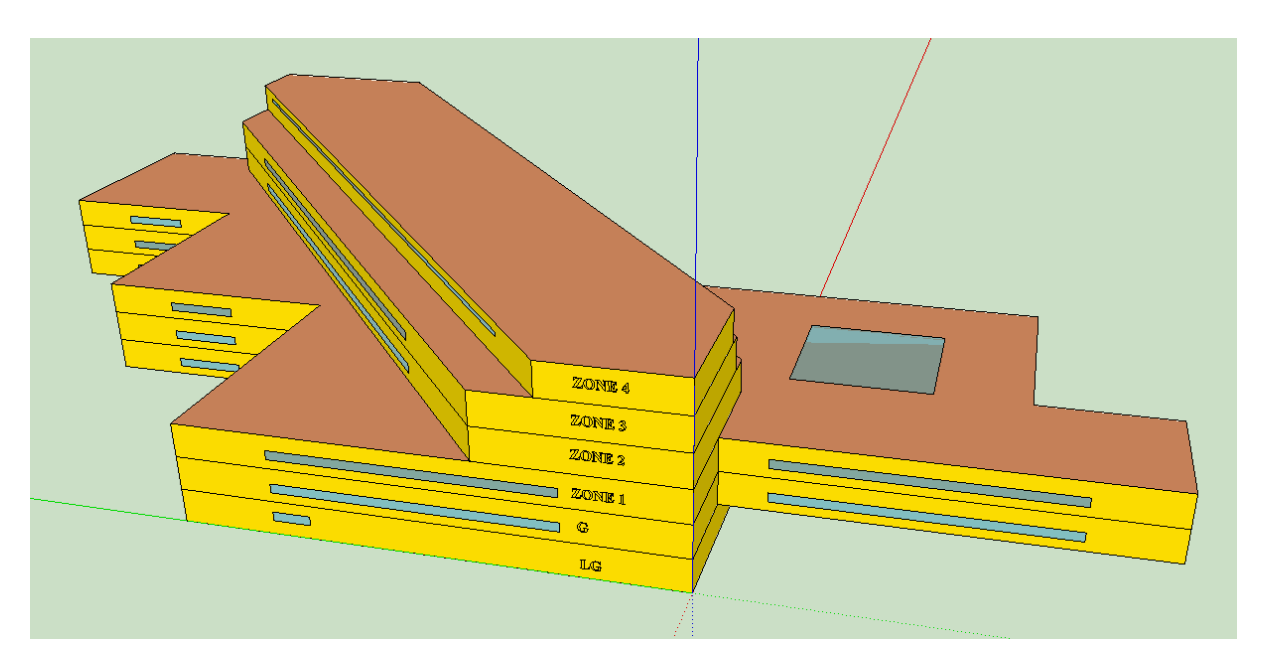


Figure 4-1: Trnsys3d building model for simulation

The building's metrological data

London metrological data (Lat 51.15°N, Lon -0.02°E) with an elevation of 77 meters was used in the TRNSYS simulation software as the external weather file GB-London-weather-C-37790.tm2 to study the weather conditions.

b) Construction types in trnsys

In TRNBuild, the construction types must be specified. Here, all the layers used by the opaque surface constructions (walls, floors, ceilings, roofs) and windows are listed [191]. The construction types used for this project included:

- EXT_WALL (External wall)

- ADJ_WALL (Adjacent wall)
- ADJ_CEILING (Adjacent ceiling)
- GROUND_FLOOR
- EXT_ROOF (External roof)
- EXT_WINDOW (External Window)

EXT_WALL (External wall) construction ranges from the "outside" (back) surface, which is exposed to ambient conditions, to the "inside" surface (front) of the wall, as illustrated in Table 4-1. The thickness of each material layer was specified using the building design, and TRNBuild calculated the total wall thickness and the standard U-value. The standard U-value was determined with combined heat transfer coefficients of 7.7 W/(m² K) inside and 25 W/(m² K) outside.

Table 4-1. EXT_WALL "Construction Type" Manager

Front (Inner surface)				
Layer number	Layer name	Thickness, x (m)	Type	
9	Inner-Gypsum board	0.0125	Massive	
8	Outer-Gypsum board	0.0125	Massive	
7	vapour-barrier	0.003	Massive	
6	Inner-Kingspan (K112	0.038	Massive	
5	Inner block	0.100	Massive	
4	Outer-Kingspan (K118) in studs	0.050	Massive	
3	Vapour -barrier	0.003	Massive	
2	Airgap	0.050	Massless	
1	Outer block	0.100	Massive	
Back (Outer surface). Wall thickness = 0.369 (m) without PCM, with PCM = 0.384 (m)				

c) Building daily occupancy schedules

Internal energy gains [178], lights, people, and equipment must be considered in relation to the building's associated occupancy time. Figure 4-2, shows the building's assumed occupancy schedule. This was based on the building being occupied by most people between 0800 and 1800. This was halved between 1800 and 2200, while a few patients, night-shift nurses, cleaning, and security staff stayed overnight from 2200 to 0800.

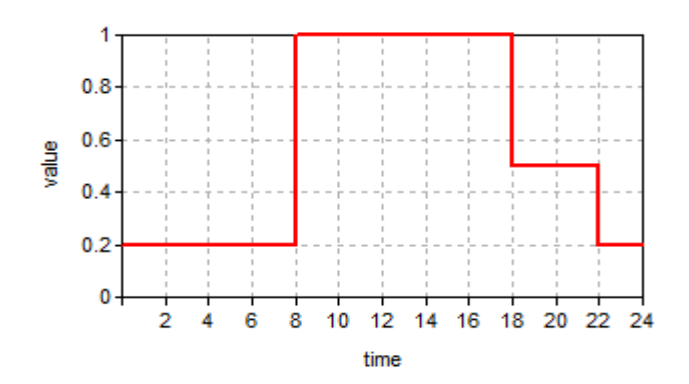


Figure 4-2: Daily Building Occupancy Schedule [178]

d) Ceiling, ground floor and side wall layout

The ceiling composition detailed in the Table 4-2 consists of a multi-layer structure designed to enhance thermal performance and energy efficiency. The inner lining was composed of a gypsum board, which provides a smooth finish, basic insulation, and fire resistance. Adjacent to this was an air gap, serving as an insulating buffer to minimise heat transfer. Following this was a layer of kingspan insulation, which significantly reduces heat loss through the ceiling. The outermost layer was another layer of gypsum board, which further reinforces insulation properties, contributing to overall energy efficiency by minimising heat loss through these surfaces.

Table 4-2 Ceiling Layout

	Layer name	Conductivity	Specific Heat	Density	Thickness	Resistance, R,
		k, (W.m ⁻¹ .K ⁻¹)	$(kJ.kg^{-1}.K^{-1})$	(kg.m ⁻³)	x, (m)	$(\mathbf{W}.\mathbf{m}^{-2}.\mathbf{K}^{-1})$
1	Gypsum_board	0.170	0.840	950.0	0.125	0.740
2	Airgap	0.024	1.005	1.200	0.050	2.083
3	Insulation, K112	0.021	1.400	40.00	0.038	1.810
4	Gypsum_board	0.170	0.840	950.0	0.125	0.740

e) Energy gains/loss type based on the occupancy schedule

In building energy simulations, internal gains from lighting, people and electrical equipment significantly influence the building's thermal load. Since these gains fluctuate throughout the day, occupancy schedules were employed in the model to capture these variations accurately. The conservation energy gains/loss for different internal sources were expressed through equations that account for the daily occupancy in TRNBuild [191].

- Convective energy gain/loss due to lights, Q_LIGHTS, is given as follows in Equation (4-1).

$$Q_{LIGHTS} = 3600 * Daily_Occupancy_schedule$$
 (4-1)

This equation determines the energy contribution from lighting based on the occupancy schedules.

- Convective energy gain/loss due to people, Q _PEOPLE is given by Equation (4-2).

$$Q_{PEOPLE} = 720 * Daily_Occupancy_schedule$$
 (4-2)

This equation quantifies the convective energy gain from occupants, reflecting how people's presence contributes to the building's heat.

- Convective energy gain/loss due to Electrical equipment, *Q_EQUIPMENT*, is given Equation (4-3).

$$Q_{EQUIPMENT} = 1000 * Daily_Occupancy_schedule$$
 (4-3)

This equation accounts for the heat generated by electrical equipment, adjusted according to the daily schedule of equipment use.

f) Infiltration

This is the rate at which ambient air infiltrates the building through cracks and crevices. Infiltration is wind speed-dependent and will affect the coupling between the zones. It is assumed that 100 kg/hr of air flows between adjacent zones. The wind speed relationship to the infiltration rate is shown as follows [191]:

$$Infiltration = 0.07 * V_{WIND} + 0.4 \tag{4-4}$$

where V_{WIND} is the wind velocity, a weather input to the building model.

g) Heating and cooling loads

Room temperature control: 26°C – 30°C

The chosen temperature range of 26°C to 30°C ensures that the PCM's phase change temperature of 27°C is consistently attained, optimising its thermal storage and release properties. This range aligns with temperature conditions in specific hospital environments such as neonatal intensive care units (26°C–29°C) [207, 208], hydrotherapy rooms (27°C–29°C) [209], swimming pools (28°C–30°C) [210], and physio-therapy/fitness centres or gyms [211], where controlled thermal conditions are essential for patient care and comfort.

- Heating: A set temperature of 26°C has been specified in the heating regime (HEAT001) for unlimited power
- Cooling: A set temperature of 30°C above which cooling is activated has been specified in the cooling regime (COOL001).

h) Outputs from TRNBuild

The output from TRNBuild are summarised in Table 4-3, showing a variety of parameters, QCOMO for instance is the convective heat transfer mode to handle the PCM, which is discussed in detail in the next section. QCOMO was significant for accurately simulating the energy performance and thermal comfort in building environments modelled in TRNSYS.

Table 4-3: Main TRNBuild Outputs Used in the Project

No	Name	Unit	Description
1	TAIR	С	Air temperature of the zone
2	TOP	C	Operative room temperature
3	TSI	C	Inside surface wall temperature
4	QHEAT	kJ/hr	Sensible heating demand of zone: heating (positive values)
5	QCOOL	kJ/hr	Sensible cooling demand of zone: heating (positive values)
6	QELEQUIP	kJ/hr	Electric energy demand by "equipment" gains of zone
7	QELLIGHT	kJ/hr	Electric energy demand by "lights" gains of zone
8	QINF	kJ/hr	Sensible infiltration energy gain of air node
9	SQHEAT	kJ/hr	Sum of heating demand of Zones: LG, G, 1, 2, 3 &4
10	SQCOOL	kJ/hr	Sum of cooling demand of Zones: LG, G, 1, 2, 3 &4
11	QCOMO	kJ/hr	Energy to the outside surface of a boundary wall - with
			positive defined as into the surface from the outside
12	PPD	%	Percentage of person dissatisfied of comfort
13	PMV		Predicted mean vote of comfort

4.3 Simulation Results

4.3.1 Introduction to Simulation Results: Overview of Thermal Performance and Energy Efficiency

This section presents the findings from simulations designed to evaluate the thermal performance of buildings with and without PCM integration. Key parameters considered in the study include inside surface temperatures, operative room temperatures, heat energy transfer rates (W/m²), Predicted Mean Vote (PMV), and Predicted Percentage of Dissatisfied (PPD).

The analysis begins with baseline simulations without PCM to provide a reference for comparison. The results show significant temperature fluctuations and heat losses, highlighting the need for

thermal regulation strategies. Subsequently, the PCM integration results focus on walls without windows. PCM positions are tested to see how they impact thermal metrics, revealing that positions between 341 mm and 356 mm, where the PCM reaches its phase change temperature of 27°C, provide the most effective thermal buffering. This section also explores how PCM affects walls with windows, finding that similar positions continue to yield the best performance despite the increased heat transfer through glazing. Finally, the full-building simulations examine the broader impact of PCM on energy demand and comfort over a year. The study shows that PCM positions 341 mm to 356 mm achieve the highest energy savings and the lowest PMV and PPD values, confirming their effectiveness in stabilising indoor temperatures and reducing heating and cooling loads.

4.3.2 Baseline Simulation Results

a) Baseline 48-hour inside temperature profile

The baseline simulation, conducted without PCM integration, provided a reference point for evaluating the effectiveness of PCM in improving thermal performance.

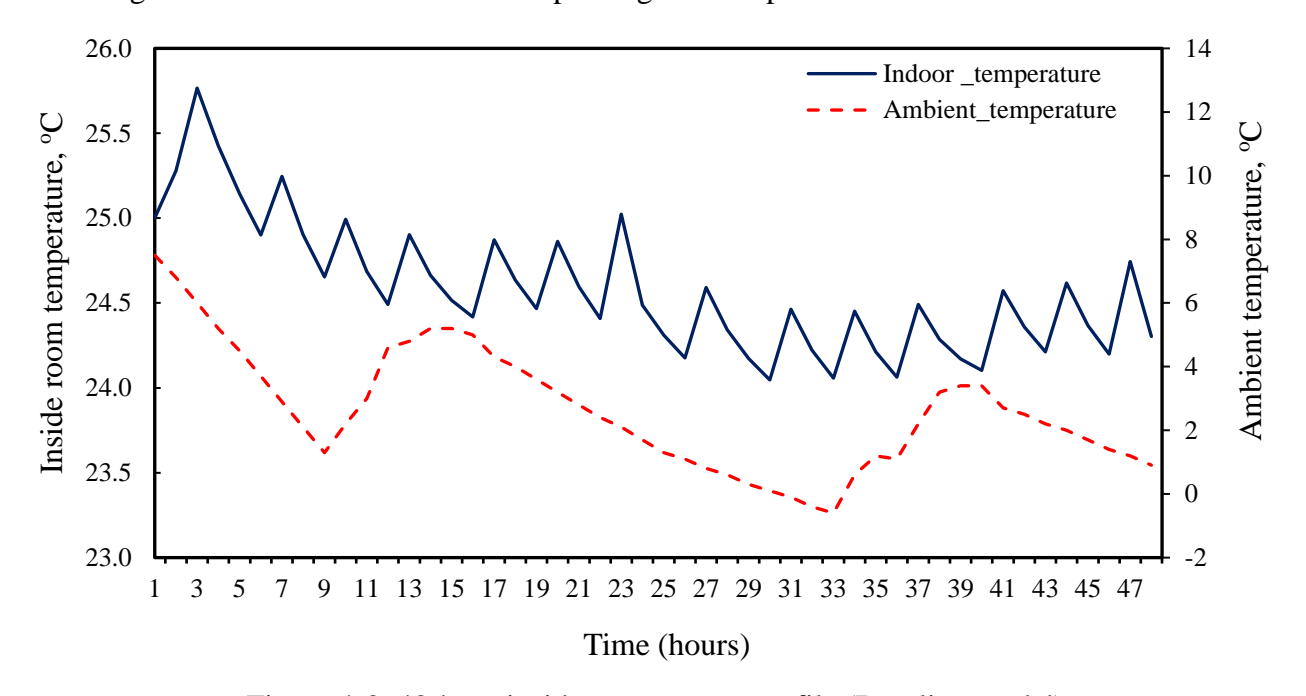


Figure 4-3. 48-hour inside temperature profile (Baseline model)

Figure 4-3 illustrates how the inside temperature fluctuates in the baseline model over 48 hours without PCM, initially set at 25° C. The indoor temperature spiked to a maximum of around 26° C in the first few hours, while the ambient temperature hovered around 5° C. Over time, the indoor temperature dropped, reaching as low as 24° C around hours 30 - 40. Notably, these fluctuations coincide with the variation in ambient temperature, which ranges from a peak of approximately 6° C

to a low of -1°C. This pronounced indoor temperature oscillation indicates the baseline model's inability to buffer against external temperature changes, emphasising the need for regulation strategies like PCM integration to achieve more stable indoor conditions.

b) Baseline room operative temperature

Figure 4-4 illustrates the variations in the room's operative temperature (TOP) over a 48-hour period for the baseline model without PCM integration. "The operative room temperature (TOP) is defined as the uniform temperature of an enclosure in which a person would exchange the same amount of heat with radiation and convection" [178]. The initial operative temperature was set at 25°C, but the graph shows a series of fluctuations as the simulation progressed. In the early hours, the operative temperature spiked to just above 25.5°C, indicating an initial response to environmental changes.

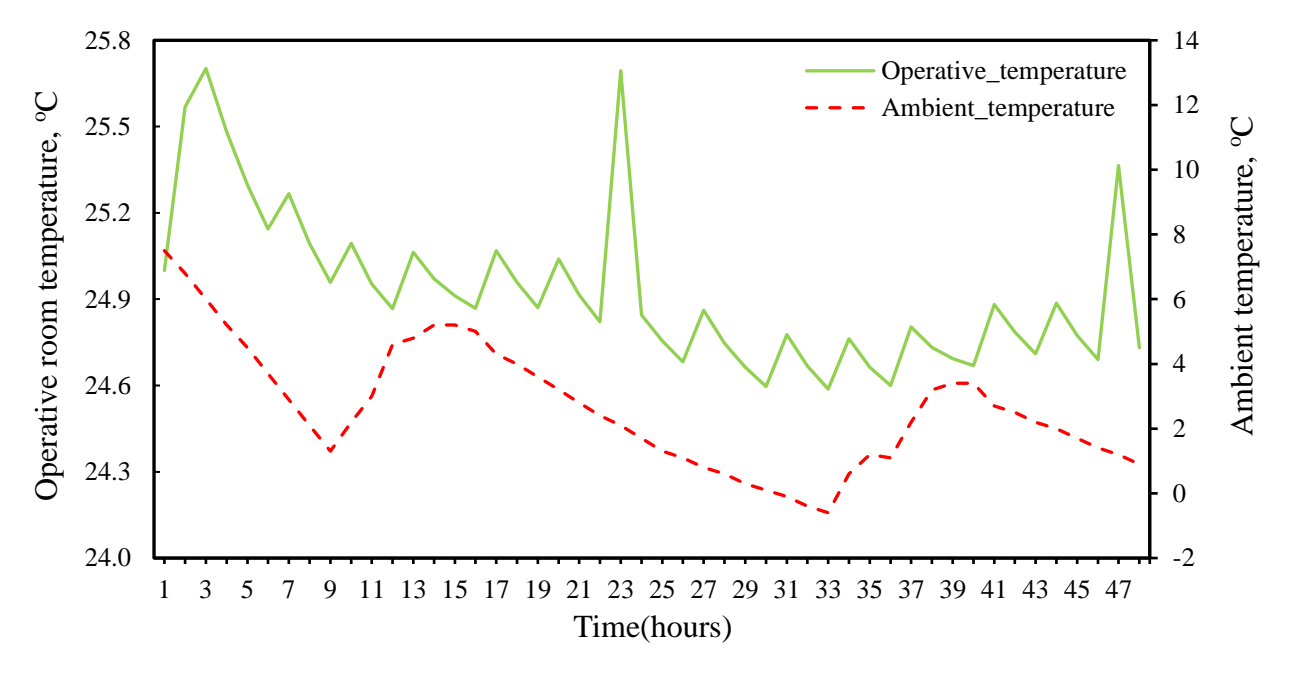


Figure 4-4. Room operative temperature (Baseline model)

The operative temperature then gradually declined, exhibiting a wavy pattern similar to the indoor temperature fluctuations seen earlier in Figure 4-3. The peaks and troughs suggest that the operative temperature was directly influenced by the ambient temperature, which ranged from a high of around 10°C to -1°C over the 48-hour period.

It can be seen that, the operative temperature maintains a relatively narrow range of about 1.1°C oscillation, between 24.6°C and 25.7°C. This pattern indicates a response to the external environment's temperature variations, showing the baseline model's limited capacity to buffer and regulate the room's thermal comfort without PCMs. The limited temperature range means a minimal luxurious comfortable temperature range and the HVAC system would work more to achieve these strict comfort conditions, which would increase energy consumption. The observed peaks at Hours 3, 23, and 47 can be attributed to a combination of occupancy levels, HVAC system activity, and ambient temperature influences. At Hour 3, high internal heat gains from occupants, lighting, and equipment, coupled with reduced cooling capacity during nighttime, result in a temperature spike despite low ambient temperatures. At Hour 23, the HVAC system restarts after a period of inactivity, and increased occupancy and activities, along with rising ambient temperatures, contribute to the peak. Similarly, at Hour 47, high occupancy levels later in the day, combined with reduced cooling efficiency and elevated ambient temperatures, lead to an accumulation of heat, causing another spike. These factors highlight the interaction between internal and external conditions in driving room temperature fluctuations.

c) Baseline Heat energy transfer rate

The heat energy transfer rate was evaluated to assess the heat entering or leaving the building through the walls.

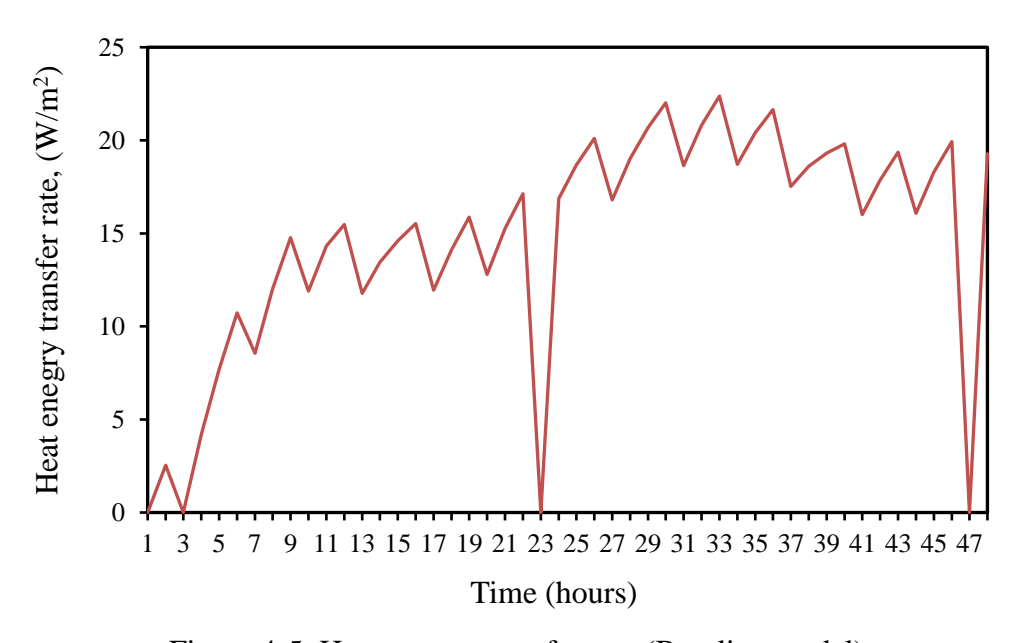


Figure 4-5. Heat energy transfer rate (Baseline model)

Figure 4-5, illustrates the heat energy transfer rate over a 48-hour period for the baseline model without PCM integration. The results show a consistent increase in heat energy transfer as time progresses, peaking at around 25 W/m², with periodic sharp drops, potentially due to short-term external environmental changes. These fluctuations indicate that the wall, in its current state, allows significant heat energy to pass through, leading to substantial losses or gains depending on the external conditions. The sharp drops in heat energy transfer rate at Hours 3, 23, and 47, correspond to periods of sudden changes in HVAC system activity or reduced cooling demand. At Hour 3, the cooling system is likely not fully operational due to night-time settings, causing the heat energy transfer rate to momentarily dip. Similarly, at Hour 23, the HVAC system restarts after an inactive or low-output period, and the reduced cooling activity results in a sharp decline in heat transfer. At Hour 47, this pattern repeats as the HVAC system may again shift operations or reduce cooling output, leading to another drop. These fluctuations highlight the interaction between occupancy schedules, HVAC settings, and internal heat gains in influencing the energy transfer dynamics within the building. This highlights the wall's inefficiency in insulating the indoor environment, thus necessitating the integration of thermal enhancement materials like PCM to mitigate these heat transfers and achieve better energy efficiency.

- Correlation between room operative temperature and heat energy transfer rate

The sharp drops in heat energy transfer rate at Hours 3, 23, and 47 in Figure 4-5 can be directly correlated with the observed peaks in operative room temperature discussed earlier in Figure 4-4. At Hour 3, while internal heat gains are high due to early occupant activities, the cooling system operates at reduced capacity during night-time, causing a sharp dip in heat transfer. This aligns with the temperature spike caused by internal heat gains outpacing cooling. Similarly, at Hour 23, the HVAC system restarting after inactivity results in a temporary drop in heat transfer, corresponding to the temperature peak driven by increased activity and rising ambient temperatures. At Hour 47, reduced cooling efficiency coupled with high late-day occupancy levels and elevated ambient temperatures causes another drop in heat transfer, correlating with the temperature spike. These patterns illustrate the interplay of internal heat gains, ambient conditions, and HVAC activity in shaping both heat transfer rates and room temperature profiles.

d) PMV and PPD Analysis

Predicted Mean Vote (PMV) is an index that predicts the average thermal sensation of a group of people on a scale from -3 (cold) to +3 (hot), with 0 being neutral comfort [212]. A lower PMV,

closer to 0, indicates better thermal comfort. Predicted Percentage of Dissatisfied (PPD) estimates the percentage of people likely to be dissatisfied with the thermal environment. Ideally, the PPD should be below 20% for acceptable comfort [213, 214]. Both PMV and PPD values were obtained from the simulation to quantify thermal comfort levels within the room.

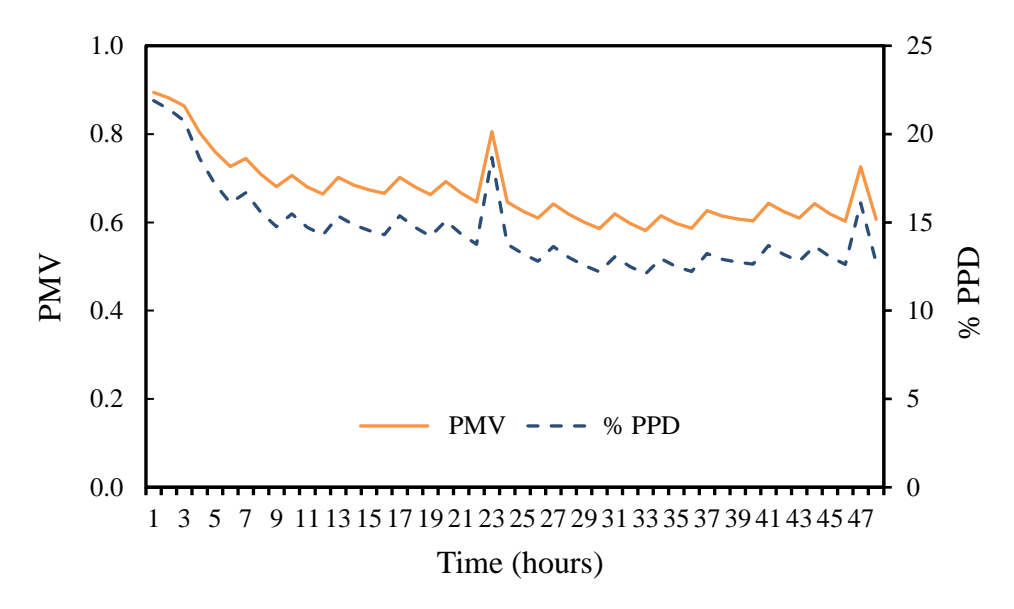


Figure 4-6. PMV and PPD values (Baseline model)

Figure 4-6 illustrates the Predicted Mean Vote (PMV) and Predicted Percentage of Dissatisfied (PPD) values over 48 hours for the baseline model without PCM. It appears that the PMV values consistently hover above 0.6, indicating a tendency towards warmer thermal sensations, corresponding to a less comfortable indoor environment. The PPD values, generally exceeding 10% of the ASHRAE Standard 55-2020, reflect a significant proportion of occupants likely to feel uncomfortable during this period. At Hour 23, the HVAC system restarts after a period of inactivity, coinciding with increased occupancy and rising ambient temperatures, leading to a sharp increase in PMV and PPD values. Similarly, at Hour 47, high occupancy levels, reduced cooling efficiency, and elevated ambient temperatures result in another peak in discomfort metrics.

In contrast, no peak is observed at Hour 3 due to relatively low cooling demand and ambient temperatures. While early activity generates internal heat gains, they are insufficient to significantly increase PMV or PPD, as thermal conditions remain balanced within comfortable limits. This reflects the influence of system operation and external conditions on thermal comfort throughout the day.

Thus, the occasional spikes in both PMV and PPD highlight moments of pronounced discomfort, reinforcing the baseline model's inadequacy in maintaining optimal thermal comfort. These results underscore the necessity of integrating PCM to stabilise indoor conditions, and reduce PMV and PPD values.

4.3.3 Simulation Results: Wall Integrated with PCM but Without a Window

The simulations focused on determining how PCM placement affects inside temperatures, room operative temperatures, heat energy transfer, PMV, and PPD values. Various PCM positions were tested to identify the optimal configuration.

a) Simulated inside room surface temperature profile for 48-hour with PCM position (wall without window)

Figure 4-7, shows the simulated inside surface room temperature for the wall without the window, comparing the thermal performance of various PCM positions over a 48-hour period, with the initial temperature set at 25°C. The employed PCM has a phase change temperature of 27°C.

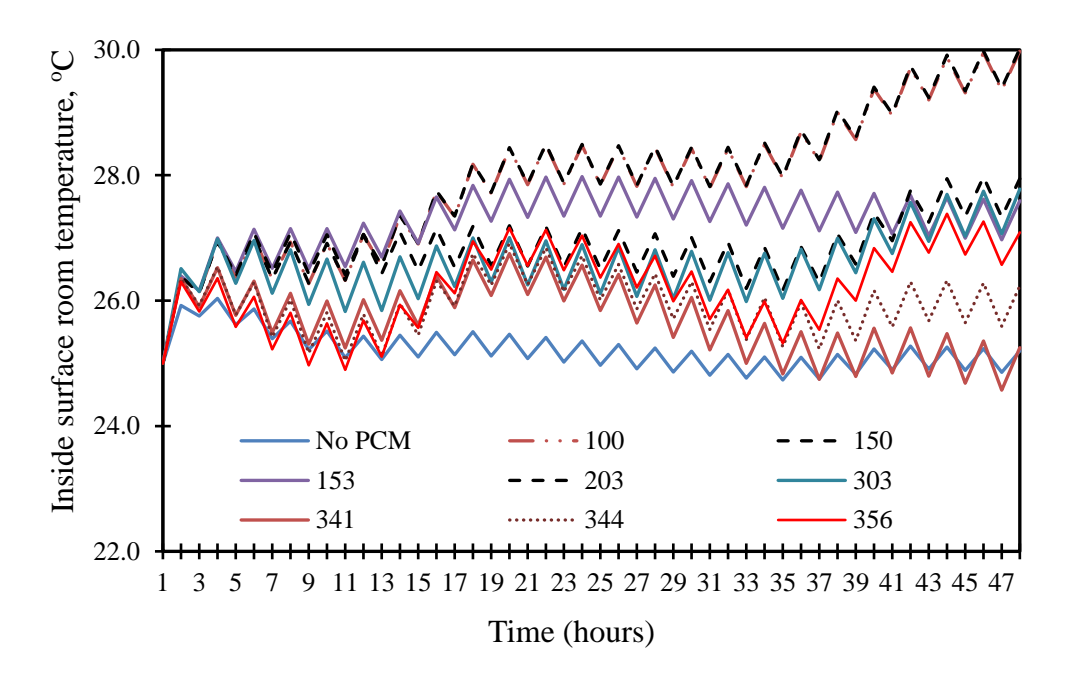


Figure 4-7. Simulated inside surface room temperature (wall without window) with PCM at various positions

It can be seen from Figure 4-7 that the baseline condition without PCM maintains relatively stable temperatures ranging from approximately 24.4°C to 2.5°C throughout the period of 48 hours. However, noticeable fluctuations highlight the wall's limited ability to buffer temperature variations, which could lead to potential thermal discomfort and increased energy demands for cooling. When PCM was placed at 100 mm and 150 mm positions, the highest surface temperatures were observed, fluctuating between 27.5°C and nearly 30°C. These temperatures sharply increased in the later stages of the simulation, suggesting that PCM in these locations failed to effectively maintain its phase change temperature due to its close proximity to the outer surface and increased heat absorption from the external sources. This inefficiency results in poor thermal buffering, indicating that these positions are unsuitable for enhancing thermal comfort or reducing energy consumption.

In contrast, PCM placements at 153 mm, 203 mm, and 303 mm show some improvement in temperature stabilisation, maintaining a range between 25°C and 27°C. However, while these positions provide moderate thermal buffering, the PCM's ability to undergo phase changes and regulate heat absorption and release is not fully optimised, resulting in continued temperature swings.

The most significant improvements in thermal regulation are observed when the PCM is placed on the positions at 341 mm, 344 mm, and 356 mm. At these locations, the inside surface temperatures are maintained within a tighter range of about 24.5°C to 27.3°C, demonstrating reduced fluctuations and more stable conditions. This suggests that the PCM effectively reached its phase change temperature, absorbing excess heat during warmer periods and releasing it during cooler times, thereby acting as an efficient thermal buffer. Consequently, this resulted in reduced reliance on mechanical heating or cooling systems, enhancing overall energy savings.

From an energy savings perspective, the PCM positions closer to the inner wall surface, particularly 341 mm to 356 mm, are optimal. These positions minimise temperature fluctuations within a temperature range of 25.3°C to 27.3°C, ensuring better thermal comfort. In contrast, PCM positions closer to the external wall surface (100 mm and 150 mm) lead to higher surface temperatures, making them less effective for energy savings and thermal comfort.

b) Simulated room operative temperature profile for 48-hours with PCM position (wall without window)

Figure 4-8 shows the simulated room operative temperature for a wall without a window, with PCM integrated at various positions over a 48-hour simulation period, while the employed PCM had a phase change temperature of 27°C. The initial temperature was set at 25°C. The operative temperature of the wall without PCM rises steadily after the initial hours, eventually peaking close to 26°C, indicating that without PCM, the wall struggles to regulate heat effectively. On the other hand, PCM placed at 100 mm and 150 mm from the external wall shows the highest operative temperatures, exceeding 29°C. This suggests that the PCM in these positions is too close to the outer wall, preventing it from efficiently reaching and maintaining its phase change temperature, making it less effective in stabilising the indoor environment.

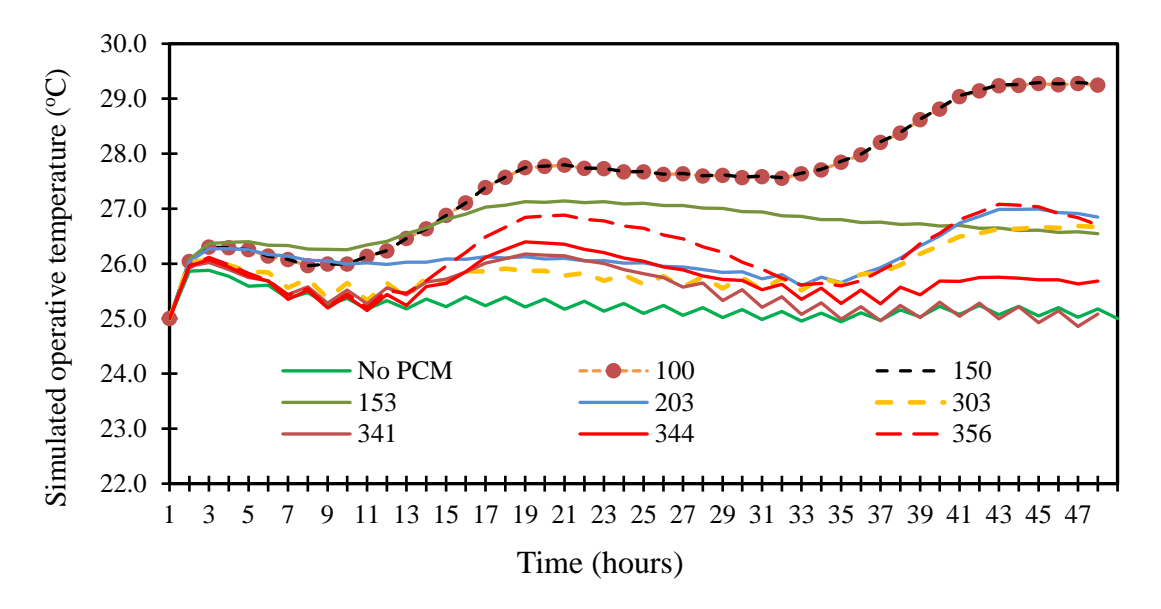


Figure 4-8. Simulated room operative temperature (wall without window) with PCM at various positions

PCM position 153 mm shows a moderate improvement in temperature regulation, but the operative temperatures still hover just under 27°C. Although this position offers some heat absorption, the PCM at this depth does not fully utilise its phase change capabilities to minimise temperature fluctuations effectively. Similarly, PCM positions at 203 mm and 303 mm demonstrate better thermal control, and buffering capacity than the previous placements, with temperatures stabilising around 26.5°C to 27°C.

As shown in Figure 4-8, the most effective PCM positions for maintaining a stable and comfortable indoor temperature are at 341 mm, 344 mm, and 356 mm, where the operative temperatures are

maintained around 25.5°C to 26°C with minimal fluctuations. These positions allow the PCM to efficiently reach its phase change temperature of 27°C, absorbing and releasing heat effectively to regulate indoor conditions. The proximity of the PCM to the internal wall surface at these positions ensures that the material undergoes phase transitions when needed, optimising its ability to stabilise indoor temperatures and reduce the cooling load.

Therefore, based on the data in Figure 4-8 PCM positions between 341 mm and 356 mm are optimal for thermal comfort and energy savings, by maintaing operative room temperatures around 25.5°C to 27°C. These positions enable the PCM to effectively absorb and release heat at its phase change temperature, minimising operative temperature fluctuations, reducing the reliance on mechanical heating and cooling systems, and helping to achieve greater energy efficiency while maintaining a comfortable indoor environment.

c) Heat energy demand with PCM

Figure 4-9 illustrates the heat energy demand for a wall without PCM (No PCM) and with PCM integrated at various positions over a 48-hour simulation period. The results clearly show significant differences in the heat energy demand behaviour depending on PCM placement.

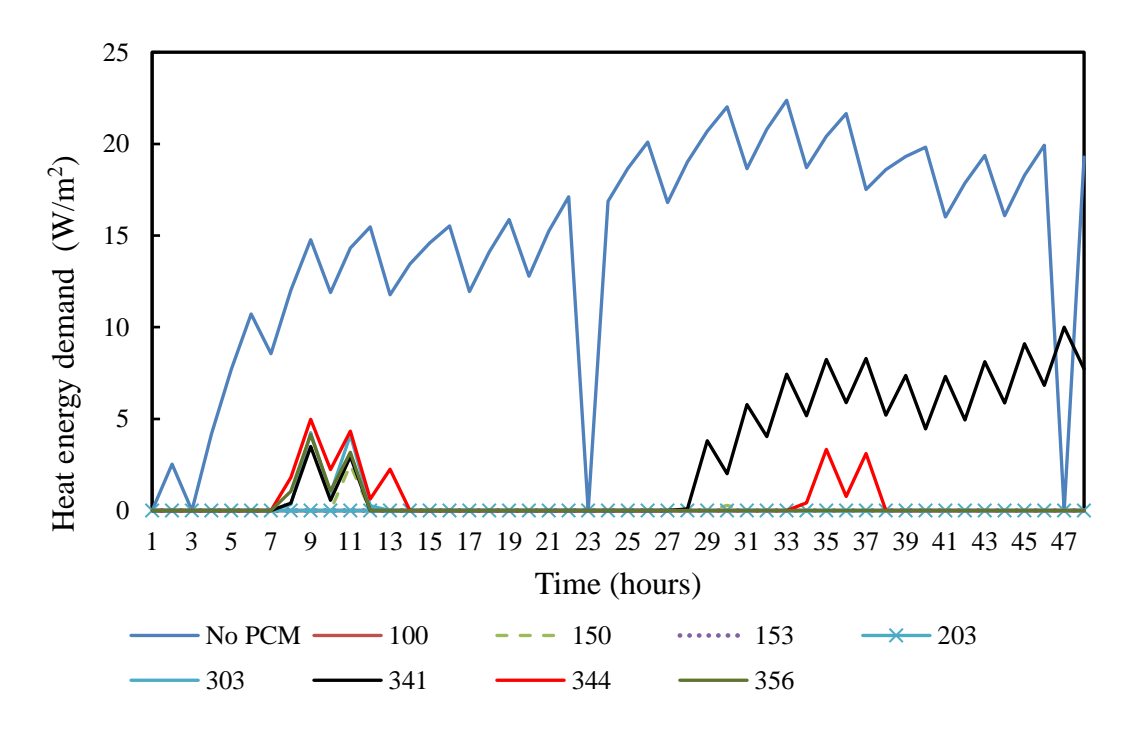


Figure 4-9. Heat energy demand with PCM at various positions

As shown in Figure 4-9, the heat energy demand for the wall without PCM exhibits a continuous upward trend, peaking at approximately 24 W/m². This indicates that the wall, without any thermal buffering, allows for a substantial amount of heat to pass through, reducing indoor temperature and potentially heating demand. There are noticeable peaks throughout the day, corresponding to periods of high ambient temperature, as indicated earlier in Figure 4-3 and Figure 4-4, which highlights the wall's inability to moderate heat gains effectively.

When PCM was integrated into the wall, the heat energy demand significantly decreased, varying based on the PCM's position. PCM placement at 100 mm and 150 mm was associated with moderate peaks in heat energy demand, indicating some reduction compared to the wall without PCM. However, the peaks still appeared, suggesting that placing the PCM too close to the external wall surface did not optimise its phase change capabilities for thermal regulation.

It can be seen that PCM positions at 153 mm, 203 mm, and 303 mm exhibit improved performance, with lower peaks in heat energy demand compared to external positions. These placements provide a degree of thermal buffering but still show fluctuations, indicating they do not fully harness the PCM's latent heat storage potential to stabilise indoor temperatures optimally.

The most effective PCM positions are observed at 341 mm, 344 mm, and 356 mm. In these positions, the observed peaks appear to indicate absorption and release of heat. The heat energy demand is low compared to the wall without the PCM for almost the entire simulation period, indicating minimal heat transfer through the wall. This suggests that when the PCM is positioned closer to the inner surface of the wall, it efficiently undergoes phase changes, absorbing excess heat during peak temperature periods and releasing it during cooler times.

From Figure 4-9 it can be seen that placing the PCM closer to the internal wall surface, particularly between 341 mm and 356 mm, provides the most effective thermal regulation. These positions minimise heat energy demand, indicating that the PCM effectively manages thermal loads by absorbing and releasing heat as required. Conversely, positions closer to the external wall surface are less effective, resulting in higher heat energy demands and reduced energy-saving potential.

d) PMV and PPD analysis with PCM

Figure 4-10 shows the simulated Baseline Predicted Mean Vote (PMV) and Predicted Percentage of Dissatisfied (PPD) values for the wall without a window, with PCM at various positions. Based on the PMV and PPD values, the objective is to identify the optimal PCM position that maximises both energy savings and thermal comfort. The acceptable limit for PPD is set at 20%.

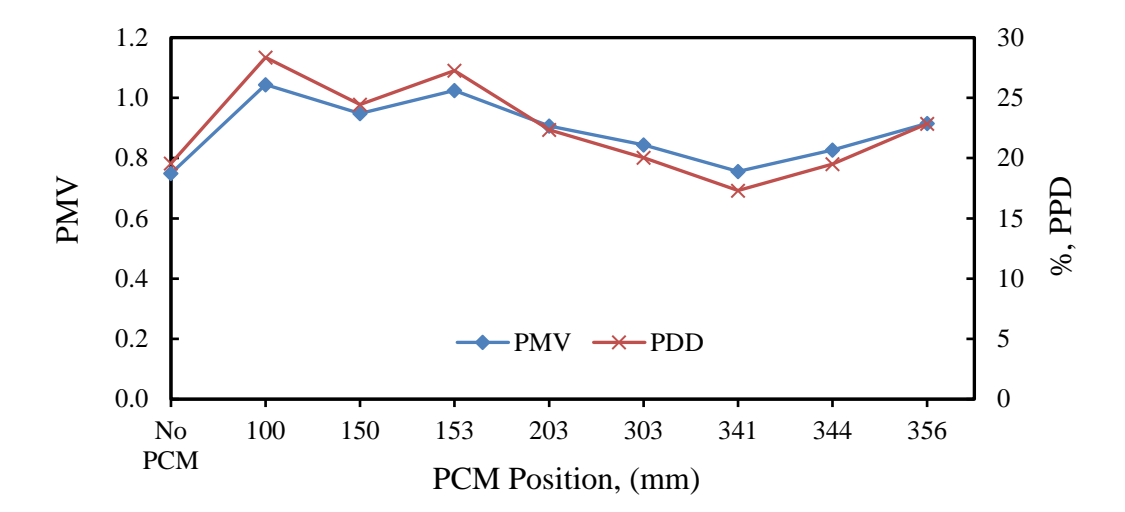


Figure 4-10. PMV and PPD values with PCM at various positions

The wall with no PCM shows relatively high PMV and PPD values. The PMV value is close to 1.0, suggesting that occupants feel warmer than neutral, while the PPD value exceeds 20%, indicating a higher percentage of dissatisfied occupants due to uncomfortable thermal conditions. This validates that without PCM integration, the wall cannot regulate indoor temperatures effectively, leading to thermal discomfort.

It can be seen that PCM at 100 mm and 150 mm is associated with high PMV values (above 1.0) and PPD values around 25%. These results indicate that the PCM at these positions does not significantly improve thermal comfort, as the occupants still feel too warm, and the percentage of dissatisfied occupants remains high. This can be attributed to the PCM not reaching its phase change temperature, limiting its ability to regulate indoor temperatures effectively.

On PCM at positions at 153 mm, 203 mm, and 303 mm in Figure 4-10, a slight improvement in PMV and PPD values can be observed, with PMV dropping to around 0.9 and PPD closer to 22%. However, these positions still do not achieve the desired comfort levels, as the PPD value remains above the acceptable threshold of 20%. This suggests that while these PCM positions provide some thermal buffering, they are still suboptimal for energy savings and occupant comfort.

By contrast, PCM at 341 mm, 344 mm, and 356 mm positions exhibit the most significant improvement in both PMV and PPD values. The PMV values are closer to 0.8, indicating a thermal sensation closer to neutral, while the PPD values drop below 20%, reaching as low as 18%. This is within the acceptable range, meaning fewer occupants feel thermally uncomfortable. These positions allow the PCM to reach its phase change temperature of 27°C, enabling it to absorb and release heat effectively, thereby reducing indoor temperature fluctuations and improving thermal comfort.

It appears that the optimal PCM positions for achieving both energy savings and thermal comfort are between 341 mm and 356 mm from the external wall surface. At these positions, the PCM reaches its phase change temperature, actively regulating the indoor environment and reducing the PPD to acceptable levels. These positions offer better thermal comfort and align with energy-saving objectives by minimising the need for active cooling and heating interventions. Conversely, PCM placed closer to the outer wall (100 mm and 150 mm) cannot maintain thermal comfort and energy efficiency, as higher PMV and PPD values indicate.

4.3.4 Simulation Results: PCM Integration in a Wall with a Window

a) Simulated inside temperature profile with PCM positions

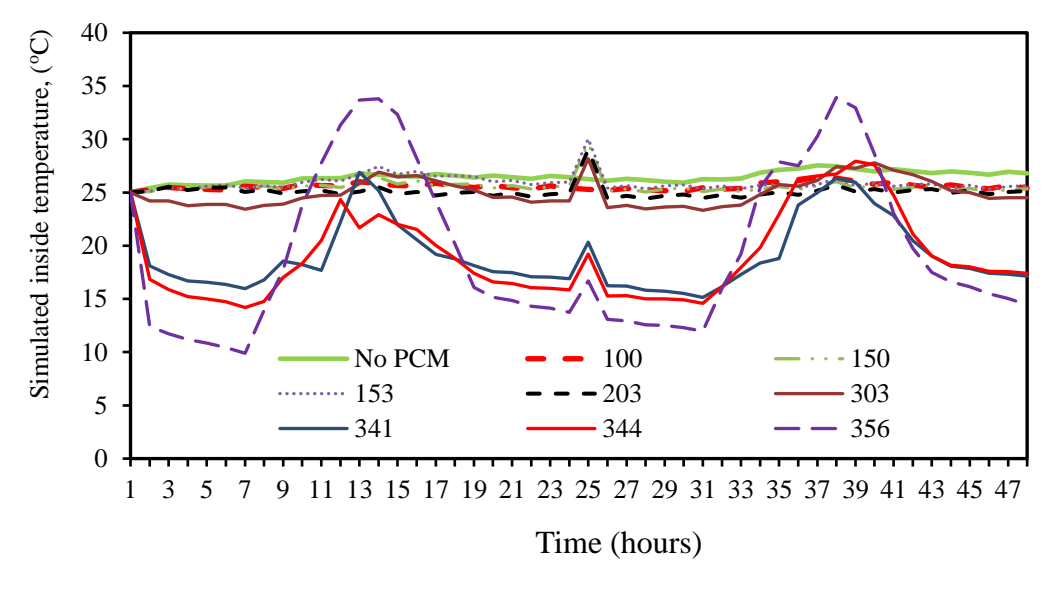


Figure 4-11. Simulated inside room temperature (wall with window) with PCM at various positions

Figure 4-11 shows the simulated inside temperature for a wall with a window, with PCM integrated at various positions over a 48-hour simulation period. The initial temperature was set at 25°C while

the employed PCM has a phase change temperature of 27°C. As seen in Figure 4-11, PCM placements at 100 mm, 150 mm, 153 mm, 203 mm, and 303 mm show relatively stable and lower inside surface temperatures, generally remaining below 27°C throughout the simulation. While this might appear advantageous for reducing temperature peaks, it indicates that the PCM in these positions does not reach its phase change temperature. Without reaching 27°C, the PCM cannot undergo phase transitions, which means it fails to absorb significant amounts of heat. As a result, its effectiveness in thermal regulation and energy storage is limited. In these positions, the PCM behaves more like traditional insulation rather than a thermal energy storage system. Although it does help moderate indoor temperature fluctuations to some extent, it does not fully exploit the PCM's latent heat capacity, which is critical for maximising energy savings and thermal comfort.

In contrast, it can be seen in Figure 4-11, PCM placements at 341 mm, 344 mm, and 356 mm are associated with higher temperature peaks, often exceeding 27°C. These peaks are likely due to the window acting as a weak point that promotes heat loss, requiring increased temperature to compensate for the deficit. Despite the larger fluctuations, these positions allow the PCM to reach and surpass its phase change temperature of 27°C. This activation enables the PCM to absorb excess heat during higher temperature periods, utilising its thermal storage capacity effectively. Therefore, PCM placements between 341 mm and 356 mm demonstrate a superior capacity for managing indoor temperatures by utilising the material's phase change properties. Among these positions, 341 mm and 344 mm appear to offer an optimal balance, as they allow the PCM to reach its phase change temperature while still moderating the indoor temperature effectively, with the lowest observed temperature around 15°C. This placement enables the PCM to act as a thermal buffer, reducing extreme highs and lows in indoor temperatures, contributing to a more energy-efficient and comfortable environment.

Conversely, PCM placements from 100 mm to 303 mm could not reach the phase change temperature, resulting in missed opportunities for heat absorption and limited energy savings.

b) Simulated operative room temperature profile with PCM position

Figure 4-12, shows the simulated operative room temperature (wall with window) with PCM at various positions over a 48-hour period. The initial temperature was set at 25°C. The wall with no PCM unlike other cases, shows relatively minor fluctuations throughout the 48-hour period, with the room temperature mostly oscillating between 25°C and 26°C. This stability suggests that, for this

particular wall configuration, the absence of PCM does not lead to significant peaks in temperature. However, the lack of PCM also means that the system is not benefiting from any potential latent heat absorption or release, which could further enhance energy savings and comfort.

As shown in Figure 4-12, PCM placements at 100 mm, 150 mm, 153 mm, 203 mm, and 303 mm result in relatively stable and lower temperature profiles, generally maintaining the room temperature just below 27°C throughout most of the simulation period. This suggests that these PCM positions do not reach the phase change temperature of 27°C frequently enough to trigger effective thermal energy absorption. While these positions help to moderate the temperature to some extent, the inability of the PCM to undergo phase transitions means that it does not fully utilise its latent heat capacity. Consequently, these positions act more like traditional insulation materials rather than efficient thermal energy storage systems, leading to limited thermal regulation and energy savings.

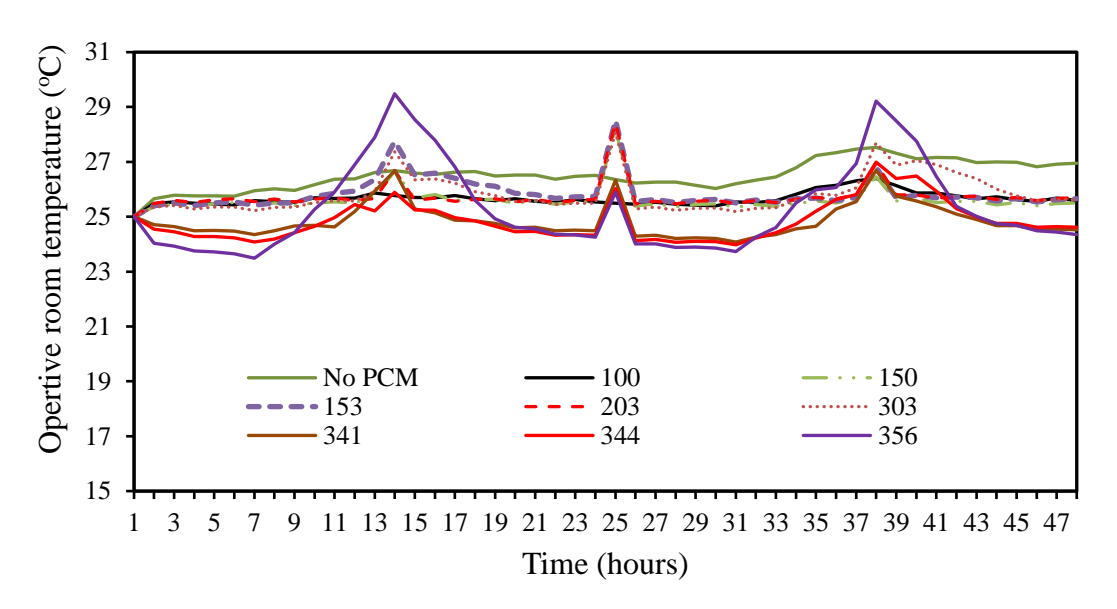


Figure 4-12. Simulated operative room temperature (wall with window) with PCM at various positions

In Figure 4-12, the PCM placed at position 344 demonstrates one of the most balanced temperature profiles. The operative room temperature maintains a narrower range, with peaks generally staying just under 28°C during the hottest periods (around hours 13–15, 23-27 and 37–39) and avoiding extreme drops during cooler periods. The temperature stays within a more desirable comfort zone of 24°C to 27°C. By reaching and occasionally surpassing its phase change temperature of 27°C, the PCM at this position effectively absorbs excess heat during warm periods and releases it during cooler

times. It is suggested that this buffering action reduces the need for mechanical cooling and heating, thereby offering improved energy efficiency and enhanced thermal comfort.

Similar to position 344, PCM at 341 also shows a favourable temperature regulation effect, and slightly peaks above 27°C during warmer hours. It maintains temperatures comfortably above 24°C during cooler periods. This indicates that the PCM at this position has reached its phase change temperature, absorbing and releasing heat effectively.

Distinctly, the 356 mm PCM position shows the highest temperature peaks, approaching 30°C during the warm periods. Although the PCM in this position has reached the phase change temperature, the higher fluctuations suggest it is not performing optimally due to the presence of the window, which likely increases the heat loss or gain. As a result, the PCM in this position provides less consistent temperature regulation, leading to more pronounced fluctuations.

In summary, the analysis of the operative room temperature profile shown in Figure 4-12 suggests that PCM positions at 341 mm and 344 mm are the most effective for temperature stabilisation and energy efficiency. These positions allow the PCM to operate within its optimal phase change range, providing enhanced thermal buffering against indoor temperature fluctuations. In contrast, positions closer to 100 mm to 303 mm only show some moderation but do not utilise the PCM's phase change capabilities to their fullest. Therefore, placing the PCM between 341 mm and 356 mm within the wall assembly appears to be the most advantageous for maintaining comfort and maximising energy savings in this scenario.

c) Heat energy demand with PCM

Figure 4-13 shows the heat energy demand (W/m²) and ambient temperature (°C) over a 48-hour period for a wall with a window, with the heat demand displayed for various PCM positions and a "No PCM" case. The initial temperature was set at 25°C. The ambient temperature fluctuated significantly between approximately 6°C and 15°C throughout the 48-hour period, with peaks occurring during the daytime and dips during the night. These fluctuations drive the need for heating or cooling as the room attempts to maintain a comfortable indoor environment. The role of PCM is to absorb excess heat when the temperature exceeds the PCM's phase change temperature (27°C), and to release stored heat when the temperature falls, thus reducing energy consumption and stabilising indoor temperature.

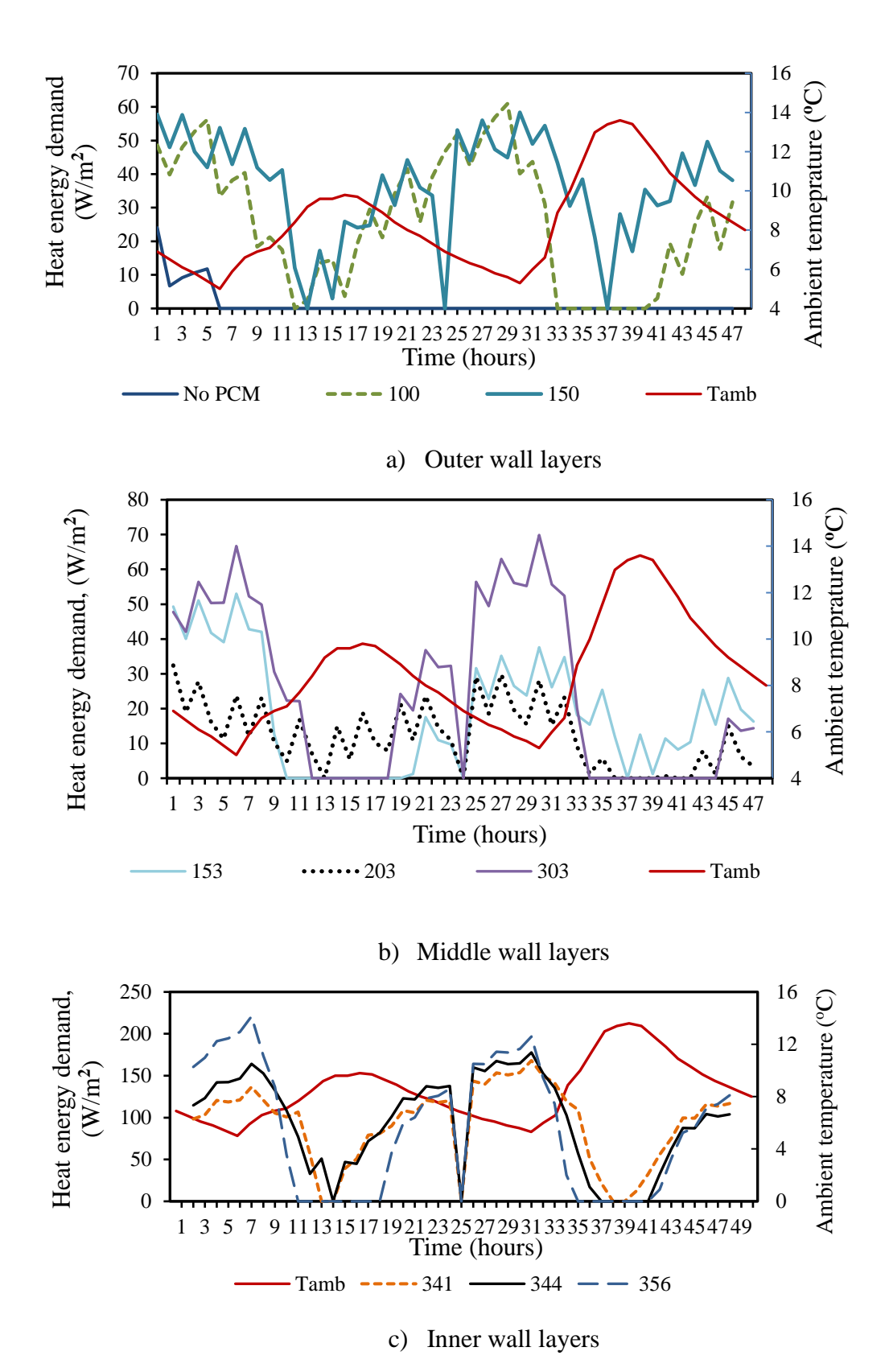


Figure 4-13. (a) – (c) Heat energy transfer rate with PCM at various positions

The wall without the PCM, showed a zero-heat demand consistently throughout the 48-hour period. This indicates that, without PCM, the room is solely reliant on the thermal insulation properties of the wall, which results in no additional heat energy demand. However, the absence of PCM also implies no thermal buffering, meaning the room would experience more significant temperature fluctuations in response to the ambient conditions. The steady zero heat demand suggests that external heating or cooling systems would be heavily relied upon without PCM to maintain comfort, likely increasing energy consumption elsewhere.

PCM Position 344

PCM at position 344 (Figure 4-13(c)), shows a peak heat demand of around 150 W/m² during the daytime. This peak occurs during periods of rising ambient temperature (around hour 12 and hour 36), indicating that the PCM is absorbing heat and reducing the demand on external heating systems. However, it also suggests that this position allows a substantial amount of heat to enter the room, as the heat energy demand increases significantly during peak hours. Despite the high heat demand, the fluctuations in demand are more moderate compared to positions like 356, indicating that PCM 344 provides better thermal regulation by absorbing and releasing heat efficiently. PCM at this position actively reduces the cooling load during peak temperature periods, thus contributing to overall energy savings, especially when ambient temperatures are high.

PCM Position 341

PCM placed at 341 mm (Figure 4-13(c)), exhibits heat demand peaks slightly lower than 150 W/m², similar to PCM 344, but with slightly smoother variations. The lower peak suggests that PCM 341 absorbs and releases heat more effectively than position 344, as it requires slightly less energy during peak periods to maintain thermal comfort. The energy demand curve for PCM 341 is less volatile, indicating a better balance between heat absorption and release. The lower peaks suggest that PCM 341 contributes to more consistent temperature regulation, reducing both cooling and heating demands throughout the 48-hour period. This makes PCM 341 one of the more efficient positions for achieving energy savings and maintaining comfort.

PCM Position 356

PCM at 356 (Figure 4-13(c)), shows the highest peak heat demand, around 200 W/m², especially during the daytime when ambient temperature is lowest (hours 6–8 and 32–34). This high heat demand indicates that PCM at position 356 mm is not efficiently managing heat, as it allows a large

amount of heat to enter the room. This position may be less optimal for heat absorption and release, as it requires significantly more energy to maintain comfortable indoor conditions. The large fluctuations in the heat demand for PCM 356 suggest that this position is unsuitable for energy savings, as it leads to higher energy requirements during peak temperature periods. This position is less effective at moderating the impact of external temperature changes on the indoor environment.

PCM Positions 100, 150, and 153

These PCM positions exhibit moderate heat demand, with peak values between 50 and 100 W/m². These positions perform better than PCM 356 but are less efficient than positions 344 mm and 341 mm. PCM positions 100 mm, 150 mm, (Figure 4-13(a)), and 153 mm (Figure 4-13(b)), still allow some heat to enter the room, but the overall energy demand is lower, indicating that they contribute to energy savings. However, their moderate performance suggests that they may not be absorbing and releasing heat as effectively as positions 344 mm and 341 mm, resulting in slightly higher energy consumption for maintaining thermal comfort.

PCM Position 203

PCM at 203 mm (Figure 4-13(b)), shows the lowest peak heat demand, around 50 W/m², during the entire 48-hour period. This suggests that PCM at position 203 mm is efficiently managing heat absorption and release, minimising the amount of energy needed to regulate indoor temperature. The smooth, low heat demand curve indicates that PCM at position 203 mm is highly effective at stabilising indoor conditions by absorbing heat during peak periods and releasing it gradually when needed. This position appears to provide excellent energy savings and is likely to offer the best balance between thermal comfort and reduced energy consumption, but due to its location, it is unlikely to attain the phase change temperature. Hence, more experimental work is necessary to correlate the findings.

PCM Position 303

PCM at 303 mm (Figure 4-13(b)), performs similarly to position 203 mm, with relatively low heat demand, peaking around 60 W/m². This suggests that PCM at 303 mm is also an efficient placement for absorbing and releasing heat, contributing to energy savings, stable indoor conditions, and minimising heat demand during peak periods, making it a suitable candidate for energy efficiency. Like position 203, PCM at this position is unlikely to attain the phase change temperature due to its location. Hence, more experimental work is necessary to correlate the findings.

Based on the analysis, PCM positions 203 and 303 are identified as the most effective for energy savings, as they demonstrate the lowest heat demand and provide consistent thermal regulation. For environments with extreme temperature fluctuations and ease of implementation or retrofits, PCM positions 341 mm and 344 mm are effective, though they require slightly higher energy input to maintain comfort.

Based on the simulation results for both a plane wall and a PCM-integrated wall with a window, PCM positions 341, 344, and 356 stand out as key configurations for different reasons. PCM at position 341 mm offers a strong balance between energy savings and thermal comfort, with relatively moderate peak heat demand (~170 W/m²), effectively absorbing and releasing heat to stabilise indoor conditions. This makes it ideal for environments requiring consistent thermal regulation without excessive energy use. PCM at position 344 mm, with a slightly higher peak heat demand (~180 W/m²), performs similarly but may be more suitable for spaces with higher thermal loads, where efficient heat absorption during peak temperatures is crucial for reducing cooling demands.

d) PMV and PPD analysis with PCM

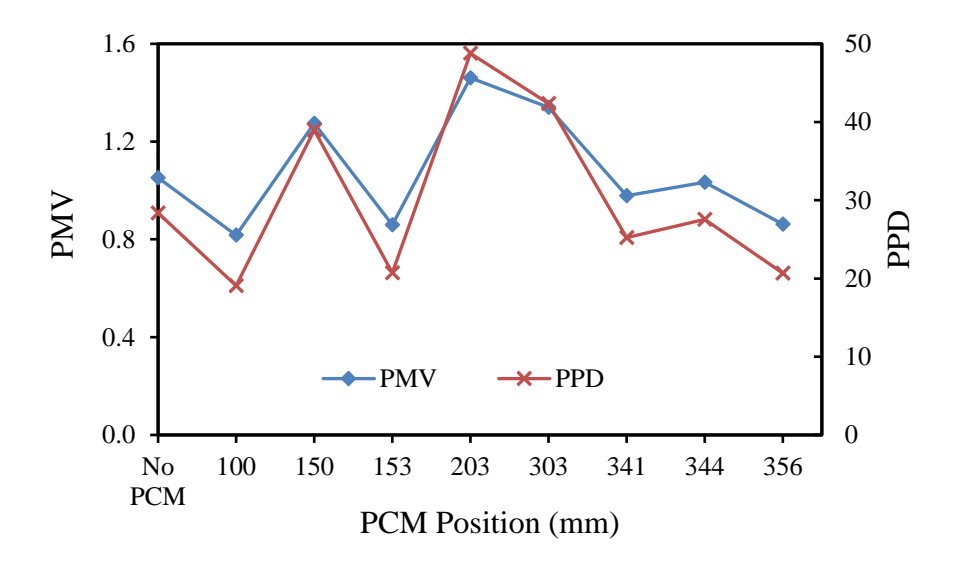


Figure 4-14. PMV and PPD values with PCM at various positions

Figure 4-14 shows the Predicted Mean Vote (PMV) and Predicted Percentage of Dissatisfied (PPD) for various PCM positions in a wall with a window. It can be seen that the wall with no PCM, has a relatively high PMV value of around 1.0, indicating discomfort due to a warmer environment. The

PPD value is around 28%, meaning that approximately 28% of occupants would likely feel dissatisfied.

The PMV values at the PCM Positions of 150 mm, 203 mm, and 303 mm positions are generally higher than 1.0, indicating that occupants would feel uncomfortably warm. PPD values reaches to as much as 48% at 203 mm, suggesting that nearly half of the occupants might feel thermally dissatisfied at this position. These positions, therefore, are not promising for achieving comfort.

By contrast, PCM Positions at 341 mm to 356 mm exhibit lower PMV values, closer to 0.9, indicating a more neutral thermal sensation. The PPD values drop significantly, especially at PCM 341 mm down to PCM 356 mm, where PPD is below 20%, meeting the acceptable threshold for thermal comfort. PCM at these positions has effectively reached its phase change temperature, resulting in better thermal regulation and comfort by storing and releasing thermal heat energy.

4.3.5 PCM in Full-Building

a) Full-Building 48-hour inside temperature profile

The full-building simulation was carried out with identified PCM positions as presented in Sections 4.3.3 - 4.3.4, having identified PCM positions 341, 344, and 356 as key configurations. The full-building simulation extended the optimal PCM placement findings to the entire building, analysing its impact on overall temperature regulation and energy consumption.

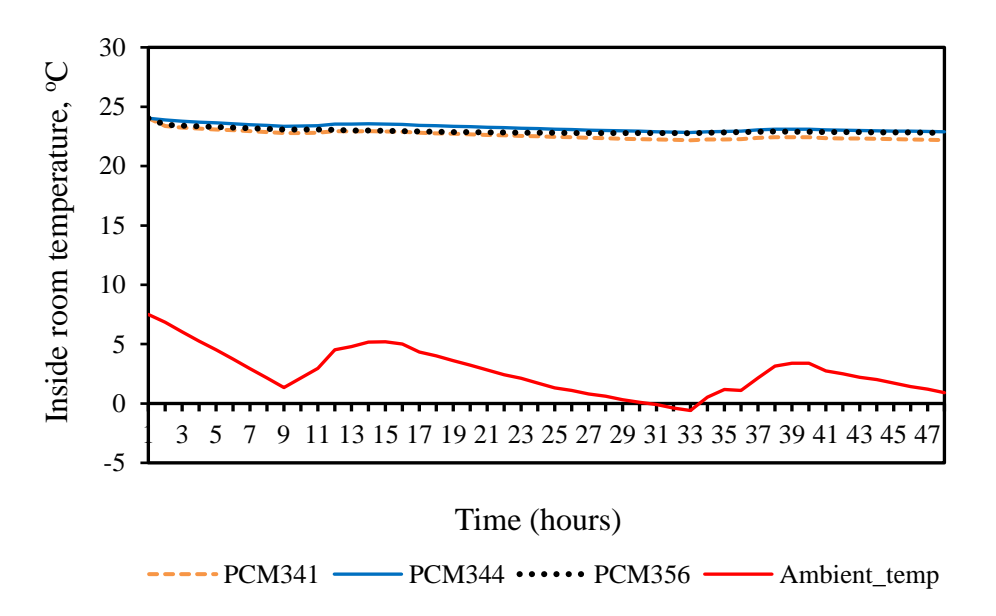


Figure 4-15. Full-building 48-hour temperature profile with optimal PCM position

Figure 4-15, shows the Full-Building temperature profile with Optimal PCM position for a period of 48 hours. It demonstrates the effectiveness of optimal PCM placement in maintaining stable indoor temperatures across the building. PCM positions at 341mm, 344mm, and 356mm successfully mitigate temperature fluctuations, keeping the indoor environment consistently around 25°C.

b) A full year full-building room operating temperature profile for various PCM positions Figure 4-16 shows the results of a full-building simulation and room operating temperatures across different PCM positions throughout the year. It can be seen that the no PCM case resulted in the highest operating temperatures across all months, demonstrating that the absence of PCM leads to less effective temperature control. The operating temperature reached a maximum in July, peaking just below 21°C, while the lowest temperatures were observed in January and December, around 18°C.

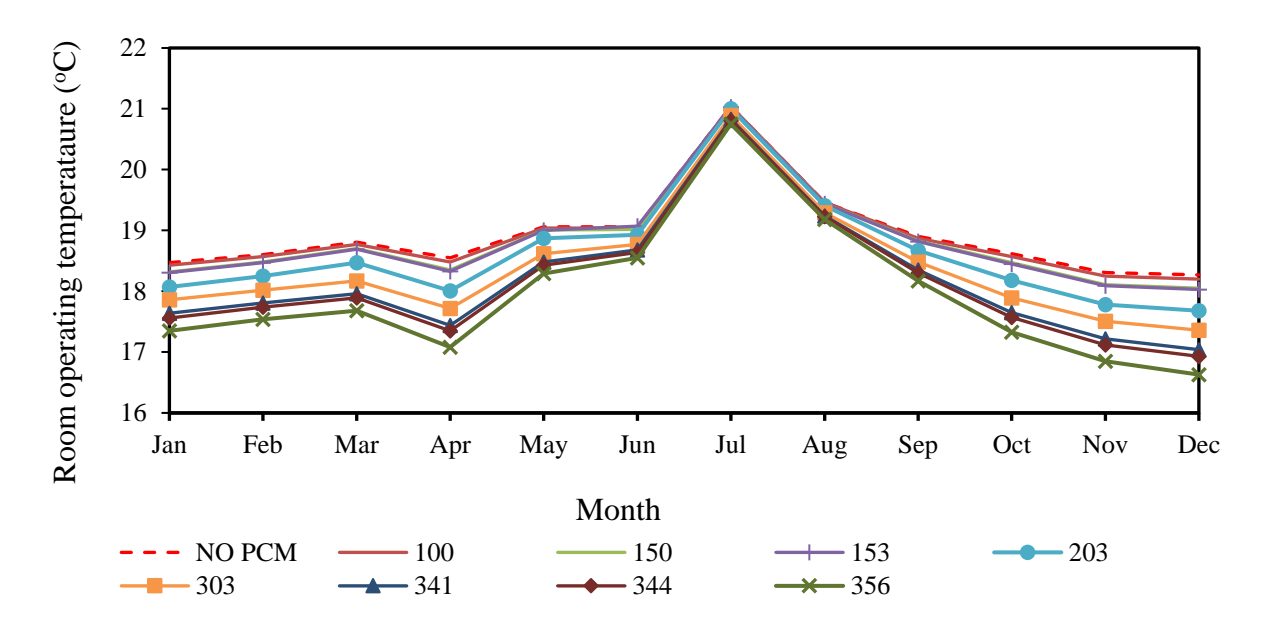


Figure 4-16. 12-month full-building simulated operative room temperature with PCM at various positions

As shown in Figure 4-16, for all PCM-integrated positions, there is a noticeable reduction in room operating temperatures compared to the no PCM scenario. The best performance is observed for PCM positioned at 341 mm and 356 mm, which consistently maintain the lowest operating temperatures throughout the year, particularly during the summer months. In July, the PCM at 341 mm and PCM at 356 mm positions exhibited operating temperatures around 17°C to 18°C, significantly reducing

the peak summer temperature observed in the no PCM case. This indicates that these positions are the most effective in mitigating heat gains during the hottest periods of the year, which is critical for reducing cooling energy demand and ensuring thermal comfort.

It can be observed from Figure 4-16 that during the winter months, PCM at 341 mm and 356 mm demonstrates superior performance, maintaining temperatures between 16.5°C and 17°C. This suggests that PCM integration at these depths helps to reduce heat loss through the wall, improving the overall thermal insulation of the building. The reduced need for additional heating during colder months translates to significant energy savings and a more comfortable indoor environment.

Conversely, PCM positions closer to the outer wall surface (100 mm, 153 mm, and 203 mm) exhibit less effective temperature control. For instance, PCM positions of 100 mm and 203 mm maintain higher room temperatures than deeper PCM positions, particularly in the summer, with operating temperatures exceeding 19°C. This suggests that the PCM is not fully utilised for thermal regulation at these depths within the wall, likely due to insufficient heat transfer, as these positions do not take full advantage of the PCM's phase change properties. Therefore, these PCM positions closer to the outer wall surface are suboptimal for both energy savings and thermal comfort, and should be used with caution.

It is clear that PCM positions between 341 mm and 356 mm are the most effective for stabilising room temperatures and reducing peak operating temperatures throughout the year. These positions consistently outperform others, making them the optimal choice for PCM integration.

The full-building simulation demonstrates that the PCM positions of 341 mm and 356 mm provide the most significant energy savings and thermal comfort improvements. By maintaining lower room operating temperatures, particularly during peak summer months, and stabilising indoor conditions throughout the year, these PCM positions optimise the phase change material's potential.

c) A full year full-building heating and cooling profile for various PCM positions

The monthly maximum heating and cooling energy demand for a full-building simulation with various PCM positions is shown in Figure 4-17 to analyse the effect of PCM placement on energy consumption for both heating and cooling. The analysis covers a whole year, providing a comprehensive understanding of PCM performance in both winter and summer. It can be seen that

during the winter months (January to March and October to December), PCM integration reduced heating energy consumption by approximately 0.5 MJ compared to the no PCM case. This suggests that PCM positioned closer to the inner wall surface can efficiently store and release heat, thereby maintaining more stable indoor temperatures. In the summer months (July and August), cooling energy savings were evident for PCM positions 341 mm to 356 mm, with a reduction in cooling energy demand by about 0.2 MJ compared to the no PCM case. This indicates the PCM's effectiveness in absorbing excess heat during the day and releasing it during cooler night-time hours, thereby reducing the need for air conditioning.

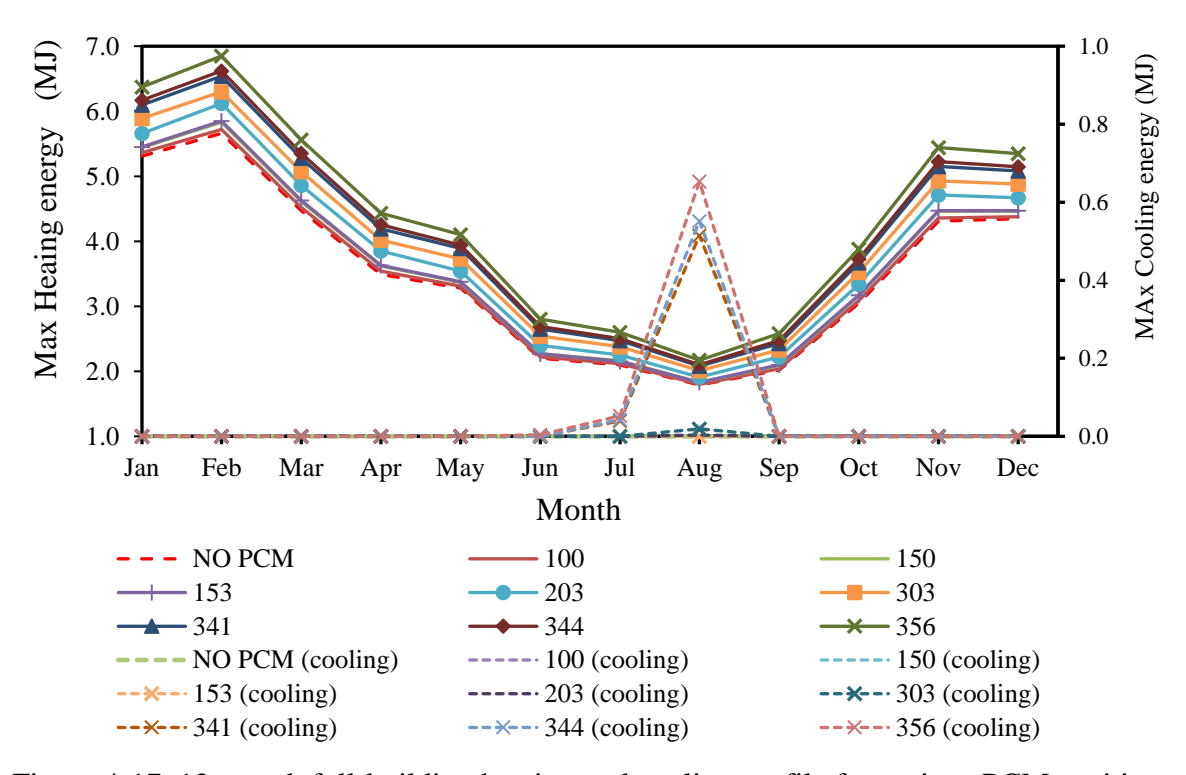


Figure 4-17. 12-month full-building heating and cooling profile for various PCM positions

A comparison between the simulated monthly and annual energy demand for full buildings at different PCM positions and the measured data from 2019 is shown in Table 4-4. It can be seen that the PCM positions between 341 mm and 356 mm have the most promising results in terms of energy savings, particularly during peak energy demand periods in January and December. In particular, PCM at position 341 yields an annual energy consumption of 49.53 MJ, representing a saving of approximately 7.5 MJ (13.12%) compared to the 2019 measured data of 57.01 MJ. Similarly, PCM positions of 344 mm and 356 mm are associated with an annual energy consumption of 50.20 MJ and 52.13 MJ, respectively, corresponding to savings of around 6.8 MJ (12%) and 4.9 MJ (8.6%),

respectively. It is evident that these positions exhibit the most consistent monthly savings, particularly in the cold months of January, February, November, and December, where heating energy demand typically peaks.

However, PCM at positions of 100, 150, 153, 203 and 303 show less energy savings and higher energy demand than the optimal PCM placements due to their proximity to the external temperatures. They are likely to fail to attain the phase change temperature. It can be seen that these positions result in annual energy demands ranging between 42.46 MJ and 47.60 MJ, indicating that the PCM at these positions does not fully utilise its phase change capabilities to absorb and release heat effectively. As a result, the energy demand for cooling and heating remains relatively high.

Table 4-4 shows that PCM at 341 mm, 344 mm and 356 mm positions are associated with the most significant reductions in energy demand, particularly in winter. Typically, PCM at position of 341 reduced the energy demand in January to 6.09 MJ, which is 0.9 MJ (12.9%) lower than the measured data. PCM at position 344 mm similarly reduced energy consumption to 6.17 MJ (11.7%) in January. PCM at position 356 achieved the least annual energy demand of 4.9 MJ (8.6%), indicating considerable energy savings, though slightly better than PCM positions 341 mm and 344 mm. it can be seen that the yearly energy demand reduction at PCM positions of 344 mm and 341 mm was 6.8% and 7.5%, respectively, reflecting a meaningful reduction compared to the baseline and non-optimal PCM positions with 26.3%.

The 14.98 MJ for no PCM configuration represents a significantly higher energy deficit compared to the measured data of 2019, indicating that the lack of a latent heat storage mechanism, which PCM configurations provide, and leads to greater temperature fluctuations and increased energy requirements to maintain indoor comfort. Without PCM, the wall lacks an effective buffer against thermal variations, resulting in reduced efficiency. These underlines both the efficacy of PCM integration in reducing energy consumption and the importance of accurate simulation to fully understand energy dynamics in building designs.

Based on the data provided, it is suggested that PCM positions between 341 mm and 356 mm are the optimal configurations for energy savings and thermal comfort, particularly during peak heating and cooling months. These positions achieve the highest annual energy savings, reaching up to 13% in the case of PCM at position of 341. The mechanism for these savings is directly related to the PCM

reaching its phase change temperature of 27°C, which allows the material to absorb excess heat during warmer periods and release stored heat during cooler periods.

Table 4-4. Comparison of Full Building Simulation Monthly and Annual Energy Demand for Various PCM Positions against 2019 Measured Data (MJ) [215]

- A f	NO	100	150	1.50	202	202	241	244	256	3.6
Month	NO	100	150	153	203	303	341	344	356	Measured
	PCM									
Jan	5.31	5.36	5.44	5.45	5.66	5.89	6.09	6.17	6.37	6.988
Feb	5.66	5.72	5.83	5.85	6.12	6.30	6.54	6.62	6.85	5.807
Mar	4.47	4.52	4.61	4.63	4.86	5.07	5.28	5.35	5.56	5.033
Apr	3.49	3.54	3.62	3.63	3.85	4.02	4.19	4.25	4.43	4.917
May	3.28	3.31	3.37	3.38	3.54	3.73	3.89	3.94	4.10	4.237
Jun	2.20	2.22	2.27	2.27	2.40	2.54	2.65	2.69	2.80	2.348
Jul	2.10	2.12	2.16	2.15	2.25	2.38	2.47	2.51	2.60	3.548
Aug	1.79	1.80	1.83	1.83	1.91	2.01	2.08	2.11	2.17	2.818
Sep	2.02	2.04	2.09	2.10	2.22	2.33	2.43	2.47	2.58	4.243
Oct	3.05	3.09	3.16	3.17	3.34	3.52	3.67	3.73	3.88	4.770
Nov	4.31	4.36	4.46	4.47	4.71	4.93	5.15	5.23	5.44	4.733
Dec	4.35	4.38	4.46	4.47	4.67	4.88	5.08	5.15	5.35	7.562
Annual	42.03	42.46	43.30	43.40	45.53	47.60	49.53	50.20	52.13	57.01
Demand	-14.98	-14.6	-13.7	-13.6	-11.5	-9.4	-7.5	-6.8	-4.9	

(1 MJ=0.27778kWh)

d) PMV and PPD Analysis with PCM

Figure 4-18 shows the Predicted Mean Vote (PMV) and Predicted Percentage of Dissatisfied (PPD) values across different PCM positions in the full building simulation. PMV and PPD are critical metrics in evaluating thermal comfort, with the acceptable PPD threshold being 20% and the ideal PMV value near zero. The PMV variation throughout the year is shown in Figure 4-18(a). The PCM positions of 341 mm, 344 mm, and 356 mm are associated with the lowest PMV values, closely tracking each other and maintaining more consistent thermal comfort. During peak summer months (July and August), the PMV values for these positions approach zero, indicating near-ideal comfort conditions, while other PCM positions show slightly higher deviations.

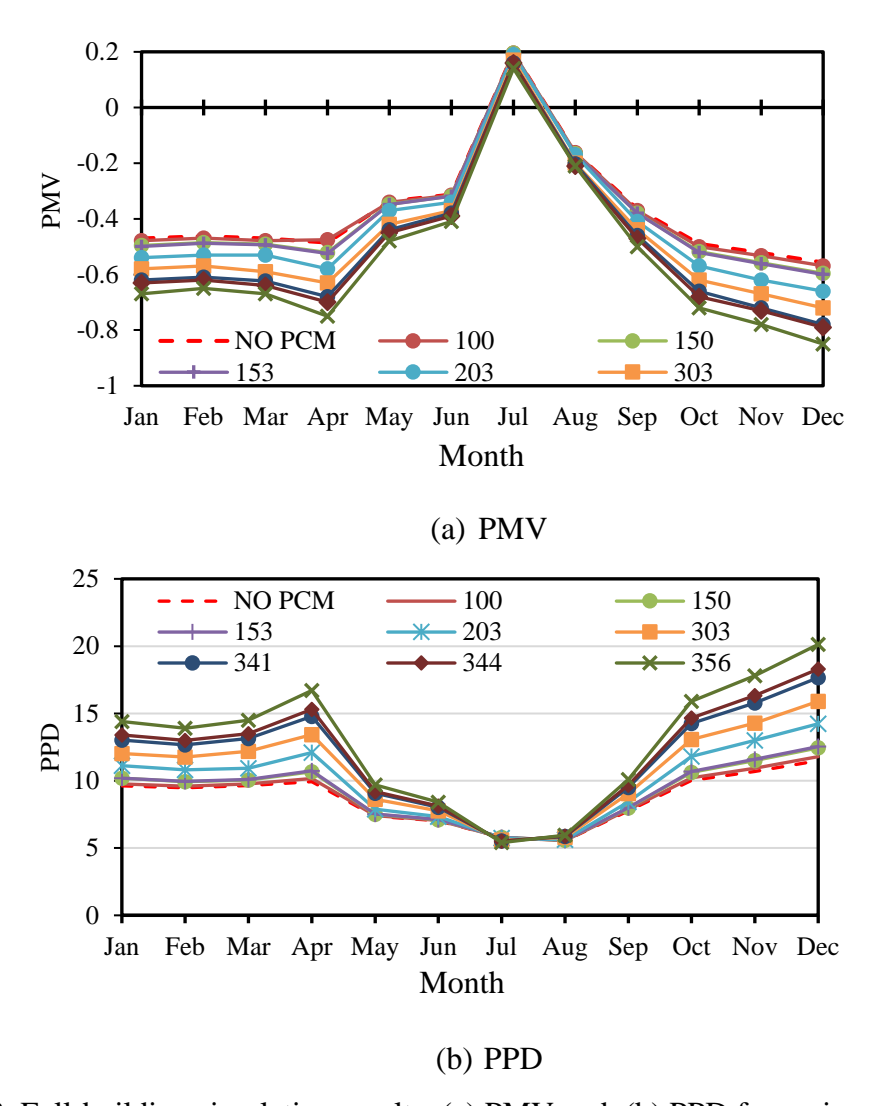


Figure 4-18. Full-building simulation results: (a) PMV and, (b) PPD for various PCM positions

Similarly, in colder months, such as January and December, these PCM positions offer better thermal performance, as evidenced by their proximity to a PMV of -0.7, indicating occupants feel cooler but within the acceptable range. However, it appears that PCM positions such as 100 mm, 150 mm, and 203 mm tend to produce less effective thermal regulation, showing PMV values further from zero throughout the year.

Figure 4-18(b) shows the PPD values. Similarly, PCM positions of 341 mm, 344 mm, and 356 mm are linked with the lowest PPD values, consistently remaining below the acceptable 20% threshold. Throughout the simulation year, these positions demonstrate lower PPD values, ensuring that a higher percentage of occupants are satisfied with the thermal conditions. Particularly during the warmer months, the PPD for the optimal positions drops to around 5%, indicating very high satisfaction with the indoor environment. In contrast, PCM positions between 100 mm and 303 mm also show low

PPD values, particularly during seasonal transitions like April and October, suggesting reduced comfort levels. However, the PCM at these positions, as seen in Table 4-4 show a high energy demand compared to the measured data in 2019, indicating that the PCM at these positions does not offer better thermal regulation due to its failure to attain phase change temperature.

Therefore, as a trade-off, PCM positions of 341 mm, 344 mm, and 356 mm provide the best thermal regulation and energy savings across different seasons. These positions consistently show low PMV values and PPD values below the 20% threshold, meeting the thermal comfort criteria while reducing heating and cooling loads. This suggests that PCM integration at these positions offers optimal energy performance and occupant satisfaction, making them the most effective configurations for PCM-enhanced building envelopes. Further investigations could explore the long-term performance of these configurations under varying operational conditions to solidify these findings.

4.4 Summary

This chapter has presented the results of dynamic simulations to evaluate the impact of Phase Change Material (PCM) integration within building walls on thermal performance and energy efficiency. Simulations were conducted using TRNSYS, focusing on different PCM positions in the wall structure, both with and without windows, to determine optimal configurations for reducing heat transfer, improving thermal comfort, and maximising energy savings.

Key performance metrics analysed include inside wall surface temperatures, room operative temperatures, heat energy transfer rates, and occupant comfort indicators such as Predicted Mean Vote (PMV) and Predicted Percentage of Dissatisfied (PPD). Baseline models without PCM served as references for comparison, allowing for a robust evaluation of PCM effectiveness.

Key Findings can be summarised as follows:

- i. The most effective PCM positions were identified between 341 mm and 356 mm from the external wall. These placements allowed the PCM to efficiently reach its phase change temperature of 27°C, optimising heat absorption and release. This significantly reduced temperature fluctuations and improved thermal comfort, making these positions ideal for maximising PCM performance.
- ii. PCM placed closer to the inner wall surface (341 mm to 356 mm) maintained inside wall surface and operative temperatures within a stable, comfortable range of 25°C to 27°C. These

- positions exhibited minimal temperature fluctuations. In contrast, PCM placed closer to the external wall surface (100 mm or 150 mm) was less effective in moderating temperature, as it struggled to reach the phase change temperature.
- Full-building simulations showed substantial energy savings with PCM integration. A specific PCM, positioned between 341 mm and 356 mm, provided annual energy savings ranging from 8.55% to 13.12%. These savings were attributed to the PCM's ability to reduce heating demand in winter and cooling demand in summer by stabilising indoor temperatures more effectively.
- iv. PMV and PPD analyses confirmed that PCM positioned between 341 mm and 356 mm delivered the most significant improvements in thermal comfort. PMV values were closer to neutral (~0.8), and PPD values dropped below the acceptable 20% threshold, ensuring occupant comfort by maintaining stable temperatures and minimising discomfort.
- v. PCM integration, especially at the optimal positions, effectively reduced heat transfer through the walls, decreasing the energy required for heating and cooling. PCM between positions 341 mm and 356 mm consistently showed lower heat transfer rates, aligning with improved energy efficiency.
- vi. The simulation model is reasonably accurate and reliable after a comparison with the experimental results (in the next chapter). The average MAPE was determined was 12.08%, which is considered as an acceptable error margin, and it was concluded that the simulation model is reasonably validated by the experimental results. The comparison between simulated data and experimental data for key PCM positions (341 mm, 344 mm, and 356 mm) yielded low error margins, with MAE values between 3.53 and 4.07, and MAPE values between 11.97% and 13.40%. The RMSE for the heat transfer rate was also 3.69, confirming the model's reliability. This indicates a degree of accuracy ensures that the simulation results are robust and can be confidently used to guide PCM integration strategies.

In conclusion, the simulation results have demonstrated that PCM placement between 341 mm and 356 mm from the external wall provides the most effective balance between energy savings and thermal comfort. The validated accuracy of the simulation results supports the reliability of these findings, offering a strong framework for optimising PCM use in building designs. Future research could further investigate the long-term performance of PCM under varying climatic conditions and explore synergies with other energy-saving technologies.

CHAPTER 5: EXPERIMENTAL ANALYSIS OF PCM INTEGRATION IN MULTI-LAYER WALLS

5.1 Introduction

The experimental validation of simulation results is a critical step in any research that seeks to apply theoretical models to real-world scenarios. This chapter details the experimental procedures conducted to assess the thermal performance of PCM-integrated wall systems, focusing on the temperature variation inside and outside the prototype, as well as across the wall layers.

This experimental approach aimed to recreate real-world building conditions, considering external factors like temperature fluctuations and internal heating requirements. This study also extended its investigation to walls incorporating glazed windows, examining how combining PCM and window systems could further optimise energy performance. The experimental findings provide an empirical validation for the earlier simulation models while offering insights into the practical challenges and benefits of PCM implementation in building designs.

5.2 Experimental Procedure

As the foundation for this study, a baseline wall model without PCM integration was constructed to assess its thermal behaviour. Subsequently, a PCM layer was subsequently introduced into various positions within the wall to observe its impact on energy consumption and thermal regulation. Using strategically placed sensors, temperature variations were measured across the wall layers, and the results were compared to the baseline, establishing the effectiveness of PCM in enhancing thermal comfort and energy efficiency.

a) Baseline Measurement

Before integrating the PCM layer, baseline temperature measurements of the wall prototype were taken across the various wall layers, including the window's inner and outer wall surfaces, to establish the prototype wall's thermal performance without PCM enhancement.

b) PCM Integration

The PCM layer was introduced into the wall at various positions, specifically at depths of 100 mm, 150 mm, 203 mm, 303 mm, 341 mm, 344 mm, and 356 mm measured from the outer wall surface. Temperature measurements were taken across the wall layers for each position to evaluate the PCM's effects on temperature regulation.

c) Data Collection

To capture temperature changes, K-type temperature thermocouple sensors were placed at strategic locations within the wall layers, including at the PCM interfaces and on the inner and outer surfaces of the window, to track the energy consumption required to maintain a stable indoor temperature of 26°C. The measurement points within the wall layers were strategically positioned at 0.5 m height (y-axis), 0.2 m depth (z-axis), and aligned along the x-axis for each individual layer. These locations ensured accurate thermal profiling and consistency with the assumption of one-dimensional heat transfer used for R-value calculations. By avoiding edge boundary effects and focusing on the central regions of the wall, the collected data provided reliable inputs for determining the thermal resistance (R-value), offering a robust connection between sensor placement and thermal performance analysis. While the chosen locations enabled precise measurement of temperature gradients and avoided edge-related inaccuracies, constraints included the inability to fully analyse three-dimensional heat flows, especially near windows. To simplify the analysis, a one-dimensional heat transfer assumption was applied. Despite these limitations, the sensor arrangement yielded reliable data on thermal gradients and PCM activation, ensuring the validity of the experimental results.

The data logger employed for the experiment operated at a 1-second sampling rate, delivering high-resolution tracking of transient and steady-state thermal behaviours. This high sampling frequency minimized errors caused by short-term fluctuations, enabling precise R-value calculations by accurately capturing heat transfer rates across the wall layers. Standard deviation analysis revealed minimal variability, such as a standard deviation of approximately ±0.6°C for PCM temperatures during steady-state conditions, confirming the reliability and consistency of the collected data. However, the rapid sampling generated a large dataset, requiring significant post-processing, which could pose challenges for extended experiments. Nevertheless, the setup proved effective for providing detailed insights into the system's thermal performance.

d) Comparison with Baseline

The data collected after PCM integration were compared with the baseline measurements to quantify the improvements in thermal performance. The impact of the PCM layer on heat transfer rates, particularly in conjunction with the window, was analysed.

e) Evaluation of Combined Effects

A combined effect of the PCM layer on energy consumption and temperature stability in both cases, the wall without a window and the wall with a double-glazed window, was evaluated. The goal was to determine how effectively the PCM in case 1 and case 2 with a window worked together to reduce heat transfer and maintain stable internal temperatures.

f) Analysis of Thermal Transmittance

The overall U-value of the wall with the integrated PCM and window was recalculated to assess any changes in thermal transmittance. This analysis helped to determine the effectiveness of the combined PCM and window setup in meeting UK Building Regulations for thermal efficiency.

5.3 PCM Wall without Window

5.3.1 Experimental Setup

A prototype wall sample, identical to the external wall of a third-floor room in a thick two-block, multi-layer external wall of a four-story CHASE FARM Hospital building in North London UK, was constructed, as shown in Figure 5-1(a)-(b), and a PCM layer was introduced into this wall sample. A 1:2 mix of cement and sieved sand was used for the mortar [216], maintaining a maximum thickness of 5mm. A series of tests were conducted to investigate the impact of integrating a PCM layer into the room's north-facing multi-layer external wall. Temperature measurements were taken across various wall layers of the prototype to evaluate the effectiveness of PCM in regulating temperatures and its energy-saving potential. The sample dimension was 1.2 m x 0.9 m x1.0 m, with a wall thickness of 384 mm, including the PCM layer, as shown in Figure 5-2(a). The total thermal transmittance value (U-value) of the wall was determined to be 0.154 W/(m².K), meeting the UK minimum standards specified in the Approved Document Part L, Dwellings 2021 Edition guidelines [217].





(a) The wall layer assembly

(b)The prototype

Figure 5-1. The prototype wall construction and assembly

The inside space of the prototype wall set-up was lagged using Rockwool between gypsum boards on all sides, including the top and bottom surfaces, allowing only one directional heat through the test wall from the inner wall surface towards the outer wall surface. An 800W (AirForce NDB-1Q-08 oil-filled radiator electric) oil heater shown in Figure 5-2(b) equipped with a thermostat was utilised to heat the space, and the indoor temperature was set to 26°C.

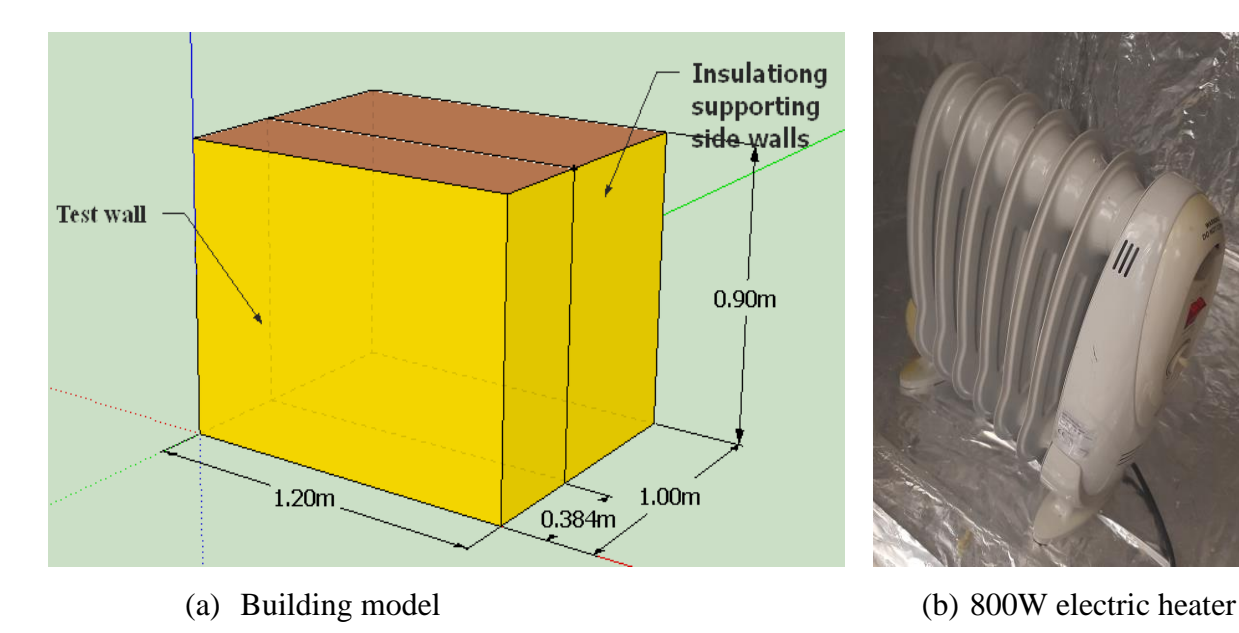


Figure 5-2. (a) Dimensions of the prototype. (b) Heater placed inside the prototype

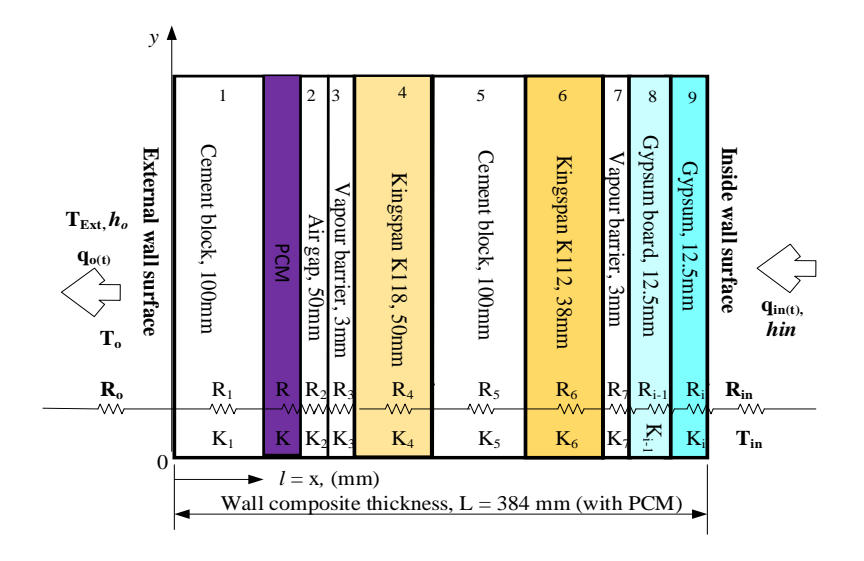


Figure 5-3. Schematic and boundary conditions in the multi-layer wall with PCM

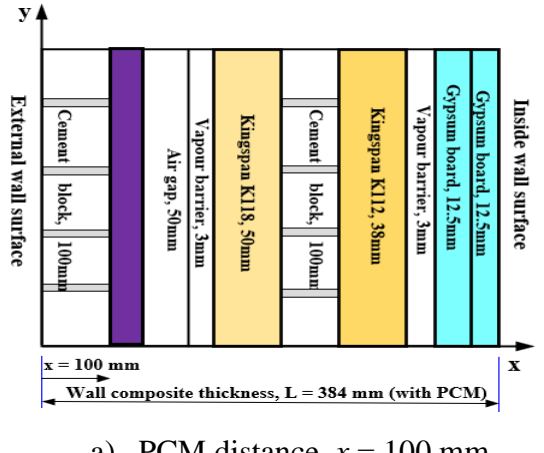
Figure 5-3 illustrates the schematic and boundary conditions of the standard wall configuration constructed in a laboratory at the University of Hertfordshire (51.7517° N, 0.2400° W). The wall assembly comprised an air gap and eight distinct layers, each serving a specific function in regulating heat transfer and maintaining thermal comfort. Temperature measurements of wall layers for various wall configurations, with and without the PCM layer, were conducted over 48-hour periodic intervals during the cold months from December to February. Data acquisition was facilitated using a Pico data logger. The temperature readings were used to calculate the overall heat transfer as seen in section 3.3.1, through the wall layers using the overall heat transfer Equation (5-1) below:

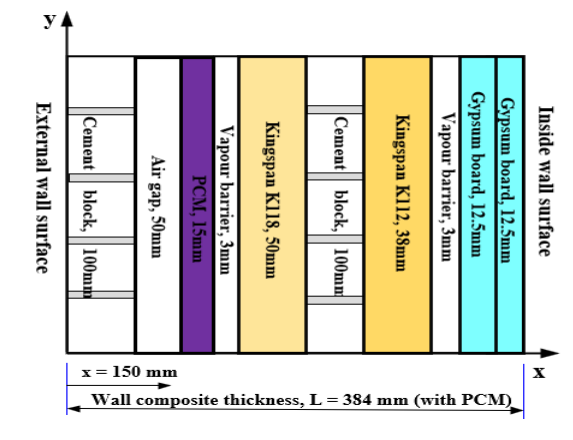
$$Q = U \times A \times \Delta T \tag{5-1}$$

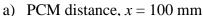
where; Q is the heat transfer (W), U is the thermal transmittance (W.m⁻².K⁻¹), A is the cross-sectional area (m²), and ΔT is the temperature change across the wall layers.

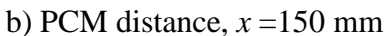
5.3.2 The Experimental Description

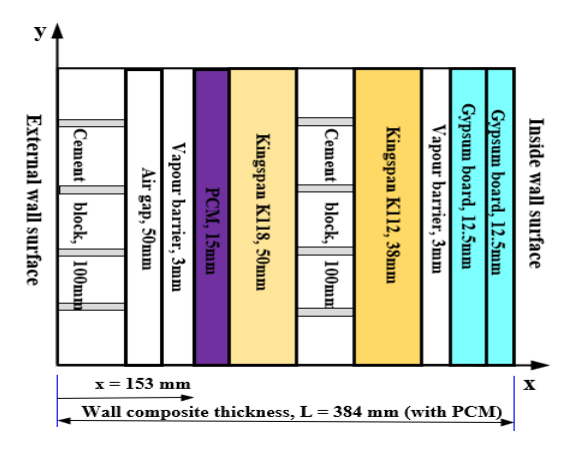
The thermophysical properties of the wall layers are shown in Table 5-1. The building materials were locally sourced and supplied by an approved University supplier.

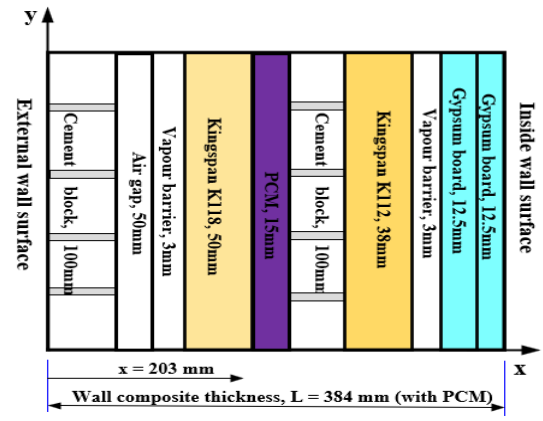






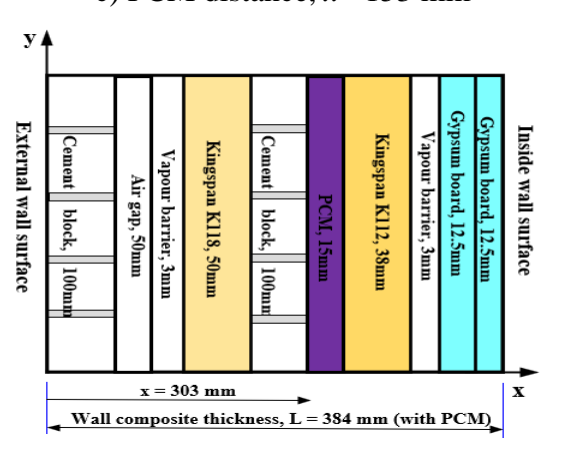


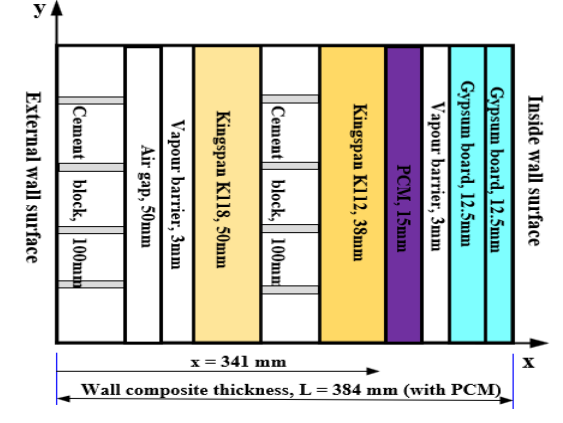




c) PCM distance, x = 153 mm

d) PCM distance, x = 203 mm





e) PCM distance, x = 303 mm

f) PCM distance, x = 341 mm

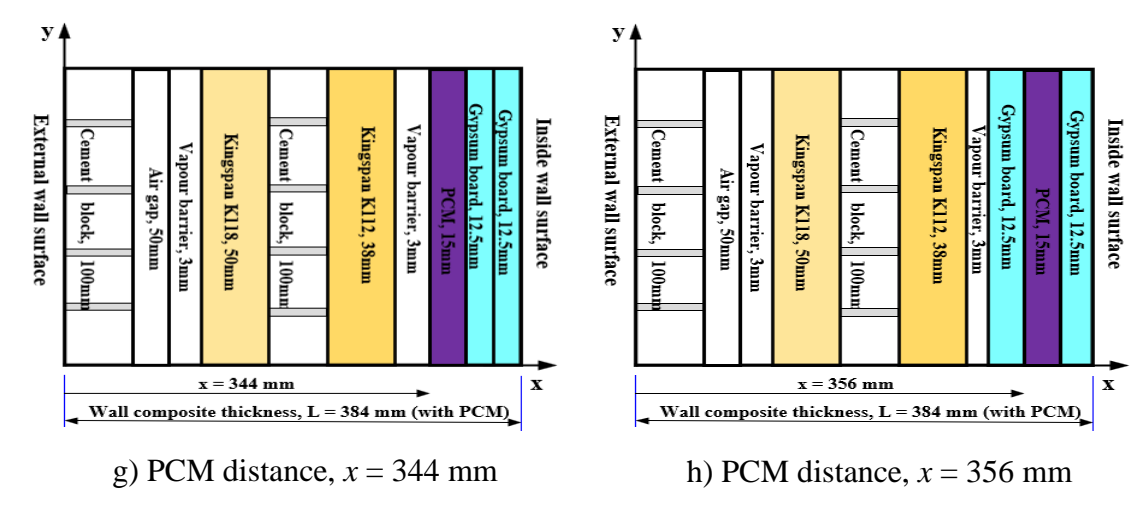


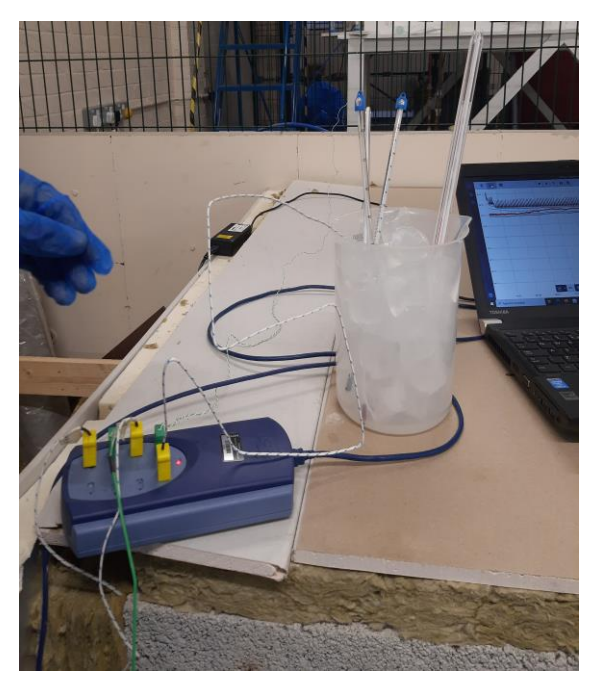
Figure 5-4. Wall configuration without window at various PCM positions

The PCM was initially positioned at x = 100mm from the wall's external wall surface and subsequently moved inwards to positions at x = 150, 153, 203, 303, 341, 344, and 356 mm, respectively, as shown in Figure 5-4 to explore all theoretical possible PCM wall positions. The convective heat transfer coefficients for the internal and external wall surfaces were 7.7 W/(m2.K) and 25 W/(m2.K), respectively. Thermal performance tests were conducted on the wall first without the PCM and subsequently with the PCM.

Table 5-1. Thermophysical Properties of the Different Layers of the Wall Construction

Layer	Layer name	Thickness,	Conductivity,	Resistance, R,	Density	Specific Heat	
		<i>x</i> (m)	k, (W.m ⁻¹ .K ⁻¹)	$(W.m^{-2}.K^{-1})$	(kg.m ⁻³)	$(kJ.kg^{-1}.K^{-1})$	
1	Outer block	0.100	1.400	0.071	1400	1.000	
2	Airgap	0.050	0.024	2.083	1.200	1.005	
3	Vapour -barrier	0.003	0.200	0.015	161.1	1.200	
4	Outer-Kingspan	0.050	0.021	2.381	40.00	1.400	
	(K118) in studs						
5	Inner block	0.100	1.400	0.071	1400	1.000	
6	Inner-Kingspan	0.038	0.021	1.810	40.00	1.400	
	(K112						
7	Vapour-barrier	0.003	0.200	0.015	161.1	1.200	
8	Outer-Gypsum	0.125	0.170	0.740	950.0	0.840	
	board						
9	Inner-Gypsum	0.125	0.170	0.740	950.0	0.840	
	board						

K-type thermocouples were used to measure the temperature of various wall layers. These thermocouples underwent in situ calibration [218], performed using ice, boiling water, and a thermobath [219, 220, 221], with observed accuracy within ± 0.5 °C (Figure 5-5). Parameters selected for validation include the interior room temperature, the inner surface wall temperature, the outer surface wall temperature, the PCM temperature, and the heat necessary to warm the room. During the tests, the experimental data was gathered using a data collector.





(a). Calibration in ice

(b). Calibration in boiling water in thermo-bath

Figure 5-5. In situ calibration of thermocouples

5.3.3 Experimental Results from PCM Wall with no Window

a) PCM temperature variations with PCM positions

Figure 5-6 illustrates the temperature variations of RT28HC a tested PCM, at different locations within the wall. As the PCM (RT28HC) was positioned closer to the heat source (inside), its temperature increased. Positions near the external wall surface of the wall (100 mm and 150 mm away from the out-surface) exhibited lower temperatures, suggesting that these positions are less effective at absorbing heat due to reduced exposure or the influence of external temperatures.

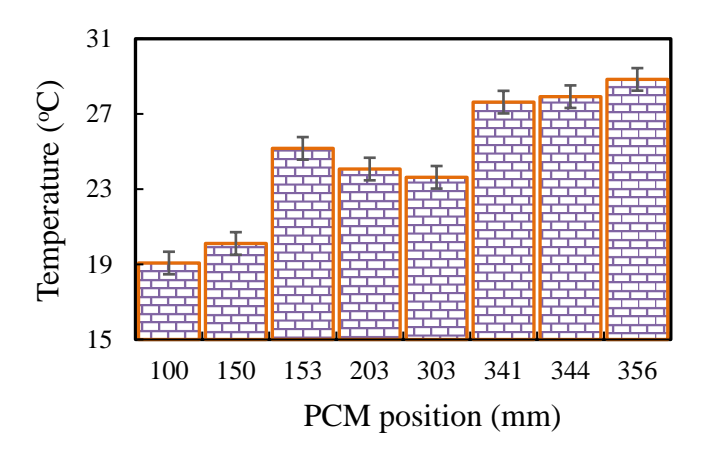


Figure 5-6. PCM temperature variation with PCM positions (measured from the wall out-surface)

A noticeable temperature increase occurred at positions 153 mm, 203 mm, and 303 mm, likely due to trapped heat in the air gap. However, the PCM at these positions did not reach phase change activity, indicating that these locations within the cement blocks are unsuitable due to lesser exposure or earlier phase change completion.

When the PCM was placed further from the external wall surface, phase changes began at position 341 mm, with temperatures ranging between 27°C and 29°C. The PCM temperature stabilised at positions between 341 mm and 356 mm, suggesting that the PCM reached its phase change threshold and was actively absorbing and releasing heat. The standard deviation of the PCM temperature during activation (27.63°C to 28.84°C) was 0.62°C, indicating minimal temperature variability and stable phase change behaviour. Therefore, positions from 341 mm to 356 mm are identified as the most effective for this PCM under the given conditions.

b) Effects of the PCM position inside the wall on temperature

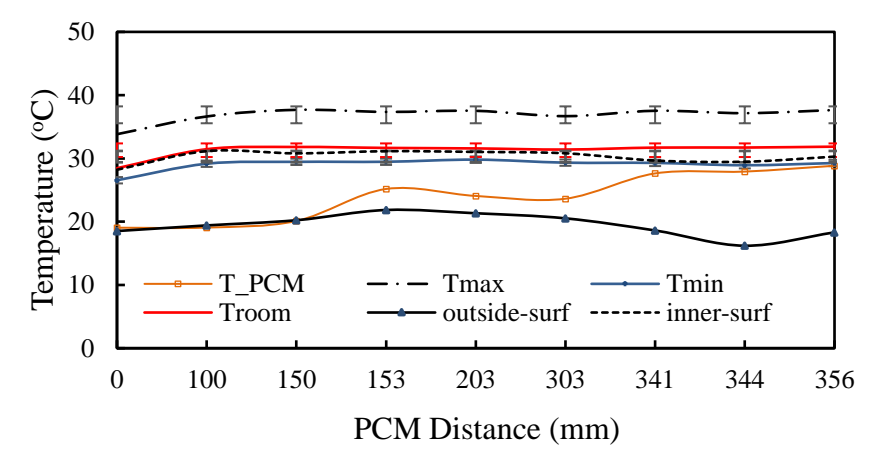


Figure 5-7. Temperature distribution against various PCM positions

Figure 5-7 shows the temperature distribution against PCM positions. It can be seen that the PCM incorporated into the wall resulted in a consistent thermal buffer of 7.9°C between the maximum and minimum room temperature values, showing flexible and astounding room-controlled environmental conditions. This regulation, as indicated by the standard deviations in Table 5-2 (1.14°C for maximum room temperature and 0.91°C for minimum room temperature), demonstrates the PCM's ability to maintain stable indoor conditions. As illustrated in Figure 5-7, the regulation of minimum and maximum temperatures by the PCM is essential during colder months and is crucial in applications prioritising maintaining a lower temperature limit over the prevention of overheating, such as certain industrial settings or climate control systems.

Table 5-2. Standard Deviation of Recorded Temperatures Across Wall Layers and Room Conditions

Measurement type	Standard deviation (°C)
Room temperature	1.02
Minimum room temperature	0.91
Max room temperature	1.14
Inner surface temperature	0.94

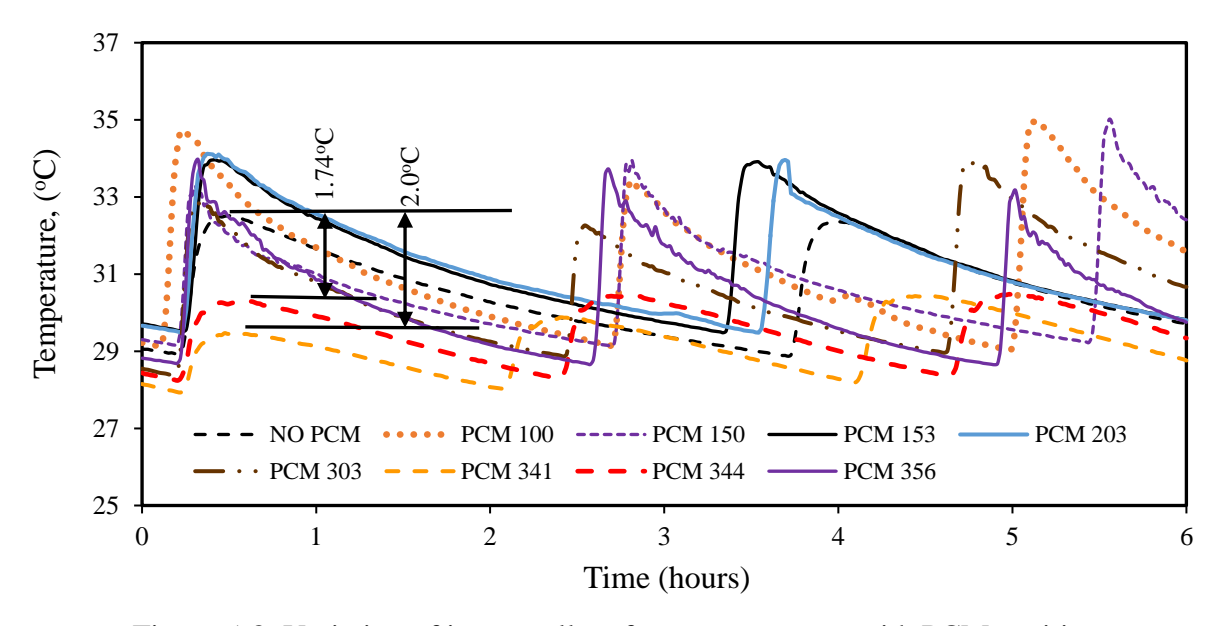


Figure 5-8. Variation of inner wall surface temperatures with PCM position

Figure 5-8 illustrates the wall's inner surface temperature variations over six hours for different PCM positions. The data shows that placing the PCM at the positions of 341 and 344 in the multi-layer wall significantly reduced the temperature amplitude on the inner surface compared to that of the wall without PCM. This positioning greatly influenced the ability to regulate inner surface temperatures. A more uniform temperature on the inner surface enhances indoor thermal comfort. When compared with the wall without any PCM, the peak temperature flow decreased by 2.0°C at the PCM position range of 341 and 1.74°C at that of 344, an indication that this leads to energy savings of 5.3% to 6.2%.

c) Temperature distribution across various PCM wall configurations

Figure 5-9 shows temperature gradients from the outer to inner wall surfaces, indicating greater heat loss without PCM (gradient of 1.4469). PCMs near the outer surface (100 mm, 150 mm and 153 mm positions) have limited impact on inner wall temperatures but improved thermal regulation by absorbing and delaying heat transfer as the PCM acted as an insulation layer. Mid-layer PCM positions (203 mm, 303 mm away from the wall out-surface) provided better temperature moderation with low-temperature gradients of 0.9905 and 0.9727, respectively. The PCM acts as a passive insulation layer but poses installation challenges for retrofitting Victorian-era buildings, making them uneconomical. PCMs positioned closer to the inner surface (at 341 mm, 344 mm & 356 mm) effectively maintained high-temperature gradients of 0.9984, 1.478 and 1.273, respectively, as the PCM reached its phase change temperature, actively absorbing and releasing heat into the inner space. The PCM at 341 mm demonstrated moderate temperatures, with a temperature gradient of 0.9984, highlighting its efficiency in balancing heat transfer and thermal regulation. Therefore, as a trade-off, the optimal PCM placement was determined to be 344 mm from the wall out-surface for efficient thermal regulation and easier installation, considering environmental conditions, desired temperatures, and wall properties.

The R^2 values in Figure 5-9 indicate the integrity of fit for the temperature distribution across wall layers for different PCM positions. PCM at 341 mm achieved a relatively a high R^2 value of 0.9522 (Figure 5-9(g)), followed closely by PCM at 344 mm (R^2 = 0.9685, Figure 5-9(h)) and PCM at 356 mm with the highest R^2 = 0.9714 (Figure 5-9(i)). These values reflect effective thermal regulation, strong temperature stability, and their impact on maintaining indoor thermal comfort. PCM at 344 mm demonstrates superior linearity in temperature distribution, ensuring optimal heat absorption and release while balancing the internal environment. Although PCM at 356 mm exhibits a slightly higher

temperature gradient (1.273), indicating more pronounced heat flux near the inner surface, all positions contribute to reducing temperature fluctuations, enhancing occupant comfort and overall thermal performance.

It can be seen from Figure 5-9 that the temperature gradients and R² values demonstrate that the effectiveness of the PCM layer is significantly influenced by the arrangement of surrounding wall layers, which affect heat transfer and temperature regulation. Conductive materials enhance heat transfer, increasing the PCM's responsiveness, while insulating layers slow the process, improving its buffering capability. Key factors such as proximity to heat sources, layer thickness, air gaps, and the alignment of phase change temperatures also play critical roles. A well-designed layer arrangement is essential for maximizing PCM efficiency and achieving optimal energy savings.

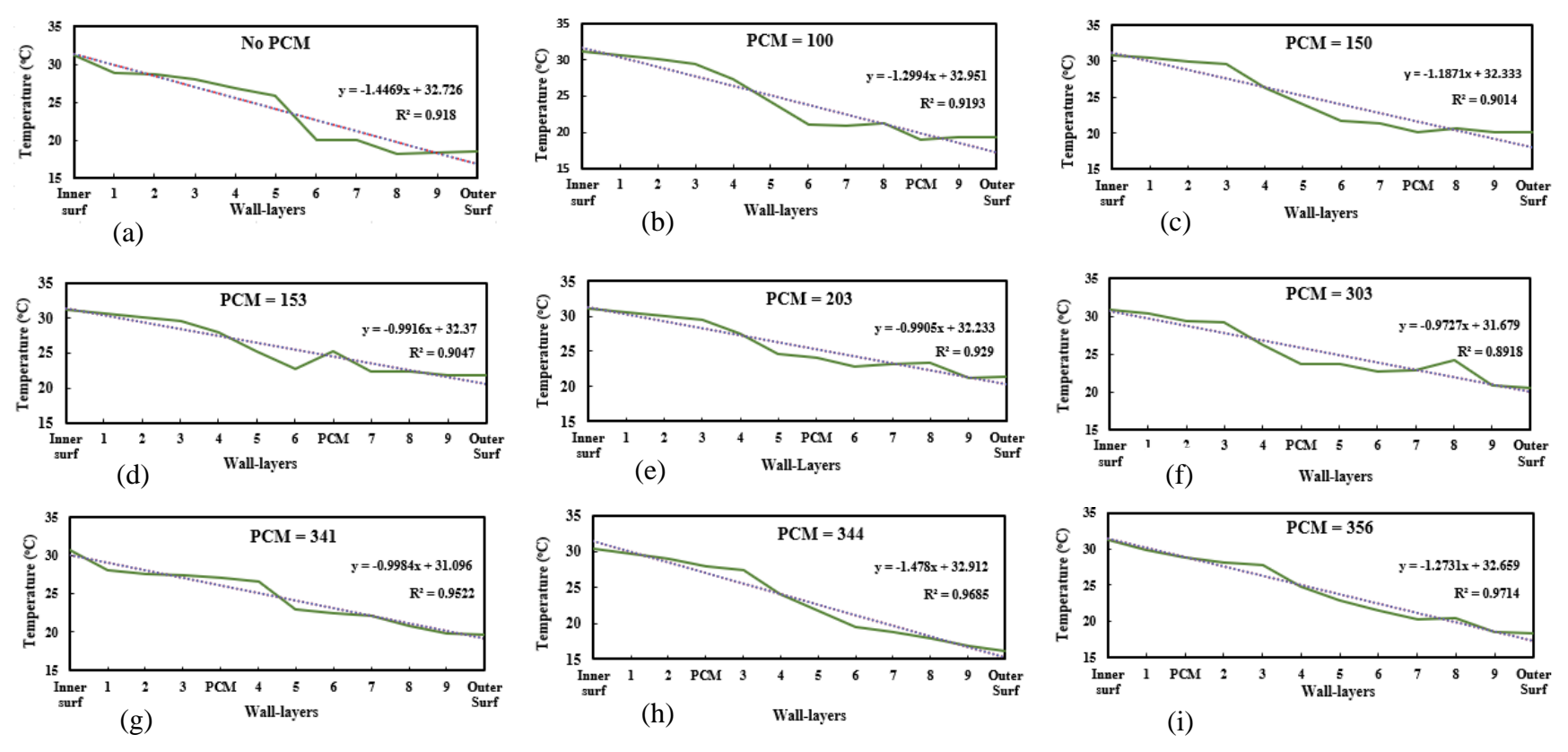


Figure 5-9. Temperature distribution across the wall thickness against PCM position

d) The effect of PCM position on heat transfer across the wall

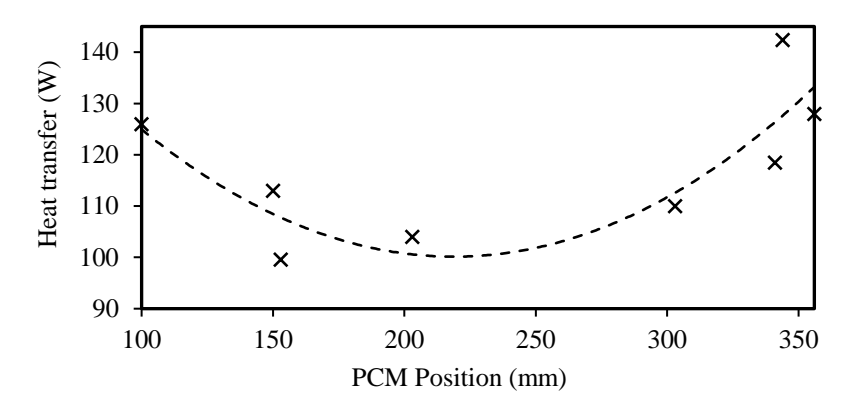


Figure 5-10. Variation of PCM position on heat transfer across the wall

Figure 5-10, delves into the PCM position's effect on heat transfer calculated using Equation (5-1), across the wall, highlighting the parabolic relationship between PCM positions within the wall and heat energy transfer. The graph vividly illustrates this relationship, showing a gradual decrease in heat transfer as the PCM is shifted from the 100 mm position to approximately 203 mm, reaching a minimum around this midpoint. Beyond the 203 mm position, as the PCM position nears the 356 mm position, the heat transfer begins to rise again, forming the other half of the parabola.

At the 100 mm PCM position, closer to the outer wall, there is a notable heat energy transfer, likely because the PCM is effectively absorbing incoming heat from the outdoor environment and becoming saturated too early during sharp temperature episodes, leading to increased heat transfer across the rest of the wall. Conversely, the significant heat transfer observed towards the end of the curve at the PCM positions 341 mm, 344 mm, and 356 mm suggests that heat is absorbed and stored in the PCM. This process diminishes its effectiveness in moderating the temperature gradient across the wall but helps to stabilise indoor temperatures. As the PCM is at its phase change temperature at these positions, it acts as a thermal buffer by absorbing excess heat from the indoor environment and releasing it back when the indoor temperature drops. This behaviour indicates that strategically placing PCM near the interior while ensuring it is effectively insulated from external temperature swings can optimise the thermal regulation properties of buildings.

Heat transfer is less pronounced in the middle positions compared to the outer regions of the wall. As observed earlier in Figure 5-6, the PCM in these positions does not reach the required phase change temperature. Without this phase change, the latent heat absorption and release processes, essential for maximising the PCM's thermal buffering capacity, are not fully activated. Consequently, the PCM

may primarily act as sensible heat storage, which limits its efficiency in stabilising heat transfer. Therefore, the reduction in heat transfer observed in these middle positions can be attributed to the PCM serving more as an additional insulation layer rather than providing the full benefits of thermal regulation through phase change. While there are still some energy savings, the PCM's optimal thermal performance is not achieved due to the absence of the phase change.

Therefore, based on these results, the hypothesis is that placing the PCM closer to the interior of building walls while insulating it from external temperature variations will enhance thermal regulation in the room. This configuration will stabilise indoor temperatures by allowing the PCM to absorb excess heat when indoor temperatures rise and release it when they drop. Such an approach enhances temperature and reduces energy consumption in a targeted and efficient manner, thus serving as a crucial strategy in a sustainable building design under BS EN ISO 15251:2007 for the indoor environmental criteria [222].

5.4 PCM Wall with a Window

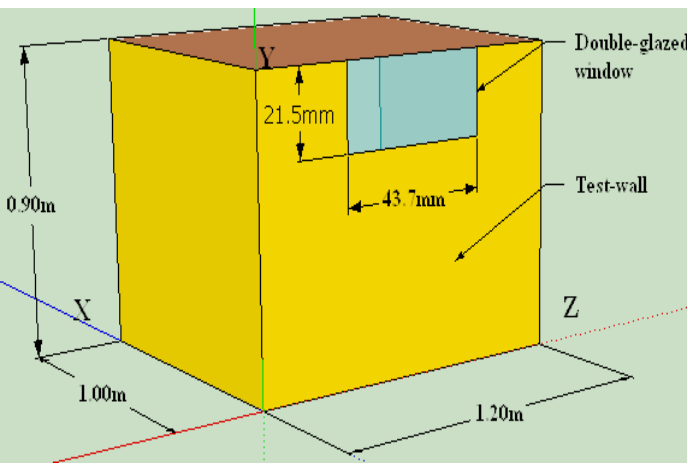
5.4.1 Experimental Setup

The experimental setup for the wall with a window followed the same procedure as the wall without a window, with adjustments made to accommodate the inclusion of a double-glazed window. The primary objective remained to investigate the impact of integrating a PCM layer into a multi-layer external wall and to assess its temperature regulation and energy-saving potential.

5.4.2 Experimental Description

A prototype wall sample was constructed, similar to the external wall of a third-floor room in a thick two-block, multi-layer external wall of a four-story North London building. The wall included a double-glazed window, as shown in Figure 5-11. A PCM layer was introduced into this wall sample to evaluate its performance alongside the window.





- a) The prototype wall integrated with a double-glazed window
- b) PCM prototype wall model with a doubleglazed window

Figure 5-11. PCM Prototype wall integrated with a double-glazed window

The wall was constructed using a 1:2 mix of cement and sieved sand for the mortar [176], with the thickness maintained at a maximum of 5mm. As shown in Figure 5-11, the sample dimensions were 1.2 m x 0.9 m x 1.0 m, with a wall thickness of 384 mm, including the PCM layer and the window with properties shown in Table 5-3. The total thermal transmittance value (U-value) of the wall, including the window, was determined to be 1.95 W/(m²·K), following UK Building Regulations [25].

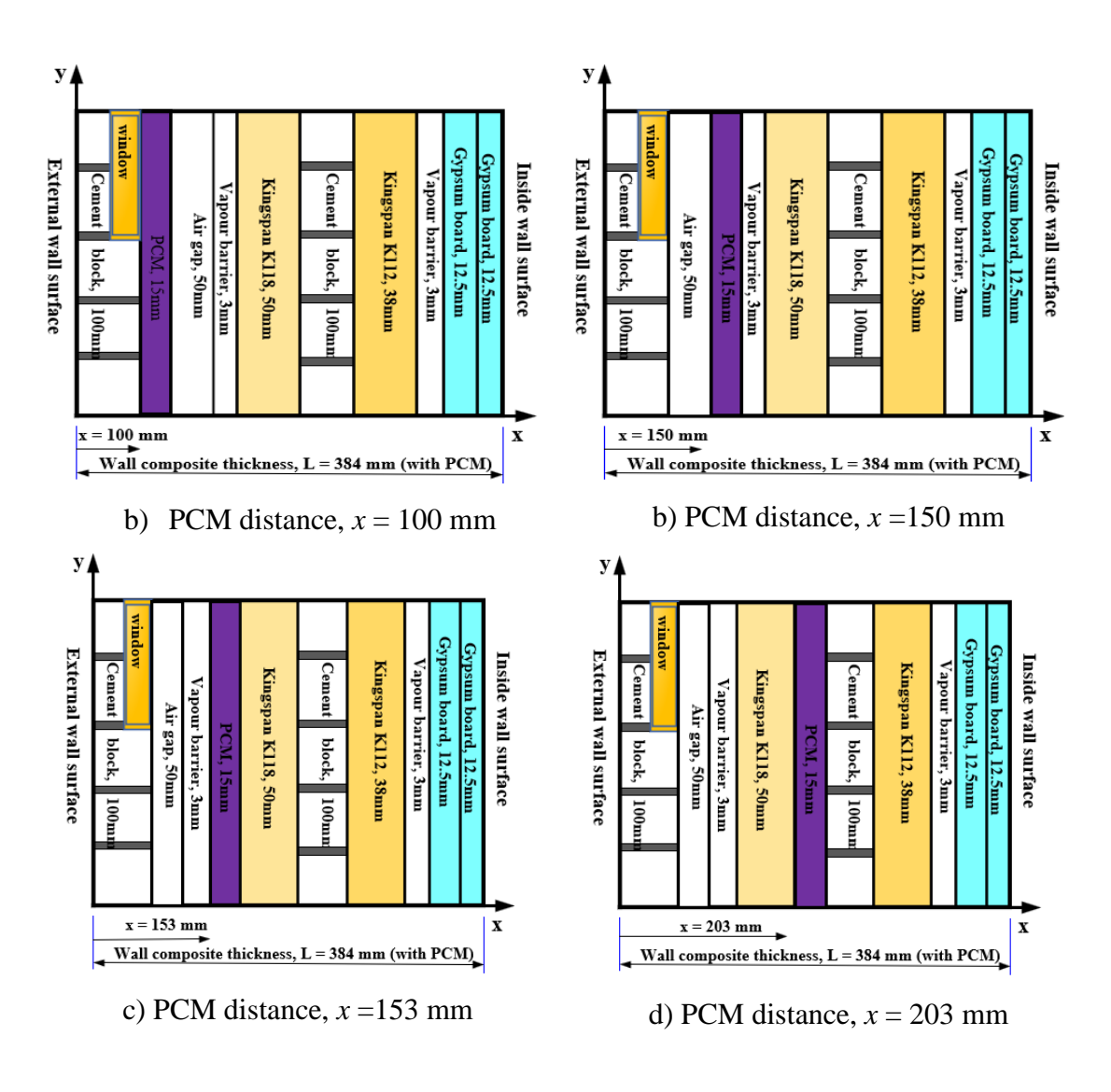
Table 5-3. The Window Properties

Property	Glass	Air
Thermal Conductivity, k (W.m ⁻¹ .K ⁻¹)	0.8	0.025
Density, ρ (kg.m ⁻³)	2500	1.225 (at sea level, 15°C)
Specific Heat, C _p (J/kg.K)	840	1005
Thickness (mm)	5	12.5

The inside space of the prototype wall setup was lagged using Rockwool between gypsum boards on all sides, including the top and bottom surfaces, allowing only one directional heat flow from the inner wall surface towards the outer wall surface. The window, measuring 43.7mm by 21.5mm, was composed of two clear 5mm thick glass panes with a thermal conductivity of 0.8 W/mK, a density of 2500 kg/m³, and a specific heat of 840 J/kg.K. It was positioned at the centre of layer 1 and its centre was 0.5m in y-axis in the yz plane of the wall, as depicted in Figure 5-11, ensuring that its impact on heat transfer could be accurately measured. An 800W (AirForce NDB-1Q-08 oil-filled radiator

electric) oil heater equipped with a thermostat was utilised to heat the inside space of the model. The indoor temperature was set to 26°C to replicate typical room conditions and assess the PCM layer's effectiveness in regulating temperature in conjunction with the window.

Numerous tests were conducted, the first on the wall without PCM (baseline), then the wall with PCM. The PCM layer was initially positioned at x = 100mm from the wall's outer surface and then systematically manually moved inwards in subsequent tests to positions x = 150, 153, 203, 303, 341, 344, and 356mm between the wall layers, as shown in Figure 5-12. The PCM was strategically placed between individual wall layers, utilizing the boundaries or splits to evaluate how material properties and thermal gradients influence its performance, thereby identifying the optimal placement within wall assemblies for practical applications without compromising the thermal and structural integrity of the multi-layer wall [223]. Additionally, the structural integrity of the wall remained unaffected by this integration [224].



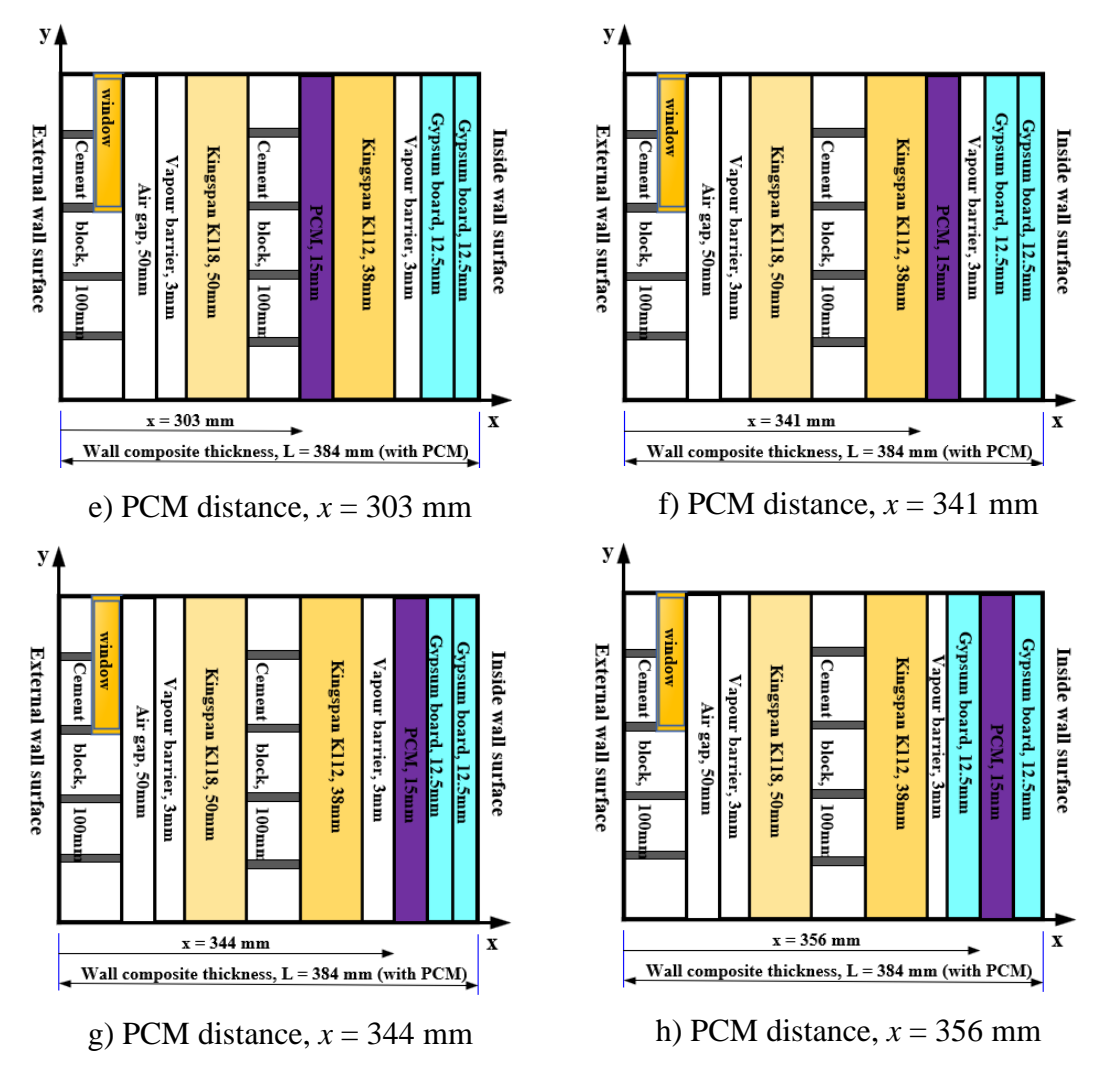


Figure 5-12. Wall configuration with window at various PCM positions

5.4.3 Experimental Results from PCM Wall with Window

a) Variation of PCM temperature across different PCM Positions in Multi-Layered wall configuration

As shown in Figure 5-13, the temperature of PCM generally increased as it was positioned closer to the heat source (inside). Notably, at position 341mm, the PCM temperature (T_PCM) rose sharply and subsequently exhibited a more stable trend, maintaining a temperature above 27°C from 341mm to 356mm. This temperature stabilisation indicates that the PCM had reached its phase change threshold. These findings suggest that positions between 341mm to 356mm are the most effective for thermal regulation in this PCM wall.

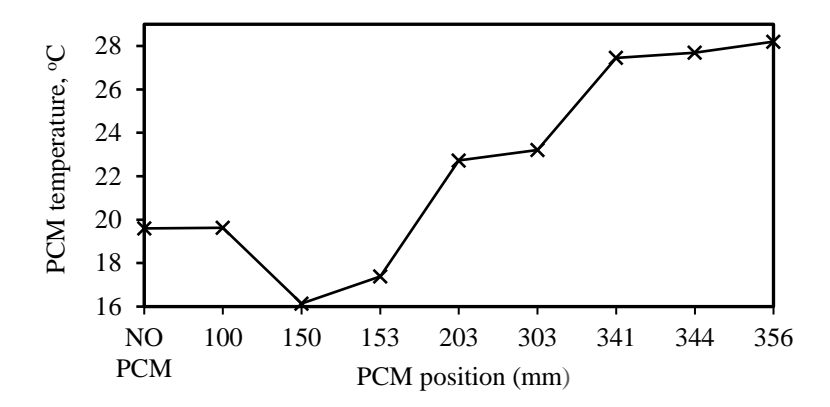


Figure 5-13. Variation of PCM temperature across different PCM positions

b) Effects of the PCM positions inside the wall on temperature

Figure 5-14 illustrates the relationship between PCM positions and the temperature under various external conditions. It appears that the temperature varies with the distances of the PCM layer from the external wall surface, ranging from 0 mm (No PCM) to 356mm. The experiment setup maintained the external temperature (Ext) consistently lower than the interior temperature, demonstrating the building envelope's effectiveness in insulating the interior from external climatic conditions, particularly when enhanced by the PCM layer.

It can be seen that when the PCM was positioned farther from the external wall, the room temperature slightly increased before stabilising, particularly beyond the 203mm mark. This trend indicates an improved thermal regulation within the room, with the PCM effectively absorbing excess heat during peak temperatures and releasing it during cooler periods. Although the PCM temperature exhibited fluctuations, it generally trended upwards with increased distance from the external wall, reaching notable peaks at positions of 341mm, 344mm, and 356mm. These peaks suggest optimal PCM positions where phase change processes are most effective, allowing for substantial energy absorption and release cycles. The inside surface wall temperature (inside-surface-wall temp) remained relatively stable and closely mirrored the trend of room temperature (Troom). This stability highlights the PCM's crucial role in maintaining a consistent thermal profile of the building's interior surfaces.

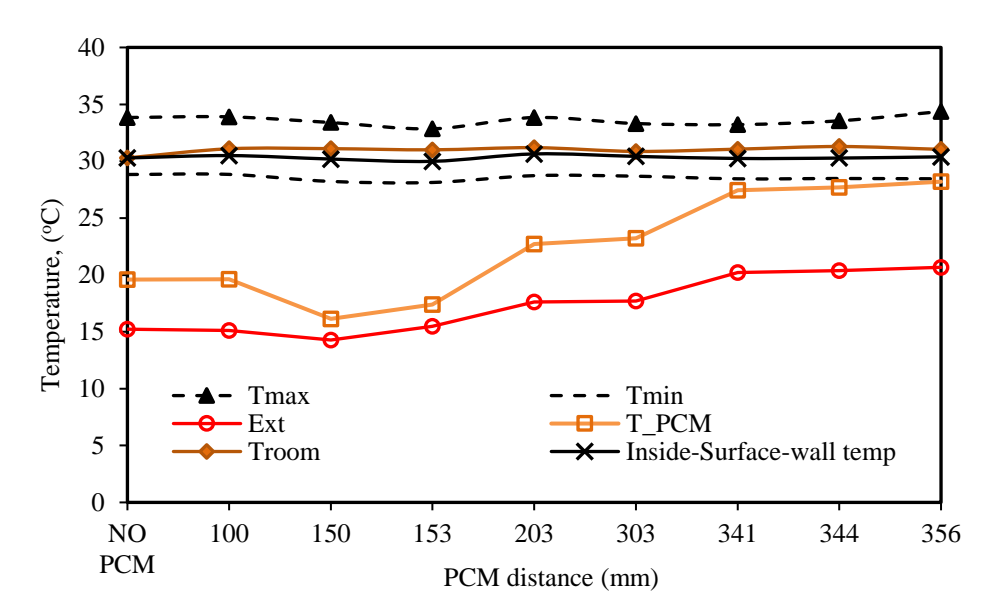


Figure 5-14. PCM and temperature variations for various PCM positions with various external conditions

This analysis indicates that positioning the PCM layer between 341mm and 356mm from the external wall surface provides optimal temperature regulation. This range is characterised by effective phase change activities, as demonstrated by the significant peaks in PCM temperature (T_PCM) and the corresponding stable room temperature profiles. These observations suggest robust phase change cycles and enhance the thermal regulation within this range. Consequently, integrating PCM strategies with existing HVAC systems is recommended to further optimise energy savings. By leveraging PCM's ability to stabilise indoor temperatures, it is possible to reduce the load on heating and cooling systems, leading to more efficient energy use.

c) Temperature distribution across various PCM configurations

A set of graphs shown in Figure 5-15(a)–(i), provide a detailed analysis of temperature distribution across wall layers for various PCM positions, including a "No PCM" baseline. The "No PCM" baseline Figure 5-15(a), has an R² value of 0.9512, indicating a strong correlation that may validate this analytical approach. It can also be observed that the temperature gradient (1.8018) of the "No PCM" baseline wall configuration is highest, suggesting significant temperature variation across the wall layers, which results in less effective thermal regulation.

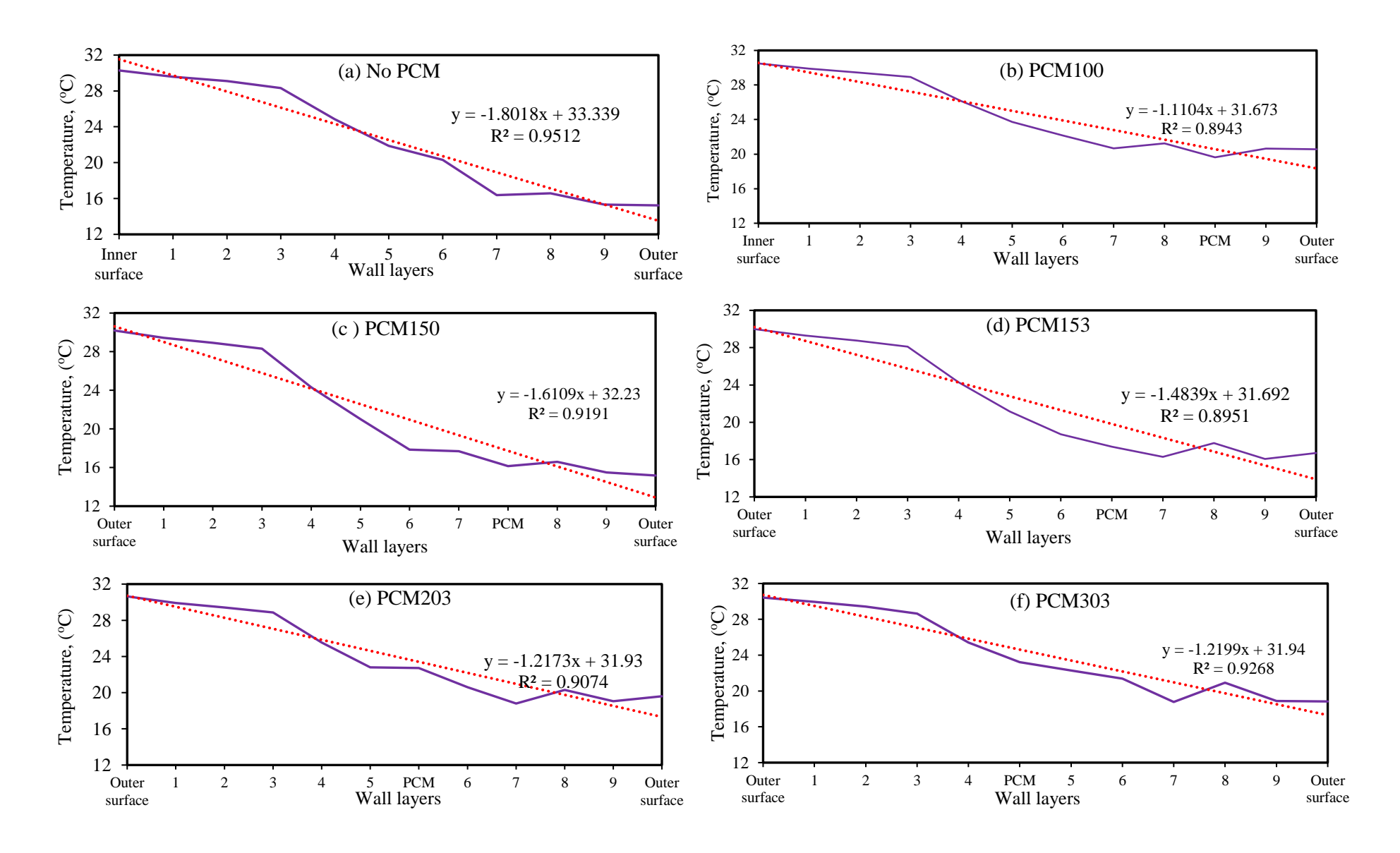
Similarly, the temperature gradients for PCM positions from 100 mm to 303 mm (Figure 5-15(b)-(f)) are relatively higher compared to those for PCM positions of 341 mm to 356 mm (Figure 5-15(g)-(i)). This indicates that PCM positions closer to the inner surface (341 mm to 356 mm) provide better

thermal regulation. PCM positions of 341 mm to 356 mm exhibit smoother temperature gradients across the wall layers compared to other PCM positions and the "No PCM" scenario. These positions show a less consistent reduction in temperature from the inner surface to the outer surface. This gradual temperature reduction benefits energy savings by indicating a more effective thermal barrier to heat transfer. With less heat passing through the wall, the indoor environment remains cooler, reducing the reliance on active cooling systems (e.g., air conditioning), directly translating into energy savings.

As shown in Figure 5-15(g), the temperature profile at PCM 341 mm remains smooth and consistent, with minimal fluctuation, making it a favourable position for reducing thermal transmission. With an R² value of 0.9418, the linear trend fit confirms a reliable and steady temperature reduction. Similarly, the PCM 356 mm configuration, shown in Figure 5-15(i) has an even stronger fit with an R² value of 0.9474, indicating an even smoother overall temperature distribution. This stability is, crucial for preventing rapid heat loss or gain, particularly when a double-glazed window is part of the structure, as shown in Figure 5-15(j), which illustrates that PCM positions from 341 to 356 mm show consistent temperature gradients and R² values. Windows are generally weak thermal weak points, and placing PCM layers closer to the inner surface (PCM positions from 341 mm to 356 mm) helps counteract additional heat transfer caused by the window.

By strategically placing PCM layers near the inner portion of the wall (positions from 341 mm to 356 mm), the wall can better regulate the flow of heat both in and out of the building, effectively offsetting any potential heat gains or losses through the window.

It is evident that PCM positions from 341mm to PCM 356 mm offer the most optimal positions for maximising energy savings and ensuring indoor comfort, especially in walls with double-glazed windows.



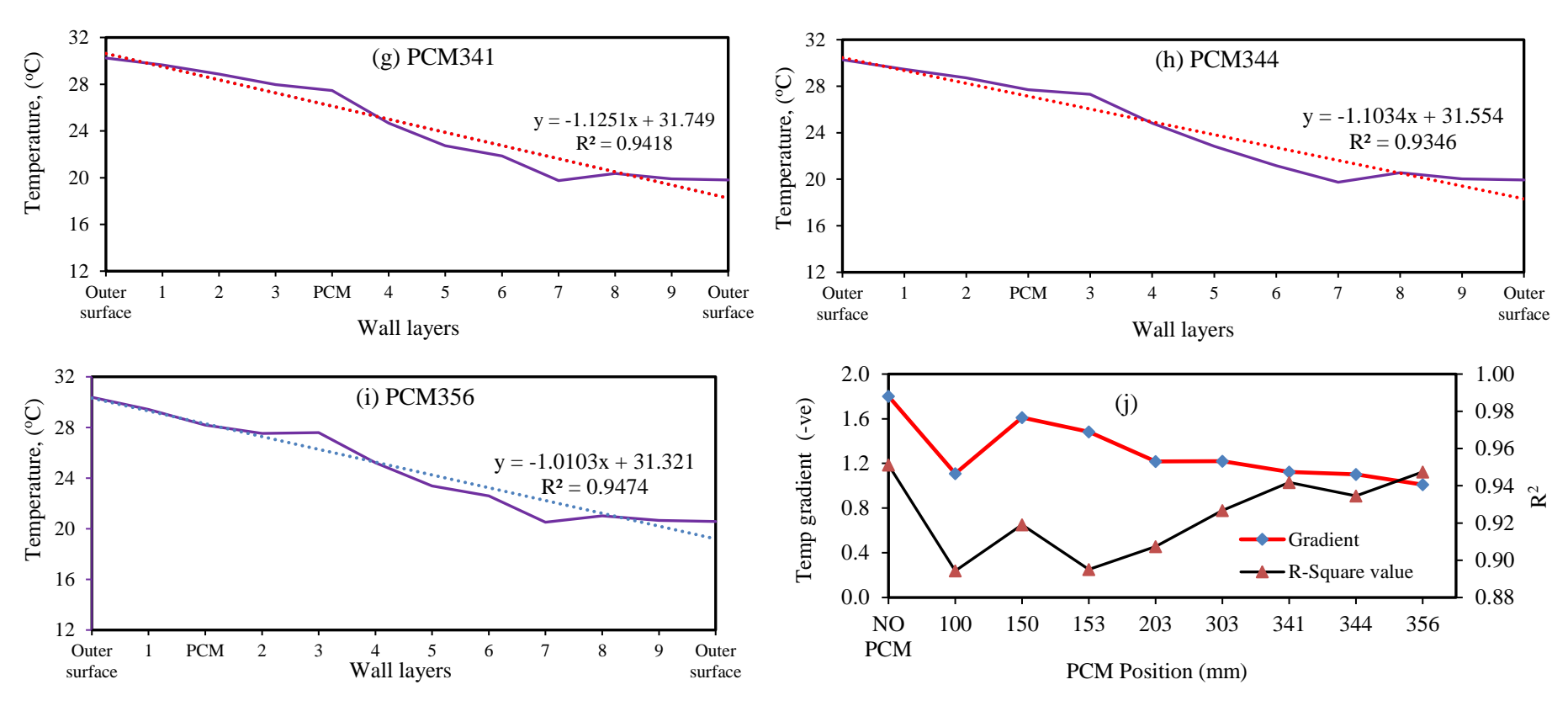


Figure 5-15. (a)-(i) Temperature distribution across various PCM configurations. (j) Temperature gradient with various PCM positions

- d) PCM position effects on energy transfer, consumption and savings
 - i). Energy transfer across the wall

The overall heat transfer rate through the wall layers and glass window can be calculated using Fourier's law in Equation (5-2) [225].

$$q_{wall/window} = -k \cdot A \cdot \frac{dT}{dx} \tag{5-2}$$

where q is the heat transfer rate (W), k is the thermal conductivity (W/mK) of layer material, A is the cross-sectional area (m²), and dT/dx is the temperature gradient across the wall layer.

The individual layer thermal resistance, R_i , and wall's total thermal resistance, R_{wall} , were calculated using Equation (5-3) [226, 225]:

$$R_i = \frac{x_i}{k_i \cdot A_i}, \qquad R_{wall} = \sum_{i=1,2,...n}^{n} R_n$$
 (5-3)

where i is the i^{th} layer, n is the number of wall layers.

The thermal resistances of glass, R_{glass} , and glass air cavity, R_{air} , were calculated as follows:

$$R_{air_gap} = \frac{x_{air}}{k_{air}.A}$$
, $R_{glass} = \frac{x_{glass}}{k_{glass}.A}$ (5-4)

where k_{glass} and k_{air} , are the thermal conductivities of glass and air, respectively. And x_{glass} and x_{air} , are the thickness of glass and air, respectively.

The total thermal resistance of the window, R_{window} , was calculated using Equation (5-5).

$$R_{window} = 2R_{glass} + R_{air_gap}$$
(5-5)

The total heat transfer rate can be obtained (W)

$$q_{total} = q_{wall} * A_{wall} + q_{window} * A_{window}$$
(5-6)

Table 5-4. Heat Transfer Rate and Energy Consumption Rates at Various PCM Positions

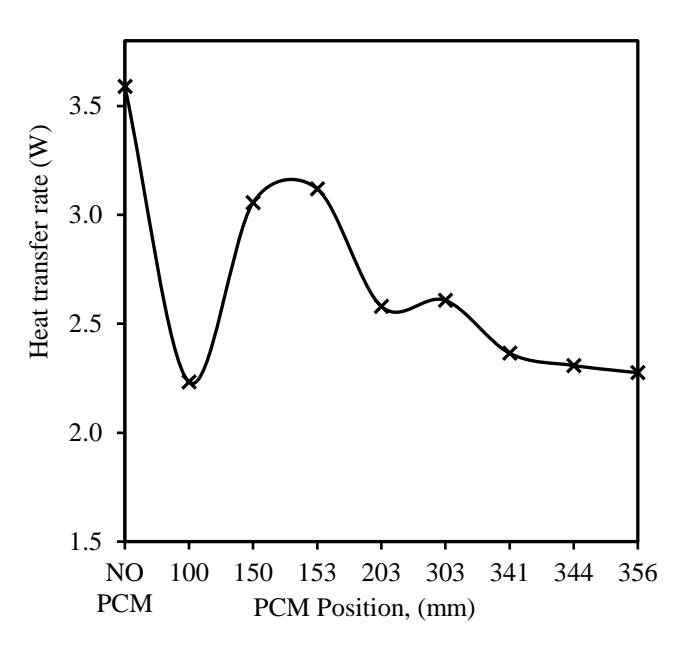
PCM Position	Resistance,	Heat transfer,	24hr Energy
	x/k , $(m^2.K/W)$	q (W)	consumption, E (wh)
NO PCM	6.594	3.59	86.28
100	6.669	2.23	53.575
150	6.669	3.06	73.4
153	6.669	3.12	74.9
203	6.669	2.58	61.9
303	6.669	2.61	62.6
341	6.669	2.37	56.8
344	6.669	2.31	55.4
356	6.669	2.28	54.6

The heat transfer rate in Table 5-4 calculated using Equations (5-3) to (5-6) relative to the PCM position from the origin shown in Figure 5-16(a), is depicted in Figure 5-16(b). It can be seen in Figure 5-16(b) that the data reveal that the heat transfer rate exhibits a sinusoidal pattern as the PCM position shifts from the outer-wall surface (the origin) to the inner-wall surface, indicating a wave-like variation in heat transfer. The baseline heat transfer rate, observed at approximately 3.59W without PCM (at the origin), is the highest. Notably, the most significant reduction in heat transfer rate, down to 2.23W, occurs at the PCM position of 100 mm, which corresponds to the valley of the sinusoidal curve. The positions between 100 mm and 150 mm represent the physical air gap where the PCM effectively extends the air gap further toward the inner wall, contributing to reduced heat transfer.

Heat loss from the interior that passes through the air gap encounters the PCM before reaching the external wall layer. This arrangement allows the PCM to act as an additional thermal buffer, reducing the overall heat transfer rate through the wall and suggesting that an optimal placement zone exists for maximising efficiency. However, previous temperature analysis has shown that PCM activation occurs between positions 341mm and 356 mm, where the PCM has reached its phase change temperature and actively absorbs and releases heat.

Figure 5-16(b) shows that up to the PCM position of 153 mm, the heat transfer rate rises to a peak that remains lower than the baseline. This indicates that the PCM at this position is less effective due to suboptimal thermal dynamics. The heat transfer rate increases slightly from PCM positions





- (a). Layered wall construction
- (b). Variation of PCM position on heat transfer

Figure 5-16. Effects of PCM positions: (a). Layered wall construction, (b) Heat transfer rate versus wall PCM position across the wall

of 203 mm and 303 mm, suggesting that while effectiveness is maintained, it is less pronounced compared to position of 153 mm. The PCM reaches its activation temperature zone nearer the inner wall surface, at positions of 341 mm, 344 mm, and 356 mm where the heat transfer rates are 2.37 W, 2.31 W, and 2.28 W, respectively. These values are comparable to those observed at position of 100 mm, suggesting that these locations also represent potentially effective areas for PCM placement.

It was observed that the sinusoidal behaviour of the heat transfer rate, as shown in Figure 5-16(b), was linked to the periodic thermal dynamics of the PCM during phase changes. This behaviour resulted from the cyclic heat absorption and release, thermal equilibrium cycles, and the interaction between the heat flux and the PCM temporary equilibria, leading to periodic fluctuations in heat transfer rates. The overall trend of declining heat transfer after the initial peak suggests an exponential fall-off in maximum heat losses, attributed to thermal saturation and enhanced insulation. This sinusoidal characteristic coupled with the exponential fall-off, indicates effective thermal management and holds significant potential for applications in energy-efficiency building designs.

Based on the analysis of the data in Figure 5-16, an empirical and hypothetical equation that models the observed trend, combining a decaying exponential function with a sinusoidal component, can be proposed as follows:

$$y = A e^{-Cx} \times Sin(Bx + D) + E$$
 (5-7)

where y is the PCM heat transfer rate (W), x is the PCM position (mm), A is the amplitude (W), B is the frequency (mm⁻¹), C is the decay (mm⁻¹), D is the phase shift, radians (rad), and E is the vertical shift (W).

The model's accuracy was validated by comparing the predicted values of heat transfer rates with the experimental data, yielding a low sum of squared residuals of 0.78. The mean absolute error (MAE) was 0.0244, and the Root Mean Squared Error (RMSE) was 0.09 [227]. Using the Excel solver, as summarised in Table 5-5, the values of variables A, B, C, D, and E in Equation (5-7) were obtained as 13.55603, 0.000020234, 0.1458, 0.0749, and 2.53, respectively. The model's accuracy is supported by generally low squared residuals between the observed heat transfer rates and fitted values, especially at key PCM positions such as 0 mm, 203mm, and 303mm to 356mm. These positions show more significant residuals, and the overall fit remains reliable, with moderate residuals at the recommended PCM positions of 341mm to 356mm, indicating a reasonable match. This consistency across most positions justifies the reliability of Equation (5-7) in predicting heat transfer rates, supporting its prediction in optimising PCM integration for thermal comfort and energy efficiency.

Using the fitted model under these conditions, the heat transfer rate, y, at any given PCM position, x, can be calculated using Equation (5-8).

$$y = 13.6 e^{-0.015x} \cdot Sin(0.000020234x + 0.0749) + 2.53$$
 (5-8)

This newly developed equation could be a significant advancement in understanding and predicting the behaviour of PCM in advanced energy-efficient building designs. Its applicability extends to other buildings, provided the thermal conductivity (K) and thermal diffusivity properties are comparable to those under which the equation was derived. When these thermal properties align, the model remains valid even for walls with different thicknesses or lengths, offering flexibility for broader application across varied architectural and material contexts.

Table 5-5. Excel Solver to Show Fitted Values and Square Residuals

PCM position	Heat Transfer	Fitted	Squared
(mm)	Rate (W)	values (W)	Residuals
0	3.59	3.55	0.002
100	2.23	2.77	0.291
150	3.06	2.65	0.167
153	3.12	2.64	0.227
203	2.58	2.59	0.00003
303	2.61	2.54	0.004
341	2.37	2.54	0.030
344	2.31	2.54	0.052
356	2.54	2.54	0.068

Its validation through the transient heat conduction equation for a semi-infinite solid and Fourier's law, which typically results in an exponential decay of temperature with distance, highlights the novel contributions of this investigation. There is a notable resemblance between this equation and Equation (3.15) for the effective heat conductivity found in the work of Yu et al [228]. Furthermore, Equation (5-8) not only accurately reflects the exponential decay in heat transfer rate with increasing PCM distance from the outer-wall wall surface but also incorporates a sinusoidal component that captures the periodic fluctuations associated with PCM phase transitions. This innovative combination effectively models the complex thermal behaviour observed, providing a robust support for the accuracy and originality of the findings.

ii) Energy consumption across the wall and

The energy savings from incorporating the PCM layer into the wall were analysed by comparing the energy consumption with and without the PCM layer. The energy consumption and energy savings were calculated using the formula given in Equations (5-9) and (5-10).

Energy consumption,
$$E = Q_{total} \times Time$$
 (5-9)

Energy Savings (%) =
$$\frac{E_{without\ PCM} - E_{with\ PCM}}{E_{without\ PCM}} \times 100$$
 (5-10)

where Q_{total} is the total heat transfer rate (W).

The energy consumption at different PCM positions is shown in Figure 5-17, where the baseline energy consumption without PCM is the highest at 86.3Wh. It can be observed that adding the PCM

layer significantly has reduced energy consumption across all wall configurations as the PCM is moved from the outer-wall toward the inner-wall. The PCM position at 100 mm shows the lowest energy consumption at 56.3Wh, indicating that this configuration is the most effective in reducing energy usage. However, the PCM had not yet reached its phase change temperature in this position.

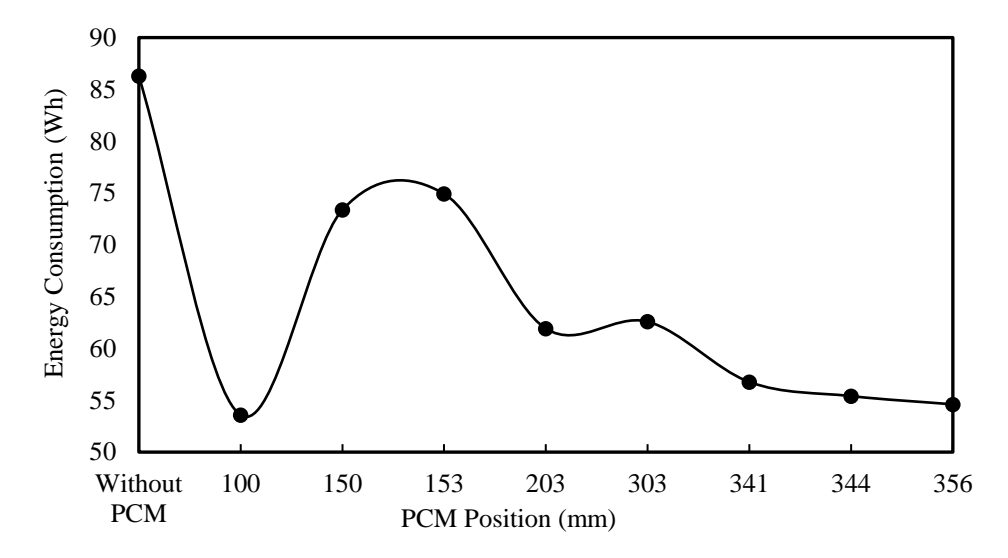


Figure 5-17. Energy consumption for various PCM positions

The PCM configurations at 150 mm and 153 mm show high energy consumption, measured at 83.06 Wh and 83.12Wh, respectively, making them the least effective compared to other positions. The high energy consumption is likely due to the PCM's proximity to the external wall surface, which allows greater heat absorption and traps heat in the air gap on warmer days.

PCM at positions of 203 mm and 303 mm exhibits relatively low energy consumption but not the lowest. In contrast, PCM configurations at 341 mm, 344 mm, and 356 mm demonstrate significantly low energy consumption, indicating that these positions are highly effective. These findings underscore the critical role of PCM positioning in enhancing building energy efficiency. By providing empirical data on various PCM configurations, Equation (5-8) could be used for valuable guidance in designing energy-efficient and thermally comfortable buildings.

iii) Energy savings and Cost-Benefit Analysis of PCM Integration in Multilayer Walls
Table 5-6 shows the energy consumption and the percentage of energy savings at different PCM
positions within the wall relative to the baseline energy consumption without PCM. The data indicate
that the PCM position at 100mm achieves the highest energy savings at 38%. However, as the prior

experimental observation pointed out, the PCM at this position had yet to reach its phase change temperature. The PCM in this position effectively increased the thermal mass and pushed the air gap further to the inner wall. As a result, any heat loss from the interior passing through the air gap encountered the PCM before reaching the external wall layer, thereby enhancing the wall's thermal buffering capacity.

Table 5-6. PCM Positions with Corresponding Energy Saving in Percentages

PCM position	Energy consumption (Wh)	Energy savings (%)	Cost Savings/m ² (£/m ²)
No PCM	86.3	-	-
100	53.6	38%	0.002085
150	73.4	15%	0.000821
153	74.9	13%	0.000726
203	61.9	28%	0.001557
303	62.6	27%	0.001511
341	56.8	34%	0.001881
344	55.4	36%	0.001970
356	54.6	37%	0.002021

As shown in Table 5-6, PCM positions of 150 and 153 are associated with the lowest savings (15% and 13%), indicating that these positions are less effective. By contrast, the PCM positions in the range of 341 to 356 show high energy savings, ranging from 34% to 37%. The consistently high savings across these positions suggest that the PCM layer's effectiveness is not solely dependent on a single position but a range of positions close to the interior. PCM positions 100 to 303 show higher energy savings due to temperature differences, but they are not ideal for retrofitting. The PCM does not reach its activation temperature in these positions, and installing it would require breaking the walls, making it impractical and costly. Therefore, despite the savings, these positions are not favourable for practical energy efficiency applications.

To evaluate the cost-benefit relationship of implementing PCM multilayer walls in historic buildings, energy consumption data for various PCM positions was compared to a baseline without PCM. Using the Ofgem Gas tariff of £0.0689/kWh [229], energy savings per square meter were calculated, with PCM341, PCM344, and PCM356 achieving savings of £0.00188/m², £0.00197/m², and £0.00202/m², respectively, as shown in Table 5-6.

The energy costs were calculated as follows:

Energy Savings (kWh) =
$$\frac{Energy\ Savings\ (Wh)}{1000}$$

For example, PCM 100

Energy Savings
$$(kWh) = \frac{(86.3 - 53.6)}{1000} kWh$$

Energy Savings $(kWh) = \frac{32.705}{1000} = 0.032705 kWh$
Cost Savings $(£) = 0.032705 \times 0.0689 = £0.002252$

From Figure 5-2(a), the prototype wall area perpendicular to the heat flow = 1.08m

Cost Savings per
$$m^2 \left(\frac{\pounds}{m^2}\right) = 0.002252/_{1.08} = £ 0.002085/m^2$$

Cost Savings per $m^2 \left(\frac{\pounds}{m^2}\right) = 0.002252/_{1.08} = £ 0.002085/m^2$ (5-11)

The other position PCM cost savings are calculated in the same manner and summarised in Table 5-6. Although the financial savings are modest, they highlight incremental energy efficiency improvements influenced by factors such as installation costs, retrofitting complexities, material properties, climate conditions, and wall construction types. This study underscores PCM's potential as a sustainable retrofitting solution, providing a foundation for further lifecycle cost analysis while aligning energy efficiency goals with the preservation standards of historic buildings.

5.5 Experimental Construction Challenges and Their Impact on PCM Wall Performance

During the construction of the prototype wall, several challenges arose, influencing the experimental outcomes. A key issue was ensuring precise alignment of the wall layers, particularly the PCM layer, to maintain consistent thermal contact and minimize thermal bridging. Misalignments could cause localized thermal anomalies, so spacers were used to ensure uniform placement during assembly. Integrating the double-glazed window presented additional difficulties due to potential air gaps and thermal leaks at the junction with the wall. A high-performance thermal stability sealant (-40°C to +120°C) was applied to eliminate air leakage and ensure accurate measurements near the window interface. Material compatibility issues also emerged, particularly due to differing thermal expansion rates between the PCM and surrounding materials. To address this, a PCM with a low thermal expansion coefficient (0.0008 1/°K) was selected to maintain consistent contact.

Moisture management was critical, as PCM is prone to moisture-related degradation. Vapour barriers and moisture-resistant aluminium compact storage modules were used to protect the PCM layer, preserving its thermal properties. Sensor network assembly and calibration also proved time-intensive, requiring careful pre-testing of thermocouples to ensure accurate and reliable data collection.

A significant logistical challenge was the delayed delivery of PCM materials, which reduced the experimental timeline and pushed testing into March and April as temperatures began to rise. While this limited the ability to fully assess the system under consistently cold conditions, colder days during this period provided sufficient data to evaluate system performance effectively.

Despite these challenges, the implemented mitigation strategies ensured reliable results. The prototype wall successfully simulated real-world conditions, demonstrating the potential of PCM-integrated walls for energy-efficient applications.

5.6 Summary

A detailed experimental investigation is presented to evaluate the thermal performance and energy efficiency of PCM-enhanced walls, particularly emphasising the optimal positioning of PCM layers for maximum energy savings and temperature regulation. The results from these experiments were compared to the earlier simulations presented in Chapter 4 to assess the accuracy of the models and identify the best strategies for PCM integration.

The key findings can be summarised as follows:

i. PCM Integration and Temperature Regulation

A PCM layer within the wall was subsequently introduced at various depths (100 mm, 150 mm, 203 mm, 303 mm, 341 mm, 344 mm, and 356 mm away from the wall's outer surface). The experimental results indicated that PCM positions closer to the interior (341 mm to 356 mm) were the most effective in stabilising indoor temperatures. The PCM maintained its phase change temperature at these depths, actively absorbing and releasing heat. This resulted in a consistent thermal buffer of 7.9°C between the maximum and minimum room temperatures, enhancing indoor comfort. For instance, the PCM at the 341 mm and 344 mm positions, reduced the peak temperature by 2.0°C to 1.74°C, respectively, thereby boosting air-conditioning performance and reducing energy consumption by 5.3% to 6.2%.

ii. Heat Transfer

For the wall without a window, the experiments revealed a parabolic relationship between the PCM positions and heat transfer rates, as illustrated in Figure 5-10. The heat transfer was lowest at the 100 mm PCM position (2.23 W) but increased as the PCM was positioned deeper within the wall, particularly near 341 mm and 356 mm.

As far to the wall with a window, the key highlight of the experimental investigation was the derivation and validation of a newly developed empirical formula, Equation (5-8), which models the heat transfer rate as a function of PCM position. This equation combines a decaying exponential function with a sinusoidal component, as given below:

$$y = 13.6 e^{-0.015x} \cdot Sin(0.000020234x + 0.0749) + 2.53$$

where y represents the PCM heat transfer rate in watts (W), and x is the PCM position in millimetres (mm). This equation accurately captures the sinusoidal fluctuations in heat transfer caused by PCM phase changes and the exponential decay as the PCM is positioned deeper in the wall. The experimental data confirmed the predictive power of this equation, with a strong correlation between the measured and predicted values, validating its utility for optimising PCM placement for efficient thermal management.

iii. Energy Consumption and Savings

For the wall incorporated with a window, PCM integration significantly reduced energy consumption across all tested wall configurations. The PCM positioned at 100 mm from the outer wall achieved the highest energy savings (38%), but the phase change threshold had not been reached at this position. The PCM configurations closer to the interior (341 mm to 356 mm) achieved slightly lower energy savings (34-37%) but were more effective in thermal regulation. This demonstrates that PCM placement deeper within the wall, particularly between 341 mm and 356 mm, optimises temperature stabilisation and energy savings. The analysis also revealed that the energy consumption without PCM was 86.3 Wh, while the most effective PCM configurations reduced consumption to as low as 54.6 Wh.

iv. Impact of PCM on Walls with Glazed Windows

When the wall was tested with a double-glazed window, PCM integration continued to demonstrate its thermal benefits. The PCM in positions closer to the interior (341 mm to 356 mm) effectively mitigated additional heat transfer caused by the window, contributing to lower energy consumption and improved thermal comfort. These positions provided smoother temperature gradients across the wall layers, especially in the presence of weak thermal points like windows.

This experimental work has demonstrated the significant potential of PCM integration to enhance thermal performance and energy efficiency in building walls. The strategic placement of PCM layers, particularly between 341 mm and 356 mm from the outer surface, was shown to optimise energy savings and temperature regulation. The new empirical formula Equation (5-8) as a predictive model for heat transfer rates further strengthens the findings, offering a practical method for determining the ideal PCM placement in real-world applications. These experimental results, in conjunction with the earlier simulation outcomes, provide valuable insights into the use of PCM for sustainable building design and energy efficiency improvement.

CHAPTER 6: DISCUSSION

6.1 Introduction

In this chapter a comparison between the simulation and experiment results has been carried out to assess the models' accuracy and reliability in predicting thermal performance and energy savings. Various PCM positions within the wall have been identified and the optimal configuration for energy efficiency and occupant thermal comfort has been identified. The effectiveness of integrating Phase Change Materials (PCMs) into multi-layered walls has been evaluated by a combined discussion of the simulation and experimental findings. This chapter has also investigated how the optimal PCM configuration can be extended to full-building simulations, comparing these results with actual building energy consumption data from 2019 as a reference to establish the benefits of PCM integration. It provides a comprehensive analysis of how PCM integration can improve building performance and contribute to energy efficiency.

6.2 An Analysis of Thermal Performance

This section evaluates the wall's thermal performance by analysing the simulated and experimental inside surface wall temperature distributions. The analysis focuses on comparing the thermal behaviour at different PCM positions for both the prototype wall without a window and that with a window to determine the impact of PCM integration on temperature regulation and energy efficiency.

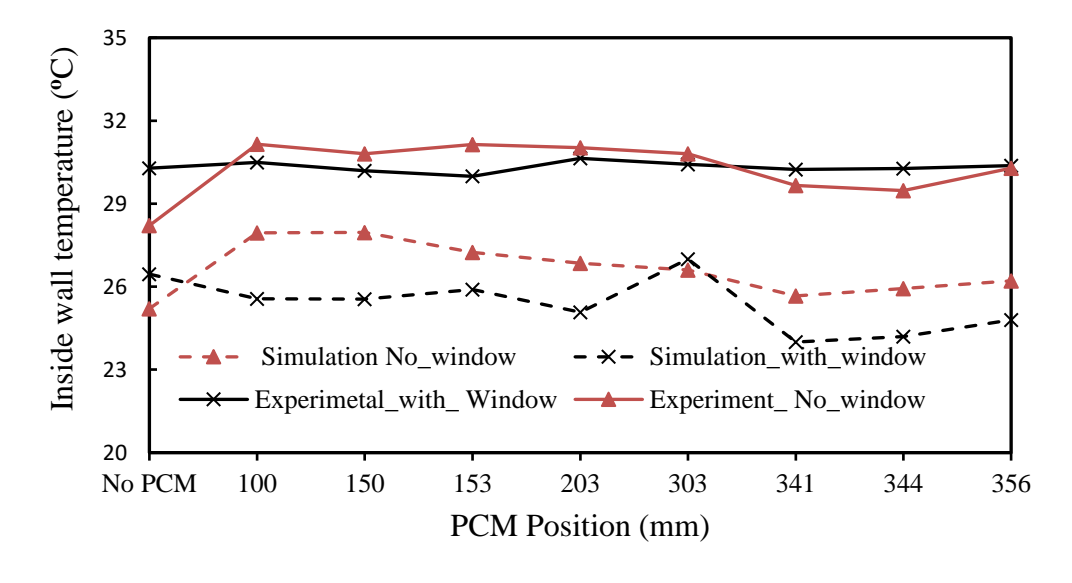


Figure 6-1. Inside wall temperature versus variation with PCM positions

Figure 6-1, shows the temperature distributions across the wall layers from both the simulation and experimental results, comparing a wall with and without a window at various PCM positions.

PCM at positions from 100 mm to 153 mm

In evaluating the thermal performance, the simulation and experimental results show elevated temperatures in these positions, often exceeding the PCM's phase change temperature of 27°C. The PCM in this region is unable to provide effective thermal buffering, leading to higher wall layer temperatures and less stable thermal performance. The wall with a window also shows even higher temperatures in this region, confirming that the window exacerbates heat transfer issues at shallow PCM depths. The window in this case allows more heat transfer into the structure, thereby diminishing the PCM's potential to reduce heat gain effectively. These positions are therefore, suboptimal for energy savings and thermal comfort.

PCM at 203 mm to 303 mm

As the PCM is positioned deeper within the wall, both simulations and experimental results show a general improvement in temperature regulation. Temperatures approach 27°C, especially in the wall with a window, where heat transfer is more pronounced. However, the PCM at these positions does not consistently maintain temperatures below 27°C, which indicates that the PCM is not fully activated. While these positions offer moderate improvements, they do not deliver optimal thermal performance.

PCM at 341 mm to 356 mm

The best thermal performance is observed when the PCM is placed between 341 mm and 356 mm, close to the inner wall surface. Both the simulation and experimental results confirm that temperatures are maintained close to or below 27°C in this region. The PCM is fully activated, allowing optimal heat absorption and release, stabilising wall layer temperatures. This holds for the wall both with and without a window, although the presence of the window results in slightly higher temperatures. These positions are the most effective in reducing heat transfer, enhancing energy savings, and maintaining indoor thermal comfort.

Therefore, both simulation and experimental results indicate that PCM placement near the inner wall surface, particularly between 341 mm and 356 mm, provides the best thermal performance. This

optimal PCM position allows the material to fully activate its phase change properties, stabilising wall temperatures and reducing heat transfer.

6.3 Performance Metrics

6.3.1 Error Metrices for Validation

The validation utilised and calculated three key error Metrics: Mean Absolute Error (MAE), Mean Absolute Percentage Error (MAPE), and Root Mean Square Error (RMSE) [166]. These metrics are crucial to comprehensively understanding the discrepancies between the simulated and measured values. The average deviation of the simulation from the actual data is determined by analysing the MAE. MAPE gives insight into the percentage error relative to the actual values, highlighting the accuracy of the simulation in relative terms. Finally, RMSE measures the standard deviation of the residuals, indicating how closely the simulation aligns with the actual measurements.

a) Mean Absolute Error (MAE)

Mean Absolute Error (MAE) is a statistical metric used to measure the average magnitude of errors in a set of predictions without considering the direction of the errors (whether they are positive or negative). MAE is calculated as the average of the absolute differences between predicted (simulated) and actual values (measured), making it a straightforward way to assess the accuracy of a predictive model. Lower MAE Values indicate that the predictions are close to the actual values, meaning the model is more accurate. On the other hand, Higher MAE Values suggest more significant deviations between the predicted and actual values, indicating lower accuracy.

The Mean Absolute Error (MAE) is calculated using Equation (6-1) [167], where n is the number of observations:

$$MAE = \frac{1}{n} \sum_{i=1}^{n} |y_{measured} - y_{simulated}|$$
 (6-1)

b) Mean Absolute Percentage Error (MAPE)

Mean Absolute Percentage Error (MAPE) is a widely used metric for evaluating the accuracy of predictive models, particularly in time series forecasting. MAPE expresses the prediction error as a percentage of the actual values, providing an easily interpretable measure of relative accuracy. It is calculated by taking the average absolute percentage errors between predicted and actual values. The

Mean Absolute Percentage Error (MAE) is calculated using Equation (6-2), where n is the number of observations:

$$MAPE = \frac{100\%}{n} \sum_{i=1}^{n} \left| \frac{y_{measured} - y_{simulated}}{y_{measured}} \right|$$

$$MAPE = \frac{100\%}{n} \sum_{i=1}^{n} Percentage\ error$$
(6-2)

c) Root Mean Square Error (RMSE)

This represents the square root of the average of the squared differences between the predicted (simulated) and actual values. Due to the squaring process, this metric is particularly sensitive to significant errors, making it more sensitive when large errors are undesirable. Lower RSME values indicate better model performance, as the predictions are closer to the actual values. If RMSE is within 10-20% of the mean of the experimental data, the simulation is considered to have good accuracy, with values within 5% of the mean often regarded as excellent [168]. The Root Mean Square Error (RMSE) is calculated using Equation (6-3), where n is the number of variables.

$$RSME = \sqrt{\frac{1}{n} \sum_{i=1}^{n} (y_{measured} - y_{simulated})^2}$$

which is also simplified as,

$$RSME = \sqrt{\frac{1}{n} \sum_{i=1}^{n} Squared Error}$$
 (6-3)

6.3.2 Thermal Comfort Indices

Indices for different PCM layer positions, the Predicted Mean Vote (PMV) and the Predicted Percentage of Dissatisfied (PPD) were calculated using the Fanger comfort model [230]. PPD value indicates the percentage of people likely to feel thermally uncomfortable. Therefore, lower values are desirable for higher thermal comfort. The design goal was to achieve PPD < 20% and $-0.5 \le PMV \le +0.5$ to assess the impact of the PCM layer on occupants' thermal comfort [213, 214]. PMV measures thermal comfort, with values typically ranging from -0.5 (cold) to +0.5 (hot), where a value close to 0 shows optimal thermal comfort [212]. The PMV can be translated into PPD according to the following formulas in Equations (6-4) - (6-11) [231].

$$PPD = 100 - 95e^{-(0.03353PMV^4 + 0.2179PMV^2)}$$
 (6-4)

where Predicted Mean Vote, PMV, can be given:

$$PMV = [0.303e^{-(0.036M)} + 0.028] \times [(M - W)$$

$$- 3.96 \times 10^{-8}T_{cl}[(I_{cl} + 273.15)^{4} - (T_{r} + 273.15)^{4}]$$

$$- f_{cl}h_{c}(T_{cl} - T_{a})$$

$$- 3.05[5.733 - 0.007(M - W) - 0.001p_{w}]$$

$$- 0.42[(M - W) - 58.15] - 0.0173M(5.867 - 0.001p_{w})$$

$$- 0.0014M(34 - T_{a})]$$
(6-5)

where: M represents metabolic rate, W denotes mechanical power, T_{cl} is clothing insulation, F_{cl} is the clothing surface area, T_a is the air temperature, T_r is the mean radiant temperature, T_{cl} also refers to the clothing surface temperature and I_{cl} represents the clothing insulation.

Partial Pressure of water vapour
$$(P_{ws})$$
 can be expressed as:

$$P_a = RH \times P_{ws}$$
(6-6)

where: P_a vapour pressure, RH(%) is relative humidity, P_{ws} is the saturation vapour pressure, which is calculated using,

$$P_{ws} = 610. \left(\frac{17.27 \times T_a}{T_a + 237.3} \right) \tag{6-7}$$

The mean radiant temperature T_r is assumed equal to the air temperature, T_a .

The clothing surface temperature T_{cl} is calculated as follows.

$$T_{cl} = 35.7 - 0.0275(M - W) - R_{cl}[3.96 \times 10^{-8} f_{cl}[(T_{cl} + 273.15)^4 - (6-8)]$$

$$(T_r + 273.15)^4] + f_{cl}h_c(T_{cl} + T_a)$$

where h_c is the convective heat transfer coefficient related to the clothing and the surrounding, R_{cl} is clothing heat resistance.

$$R_{cl} = 0.155I_{cl} (6-9)$$

Convective heat transfer coefficient (h_c) for natural and forced convection, is given by Equation (6-10). The natural heat transfer coefficient case is assumed.

$$h_c = \begin{cases} 2.38 * |T_{cl} - T_a|^{0.25}, 2.38 * |T_{cl} - T_a|^{0.25} > 12.1\nu^{0.5} \\ 12.1\nu^{0.5}, 2.38 * |T_{cl} - T_a|^{0.25} \le 12.1\nu^{0.5} \end{cases}$$
(6-10)

where v is the air velocity.

Clothing surface area (f_{cl}) is given by Equation (1).

$$f_{cl} = \begin{cases} 1.0 + 0.2I_{cl}, & I_{cl} \le 0.5clo \\ 1.0 + 0.1I_{cl}, & I_{cl} > 0.5clo \end{cases}$$

$$(6-11)$$

For most indoor activities, the external work, W, is considered negligible.

6.3.3 An Analysis of Inside Wall Surface Temperature

a) Validation of Simulated vs. Experimental Temperatures for PCM-Integrated Walls Table 6-1 presents a comparison between the simulated and experimental inside wall surface temperatures for different PCM positions. To validate the simulation results against the experimental data, the Mean Absolute Error (MAE), Mean Absolute Percentage Error (MAPE), and Root Mean Square Error (RMSE) values were calculated and presented in the table.

Table 6-1. Comparison of the Prototype Inside Wall Surface Temperatures at different PCM Positions: Simulation vs Experimental results

	Simulation	Experimental	Error	ABS Error	% Error	(Error) ²	Deviation
NO PCM	25.21	28.21	3.00	3.00	10.65	9.02	1.41
100	27.95	31.15	3.20	3.20	10.28	10.26	1.60
150	27.96	30.80	2.84	2.84	9.21	8.05	1.42
153	27.24	31.14	3.90	3.90	12.52	15.20	1.95
203	26.85	31.03	4.18	4.18	13.47	17.47	2.09
303	26.61	30.81	4.20	4.20	13.63	17.64	2.09
341	25.66	29.66	4.00	4.00	13.49	16.00	2.01
344	25.94	29.48	3.54	3.54	12.01	12.53	1.77
356	26.21	30.28	4.07	4.07	13.44	16.56	2.03
Average	26.63	30.28	3.66	12.08	12.08	13.64	-
MAE	3.66						
MAPE (%)	12.08						
RSME	3.69						

Table 6-1 shows that the MAE value is 3.66, indicating that, on average, the simulated temperatures deviate from the experimental values by about 3.66°C. This is a relatively moderate error and gives

a direct sense of the average discrepancy between the two sets of data. The MAPE value is 12.08%, which means that the average percentage difference between the simulated and experimental results is around 12.08%. The RMSE value is 3.69, which gives more weight to larger errors due to the squaring of differences. It is slightly higher than the MAE, highlighting some larger discrepancies in specific PCM positions. However, the RMSE is still within a tolerable range, indicating the simulation's overall reliability. The individual percentage errors for each PCM position are also shown in Table 6-1, with all values falling under 13.7%. The highest percentage error is 13.63% for the PCM at the position of 303 mm.

Since the percentage errors fall under 20% [232], which is considered as an acceptable error margin, it can be concluded that the simulation model is reasonably validated by the experimental results. The standard deviations for most PCM positions remain relatively small. Thus, the numerical simulation model can be used to predict the thermal behaviour of PCM-integrated walls with a fair degree of confidence. Further refinements could focus on reducing errors at specific PCM positions to enhance the model's precision.

A comparison of error metrics is shown in Evaluation of Inner-wall Positions PCM Placement Accuracy in Walls with and Without Windows: Error Metrics Analysis

Table 6-2 and the metrices include Mean Absolute Error (MAE), Mean Absolute Percentage Error (MAPE), and Root Mean Square Error (RMSE) for simulated and experimental data for PCM positions of 341 mm, 344 mm, and 356 mm in two configurations: wall with and without window.

b) Evaluation of Inner-wall Positions PCM Placement Accuracy in Walls with and Without Windows: Error Metrics Analysis

Table 6-2. Comparison of Error Metrics (MAE, MAPE, RMSE) for Simulated and Experimental Data at Different PCM Positions for Walls with and Without Window

Metrix	PCM at	341	PCM at 344		PCM at 356	
	No window	Window	No window	Window	No window	Window
Average	13.37	33.96	11.97	34.45	13.40	32.14
Error (%)						
MAE	3.97	119.59	3.53	128.43	4.07	151.47
MAPE (%)	13.37	33.96	11.97	34.45	13.40	32.14
RSME	16.44	10.28	12.79	10.44	17.52	10.41

It can be seen that for the wall without a window, PCM at position of 344 mm shows the lowest MAE (3.53), followed closely by PCM at position of 341 mm (3.97), indicating that PCM at position of 344 mm best matches the simulated and experimental results. It appears that the MAE is considerably higher for the wall with a window, with PCM at position of 356 mm showing the highest error (151.47). This suggests that the window's presence introduces additional complexity that the simulation does not fully capture, possibly due to heat transfer through the glass.

Like MAE, PCM at position of 344 mm in the wall without a window has the lowest MAPE (11.97%), followed by PCM at position of 341 mm (13.37%), further validating PCM at position of 344 mm as the most accurate position in the no-window configuration. For the wall with a window, PCM at position of 356 mm has the lowest MAPE (32.14%). It appears that, all windowed cases show higher error percentages, indicating more significant discrepancies between simulated and experimental data when a window is present.

As shown in the third matrix in Evaluation of Inner-wall Positions PCM Placement Accuracy in Walls with and Without Windows: Error Metrics Analysis

Table 6-2PCM at position of 344 for the wall without a window has the lowest RMSE (12.79), followed by PCM at position of 341 mm (16.44), making PCM at position of 344 the optimal choice for energy savings and accuracy in this scenario. However, for the wall with a window, PCM at positions of 344 mm and 356 mm gives similar RMSE values (10.44 and 10.41, respectively), indicating comparable performance for these two positions in the windowed scenario.

As for the wall without a window PCM at position of 344 mm consistently shows the lowest errors across all metrics, suggesting that this PCM position is the most effective in providing energy savings and thermal regulation. So it is suggested that the simulation model has good accuracy in this configuration, with MAE, MAPE, and RMSE values remaining within acceptable limits.

By contrast, the wall with window appears more difficult in simulations. The significantly higher error metrics in the windowed cases indicate that the presence of the window introduces challenges that are not as accurately captured by the simulation model. However, PCM positions 341 mm and 356 mm still perform relatively well regarding RMSE. The discrepancy may be due to variations in

heat transfer through the window or interactions between the PCM and window materials that are not fully accounted for in the simulations.

Regarding model simulations, the lower error values for the wall without a window validate the simulation model's accuracy in simpler wall configurations. However, the higher errors in the windowed scenario suggest that the model could be improved by refining the simulation of thermal interactions in walls with windows. While PCM position of 344 mm shows the best overall performance in the wall without a window, PCM positions of 341 mm and 356 mm may still offer benefits in the windowed configuration due to their relatively lower RMSE values.

Further investigation into how windows affect heat transfer and the PCM's behaviour would help refine the model, especially for scenarios involving complex multi-layered walls with windows.

6.3.4 Energy Consumption Analysis

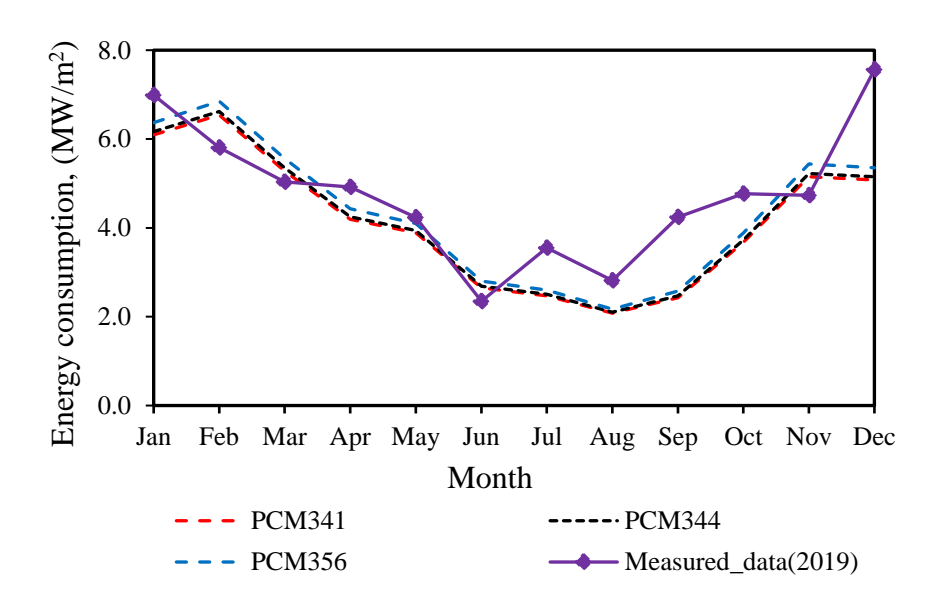


Figure 6-2. Comparison of simulated energy consumption vs. 2019 measured data

A comparison between the energy consumption at different PCM positions (341 mm, 344 mm, 356 mm) against measured data (without PCM) from 2019, is shown in Figure 6-2. It appears that the simulated energy consumption at all PCM positions follows a similar trend throughout the year, with energy usage peaking in the winter months (January and December) and decreasing in the summer months (June to August). The measured 2019 data consistently shows higher energy consumption,

particularly during the peak winter months, indicating that PCM integration helps reduce energy consumption.

It can be seen that PCM positions of 341 mm, 344 mm, and 356 mm indicate comparable performance, with PCM at position of 341 mm demonstrating slightly lower energy consumption overall. This suggests that PCM positioning near 341 mm is optimal for energy savings.

Table 6-3 presents a comparison of simulated energy consumption data (in MJ/m²) for PCM placed at position of 341 mm with measured energy consumption data from 2019 across different months. It includes columns for the absolute error, percentage error, and square error, providing an analysis of how closely the simulation results align with the actual measured data.

Table 6-3. Data Analysis of the Energy Consumption from PCM at Position 341, and 2019 Data

Month	PCM341	Measured	Absolute	Percentage	Square
	Simulated	2019 data,	Error	Error (%)	Error
	(MJ/m^2)	(MJ/m^2)			
	${oldsymbol{y}_{simulated}}$	Y measured			
January	6.096	6.988	0.89	12.77	0.796
February	6.540	5.807	0.73	12.63	0.538
March	5.280	5.033	0.25	4.90	0.061
April	4.190	4.917	0.73	14.78	0.528
May	3.890	4.237	0.35	8.18	0.120
June	2.650	2.348	0.3	12.85	0.091
July	2.470	3.548	1.08	30.39	1.163
August	2.080	2.818	0.74	26.20	0.545
September	2.430	4.243	1.81	42.73	3.288
October	3.670	4.770	1.10	23.06	1.210
November	5.150	4.733	0.42	8.80	0.174
December	5.080	7.562	2.48	32.82	6.159

From Table 6-3, an analysis of energy savings during colder months can be observed by focusing on the months of January, February, March, November, and December, which typically represent cold weather conditions in a cold climate (UK). In January and February, the absolute errors between the

simulated and measured data are 0.89 MJ/m² and 0.73 MJ/m², respectively, with percentage errors of 12.77% and 12.63%. This indicates a relatively close match between the simulation and measured values, reflecting good accuracy in predicting energy consumption during these colder months. March, in particular, shows an absolute error of only 0.25 MJ/m² and a percentage error of 4.90%, which is one of the lowest in the dataset, suggesting that the model performed well in capturing energy consumption during this early spring period.

In contrast, November also showed a decent prediction with an absolute error of 0.42 MJ/m² and a percentage error of 8.80%, demonstrating effective energy savings during this moderate cold month. However, December exhibits a significant discrepancy, with an absolute error of 2.48 MJ/m² and a percentage error of 32.82%, highlighting a higher deviation between the predicted and actual energy consumption. This suggests that the model may have limitations in accurately capturing energy demands during mid-winter, potentially due to unaccounted external factors such as unusual cold spells.

The simulated energy consumption values for these colder months are consistently lower than the measured 2019 data for most months, suggesting potential energy savings if PCM integration is implemented. For example, in January, the simulated value is 6.096 MJ/m², which is lower compared to the measured value of 6.988 MJ/m². The close alignment seen in March implies effective energy savings with minimal discrepancies, indicating a positive outcome from the PCM implementation during moderate cold conditions.

Overall, the PCM at position of 341 mm demonstrates effective thermal regulation during moderate cold months, reducing energy consumption discrepancies as indicated by relatively low percentage errors. However, the significant deviation observed in December suggests challenges in maintaining optimal energy savings during the coldest periods of the year. This indicates that while PCM integration provides notable benefits, further model refinement or additional thermal solutions may be necessary to enhance efficiency in extreme winter conditions.

Further analysis using Mean Absolute Error (MAE), Mean Absolute Percentage Error (MAPE), and Root Mean Square Error (RSME) is carried out to quantify the simulations' accuracy against the measured data and further to understand the energy savings potential for each PCM position.

The three metrics are calculated as shown below as follows:

a) Mean Absolute Error (MAE), using in Equation (6-1).

$$MAE = \frac{1}{n} \sum_{i=1}^{n} |y_{measured} - y_{simulated}|$$

$$MAE = \frac{1}{12} \sum_{i=1}^{12} Absolute Error$$

$$MAE = \frac{1}{12} \sum_{i=1}^{12} (0.89 + 0.73 + 0.25 + 0.73 + 0.35 + 0.3 + 1.08 + 0.74 + 1.81 + 1.10 + 0.42 + 2.48)$$

$$MAE = \frac{10.88}{12} = 0.91 \tag{6-12}$$

The calculated Mean Absolute Error (MAE) of 0.91 indicates that, on average, the model's predictions are off by 0.91(MJ/m²) from the actual observed values. Given that the values in the data set range from 2 to 8 (MJ/m²), an MAE of 0.91(MJ/m²) suggests a relatively small error level.

b) Mean Absolute Percentage Error (MAPE), using Equation (6-2).

$$MAPE = \frac{100\%}{n} \sum_{i=1}^{n} \left| \frac{y_{measured} - y_{simulated}}{y_{measured}} \right|$$

$$MAPE = \frac{100\%}{12} \sum_{i=1}^{12} Percentage \ error$$

$$MAPE = \frac{100\%}{12} (0.128 + 0.126 + 0.049 + 0.148 + 0.082 + 0.129 + 0.304 + 0.262 + 0.427 + 0.231 + 0.088 + 0.328)$$

$$MAPE = \frac{100\%}{12} (2.302) = \underline{19.18\%}.$$

$$(6-13)$$

A MAPE value of 19.18% suggests that the simulation tool predictive model's accuracy is reasonable and within an acceptable range for many applications.

c) Root Mean Square Error (RMSE), using Equation (6-3).

$$RSME = \sqrt{\frac{1}{n} \sum_{i=1}^{n} (y_{measured} - y_{simulated})^{2}}$$

$$RSME = \sqrt{\frac{1}{12} \sum_{i=1}^{12} Squared Error}$$

$$RSME = \sqrt{\frac{1}{12} (0.796 + 0.538 + 0061 + 0.528 + 0.120 + 0.091 + 1.163 + 0.545 + 3.288 + 1.210 + 0.174 + 6.159)}$$

$$RSME = \sqrt{\frac{14.673}{12}} = \underline{1.11}$$

$$(6-14)$$

The RMSE value of 1.11 indicates that the simulation tool's predictions are reasonably accurate compared to the measured values, with an average deviation of 1.11 units from the actual data. Overall, the model is considered reliable for a general use.

Table 6-4 presents the summary of monthly energy consumption in kilowatt-hours (kWh) for the three simulated PCM positions of 341 mm, 344 mm, and 356 mm compared to the measured energy data from 2019. Additionally, the table includes annual energy consumption, annual energy savings in percentage, and three key validation metrics: MAE, MAPE, and RSME.

a) Energy Savings

It can be seen that PCM341 results in the lowest annual energy consumption, with a total of 13.76 kWh consumed throughout the year. This represents a 13.12% energy savings compared to the 2019 measured data, the highest among all PCM positions. Another good position is PCM at position of 344 mm which also offers significant savings, consuming 13.94 kWh annually and saving 11.95%. PCM, at position of 356 mm, provides the least energy savings among the three, with an 8.55% reduction in energy use, resulting in a total consumption of 14.48 kWh. It is clear that PCM at position 341 mm is the optimal PCM position for maximising energy savings. PCM at position of 344 is slightly less efficient but still performs well, while PCM at position of 356, although beneficial, is the least effective.

The energy savings results have demonstrated that PCM at position of 341 provides the highest annual energy savings (13.12%) while also exhibiting a solid validation performance with MAE and MAPE

metrics. Although PCM at position of 344 also performs well, its slightly higher error values suggest that PCM at position of 341 mm is the optimal choice for PCM placement. PCM at position of 356, while showing the lowest RMSE, provides less overall energy savings. Therefore, based on the energy consumption and validation metrics, PCM at position of 341 mm emerges as the most effective PCM position for reducing energy consumption and improving building energy performance.

b) Seasonal Performance

During the cold months (January to March), PCM at position of 341 mm shows consistently lower energy consumption than PCM at the other two positions of 344 mm and 356 mm, validating its better thermal regulation during these heating-dominated periods. Similarly, during the cooling months (July to August), PCM at position of 341 mm also shows lower energy consumption, suggesting it provides better insulation and temperature regulation, thereby reducing cooling demands. The summer months, particularly August, show a notable deviation in energy consumption compared to the measured data.

Table 6-4. Summary Comparison of Monthly and Annual Energy Consumption for Simulated PCM Positions against 2019 Measured Data with Energy Savings and Validation Metrics

Month	PCM341 (MJ)	PCM344 (MJ)	PCM356 (MJ)	Measured, MJ, (2019)
January	6.096	6.170	6.370	6.988
February	6.540	6.620	6.850	5.807
March	5.280	5.352	5.560	5.033
April	4.190	4.253	4.430	4.917
May	3.890	3.939	4.100	4.237
June	2.650	2.688	2.800	2.348
July	2.470	2.503	2.600	3.548
August	2.080	2.101	2.170	2.818
September	2.430	2.471	2.580	4.243
October	3.670	3.726	3.880	4.770
November	5.150	5.224	5.440	4.733
December	5.080	5.148	5.350	7.562
Total Energy	49.526	50.195	52.130	57.005
(Annual)	(13.757 kWh)	(13.943 kWh)	(14.48 kWh)	(15.835 kWh)
Annual Energy	7.479	6.810	4.875	-
Savings				
Savings (%)	13.12	11.95	8.55	-
MAE	0.91	0.89	0.86	-
MAPE (%)	19.18	24.94	18.45	-
RSME	1.11	1.08	0.94	-

(1 MJ=0.27778 kWh)

c) Model comparison

The model compares well with the 2019 consumption data using three statistical metrics:

MAE shows a value of 0.91 for PCM at position of 341 mm, 0.89 for PCM at position of 344 mm, and 0.86 for PCM at position of 356 mm, indicating a low deviation between simulated and actual measured data, with PCM at position of 356 mm showing the best performance in terms of absolute error.

In the Mean Absolute Percentage Error (MAPE), it ranges from 19.18% for PCM at position of 341 mm to 24.94% for PCM at position of 344, suggesting that PCM at position of 341 mm offers the lowest relative error compared to the other PCM positions.

In the Root Mean Square Error (RSME), which emphasises more significant errors, is lowest for PCM at position of 356 at 0.94, followed by PCM at position of 344 at 1.08 and PCM at position of 341 mm at 1.11. This suggests that while PCM at position of 341 and PCM at position of 344 mm show more substantial overall energy savings, PCM at position of 356 mm has a slightly more consistent error distribution.

It is suggested that this model can be considered validated, with all PCM positions showing reasonable alignment between simulated and measured data. The discrepancies seen in cooling months could be further explored by analysing other factors, such as HVAC system efficiency or potential differences in internal heat gains in the measured building.

6.3.5 Cost-Benefit Analysis of PCM Integration RT28HC

This section evaluates the energy savings for integrating PCM (RT28HC) into the multilayer walls of a historic building. Calculations are based on energy consumption data from Table 6-4, and Ofgem energy prices (Gas: 6.89 pence per kWh and 31.65 pence daily standing charge, 1 January to 31 March 2025) [229].

Annual Energy Savings

The total annual energy consumption for the building without PCM was 15.835 kWh, as seen in Table 6-4. For the inner wall PCM configurations:

PCM341 consumed 13.757 kWh, saving 15.835 - 13.757 = 2.078 kWh annually

PCM344 consumed 13.943 kWh, saving 15.835 - 13.943 = 1.892 kWh annually

PCM356 consumed 14.48 kWh, saving 15.835 - 14.480 = 1.355 kWh annually

Annual Energy Cost Savings

Using the Ofgem 2025 gas tariff 6.89 pence per kWh and £0.3165 daily standing charge (i.e. the total annual standing charge is $(£0.3165 \times 365) = £115.52$.

$$PCM341: (2.078 \times 0.0689) + £115.52 = £115.66 per year$$
 (6-15)

$$PCM344: (1.892 \times 0.0689) + £115.52 = £115.64 per year$$
 (6-16)

$$PCM356: (1.355 \times 0.0689) + £115.52 = £115.61 per year$$
 (6-17)

The energy cost savings described above are based on the total annual energy consumption for the building rather than being calculated per unit meter or volume. Using the Ofgem Gas tariffs, PCM341 demonstrates the highest annual savings of £115.66, PCM344 saves £115.64, and PCM356 saves £115.61annually, based on total energy use. These savings, however, depend on several critical factors, including the specific cost per square meter of PCM installation, which involves labour, material properties, and retrofitting complexities unique to historic buildings. Climate conditions, wall construction types, and material thermal properties further influence PCM activation and energy efficiency. While PCM integration offers potential energy benefits, assessing the savings relative to installation costs and long-term performance requires detailed per-unit metrics to provide an accurate lifecycle cost analysis.

6.3.6 Predicted Mean Vote (PMV) and Predicted Percentage of Dissatisfied (PPD)

The Predicted Mean Vote (PMV) and the Predicted Percentage of Dissatisfied (PPD) values are calculated using Equations (6-4) to (6-11). The external work, W, is assumed to be negligible; the radiant mean temperature is equal to the indoor temperature. Table 6-5, shows the variables used in the calculation of PMV and PPD.

Table 6-5. PMV and PPD variables

Parameter	Value	Unit
Relative Humidity (RH)	50	%
Air Velocity (v)	0.1	m/s
Metabolic Rate (M)	560	Met
Clothing factor (I_{cl})	0.5	Clo
Saturated water vapour Pressure (P_{ws})	4314.01	Pa
Partial pressure P_a)	2157	Pa
External work (W)	0	W/m ²

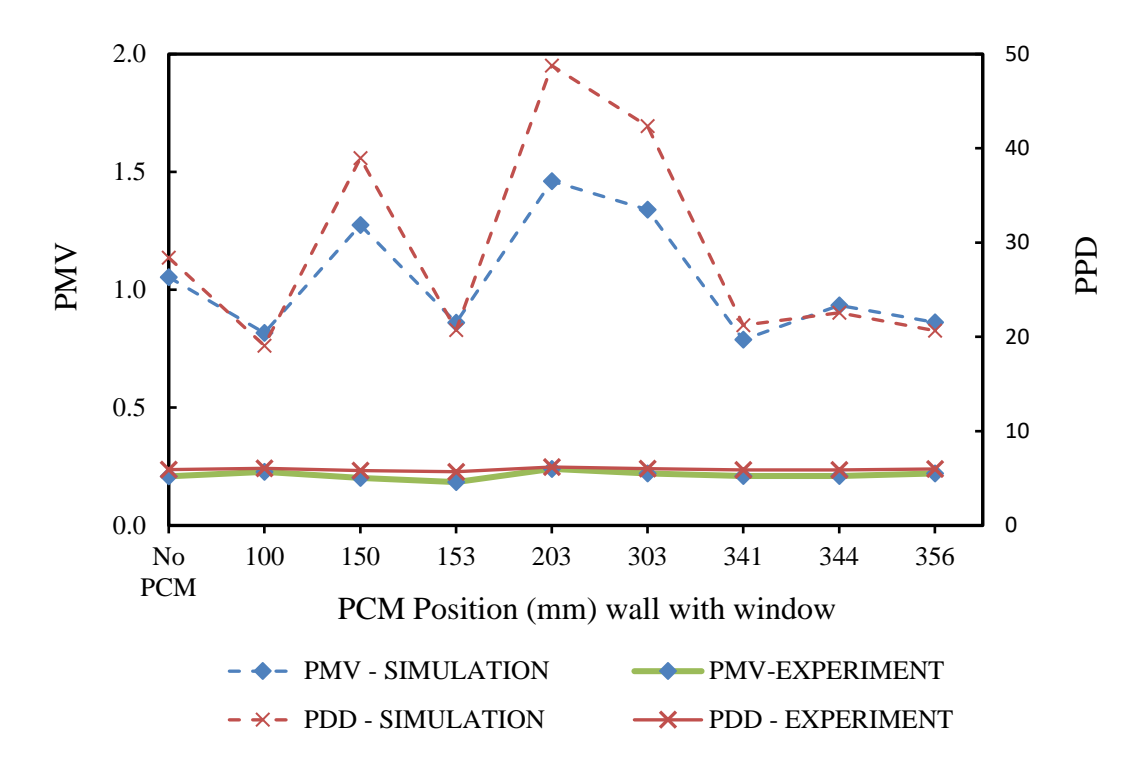


Figure 6-3. PPD and PMV values versus various PCM positions of a wall with a window

a) Wall with a window

Figure 6-3 depicts the experimental and simulation PMV and PPD trends for walls with windows. It can be observed that the PCM positions from 341 mm to 344 mm yield the lowest simulated and experimental PPD values, which are around the acceptable thermal comfort range of 20%. The experimental PPD values show minimal variation across different PCM positions, remaining relatively low, except for a slight increase at PCM positions of 153 mm and 203 mm. The PMV values, which represent the occupants' thermal sensation, also align closely with the simulated and experimental results at PCM positions between 341 mm and 356 mm. At these positions, the PMV values are closest to the neutral comfort range (PMV = 0), indicating that these positions provide the highest thermal comfort levels.

However, the PCM position at 203 mm shows the highest deviation in both PMV and PPD values, where the comfort levels are far from optimal, suggesting that this position may not be ideal for PCM integration. The significant variations observed in simulated and experimental data at this position highlight the need for further refinement or consideration of additional factors that could influence the results.

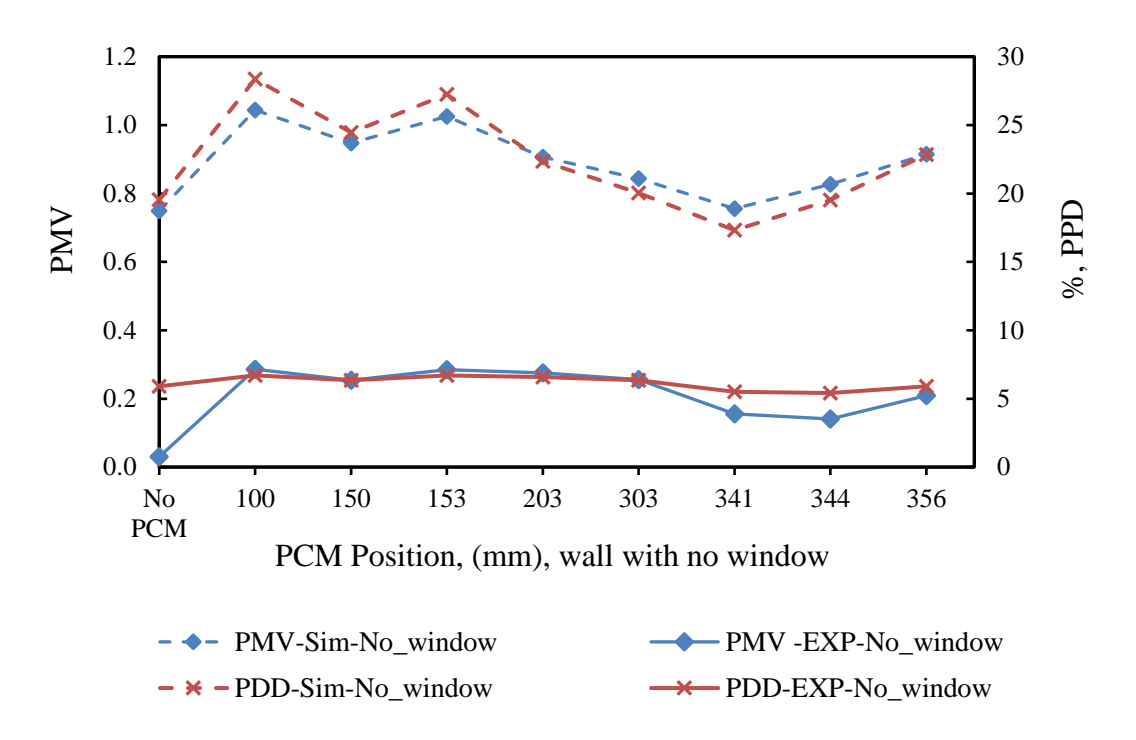


Figure 6-4 PPD and PMV values for various PCM positions of a wall no window

b) Wall without a window

Figure 6-4 shows that both simulation and experimental results follow a more consistent trend. The experimental results showed a better trend with consistently low PMV (below 0.3) and PPD (less than 7%). Similarly, the simulation results showed a good trend, particularly PCM at position 341 with PMV value (0.8) and PPD (17%). The PCM positions of 341 mm and 344 mm again stand out as providing optimal thermal comfort, with PPD values dropping below 10% for the experimental work, which is well within the acceptable range for thermal comfort. These positions also show minimal variation between the simulation and experimental PMV values, suggesting a good alignment between the model and the experimental findings.

On the other hand, PCM positions of 100 mm to 203 mm show relatively higher PPD and PMV simulated values, indicating that these positions do not provide the same level of thermal regulation as the positions closer to the wall's inner surface (341 mm to 356 mm). The general trend in the wall without a window case is smoother than that of the wall with a window, in Figure 6-3. This could be due to the added complexity and variability that the window introduces, affecting heat transfer and thermal comfort distribution.

c) Validation of simulation results

By comparing the simulated and experimental results, it is clear that the PCM positions closer to the inner surface of the wall (341 mm to 356 mm) consistently provide better thermal comfort, as evidenced by lower PPD values and PMV values close to zero. These positions are ideal for maintaining thermal comfort and reducing energy consumption for both wall configurations (with and without windows). The discrepancies at certain PCM positions, particularly 150 mm and 203 mm, suggest that the model may require further calibration to account for specific dynamic factors, such as heat gain from the window or external environmental conditions.

The validation process has compared simulated and experimental results, showing that the model used for simulating thermal comfort with PCM integration is generally reliable, particularly at the PCM positions that reach the phase change temperature of 27°C (341 mm, 344 mm, and 356 mm). However, further refinement could be required to improve accuracy at positions where significant deviations between simulated and experimental results are observed.

6.3.7 Implications for Building Design and Energy Efficiency

The integration of phase change materials (PCMs) in building envelopes, particularly in the positions identified as optimal through simulation and experimental validation (341 mm to 356 mm), holds significant implications for both building design and energy efficiency. Positioning the PCM near the inner surface of the wall, where temperatures fluctuate around the PCM's phase change temperature of 27°C makes it possible to leverage the material's latent heat properties to stabilise indoor temperatures more effectively.

i). Two key factors in buildings: thermal comfort and energy savings

One of the critical outcomes of PCM integration at the optimal positions is the substantial improvement in thermal comfort. The PMV and PPD results have consistently demonstrated that PCM positions closer to the inner surface (341 mm, 344 mm, and 356 mm) are more effective at maintaining comfortable indoor environments. For both walls with and without windows, these positions show the lowest PPD and PMV values closest to neutral, indicating minimal thermal discomfort for occupants. This suggests that building designs incorporating PCM at these positions could reduce the need for active heating and cooling systems while maintaining high thermal comfort levels.

The implications for energy efficiency are equally significant. The comparison between simulated and experimental energy consumption data reveals that buildings utilising PCM in the optimal positions experience reduced energy demand, particularly during peak heating and cooling periods. This is most clearly reflected in the energy savings of up to 13.12% in the case of PCM at position of 341 mm, as shown in the previous analysis. This reduction in energy use translates to cost savings for building operators and contributes to broader sustainability goals by reducing the building's carbon footprint. It is suggested that PCM integration at the optimal positions in building walls has the potential for significant energy savings.

Additionally, the integration of PCM can help mitigate extreme temperature fluctuations, reducing the peak loads on HVAC systems. This not only prolongs the lifespan of mechanical systems by reducing their operational strain but also enhances the overall energy efficiency of the building. The simulations have indicated that buildings with PCM integrated at the optimal positions can achieve lower maximum heating and cooling demands, as observed in the monthly energy consumption graphs. The smoother temperature regulation afforded by the PCM reduces the need for constant adjustments to the heating and cooling systems, which can otherwise contribute to energy inefficiency.

ii). Application in Modern and Retrofitted Buildings

The findings of this study are highly relevant for both new construction and retrofitting projects. In modern building design, integrating PCMs into external walls, particularly those with large, glazed surfaces, can help offset the heat losses and gains typically associated with windows. For retrofitting older buildings, especially those with poor insulation or significant thermal bridges, PCM integration offers a cost-effective solution to enhance thermal performance without requiring extensive structural modifications.

The impact of PCM integration is particularly important for buildings in temperate climates, where daily and seasonal temperature variations can place a high demand on heating and cooling systems. By incorporating PCMs into the design, architects and engineers can reduce reliance on mechanical systems, improve the building's passive thermal performance, and achieve energy savings that align with increasingly stringent energy regulations.

iii). Design Considerations and Limitations

While integrating PCMs is promising to improve building energy efficiency, several design considerations must be addressed. First, the specific placement of the PCM within the wall assembly is critical. The results of this study have demonstrated that PCM placement significantly affects thermal performance, with positions closer to the inner wall surface being the most effective. This requires careful planning during the design phase to ensure that PCMs are optimally located based on the building's thermal loads and operational profile.

Moreover, the effectiveness of PCMs is influenced by the building's orientation, window-to-wall ratio, and exposure to solar gains. For instance, buildings with high solar exposure may require additional shading or glazing treatments to optimise PCM performance. Similarly, the integration of PCMs into lightweight structures, such as timber-framed buildings, may yield different results due to the lower thermal mass of the surrounding materials. As such, designers must account for these factors when considering PCM integration to maximise its energy-saving potential.

6.4 Importance of PCM Location for Heat Transfer Efficiency and Thermal Comfort

The location of the PCM layer within a multi-layered wall system plays a critical role in optimizing heat transfer efficiency and maintaining thermal comfort levels. PCMs regulate temperature by absorbing and releasing latent heat during phase transitions, which is most effective when their placement aligns with the thermal gradients and heat flux patterns of the wall.

The results of this study demonstrate that PCM positions closer to the interior surface, such as those of 341 mm and 344 mm as shown in Figure 5-9, consistently provided superior thermal performance. These locations allowed the PCM to interact more directly with internal heat flux, enabling it to stabilize indoor temperatures effectively. The PCM at the position of 341 mm (Figure 5-9), demonstrated moderate temperatures, with a temperature gradient of 0.9984, highlighting its efficiency in balancing heat transfer and thermal regulation. In contrast, PCM placed further away from the interior, such as at the position of 203 mm, showed reduced performance due to insufficient heat absorption, underscoring the importance of strategic positioning. Moreover, PCM near the interior surface acts as a thermal buffer, reducing temperature amplitude and enhancing occupant comfort. By maintaining indoor temperatures within a narrow range, the PCM minimises the need for active heating and cooling systems, which aligns with energy efficiency goals. This behaviour is

particularly crucial in temperate climates where temperature fluctuations are moderate but require effective management to prevent discomfort.

These findings highlight that the placement of PCM must be carefully designed to align with the wall's thermal dynamics. Future applications should consider proximity to heat sources, wall material composition, and the intended climate conditions to maximize energy savings and thermal comfort.

6.5 Contributions to the Field

This study significantly contributes to building design and energy efficiency by integrating PCMs into multi-layered wall systems with and without windows. The research addresses a crucial gap in optimising the position of PCM layers within building walls, focusing on thermal comfort, energy savings, and overall building performance. The findings contribute to the knowledge on how PCMs can be strategically placed to maximise their potential in reducing heating and cooling demands, particularly in temperate climates where buildings experience wide fluctuations in external temperatures.

One of the major contributions of this research is the comprehensive analysis of the thermal performance of PCMs integrated into walls with different configurations. This work used advanced simulation tools and experimental validation to test PCM performance across various scenarios. This research bridges the gap between theoretical energy savings associated with PCM use and practical implementation in real-world applications. The comparison of simulated and experimental results provides a high level of validation for the simulation models, supporting their use in future PCM research and building energy simulations.

Specifically, this study enhances understanding in the following areas:

i). Optimised PCM Positioning for Energy Efficiency

The research identifies that the PCM positions between 341mm and 356mm within the wall structure yield the greatest thermal benefits. These positions allow the PCM to effectively reach its phase change temperature (27°C), facilitating heat absorption during peak indoor temperatures and heat release during colder periods. This contributes to significant energy savings by reducing heating loads in winter and cooling loads in summer. The findings indicate that PCM placement plays a crucial role in achieving thermal comfort, with optimal positioning leading to an average annual energy savings

of up to 13.12% compared to a non-PCM configuration. This optimal placement was validated both experimentally and through simulation.

ii). Contribution to Thermal Comfort and Indoor Environmental Quality

The research demonstrates that properly positioned PCM layers contribute to improved thermal comfort, as quantified by the Predicted Mean Vote (PMV) and Predicted Percentage of Dissatisfied (PPD) indices. When PCM is integrated into the walls at the optimal positions (341 mm to 356 mm), PMV values are closer to neutral, and PPD values remain well below the acceptable threshold of 20%. This demonstrates that PCM integration saves energy and contributes to occupant comfort by reducing temperature fluctuations and maintaining indoor conditions within comfortable ranges.

iii). Impact of Windows on PCM Performance

A novel aspect of this study is its investigation into the impact of integrating PCM with double-glazed windows. Previous research has largely focused on walls without accounting for the influence of windows, which are significant sources of heat loss or gain. This study highlights the additional complexities windows introduce and shows how PCM can still deliver energy savings and comfort improvements even when windows are present. The results indicate that walls with windows exhibit higher heat transfer rates. Still, the strategic placement of PCM can mitigate these effects, making windows less of a thermal weak point in the building envelope.

iv). Validation of Simulation Models with Experimental Data

The study demonstrates the reliability of simulation models through rigorous experimental validation. Comparisons of simulated and measured data for energy consumption, temperature distribution, and heat transfer rates show close alignment, with Mean Absolute Percentage Error (MAPE) values typically below 20% and Root Mean Square Error (RMSE) values showing high accuracy. This level of validation ensures that the simulation models used in this research can be confidently applied in future studies to optimise PCM integration into building designs. Additionally, the research showcases how advanced simulation tools like TRNSYS can streamline the design process by enabling precise predictions of PCM performance before full-scale implementation.

v). Framework for PCM Integration in Historical and Modern Buildings

The research offers a framework for practically integrating PCMs into historical and modern buildings. By testing the technology in walls typical of Victorian-era buildings and comparing it with modern cavity wall constructions, the study provides guidelines for retrofitting heritage buildings with energy-efficient materials. The findings highlight that PCMs can be incorporated into different architectural styles to enhance energy performance without compromising the building's structural integrity or aesthetic value.

Overall, this study contributes to the ongoing efforts to reduce the built environment's carbon footprint by providing actionable insights into how PCMs can be optimised for energy efficiency and comfort. The findings pave the way for further research into scalable solutions for incorporating PCMs into various types of buildings, potentially informing updates to building codes and standards for energy efficiency.

6.6 Limitations of the Study

While this research makes significant contributions to energy-efficient building design by integrating PCMs in wall systems, several limitations must be acknowledged. These limitations present opportunities for future research but also introduce potential sources of uncertainty that should be carefully considered when interpreting the findings.

i). Experimental Scope and Scale

One of the primary limitations of this study is the scale of the experimental setup. The research was conducted on prototype wall samples, scaled-down versions of full-sized walls commonly found in buildings. Although the experimental prototypes were designed to mimic real-world conditions as closely as possible, it is essential to note that the results may not fully capture all the complexities and variables present in full-scale building applications. Heat transfer dynamics, airflow, and structural interactions in actual buildings could differ from the laboratory conditions, potentially affecting the generalisability of the results. A full-scale building experiment would provide a more comprehensive understanding of the long-term behaviour of PCMs in real-world settings.

ii). Simplified Material Properties and Assumptions

The simulations and experiments conducted in this study relied on simplified assumptions for material properties such as thermal conductivity, specific heat capacity, and density. Although these properties were obtained from manufacturer specifications or literature, they may vary depending on installation quality, environmental conditions, and material ageing. For instance, the PCM properties were assumed to remain constant over time, but the actual performance of PCMs may degrade due to repeated thermal cycling or material fatigue. These assumptions may have introduced some inaccuracies in the simulations and experimental results, particularly in the long-term predictions of PCM behaviour.

iii). Choice and Limitation of PCM RT28HC

RT28HC PCM was chosen for its phase change temperature range of 27°C to 29°C [194] (Appendix 10), aligning with thermal comfort requirements in temperate climates and offering highly effective

thermal regulation. It stores and releases heat at nearly constant temperatures with consistent performance over thousands of cycles. Operating across a broad range (-10°C to 90°C), RT28HC is durable, non-toxic, easy to handle, and well-suited for energy efficiency in temperate climates, including applications in both historical structures and modern office buildings. Its robust aluminium encapsulation enhances thermal conductivity and ensures suitability for heritage buildings with limited maintenance access, while contributing to their preservation. However, its narrow activation range may limit its effectiveness in extreme climates, and the low thermal conductivity of paraffin-based PCMs necessitates advanced integration techniques to optimize performance. High initial costs also remain a barrier to retrofitting projects in both historic and modern office buildings, underscoring the need for research to expand PCM applicability and improve cost-effectiveness.

iv). Focus on Specific Climate Conditions

This research was primarily conducted under the assumption of temperate climate conditions similar to those in the UK, where the experiments and simulations were based. As a result, the findings may not be directly applicable to regions with extreme climates, such as tropical, arid, or polar climates. The effectiveness of PCM integration for energy savings and comfort can vary significantly depending on local temperature fluctuations, humidity levels, and solar radiation. Therefore, further research is needed to investigate the performance of PCMs under a wider range of climate conditions to provide a more global perspective on their applicability.

v). Window Impact and Shading Considerations

While this study explored the integration of PCMs in walls with and without double-glazed windows, it did not account for the effect of shading devices or dynamic window glazing on thermal performance. Windows, being significant sources of heat gain and loss, can benefit from shading devices like blinds, curtains, or external shading systems that could further enhance the thermal efficiency of buildings. The omission of these factors represents a limitation in the overall analysis of PCM integration with Windows. Future research could expand on the current work by including dynamic shading strategies and their interactions with PCM-enhanced walls to achieve more comprehensive energy efficiency.

vi). Limited Duration of Experimental Observations

The experimental validation in this study was conducted over a relatively short period of time, typically ranging from a few days to weeks. This limited time frame may not fully capture the seasonal variations and long-term effects on PCM performance. PCMs are designed to handle a wide range of temperature cycles, and their effectiveness may evolve over time as they experience repeated thermal charging and discharging cycles. Long-term experiments spanning multiple seasons or years would

provide more accurate insights into the durability and sustained performance of PCMs, especially in regions with significant seasonal temperature variations.

vii). Modelling and Simulation Constraints

Despite the high level of accuracy demonstrated by the TRNSYS simulation models, certain modelling constraints were present in this study. For example, boundary conditions such as infiltration rates, occupant behaviour, and internal heat gains were simplified to enable more manageable computations. In reality, buildings experience dynamic conditions due to variations in occupant behaviour, appliance usage, and ventilation patterns, which can significantly impact overall energy consumption and comfort levels. The simplification of these conditions limits the precision of the simulation in reflecting real-world building performance, especially in non-controlled environments.

viii). Lack of Consideration for Occupant Behaviour

The study assumes static indoor environmental conditions and does not factor in occupant behaviour, which can significantly affect both energy consumption and thermal comfort. Variables such as window opening behaviour, thermostat settings, and internal heat generation from appliances and lighting are not fully modelled in the simulations. These behaviours can have a substantial impact on the thermal dynamics of a building and, thus, on the effectiveness of PCM integration. Incorporating more realistic occupant behaviour models into future simulations could enhance the accuracy of energy-saving predictions and improve building design strategies that integrate PCMs.

ix). Limited Scope of Thermal Comfort Metrics

Although the Predicted Mean Vote (PMV) and Predicted Percentage of Dissatisfied (PPD) were utilised to assess thermal comfort, these indices do not account for all aspects of human thermal comfort. Factors such as radiant asymmetry, draft, and local discomfort were not included in the evaluation. Additionally, the study assumes uniform thermal preferences across all building occupants, which may not reflect individual preferences and sensitivities. Future research could include additional comfort metrics, such as adaptive thermal comfort models or personal comfort preferences, to provide a more holistic view of how PCMs affect thermal comfort.

x). Limitation and Applicability to PCM Integration

The experimental setup and simulations were based on specific material properties, including the thermal conductivity, density, and specific heat of the materials used in the prototype wall. While these properties are representative of local materials, the results may not directly translate to buildings constructed with significantly different materials, such as lightweight composites or highly porous bricks. Moreover, the model assumes a uniform heat transfer mechanism, which may not account for

localized anomalies or three-dimensional heat flows, especially in walls with complex architectural elements.

Additionally, while the proposed model captures heat transfer dynamics under temperate climatic conditions, its applicability to extreme climates may require adjustments, such as modifying the phase change temperature or PCM thickness to align with local thermal demands. This highlights the need for further validation under diverse environmental and operational conditions. The absence of long-term performance data, particularly concerning PCM degradation and maintenance needs, also limits the generalizability of the findings for extended lifespans.

xi). Transferability and Applicability

The confidence in this work's ability to support preliminary studies lies in the robustness of the experimental methodology and the derivation of the predictive model. The proposed equation (5-8) is grounded in well-characterized thermal properties and validated experimental data, offering a reliable basis for adapting PCM configurations to buildings with similar thermal conductivity and diffusivity properties. However, when applied to other materials, careful consideration must be given to variations in material properties and wall assemblies, as these factors significantly influence heat transfer and PCM activation mechanisms.

The generalizations made in this study are most valid for temperate climates, where the proposed PCM phase change temperature aligns well with typical seasonal variations. For other climates, adjustments to the PCM properties or the incorporation of additional layers for enhanced thermal buffering may be required. The model's assumptions, including one-dimensional heat transfer, simplify calculations but may overlook certain complexities in real-world applications, such as thermal bridging or moisture infiltration.

Despite its strengths, the study's limitations underscore the importance of material-specific considerations and climate adaptability when generalizing the findings to other contexts. By addressing these limitations and refining the model for diverse conditions, this work provides a strong foundation for future research and the broader application of PCM technologies in energy-efficient building designs. Furthermore, the research serves as a critical step toward achieving sustainable energy solutions, contributing to climate neutrality goals while preserving cultural heritage.

6.7 Summary

A detailed comparison between simulation and experimental results has been conducted, providing key insights into the optimal positioning of PCM layers for maximising thermal performance and energy savings in buildings. By examining the thermal performance of walls with and without windows, the most effective PCM positions and validation of predictive accuracy of the simulation models have been identified.

The comparison analysis highlights that PCM positions between 341 mm and 356 mm from the outer wall surface consistently yield the best thermal performance. These positions allow the PCM to fully activate, effectively absorbing and releasing heat at its phase change temperature (27°C), which contributes to stabilising wall temperatures and reducing heat transfer. This finding is supported by both simulation and experimental results, with close alignment between the two methods, particularly for walls without windows. Key Findings are summarised as follows:

- i. Both the simulation and experimental results have indicated that PCM positioned between 341 mm and 356 mm from the outer surface provided the best thermal regulation. These positions maintained temperatures close to 27°C, ensuring full activation of the PCM's heat storage and release properties.
- ii. The accuracy of the simulation models was validated using three error metrics: MAE, MAPE, and RMSE. For walls without windows, PCM at 344 mm showed the lowest MAE (3.53), while PCM at 356 mm had the lowest RMSE (10.41) for walls with windows. The overall error analysis confirmed that the simulation models have accurately predicted PCM performance, with deviations primarily occurring in window scenarios.
- iii. The sinusoidal relationship captured by the newly developed empirical formula, Equation (5-8) accurately modelled the heat transfer rate for various PCM positions of the prototype wall under study, (384 mm thick). This equation effectively described the periodic thermal behaviour of PCM during phase transitions, validating its use in optimising PCM placement for thermal comfort and energy efficiency.
- v. The simulation results showed that PCM positioned at 341 mm achieved the highest annual energy savings, reducing consumption by 13.12% compared to the baseline. PCM at 344 mm and 356 mm also contributed to substantial energy savings (11.95% and 8.55%, respectively), with all PCM configurations outperforming the 2019 measured data in terms of energy efficiency.

vi. The PMV and Predicted PPD metrics showed that PCM positions between 341 mm and 356 mm provided the reasonable thermal comfort. PPD values remained within acceptable limits (<15%), and PMV values were close to zero, indicating optimal comfort for occupants.

This chapter underscores the importance of PCM positioning within wall structures, with positions between 341 mm and 356 mm providing optimal thermal regulation, energy savings, and occupant comfort. The simulation models, validated by experimental data, offer a reliable tool for predicting the thermal performance of PCM-enhanced walls, enabling informed design decisions for energy-efficient buildings. Additionally, the combined results emphasise the role of PCM integration in both new constructions and retrofitting projects, particularly in improving the thermal performance of walls with windows.

CHAPTER 7: CONCLUSIONS AND RECOMMENDATIONS

This chapter provides a comprehensive conclusion of the research, which aimed to investigate the integration of Phase Change Materials (PCMs) in enhancing energy conservation across different building types, including Victorian-era structures and modern hospitals or contemporary office buildings. This research aligned with global sustainability goals, such as the UK's Net Zero Emissions by 2050 initiative.

The study was structured around a series of precise objectives: beginning with the aim to reduce the energy cost of Chase Farm Hospital's main building energy consumption through the application of PCMs. The integration of PCMs has demonstrated the potential to significantly lower operational energy consumption by regulating indoor temperatures and reducing reliance on mechanical heating and cooling systems. This outcome aligns with energy efficiency strategies and sustainability goals, contributing to the broader objective of reducing energy consumption in healthcare settings.

With this foundation, the investigation delved into evaluating the thermal performance and energy-saving potential of PCM multi-layer walls in Victorian-era buildings. The research has highlighted that PCM integration can effectively reduce energy consumption while preserving the architectural and historical integrity of these structures. By moderating temperature fluctuations without requiring invasive changes to the building's design, PCMs offer a valuable solution for retrofitting historic buildings in a way that respects both heritage preservation and energy efficiency.

Then, this research focused on understanding the optimisation and impact of PCM-enhanced cavity walls with integrated windows in modern hospitals and office buildings. By studying the configuration of PCM within walls and its interaction with windows, the research has demonstrated how PCM could achieve both aesthetic and functional design goals while improving thermal performance. The findings have indicated that proper PCM placement stabilises indoor temperatures and reduces energy consumption in these modern building types, particularly by balancing heat gain and loss through windows.

To validate the simulation results, a series of lab tests were conducted to evaluate PCM performance under real-world conditions. The experimental investigations confirmed the accuracy and reliability of the simulations, demonstrating that PCMs can be effectively utilised to regulate temperatures and provide energy savings. This validation ensured that PCM applications were not only theoretically sound but also practically feasible in diverse building settings. As a result, this study has provided practical guidelines and design recommendations for incorporating PCM-drywalls in building upgrades and new constructions. The findings have culminated in strategies for optimising PCM use in hospitals, Victorian-era structures, and modern office buildings to maximise energy efficiency and sustainability. These guidelines offer actionable insights for architects, engineers, and building managers seeking to implement PCM technology for energy savings and enhanced thermal regulation.

This final chapter has summarised the significant insights gained from the study, evaluated how these findings meet the initial research objectives, and discussed potential directions for future research in this vital field of energy technology. Based on the results and discussion, the following conclusions are drawn:

7.1 Conclusions

7.1.1 Impacts of PCM on Building Walls

The study identified that placing PCM at positions between 341 mm and 356 mm from the outer wall surface provided the best thermal performance. Specifically, PCM placement at 341 mm resulted in the most significant energy savings and thermal regulation, fully allowing the PCM to activate at its phase change temperature of 27°C. For instance, PCM at the positions of 341 mm and 344 mm reduced the peak temperature by 2.0°C and 1.74°C, respectively, thereby boosting air-conditioning performance and reducing energy consumption by 5.3% to 6.2%.

- i. This optimal positioning led to smoother temperature profiles across the wall layers and minimised heat transfer, both in walls with and without windows.
- ii. The PCM placement at 341 mm delivered a notable 13.12% annual energy savings, reducing energy consumption from 57.005 MJ to 49.526 MJ in a simulated office building with a double-glazed window. PCM at positions of 344 mm and 356 mm also provided substantial energy savings of 11.95% and 8.55%, respectively. These savings were validated against 2019 measured data, emphasising the potential of PCM to reduce heating and cooling loads.

- iii. The Predicted Mean Vote (PMV) and Predicted Percentage of Dissatisfied (PPD) metrics have indicated an enhanced occupant comfort with PCM integration. PMV values for PCM positions between 341 mm and 356 mm ranged between -0.5 and +0.5, aligning with optimal comfort levels. PPD values remained under 15%, highlighting the significant improvement in maintaining a stable indoor environment. These findings have demonstrated that PCM saved energy and ensured higher thermal comforts for occupants.
- iv. In buildings with double-glazed windows, heat transfer was higher due to the window's inherent thermal weaknesses. However, PCM placement near the inner wall surface (341 mm to 356 mm) still mitigated these effects, reducing energy loss through windows and stabilising indoor temperatures. For instance, the PCM at the position of 341 mm in a wall with windows reduced energy consumption by 7.479 MJ annually.
- v. The accuracy of the simulation models was confirmed through a solid alignment with experimental data. Metrics such as Mean Absolute Error (MAE) and Mean Absolute Percentage Error (MAPE) have showed low error rates. Specifically, the MAE for PCM 341 mm was 0.91 MJ/m², while the MAPE was 19.18%, indicating reliable predictions of PCM performance. These metrics validated the model for predicting energy consumption and temperature regulation in different building types.
- vi. PCM integration was especially effective during peak heating and cooling periods. In cold months (January to March), PCM at the position of 341 mm particularly in January showed 6.096 MJ of energy use compared to the baseline of 6.988 MJ/m². Similarly, during the summer months (July and August), the PCM reduced cooling loads significantly, consuming 2.080 MJ/m² in August compared to the measured data of 2.818 MJ/m². These seasonal results have demonstrated the PCM's ability to buffer extreme temperatures.

7.1.2 Impacts on Classic Buildings and Modern Office Buildings

- i. The effectiveness of PCMs in improving energy efficiency across diverse building types, including classic Victorian-era buildings and modern office spaces has been demonstrated. PCM integration offers a valuable retrofit solution for classic buildings, particularly those with poor insulation. By positioning the PCM optimally near the inner wall surface, energy savings of up to 13.12% were achieved, making this a viable strategy for conserving energy while preserving the architectural integrity of older structures.
- ii. In modern office buildings, where large, glazed surfaces contribute to higher energy demands, PCM integration effectively can reduce heating and cooling loads. Double-glazed windows

typically present thermal challenges, but PCM placed near the inner surface mitigated heat loss. The PCM positions in the range of 341 to 356 show high energy savings, ranging from 34% to 37%. These savings align with global energy efficiency targets, contributing to lower operational costs and reduced carbon footprints.

- iii. The experimental analysis revealed a parabolic relationship between PCM positioning and heat transfer rates for the classic buildings. The lowest heat transfer rate (2.23 W) was observed at the 100 mm position, while deeper PCM placements, particularly at 341 mm and 356 mm, demonstrated higher heat transfer rates. This indicates that placing the PCM deeper (closer to the inner surface) within the classic building wall could enhance its ability to manage heat more effectively.
- iv. For a Modern office building wall with a window, the key highlight was the derivation and validation of an empirical formula, Equation (5-8), which can model the heat transfer rate as a function of PCM position. This empirical formula has combined a decaying exponential function and a sinusoidal component to account for fluctuations caused by PCM phase changes and the decreasing heat transfer as the PCM is placed deeper within the wall. This equation was validated through experimental data, showing a strong correlation between predicted and measured values, thus confirming its effectiveness for optimising PCM placement to achieve efficient thermal management.

7.1.3 PCM Location and Moisture Management in Multi-Layer Walls

The placement of PCM layers in multi-layer walls must account for their proximity to water barriers to prevent moisture infiltration, which could compromise both the PCM's thermal performance and the structural integrity of the wall. This is particularly crucial in the UK climate, known for its high humidity and frequent rainfall. Effective moisture management becomes even more significant in historic buildings where preserving traditional materials is a priority.

PCM layers should be positioned on the interior side of a robust water barrier to shield them from external moisture ingress. This placement prevents the PCM from absorbing moisture, which could alter its thermal properties and reduce its energy efficiency. Additionally, a vapor control layer can be incorporated between the PCM and the internal wall layers to mitigate moisture movement caused by condensation, particularly in the environment prone to temperature fluctuations.

The use of breathable materials, such as lime plaster, is also recommended for managing moisture effectively. These materials allow for moisture movement without trapping it near the PCM, making them especially suitable for historic buildings. Proper sealing of wall joints and edges, combined with the use of desiccants or moisture-absorbing materials, can further reduce the risk of moisture-related issues. A slight slope or drainage system can also be designed to direct water away from critical areas. To ensure long-term performance, monitoring systems such as moisture sensors can be installed within the wall structure. These sensors provide real-time data on humidity levels, allowing for the early detection of potential issues before a significant damage occurs. For historic buildings, this combination of preventive measures and continuous monitoring helps to balance the energy efficiency with the preservation of architectural integrity. By addressing moisture concerns effectively, PCM integration in multi-layer walls can achieve sustainable performance while safeguarding the unique characteristics of historic structures.

7.2 Recommendations for Practice and Policy

i. Incorporate PCM Standards in Building Codes

buildings' aesthetics or structural integrity.

- PCM technology has proven effective from the findings, making it worth a serious consideration by governments and industry regulators. They should consider integrating PCM into national and international building codes and energy efficiency standards. By including PCM in these regulations, its use can be encouraged in both new constructions and retrofits, thereby enhancing thermal performance, reducing energy consumption, and supporting broader sustainability and EU 2050 goals.
- Encourage PCM Use in Retrofit Programs
 Retrofit initiatives for older, historically significant buildings ought to incentivise a PCM integration. This can significantly improve energy efficiency without compromising classic
- iii. Promote PCM Application in Modern Office Design

 Architects and building engineers should integrate PCMs in modern building envelopes,
 particularly in office spaces with large, glazed areas. This strategy would optimise energy
 savings and contribute to achieving sustainability targets.

7.3 Reflections and Overall Assessment of the Research Project

The primary aim of this research was to investigate the effectiveness of Phase Change Materials (PCMs) in enhancing energy efficiency across various building types, including Victorian-era

buildings, modern hospital buildings and office structures with cavity walls and integrated double-glazed glass windows. The research sought to contribute to the global efforts in reducing energy consumption and meeting sustainability targets such as the UK, DESNEZ and the Europe 2030 targets, which align with the goal of achieving Net Zero Emissions by 2050.

The project objectives were systematically addressed and successfully completed, resulting in significant outcomes. The first objective, which aimed to reduce the energy cost of CHASE FARM Hospital's main building, was achieved through detailed analysis and application of PCM-enhanced walls. This has shown a substantial reduction in operational energy costs, supporting both the hospital's energy efficiency and sustainability goals. The second objective, evaluating the thermal performance of PCM multi-layer walls in Victorian-era buildings, was also achieved, demonstrating that PCM integration could reduce energy consumption while maintaining the architectural integrity of these historical structures.

For modern hospital and office buildings, the study optimised PCM-enhanced cavity walls with integrated windows, meeting the third objective by providing insights into how PCM configuration, combined with window integration, improves thermal performance and reduces energy consumption. Laboratory testing and experimental validation of the simulation results, as outlined in the fourth objective, were successfully conducted. These tests confirmed the reliability of the simulation outcomes and ensured that PCM performance in real-world settings was accurately reflected.

In particular, this research has provided practical design recommendations and guidelines for incorporating PCM in building retrofits or new constructions, fulfilling the fifth objective. The final objective, which aimed to align the study's findings with the UK, DESNEZ and the Europe 2030 targets, was also accomplished. The study has contributed to the broader understanding of PCM applications in diverse building contexts, supporting global efforts to reduce greenhouse gas emissions and promote sustainable energy practices.

Overall, this research project is successful in meeting its aim and objectives. It has not only demonstrated the energy-saving potential of PCMs in various building types but also provided validated, practical guidelines for future applications.

7.4 Recommendations and Suggestions for Future Research

This study has provided valuable insights into integrating Phase Change Materials (PCMs) in building walls for energy efficiency and thermal regulation. However, future research should focus on long-term performance studies of PCMs in real-world environments, particularly in regions with extreme climates, to assess their durability and effectiveness over time. Exploring PCM performance in diverse climate conditions, such as tropical, arid, and polar climates would broaden the understanding of the applicability and efficiency of PCM technology across a wider range of building types and temperature extremes.

Additionally, while scaled-down prototypes were used in this study, future research should involve full-scale buildings to capture other complex dynamics of real-world conditions more accurately. Long-term monitoring across various climates and seasons will provide better insights into sustained performance of PCMs, offering a more realistic assessment of their applicability.

Incorporating more complex occupant behavioural models into PCM simulations should also be considered. These models, which account for actions like window operation and thermostat adjustments, would provide a more realistic picture of how internal heat gains affect energy consumption. Machine learning algorithms could further enhance PCM positioning, allowing for real-time adjustments based on environmental conditions.

Finally, future research should examine the long-term effects of thermal cycling on PCM performance and explore how repeated phase transitions affect the material's efficiency. More comprehensive cost-benefit analyses and life cycle assessments (LCA) should also be conducted to determine the economic feasibility and environmental impact of PCM integration in buildings, ensuring practical application in various contexts.

These areas of research will deepen the understanding of PCMs and help optimise their use in sustainable building design.

7.5 Publications

i). Ronny Achaku, Liang Li and Yong Kang Chen. "An Experimental Investigation of Phase Change Material (PCM) - Enhanced Cavity Walls with Integrated Windows in Office

- Buildings: Optimising Energy Savings" Sustainable Energy Technologies and Assessments, pp. 1-22, 2024. (2nd review process)
- ii). Ronny Achaku, Liang Li and Yong Kang Chen. "A Study of Phase Change Materials for Energy Conservation in Classic Multi-Layered Victorian-era Buildings: A Practical Approach for Balancing Heritage Preservation and Climate Neutrality" *Construction and Building Materials*, vol. 464, no. 140075, pp. 1-12, (2025).
- iii). Ronny Achaku, Liang Li and Yong Kang Chen. "An Experimental Analysis of Energy Conservation of a typical Hospital Building with PCM Multi-Layer Wall" *SPECS Research Conference, University of Hertfordshire*, 12th June 2024
- iv). Ronny Achaku, Liang Li and Yong Kang Chen. "Optimising PCM Integration in Thick Multi-layer Walls for Energy Efficiency: Experimental Insights on Heating Demand Reduction" International Conference on Renewable Energy Sources and Energy Conversion Processes (ICRESECP-24), 17th 18th October 2024 (in review process)

REFERENCES

- [1] Y. Ma, D. Li, R. Yang, M. Arici and C. Liu, "Energy and daylighting performance of a building containing an innovative glazing window with solid-solid phase change material and silica aerogel integration," *Energy Conversion and Management*, vol. 271, no. 116341, pp. 1-16, (2022).
- [2] Z. Said and A. K. Pandey, "Phase Change Materials (PCMs)," in *Nano Enhanced Phase Change Materials. Materials Horizons. Preparation, Properties and Applications*, Singapore, Springer, 2023, pp. P11-44.
- [3] A. Bozzhigitov, S. A. Memon and I. Adilkhanova, "Sensitivity of energy performance to the selection of PCM melting temperature for the building located in Cfb climate zone," *Energy Reports*, vol. 8, pp. 6301-6320, 2022.
- [4] International Energy Agency, "International Energy Agency," Buildings, 2024. [Online]. Available: https://www.iea.org/energy-system/buildings. [Accessed 06 05 2024].
- [5] Y. Wang, H. Chen and X. Zhang, "Energy Storage and Future Carbon-Neutral Energy Systems (ES-CNES)," *Energy Reports*, vol. 8, pp. 13959-13961, 2022.
- [6] A. Maturo, C. Vallianos, A. Buonomano and A. Anthienitis, "A novel multi-level predictive management strategy to optimize phase-change energy storage and building-integrated renewable technologies operation under dynamic tariffs," *Energy Conversion and Management*, vol. 291, no. 117220, pp. 1-16, (2023).
- [7] R. A. Kishore, M. V. Bianchi, C. Booten, J. Vidal and R. Jackson, "Enhancing building energy performance by effectively using phase change material and dynamic insulation in walls," *Applied Energy*, vol. 283, no. 116306, pp. 1-17, (2021).
- [8] L. Li, Y. T. Ge, X. Luo and S. A. Tassou, "Design and dynamic investigation of low-grade power generation systems with CO2 transcritical power cycles and R245fa organic Rankine cycles," *Thermal Science and Engineering Progress*, vol. 8, pp. 211-222, (2018).
- [9] Gov.Uk, "Department of Energy Security & Net Zero," Government Digital Service, 2023-2024. [Online]. Available: https://www.gov.uk/government/organisations/department-forenergy-security-and-net-zero/about. [Accessed 10 August 2024].

- [10] C. Amaral, R. Vicente, P. A. Marques and A. Barros-Timmons, "Phase change materials and carbon nanostructures for thermal energy storage: A literature review," *Renewable and Sustainable Energy Reviews*, vol. 79, pp. 1212-1228, 2017.
- [11] J. S. Ramos, S. Á. Domínguez, M. P. Moreno, M. G. Delgado, L. R. Rodríguez and J. A. T. Ríos, "Design of the Refurbishment of Historic Buildings with a Cost-Optimal Methodology: A Case Study," *Applied Sciences*, vol. 9(15), no. 3104, pp. 1-21, 2019.
- [12] G. Nair, L. Verde and T. Olofsson, "A Review on Technical Challenges and Possibilities on Energy Efficient Retrofit Measures in Heritage Buildings," *Energies*, vol. 15, no. 7472, pp. 1-20, 2022.
- [13] V. BBC, "Grenfell Tower: What happened," BBC News, 29 October 2019.
- [14] Y. Ma, D. Li, R. Yang, M. Arici and C. Liu, "Energy and daylighting performance of a building containing an innovative glazing window with solid-solid phase change material and silica aerogel integration," *Energy Conversion and Management*, vol. 271, no. 116341, pp. 1-16, (2022).
- [15] L. Zhang, Q. Zhang, L. Jin, X. Cui and X. Yang, "Energy, economic and environmental (3E) analysis of residential building walls enhanced with phase change materials," *Journal of Building Engineering*, vol. 84, no. 108503, pp. 1-26, 2024.
- [16] A. Maturo, C. Vallianos, A. Buonomano and A. Anthienitis, "A novel multi-level predictive management strategy to optimize phase-change energy storage and building-integrated renewable technologies operation under dynamic tariffs," *Energy Conversion and Management*, vol. 291, no. 117220, pp. 1-16, (2023).
- [17] N. Farouk, A. A. Alotaibi, A. H. Alshahri and K. H. Almitani, "Using PCM in buildings to reduce HVAC energy usage taking into account Saudi Arabia climate region," *Journal of Building Engineering*, vol. 50, no. 104073, pp. 1-12, (2022).
- [18] Z. Zhang, H. Su, H. Guo, M. Song, C. Xu, X. Chen and X. Li, "A numerical study on summer operation performance of PCM wallboard cooling tower coupling system in hot-summer and cold-winter regions of China," *Journal of Building Engineering*, vol. 95, no. 110100, pp. 1-25, 2024.
- [19] R. A. Kishore, M. V. Bianchi, C. Booten, J. Vidal and R. Jackson, "Enhancing building energy performance by effectively using phase change material and dynamic insulation in walls," *Applied Energy*, vol. 283, no. 116306, pp. 1-17, (2021).

- [20] L. Li, Y. T. Ge, X. Luo and S. A. Tassou, "Design and dynamic investigation of low-grade power generation systems with CO2 transcritical power cycles and R245fa organic Rankine cycles," *Thermal Science and Engineering Progress*, vol. 8, pp. 211-222, (2018).
- [21] X. Li, W. S. Su, W. X. Xu, B. Dai, J. Li and L. Li, "Editorial: CO2-based energy systems for cooling, heating, and power," *Frontiers in Energy Research*, pp. 1-2, 16 August (2022).
- [22] S. H. Choi, J. Park, H. S. Ko and S. W. Karng, "Heat penetration reduction through PCM walls via bubble injections in buildings," *Energy Conversion and Management*, vol. 221, no. 113187, pp. 1-14, (2020).
- [23] C. Li, X. Wen, W. Cai, J. Wu, J. Shao, Y. Yang, H. Yu, D. Liu and M. Wang, "Energy performance of buildings with composite phase-change material wallboards in different climatic zones of China," *Energy and Buildings*, vol. 273, no. 112398, pp. 1-21, (2022).
- [24] A. Kurdi, N. Almoatham, M. Mirza, T. Ballweg and B. Alkahlan, "Potential Phase Change Materials in Building Wall Construction—A Review," *Materials*, vol. 14, no. 5328, pp. 1-35, (2021).
- [25] R. Daneshazarian, A. M. Bayomy and S. B. Dworkin, "NanoPCM based thermal energy storage system for a residential building," *Energy Conversion and Management*, vol. 254, no. 115208, pp. 1-14, (2022).
- [26] R. Ji, X. Li and C. Lv, "Synthesis and evaluation of phase change material suitable for energy-saving and carbon reduction of building envelopes," *Energy and Buildings*, vol. 278, no. 112603, pp. 1-11, (2023).
- [27] S. W. Sharshir, A. Joseph, M. Elsharkawy, M. A. Hamada, A. W. Kandeal, M. R. Elkadeem, A. K. Thakur, Y. Ma, M. E. Moustapha, M. Rashad and M. Arici, "Thermal energy storage using phase change materials in building applications: A review of the recent development," *Energy and Buildings*, vol. 285, no. 112908, pp. 1-28, (2023).
- [28] O. Acuña-Díaz , N. Al-Halawani, M. Alonso-Barneto, A. Ashirbekov, C. Ruiz-Flores and L. Rojas-Solórzano, "Economic viability of phase-changing materials in residential buildings A case study in Alice Springs, Australia," *Energy and Buildings*, vol. 254, no. 111612, pp. 1-10, (2022).
- [29] Q. A. PCM, "RAL Quality Association PCM," eRecht24, 2020. [Online]. Available: https://www.pcm-ral.org/pcm/en/pcm/. [Accessed 13-Jun-2021 January 2020].

- [30] N. Kulumkanov, S. A. Memon and S. A. Khawaja, "Evaluating future building energy efficiency and environmental sustainability with PCM integration in building envelope," *Journal of Building Engineering*, vol. 93, no. 109413, pp. 1-34, (2024).
- [31] K. A. Samiev, M. S. Mirzaev and U. X. Ibragimov, "Annual thermal performance of a passive solar heating system," *Earth and Environmental Science*, vol. 1070, no. 012022, pp. 1-7, (2022).
- [32] A. Vukadinovic, J. Radosavljevic and A. Dordevic, "Energy performance impact of using phase-change materials in thermal storage walls of detached residential buildings with a sunspace," *Solar Energy*, vol. 206, no. 2020, pp. 228 244, (2020).
- [33] Z. X. Li, A. A. Al-Rashed, M. Rostamzadeh, R. Kalbasi, A. Shashavar and M. Afrand, "Heat transfer reduction in buildings by embedding phase change material in multi-layer walls: Effects of repositioning, thermophysical properties and thickness of PCM," *Energy Conversion and Management*, vol. 195, pp. 43-56, (2019).
- [34] Y. Dong, L. Zhang, P. Wang, Z. Liu, X. Su, H. Liao and X. Jiang, "Potential evaluation of energy flexibility and energy-saving of PCM-integrated office building walls," *Journal of Building Engineering*, vol. 79, no. 107857, pp. 1-17, (2023).
- [35] S. Dardouri, S. Mankai, M. M. Almoneef, M. Mbarek and J. Sghaier, "Energy performance based optimization of building envelope containing PCM combined with insulation considering various configurations," *Energy Reports*, vol. 10, pp. 895-909, 2023.
- [36] P. K. S. Rathore and S. K. Shukla, "An experimental evaluation of thermal behavior of the building envelope using macroencapsulated PCM for energy savings," *Renewable Energy*, vol. 149, pp. 1300-1313, 2020.
- [37] Z. Abilkhassenova, S. A. Memon, A. Ahmad, A. Saurbayeva and J. Kim, "Utilizing the Fanger thermal comfort model to evaluate the thermal, energy, economic, and environmental performance of PCM-integrated buildings in various climate zones worldwide," *Energy and Buildings*, vol. 297, no. 113479, 2023.
- [38] C. Baylis and C. A. Cruickshank, "Parametric analysis of phase change materials within cold climate buildings: Effects of implementation location and properties," *Energy and Buildings*, vol. 303, no. 113822, pp. 1-10, (2024).
- [39] M. Ghamari, C. H. See, D. Hughes, T. Mallick, K. S. Reddy, K. Patchigolla and S. Sundaram, "Advancing sustainable building through passive cooling with phase change materials, a

- comprehensive literature review," *Energy and Buildings*, vol. 312, no. 114164, pp. 1-28, (2024).
- [40] F. Guarino, A. Athienitis, M. Cellura and D. Bastien, "PCM thermal storage design in buildings: Experimental studies and applications to solaria in cold climates," *Applied Energy*, vol. 185, no. Part 1, pp. 95-106, 2017.
- [41] P. Besen, "Heritage for the Future: Integrating Energy Retrofitting to Seismic Upgrades of Unreinforced Masonry Buildings in Aotearoa New Zealand," University of Auckland, New Zealand, (2020).
- [42] T. Zhou, Y. Xiao, H. Huang and J. Lin, "Numerical study on the cooling performance of a noval passive system: Cylindrical phase change material-assisted earth-air heat exchanger," *Journal of Cleaner Production*, vol. 245, no. 118907, pp. 1-14, (2020).
- [43] C. Baylis and C. A. Cruickshank, "Parametric analysis of phase change materials within cold climate buildings: Effects of implementation location and properties," *Energy and Buildings*, vol. 303, no. 113822, pp. 1-10, (2024).
- [44] F. Karimi, N. Valibeig, G. Memarian and A. Kamari, "Sustainability Rating Systems for Historic Buildings: A Systematic Review," *Sustainability*, vol. 14(19), no. 12448, pp. 1-22, 2022.
- [45] L. F. Cabeza, A. de Gracia and A. L. Pisello, "Integration of renewable technologies in historical and heritage buildings: A review," *Energy and Buildings*, vol. 177, pp. 96-111, 2018.
- [46] G. Passerini and M. N, WIT Transactions on Ecology and the Environment, Southhampton, Boston: WITPRESS, 2018.
- [47] T. A. Mukram and J. Daniel, "A review of novel methods and current developments of phase change materials in the building walls for cooling applications," *Sustainable Energy Technologies and Assessments*, vol. 49, no. 101709, pp. 1-27, (2021).
- [48] O. Acuña-Díaz, N. Al-Halawani, M. Alonso-Barneto, A. Ashirbekov, C. Ruiz-Flores and L. Rojas-Solórzano, "Economic viability of phase-changing materials in residential buildings A case study in Alice Springs, Australia," *Energy and Buildings*, vol. 254, no. 111612, pp. 1-10, (2022).
- [49] The European Commission, "Climate Action," Directorate-General for Climate Action (DG CLIMA), [Online]. Available: https://climate.ec.europa.eu/index_en. [Accessed (2024) April 24].

- [50] F. Wise, A. Moncaster and D. Jones, "Rethinking retrofit of residential heritage buildings," *Buildings & Cities*, vol. 2, no. 1, pp. 495-517, 2021.
- [51] A. Ahmad and S. A. Memon, "A novel method to evaluate phase change materials' impact on buildings' energy, economic, and environmental performance via controlled natural ventilation," *Applied Energy*, Vols. 353, Part B, no. 122033, pp. 1-26, (2024).
- [52] D. Li, B. Zhuang, Y. Chen, B. Li, V. Landry, A. Kaboorani, Z. Wu and X. A. Wang, "Incorporation technology of bio-based phase change materials for building envelope: A review," *Energy and Buildings*, vol. 260, no. 111920, pp. 1-17, (2022).
- [53] L. D. Pereira, V. Tavares and N. Soares, "Up-To-Date Challenges for the Conservation, Rehabilitation and Energy Retrofitting of Higher Education Cultural Heritage Buildings," *Sustainability*, vol. 13, no. 2061, pp. 1-12, 2021.
- [54] O. K. Akande, N.-D. Odeleye and A. Coday, "Energy efficiency for sustainable reuse of public heritage buildings: the case for research," *International Journal of Sustainable Development and Planning*, vol. 9, no. 2, pp. 237-250, 2023.
- [55] A. L. Webb, "Energy retrofits in historic and traditional buildings: A review of problems and methods," *Renewable and Sustainable Energy Reviews*, vol. 77, pp. 748-759, 2017.
- [56] C. M. González, A. L. Rodríguez, R. S. Medina and J. R. Jaramillo, "Effects of future climate change on the preservation of artworks, thermal comfort and energy consumption in historic buildings," *Applied Energy*, vol. 276, no. 15, pp. 1-12, 2020.
- [57] O. Imghoure, N. Belouggadia, M. Ezzine, R. Lbibb and Z. Younsi, "Evaluation of phase change material and thermochromic layers in a "smart wall" in different climates for improving thermal comfort in a building," *Journal of Building Engineering*, vol. 56, no. 104755, pp. 1-24, (2022).
- [58] M. Krajčík, . M. Arıcı and Z. Ma, "Trends in research of heating, ventilation and air conditioning and hot water systems in building retrofits: Integration of review studies," *Journal of Building Engineering*, vol. 76, no. 107426, pp. 1-18, (2023).
- [59] F. L. Rashid, M. A. Al-Obaidi, A. Dulaimi, L. F. A. Bernardo, M. A. Eleiwi, H. B. Mahood and A. Hashim, "A Review of Recent Improvements, Developments, Effects, and Challenges on Using Phase-Change Materials in Concrete for Thermal Energy Storage and Release," *Journal of Composites Science*, vol. 7(9), no. 352, pp. 1-34, (2023).

- [60] M. Jaradat, H. Al Majali, C. Bendea, C. C. Bungau and T. Bungau, "Enhancing Energy Efficiency in Buildings through PCM Integration: A Study across Different Climatic Regions," *Buildings*, vol. 14(1), no. 40, pp. 1-27, (2024).
- [61] A. Kurdi, N. Almoatham, M. Mirza, T. Ballwg and B. Alkahlan, "Potential Phase Change Materials in Building Wall Construction—A Review," *Materials*, vol. 14(18), no. 5328, pp. 1-35, (2021).
- [62] A. Al-Habaibeh, A. Hawas, L. Hamadeh, B. Medjdoub, J. Marsh and A. Sen, "Enhancing the sustainability and energy conservation in heritage buildings: The case of Nottingham Playhouse," *Frontiers of Architectural Research*, vol. 11, no. 1, pp. 142-160, (2022).
- [63] K. Fouseki, D. Newton, K. S. Camacho, S. Nandi and T. Koukou, "Energy Efficiency, Thermal Comfort, and Heritage Conservation in Residential Historic Buildings as Dynamic and Systemic Socio-Cultural Practices," *Atmosphere*, vol. 11(6), no. 604, pp. 1-22, (2020).
- [64] E. RESOURCES, "US. Department of Energy. Update or Replace Winodws," Energy Saver, 2023. [Online]. Available: https://www.energy.gov/energysaver/update-or-replace-windows#:~:text=Heat%20gain%20and%20heat%20loss,heating%20and%20cooling%20ene rgy%20use.. [Accessed 26 June 2024].
- [65] E. Cuce, P. M. Cuce and S. Riffat, "Thin film coated windows towards low/zero carbon buildings: Adaptive control of solar, thermal, and optical parameters," *Sustainable Energy Technologies and Assessments*, vol. 46, no. 101257, pp. 1-8, 2021.
- [66] M. Che-Pan, E. Simá, A. Ávila-Hernández, J. Uriarte-Flores and R. Vargas-López, "Thermal performance of a window shutter with a phase change material as a passive system for buildings in warm and cold climates of México," *Energy & Buildings*, pp. 1-20, 2023.
- [67] Z. A. Al-Absi, M. H. M. Isa and M. Ismail, "Phase Change Materials (PCMs) and Their Optimum Position in Building Walls," *Sustainability*, vol. 112, no. 1294, pp. 1-25, 2020.
- [68] B. Patel, P. K. S. Rathore, N. K. Gupta, B. S. Sikarwar, R. K. Sharma, R. Kumar and A. K. Pandey, "Location optimization of phase change material for thermal energy storage in concrete block for development of energy efficient buildings," *Renewable Energy*, vol. 218, no. 119306, pp. 1-10, 2023.
- [69] W. Jiang, B. Liu, X. Zhang, T. Zhang, D. Li and L. Ma, "Energy performance of window with PCM frame," *Sustainable Energy Technologies and Assessments*, vol. 45, no. 101109, pp. 1-9, 2021.

- [70] R. Tafakkori and A. Fattahi, "Introducing novel configurations for double-glazed windows with lower energy loss," *Sustainable Energy Technologies and Assessments*, vol. 43, no. 100919, pp. 1-10, 2021.
- [71] S. Organ, "Minimum energy efficiency is the energy performance certificate a suitable foundation?," *International Journal of Building Pathology and Adaptation*, vol. 394, no. 4, pp. 581-601, 2020.
- [72] M. Shan and B.-g. Hwang, "Green building rating systems: Global reviews of practices and research efforts," *Sustainable Cities and Society*, vol. 39, pp. 172-180, 2018.
- [73] S. Sustainable Investment Group, "Top 12 Green Building Rating Systems," Sustainable Investment Group (SIG), 01 June 2020. [Online]. Available: https://sigearth.com/top-12-green-building-rating-systems/. [Accessed 10 August 2024].
- [74] E. Commission, "The European Green Deal," Directorate-General for Communication, 09 July 2024. [Online]. Available: https://commission.europa.eu/strategy-and-policy/priorities-2019-2024/story-von-der-leyen-commission/european-green-deal_en. [Accessed 10 August 2024].
- [75] G. DESNZ, "Department for Energy Security & Net Zero," GOV.UK, 09 July 2024. [Online]. Available: https://www.gov.uk/government/organisations/department-for-energy-security-and-net-zero. [Accessed 10 August 2024].
- [76] Y. Elaouzy and A. El Fadar, "Energy, economic and environmental benefits of integrating passive design strategies into buildings: A review," *Renewable and Sustainable Energy Reviews*, vol. 167, no. 112828, pp. 1-18, 2022.
- [77] X. Kong, . L. Wang, H. Li, G. Yuan and C. Yao, "Experimental study on a novel hybrid system of active composite PCM wall and solar thermal system for clean heating supply in winter," *Solar Energy*, vol. 195, pp. 259-270, 2020.
- [78] X. Qiao, X. Kong, H. Li, L. Wang and H. Long, "Performance and optimization of a novel active solar heating wall coupled with phase change material," *Journal of Cleaner Production*, vol. 250, no. 119470, pp. 1-17, 2020.
- [79] G. Gholamibozanjani and M. Farid, Peak Load Shifting Using a Price-Based Control in PCM-Enhanced Buildings; Thermal Energy Storage with Phase Change Materials, Boca Raton: CRC Press, 2021.

- [80] X. Sun, Z. Gou and S. S.-Y. Lau, "Cost-effectiveness of active and passive design strategies for existing building retrofits in tropical climate: Case study of a zero energy building," *Journal of Cleaner Production*, vol. 183, pp. 35-45, 2018.
- [81] R. Stropnik, R. Koželj, E. Zavrl and U. Stritih, "Improved thermal energy storage for nearly zero energy buildings with PCM integration," *Solar Energy*, vol. 190, pp. 420-426, 2019.
- [82] L. Gibbons and S. Javed, "A review of HVAC solution-sets and energy performace of nearly zero-energy multi-story apartment buildings in Nordic climates by statistical analysis of environmental performance certificates and literature review," *Energy*, Vols. 238, Part A, no. 121709, pp. 1-14, 2022.
- [83] Q. A. PCM, "RAL Quality Association PCM," eRecht24, 2020. [Online]. Available: https://www.pcm-ral.org/pcm/en/pcm/. [Accessed 13 January 2020].
- [84] M. Rathod, "Phase Change Materials and Their Applications," in *Chapter 3*, Surat, Gujarat, India, Intech Open, 2018, pp. 37-57.
- [85] M. A. Boda, A. C. Kotali and V. R. Phand, "Various Applications of Phase Change Materials," Thermal Energy Storing materials. Internal Journal of Emerging research in Management & Technology, pp. 167-170, 2017.
- [86] H. Yang, Y. Wang, Z. Liu, D. Liang, F. Liu, W. Zhang, X. Di, C. Wang, H. Ho and W. Chen, "Enhanced thermal conductivity of waste sawdust-based composite phase change materials with expanded grahite for thermal energy storage," *Bioresources and Bioprocessing*, vol. 4, pp. 1-12, 2017.
- [87] M. Frigione, M. Lettieri and A. Sarcinella, "Phase Change Materials for Energy Efficiency in Buildings and Their Use in Mortars," *Materials (Basel)*, vol. 12, no. 1260, pp. 1-25, 2019.
- [88] M. Y. Abdelsalam, M. F. Lightstone and J. S. Cotton, "A novel approach for modeling thermal energy storage with phase change materials and immersed coil heat exchangers," *International Journal of Heat and Mass Transfer*, vol. 136, pp. 20-33, 2019.
- [89] C. R. C. Rao, K. Vigneshwaran, H. Niyas and P. Muthukumar, "Performance investigation of lab-scale sensible heat storage prototypes," *International Journal of Green Energy*, vol. 16, no. 14, pp. 1363-1378, 2019.
- [90] H. S. C. Pinterest, "Latent heat of fusion/vaporization," Pinterest, 2020. [Online]. Available: https://www.pinterest.com/pin/487373990898831528/. [Accessed 11 April 2020].

- [91] K. Mason, "theNBS.com," theNBS.com, 2020. [Online]. Available: https://www.thenbs.com/knowledge/phase-change-materials-applications-in-the-built-environment. [Accessed 13 January 2020].
- [92] B. P. Jelle and S. E. Kalnaes, "Chapter 3: Phase Change Materials for Application in Energy-Efficient Buildings," in *Cost-Effective Energy Efficient Building Retrofitting*, Elsevier, 2017, pp. 57-118.
- [93] J. Lizana, R. Charcartegui, A. Barrios-Padura, J. M. Valverde and C. Ortiz, "Identification of best available thermal energy storage compounds for low-to-moderate temperature storage applications in buildings," *Materials de Construction*, vol. 68, no. 331, pp. 1-36, 2018.
- [94] A. Mostafavi and A. J. Parhizi, "Theoretical modeling and optimization of fin-based enhancement," *International Journal of Heat and Mass Transfer*, vol. 145, pp. 1-10, 2019.
- [95] S. Wi, S. Yang, J. H. Park, S. J. Chang and S. Kim, "Climatic cycling assessment of red clay/perlite and vermiculite composite PCM for improving thermal inertia in buildings," *Building and Environment*, vol. 167, pp. 1-12, 2020.
- [96] A. Gounni and M. El Alami, "The optimal allocation of the PCM within a composite wall for surface temperature and heat flux reduction: An experimental Approach," *Applied Thermal Engineering*, vol. 127, pp. 1488-1494, 2017.
- [97] S. Ramakrishnan, X. Wang, J. Sanjayan and J. Wilson, "Experimental and Numerical study on Energy Performance of Buildings Integrated with Phase change materials," *Energy Procedia*, vol. 105, p. 2214 2219, 2017.
- [98] A. R. M. Siddique, S. Mahmud and B. V. Heyst, "A comprehensive rview on a passive (phase change materials) and an active (thermoelectric cooler) battery thermal management system and their limitations," *Journal of Power Sources*, vol. 401, pp. 224-237, 2018.
- [99] X. Kong, P. Jie, C. Yao and Y. Liu, "Experimental study on thermal performance of phase change material passive and active combined using for bulding application in winter," *Applied Energy*, vol. 206, pp. 293-302, 2017.
- [100] M. Saffari, A. d. Gracia, C. Fernandez and L. F. Cabeza, "Simulation-based optimization of PCM melting temperature to improve the energy perfomance in buildings," *Applied Energy*, vol. 202, pp. 420-434, 2017.

- [101] A. Agnihotri, W. S. Ali, A. Das and R. Alagirusamy, "Chapter 11: Insect-repellent textiles using green and sustainable approaches," in *The Impact and Prospects of Green Chemistry for Textile Technology*, Elsevier, 2019, pp. 307-325.
- [102] A. Marani and M. L. Nehdi, "Integrating phase change materials in construction materials: Critical review," *Construction and Building Materials*, vol. 217, pp. 36-49, 2019.
- [103] M. Li, G. Gui, L. Jiang, H. Pan and X. Wang, "Numerical Thermal Characterisation and Performance Metrics of Building Envelopes Containing Phase Change Materials for Energy-Efficient Buildings," *Sustainability*, vol. 10, no. 2657, pp. 1-23, 2018.
- [104] Q. Wang, R. Wu, Y. Wu and C. Y. Zhao, "Parametric analysis of using PCM walls for heating loads reduction," *Energy and Buildings*, vol. 172, pp. 328-336, 2018.
- [105] M. Parhizi and A. Jain, "Theoretical modelling of a phase change heat transfer problem with a pre-melted or pre-solidified region," *International journal of Heat and Mass Transfer*, vol. 136, pp. 635-641, 2019.
- [106] M. Yasin, E. Scheidemantel, F. Klinker, H. Weinläder and S. Weismann, "Generation of a simulation model for chilled PCM ceilings in TRNSYS and validation with real scale building data," *Journal of Building Engineering*, vol. 22, pp. 372-382, 2019.
- [107] T. Yamamoto, A. Ozaki, M. Lee and H. Kusumoto, "Fundamental study of coupling methods between energy simulation and CFD," *Energy and Buildings*, vol. 159, pp. 587-599, 2018.
- [108] M. Kuta, D. Matuszewska and T. M. Wójcik, "Maximization of performance of a PCM based thermal energy storage systems," *Web of Conferences*, vol. 213, no. 02049, pp. 1-6, 2019.
- [109] J. Xie, W. Wang, J. Liu and S. Pan, "Solar energy," *Thermal performance analysis of PCM wallboard for building application based on numerical simulation*, vol. 162, pp. 533-540, 2018.
- [110] H. A. Jebaei, A. Aryal, I. K. Jeon, A. Azzam, Y.-R. Kim and J.-C. Baltazar, "Evaluating the potential of optimized PCM-wallboards for reducing energy consumption and CO2 emission in buildings," *Energy and Buildings*, vol. 15, no. 114320, pp. 1-10, 2024.
- [111] T. Tamer, I. G. Dino, D. K. Baker and C. M. Akgül, "Coupling PCM wallboard utilization with night Ventilation: Energy efficiency and overheating risk in office buildings under climate change impact," *Energy and Buildings*, vol. 298, no. 113482, pp. 1-19, 2023.

- [112] R. A. Kishore, M. V. Bianchi, C. Booten, J. Vidal and R. Jackson, "Optimizing PCM-integrated walls for potential energy savings in U.S. Buildings," *Energy and Buildings*, vol. 226, no. 110355, pp. 1-14, 2020.
- [113] A. Mourid, M. E. Alami and F. Kuznik, "Experimental investigation on thermal behavior and reduction of energy consumption in a real scale building by using phase change materials on its envelope," *Sustainable Cities and Society*, vol. 41, pp. 35-43, 2018.
- [114] L. Yang, Y. Qiao, X. Zhang, C. Zhang and J. Liu, "A kind of PCMs-based lightweight wallboards: Artificial controlled condition experiments and thermal design method investigation," *Building and Environment*, vol. 144, pp. 194-207, 2018.
- [115] D. G. Antinafu, W. Dong, X. Huang, H. Gao and G. Wang, "Introduction of organic-organic eutectic PCM in mesoporous N-doped carbons for enhanced thermal conductivity and energy storage capacity," *Applied Energy*, vol. 211, pp. 1203-1215, 2018.
- [116] A. Ahmed, M. Mateo-Garcia, D. McGough, C. Kassim and Z. Ure, "Experimenetal evaluation of passive cooling using phase change materials (PCM) for reducing overheating in public heating," *Web of conferences*, vol. 32, no. 01001, pp. 1-4, 2018.
- [117] J. Jaguemont, N. Omar, P. V. d. Bossche and J. Mierlo, "Phase-Change materials (PCM) for automotive applications: A review," *Applied Thermal Engineering*, vol. 132, pp. 308-320, 2018.
- [118] S.-M. Wang, P. Matiasovsky, P. Mihalka and C.-M. Lai, "Experimental investigation of the daily thermal performance of a mPCM honeycomb wallboard," *Energy and Buildings*, vol. 159, pp. 419-425, 2018.
- [119] J. A. Noël and M. A. White, "Heat capacities of potential organic phase change materials," *J. Chem. Thermodynamics*, vol. 128, pp. 127-133, 2019.
- [120] A. Aljehani, L. C. Nitsche and S. Al-Hallaj, "Numerical nodeling of transient heat transfer in a phase change composite thermal energy storage (PCC-TES) system for air conditioning applications," *Applied Thermal engineering*, vol. 164, no. 114522, pp. 1-12, 2020.
- [121] T. Zhou, Y. Xiao, H. Huang and J. Lin, "Numerical study on the cooling performance of a noval passive system: Cylindriucal phase change material-assisted earth-air heat exchanger," *Journal of Cleaner Production*, vol. 245, no. 118907, pp. 1-14, 2020.
- [122] Z. X. Li, A. A. Al-Rashed, M. Rostamzadeh, R. Kalbasi, A. Shashavar and M. Afrand, "Heat transfer reduction in buildings by embedding phase change material in multi-layer walls:

- Effects of repositioning, thermophysical properties and thickness of PCM," *Energy Conversion and Management*, vol. 195, pp. 43-56, 2019.
- [123] S. Talukdar, H. m. M. Afroz, A. M. Hossain, M. A. Aziz and M. M. Hossain, "Heat transfer enhancement of charging and discharging of phase change materials and size optimization of a latent thermal energy storage system for solar cold storage application," *Journal of Energy Storage*, vol. 24, no. 100797, pp. 1-13, 2019.
- [124] F. Goia, G. Chaudhary and S. Fantucci, "Modeling and experimental validation of an algorithm for simulation of hysteresis effects in phase change materials for building components," *Energy & Buildings*, vol. 174, pp. 54-67, 2018.
- [125] Y. Xie, M. S. Gilmour, Y. Yaun, H. Jin and H. Wu, "A review on house design with energy saving system in the UK," *Renewable and Sustainable Energy Reviews*, vol. 71, pp. 29-52, 2017.
- [126] L. Bai, J. Xie, M. M. Farid, W. Wang and J. Liu, "Analytical model to study the heat storage of phase change material envelopes in lightweight passive buildings.," *Building and Environment*, vol. 169, no. 106531, pp. 1-10, 2020.
- [127] H. Nazir, M. Batool, F. J. B. Osorio, M. Isaza-Ruiz, X. Xu, K. Vignarooban, P. Phelan, Inamuddin and A. M. Kannan, "Recent developments in phase change materials for energy storage applications: A review," *International Journal of Heat and Mass Transfer*, vol. 129, pp. 491-523, 2019.
- [128] S. S. Chandel and T. Agarwal, "Review of current state of research on energy storage,toxicity,health hazards and commercialization of phase changing materials," *Renewable and Sustainable Energy Reviews*, vol. 67, pp. 581-596, 2017.
- [129] D. K. Bhamare, M. K. Rathod and J. Banerjee, "Passive cooling techniques for building and their applicability in different climatic zones—The state of art," *Energy & Buildings*, vol. 198, pp. 467-490, 2019.
- [130] E. Solgi, Z. Hamedani, R. Fernando, H. Skates and N. E. Orji, "A literature review of night ventilation strategies in buildings," *Energy & Buildings*, vol. 173, pp. 337-352, 2018.
- [131] A. Figueiredo, R. Vicente, J. Lapa, C. Cardoso, F. Rodrigues and J. Kämpf, "Indoor thermal comfort assessment using different constructive solutions incorporating PCM," *Applied Energy*, vol. 208, pp. 1208-1221, 2017.

- [132] L. Liu, D. Su, Y. Tang and G. Fang, "Thermal conductivity enhancement of phase change materials for thermal energy storage: A review," *Renewable and Sustainable Energy Reviews*, vol. 62, pp. 305-317, 2016.
- [133] K. A. Samiev, M. S. Mirzaev and U. X. Ibragimov, "Annual thermal performance of a passive solar heating system," *Earth and Environmental Science*, vol. 1070, no. 012022, pp. 1-7, 2022.
- [134] C. The Intergovernmental Panel on Climate, "Intergovernmental Panel on Climate Change (IPCC), Sixth Assessment Report (AR6), Working Group III: Climate Change Mitigation," The Intergovernmental Panel on Climate Change, Switzerland, 2022.
- [135] A. Mavrigiannaki and E. Ampatzi, "Latent heat storage in building elements: A systemetic review on properties and contextual performance factors," *Renewable and Sustainable Energy Reviews*, vol. 60, pp. 852-866, 2016.
- [136] A. Fateh, F. Klinker, M. Brutting and H. Weinlader, "Numerical and experimental investigation of an insulation layer with phase change materials (PCMs)," *Energy and Buildings*, vol. 153, pp. 231-240, 2017.
- [137] G. Nair, L. Verde and T. Olofsson, "A Review on Technical Challenges and Possibilities on Energy Efficient Retrofit Measures in Heritage Buildings," *Energies*, vol. 15(20), no. 7472, pp. 1-20, 2022.
- [138] E. Elnajjar, "Using PCM embedded in building material for thermal management:Performance assessment study," *Energy and Buildings*, vol. 151, pp. 28-34, 2017.
- [139] P. Devaux and M. M. Farid, "Benefits of PCM underfloor heating with PCM wallboards for space heating in winter," *Applied Energy*, vol. 191, p. 593–602, 2017.
- [140] A.-A. Zeyad, H. M. I. Mohd and I. Mazran, "Phase Change Materials (PCMs) and Their Optimum Position in Building Walls," *Sustainability*, vol. 12, no. 1294, pp. 1-25, 2020.
- [141] M. Arici, F. Bilgin, M. Krajcik, S. Nizetic and H. Karabay, "Energy saving and CO2 reduction potential of external building walls containing two layers of phase change material," *Energy*, vol. 252, no. 124010, pp. 1-13, 2022.
- [142] R. A. Kishore, M. V. Bianchi, C. Booten, J. Vidal and R. Jackson, "Enhancing building energy performance by effectively using phase change material and dynamic insulation in walls," *Applied Energy*, vol. 283, no. 116306, pp. 1-17, 2021.
- [143] M. Faraji, "Numerical study of thermal behavior of a novel Composite PCM/concrete wall," *Energy Procedia*, vol. 139, pp. 105-110, 2017.

- [144] I. Vigna, L. Bianco, F. Goia and V. Serra, "Phase Change Materials in Transparent Building Envelopes: A Strengths, Weakness, Opportunities and Threats (SWOT) Analysis," *Energies*, vol. 11, no. 111, pp. 1-19, 2018.
- [145] T. A. Mukram and J. Daniel, "A review of novel methods and current developments of phase change materials in the building walls for cooling applications," *Sustainable Energy Technologies and Assessments*, vol. 49 (2022), no. 101709, pp. 1-27, 2021.
- [146] C. Zhang, M. Yu, Y. Fan, X. Zhang, Y. Zhao and L. Qui, "Numerical study on heat transfer enhancement of PCM using three combined methods based on heat pipe," *Energy*, vol. 195, p. 116809, 2020.
- [147] E. B. Jebasingh and V. A. Arasu, "A comprehensive review on latent heat and thermal conductivity of nanoparticle dispersed phase change material for low-temperature applications," *Energy Storage Materials*, vol. 24, pp. 52-74, 2020.
- [148] G. Wei, G. Wang, C. Xu, X. Ju, L. Xing, X. Du and Y. Yang, "Selection principles and thermophysical properties of high temperature phase change materials for thermal energy storage: A review," *Renewable and Sustainable Energy Reviews*, vol. 81, pp. 1771-1786, 2018.
- [149] O. Enearu, Y. K. Chen and C. Kalyvas, "A New Approach to Modelling of PEMFC Flow Field," The 9th International Conference on Modelling, Identification and Control, pp. 958-964, 2017.
- [150] B. Delcroix, M. Kummert and A. Daoud, "Development and numerical validation of a new model for walls with phase change materials implemented in TRNSYS," *Journal of Building Performance Simulation*, vol. 10, no. 4, pp. 422-437, 2017.
- [151] Y. Abbassi, E. Baniasadi and H. Ahmadikia, "Transient energy storage in phase change materials, development and simulation of a new TRNSYS component," *Journal of Building Engineering*, vol. 50, no. 104188, pp. 1-16, 2022.
- [152] X. Sui, H. Liu, Z. Du and S. Yu, "Developing a TRNSYS model for radiant cooling floor with a pipe-embedded PCM layer and parametric study on system thermal performance," *Journal of Energy Storage*, vol. 71, no. 108024, pp. 1-19, 2023.
- [153] K. Biswas, Y. Shukla, A. Desjarlais and R. Rawal, "Thermal characterization of full-scale PCM products and numerical simulations, including hysteresis, to evaluate energy impacts in an envelope application," *Applied Thermal Engineering*, vol. 138, pp. 501-512, 2018.

- [154] L. Liu, X. Zhang, X. Xu, Y. Zhao and S. Zhang, "The research progress on phase change hysteresis affecting the thermal characteristics of PCMs: A review," *Journal of Molecular Liquids*, vol. 317, no. 113760, pp. 1-9, 2020.
- [155] F. Goia, G. Chaudhary and S. Fantucci, "Modelling and experimental validation of an algorithm for simulation of hysteresis effects in phase change materials for building components," *Energy & Buildings*, vol. 174, pp. 54-67, 2018.
- [156] W. Zeitoun, M. Labat, S. Lorente and M. Cézard, "Numerical study of a ventilated ceiling that integrates a phase change material for design improvement," *Applied Thermal Engineering*, vol. 7, no. 124090, pp. 1-36, 2024.
- [157] J. H. Park, J. Jeon, J. Lee, S. Wi, B. Y. Yun and S. Kim, "Comparative analysis of the PCM application according to the building type as retrofit system," *Building and Environment*, vol. 151, pp. 291-302, 2019.
- [158] E. Paroutoglou, A. Afshari, N. . C. Bergsøe, P. Fojan and G. Hultmark, "A PCM based cooling system for office buildings: a state of the art review," *E3S Web of Conferences*, vol. 111, no. 01026, pp. 1-8, 2019.
- [159] M. Prabhakar, M. Saffari, A. de Gracia and L. F. Cabeza, "Improving the energy efficiency of passive PCM system using controlled natural ventilation," *Energy and Buildings*, vol. 228, no. 110483, 2020.
- [160] A. Mechouet, E. M. Oualim and T. Mouhib, "Effect of mechanical ventilation on the improvement of the thermal performance of PCM-incorporated double external walls: A numerical investigation under different climatic conditions in Morocco," *Journal of Energy Storage*, vol. 38, no. 102495, pp. 1-16, 2021.
- [161] S. A. Khawaja and S. A. Memon, "Novel indicators to evaluate PCM performance under different ventilation strategies by considering the impact of climate change," *Journal of Building Engineering*, vol. 74, no. 106848, pp. 1-29, 2023.
- [162] C. Piselli, M. Prabhakar, A. de Gracia, M. Saffari, A. L. Pisello and L. F. Cabeza, "Optimal control of natural ventilation as passive cooling strategy for improving the energy performance of building envelope with PCM integration," *Renewable Energy*, vol. 162, pp. 171-181, 2020.
- [163] Y. Cascone, A. Capozzoli and M. Perino, "Optimisation analysis of PCM-enhanced opaque building envelope components for the energy retrofitting of office buildings in Mediterranean climates," *Applied Energy*, vol. 211, pp. 929-953, 2018.

- [164] O. J. Imafidon and D. S.-K. Ting, "Retrofitting buildings with Phase Change Materials (PCM)
 The effects of PCM location and climatic condition," *Building and Environment*, vol. 236, no. 110224, pp. 1-13, 2023.
- [165] F. Fatiguso, M. De Fino and E. Cantatore, "An energy retrofitting methodology of Mediterranean historical buildings," *Management of Environmental Quality*, vol. 26, no. 6, pp. 984-997, 2015.
- [166] J. Fernandes, M. C. Santos and R. Castro, "Introductory Review of Energy Efficiency in Buildings Retrofits," *Energies*, vol. 14, no. 8100, pp. 1-18, 2021.
- [167] H. Lee, Thermal Design, 2nd Edition, kalamazoo, MI, USA: Wiley, 2022.
- [168] M. Asker, H. Ganjehsarabi and T. M. Coban, "Numerical investigation of inward solidification inside spherical capsule by using temperature transforming method," *Ain Shams Engineering Journal*, vol. 9, no. 4, pp. 537-547, 2018.
- [169] Y. Huo and Z. Rao, "The improved enthalpy-transforming based lattice Boltzmann model for solid-liquid phase change," *International Journal of Heat and Mass Transfer*, vol. 133, pp. 861-871, 2019.
- [170] J. H. Lu, H. Y. Lei and C. S. Dai, "A unified thermal lattice Boltzmann equation for conjugate heat transfer problem," *International Journal of Heat and Mass Transfer*, Vols. 126, Part B, pp. 1275-1286, 2018.
- [171] A. Alongi, A. Angelotti, A. Rizzo and A. Zanelli, "A numerical model to simulate the dynamic performance of Breathing Walls," *Journal of Building Performance Simulation*, vol. 14, no. 2, pp. 155-180, 2021.
- [172] S. N. Al-Saadi and Z. J. Zhiqiang, "Modeling phase change materials embedded in building enclosure: A review," *Renewable and Sustainable Energy Reviews*, vol. 21, pp. 659-673, 2013.
- [173] M. Faden, A. König-Haagen, S. Höhlein and D. Brüggemann, "An implicit algorithm for melting and settling of phase change material inside macrocapsules," *International Journal of Heat and Mass Transfer*, vol. 117, pp. 757-767, 2018.
- [174] TRNSYS, "TRNSYS," Thermal Energy System Specialists, LLC, 2019. [Online]. Available: https://www.trnsys.com/index.html. [Accessed 03 June 2022].
- [175] T. E. S. TRNSYS Coordinator, "TRNSYS 18," Solar Energy Laboratory, University of Wisconsin-Madison, Madison, 2018.

- [176] M. R. Di Biasi, G. V. Ochoa and L. O. Quiñones, "ClosedSystem: A New Educational Software to Study the First Law of Thermodynamics in Closed Systems Using Matlab," *Contemporary Engineering Sciences*, vol. 10, no. 22, pp. 1075-1084, 2017.
- [177] T. T. 3. Mathematical Reference -, 7.7 Type 1270: Phase Change Material (PCM) Wall Layer for Type 56, Tess Libraries, 2019.
- [178] SCI, TRANSOSOLAR Energietechnik, CSTB, TESS, "Trnsys 18 Vol 9 Tutorials: TRNSYS 18 a TRaNsient SYstem Simlation program," 2019. [Online]. Available: http://sel.me.wisc.edu/trnsys. [Accessed 23 Jun 2024].
- [179] TRANSSOLAR, "Trnsys3d Tutorial," March 2012. [Online]. Available: http://www.trnsys.de/. [Accessed 27 Jul 2022].
- [180] K. M. Laxmi and V. V. KesavaRao, "Estimation of Cooling Load of a Residential House using TRNSYS," *Applied Research Journal of Science and Technology*, vol. 2, no. 1, pp. 1-24, 2020.
- [181] T. KlimaEngineering, "7.1 Type 1270: Phase Change Material (PCM) Wall Layer for Type 56," Transsolar, Stuttgart, 20112.
- [182] D. Mazzeo, N. Matera, C. Cornaro, G. Oliveti, P. Romagnoni and L. De Santoli, "EnergyPlus, IDA ICE and TRNSYS predictive simulation accuracy for building thermal behaviour evaluation by using an experimental campaign in solar test boxes with and without a PCM module," *Energy and Buildings*, vol. 212, no. 109812, pp. 1-30, 2020.
- [183] M. A. Adesanya, W.-H. Na, A. Rabiu, Q. O. Ogunlowo, T. D. Akpenpuun, A. Rasheed, Y.-C. Yoon and H.-W. Lee, "TRNSYS Simulation and Experimental Validation of Internal Temperature and Heating Demand in a Glass Greenhouse," *Sustainability*, vol. 14, no. 14, pp. 1-30, 2022.
- [184] M. Saffari, A. de Gracia, S. Ushak and L. F. Cabeza, "Passive cooling of buildings with phase change materials using whole-building energy simulation tools: A review," *Renewable and Sustainable Energy Reviews*, vol. 80, pp. 1239-1255, 2017.
- [185] BroadTech Engineering Consultancy, "Simulation Tools to Discover Better Designs, Faster," BroadTechEngineering, 2019. [Online]. Available: https://broadtechengineering.com/star-ccm/. [Accessed 10 May 2020].
- [186] C.-a. STAR-CCM+, STAR-CCM+ Training Handbook, CD-adapco, 2014.
- [187] T. E. S. Specialists, "TRNSYS 17 a TRansient SYstem Simulation program," [Online]. Available:

- https://sel.me.wisc.edu/trnsys/features/t17_1_updates.pdf#page=25&zoom=100,140,242. [Accessed 15 July 2024].
- [188] J.-B. Bouvenot, V. Jimenez and L. Desport, "Dynamic thermal behaviour characterization of integrated insulation clay hollow blocks for buildings energy simulations applications," *Journal of Building Performance Simulation*, vol. 14, no. 5, pp. 515-535, 2021.
- [189] TRNSYS, "Tess-libraries," TRNSYS, 2019. [Online]. Available: http://www.trnsys.com/c/individual-components.php.html. [Accessed 22 September 2022].
- [190] A. Wang, Z. Liu, H. Wu, A. Lewis and T. Loulou, "Numerical and Experimental Investigation on Single-Point Thermal Contact Resistance," in *Advances in Heat Transfer and Thermal Engineering: Proceedings of 16th UK Heat Transfer Conference (UKHTC2019)*, Singapore, 2021.
- [191] TRANSSOLAR, TESS, CSTB & SCL, "Trnsys 18 Vol 5 Multizone Building modeling with Type56 and TRNBuild," March 2017. [Online]. Available: http://www.transsolar.com, http://www.tess-inc.com, http://software.cstb.fr & https://sel.me.wisc.edu/trnsys/. [Accessed 27 Jul 2022].
- [192] J. Skovajsa, P. Drabek, S. Sehnalek and M. Zalesak, "Design and experimental evaluation of phase change material based cooling ceiling system," *Applied Thermal Engineering*, vol. 205, no. 118011, pp. 1-16, 2022.
- [193] R. C. Loonen, F. Favoino, J. L. Hensen and M. Overend, "Review of current status, requirements and opportunities for building performance simulation of adaptive facades," *Journal of Building Performance Simulation*, vol. 10, no. 2, pp. 205-223, 2017.
- [194] Rubitherm, "Rubitherm Phase Change Material," Rubitherm Technologies GmbH Imhoffweg 6 12307 Berlin, (2023). [Online]. Available: https://www.rubitherm.eu/media/products/datasheets/Techdata_-RT28HC_EN_09102020.PDF. [Accessed 13) November (2023].
- [195] P. Rolka, T. Przybylinski, R. Kwidzinski and M. Lackowski, "Thermal properties of RT22 HC and RT28 HC phase change materials proposed to reduce energy consumption in heating and cooling systems," *Renewable Energy*, vol. 197, pp. 462-471, 2022.
- [196] Ç. Susantez and A. Caldeira, "INVESTIGATION OF THE TIME DEPENDENT THERMAL BEHAVIOR OF A CONTAINER WITH PCM WALLS DURING A HOT SUMMER DAY," *Journal of Thermal Science and Technology*, vol. 40, no. 2, pp. 221-235, 2020.

- [197] L. Bouzyan, C. Toublanc and A. Ousegui, "Numerical Investigation on the Charging Process of Phase Change Materials (PCM) in Thermal Energy Storage Systems," in *Innovative Research in Applied Science, Engineering and Technology (IRASET)*, Morocco, 2024.
- [198] I. H. P. (IHP), "CRM846 IHP Chase Farm Hospital," Createmaster Ltd, [Online]. Available: https://www.docpark2.createmaster.co.uk/index.aspx#/documents. [Accessed 10 January 2020].
- [199] Chase Farm Hospital, "Royal free London NHS Foundation Trust," Electric Putty, [Online]. Available: https://www.royalfree.nhs.uk/chase-farm-hospital/. [Accessed 19 July 2019].
- [200] S. Seyam, "Chapter 4: Types of HVAC Systems," in *HVAC Systems*, Toronto, IntechOpen, 2018, pp. 49-66.
- [201] O. A. Qureshi, E. Trepci, A. A. Shahzad, P. Manandhar and E. Rodriguez-Ubinas, "Quantitative assessment of the HVAC system of zero-energy houses of the Solar Decathlon Middle East 2021," *Energy Reports*, vol. 9, no. 8, pp. 1050-1060, 2023.
- [202] Designing Buildings Ltd, 2020, "Designing Buildings Wiki," Designing Buildings Ltd, 3 September 2019. [Online]. Available: https://www.designingbuildings.co.uk/wiki/Heating_ventilation_and_air_conditioning_HVA C. [Accessed 23 February 2020].
- [203] X. Li, W. Su, W. Xu, B. Dai, J. Li and L. Li, "CO2-based energy systems for cooling, heating, and power," *Frontiers in Energy Research*, 16 August 2022.
- [204] L. Li, Y. T. Ge, X. Luo and S. A. Tassou, "Design and dynamic investigation of low-grade power generation systems with CO2 transcritical power cycles and R245fa organic Rankine cycles," *Thermal Science and Engineering Progress*, vol. 8, pp. 211-222, 2018.
- [205] The Guardian, "Hospitals struggling to afford new equipment after NHS budget cuts," Guardian News & Media Limited 2020, 18 May 2018. [Online]. Available: https://www.theguardian.com/society/2018/may/22/hospitals-struggling-to-afford-new-equipment-after-nhs-budget-cuts. [Accessed 26 April 2020].
- [206] NHS.UK, "Funding and Efficiency," NHS.UK, 2020. [Online]. Available: https://www.england.nhs.uk/five-year-forward-view/next-steps-on-the-nhs-five-year-forward-view/funding-and-efficiency/. [Accessed 26 April 2020].
- [207] W. A. Hodson, "29 Temperature Regulation," Avery's Diseases of the Newborn (Tenth Edition), vol. 2018, pp. 361-367.el, 2018.

- [208] D. Sharma, "Golden hour of neonatal life: Need of the hour," *Maternal Health, Neonatology, and Perinatology*, vol. 3, no. 16, pp. 1-21, 2017.
- [209] R. Kumar, A. Rani, D. Sharma and S. Chaitanya, "Fabrication and analysis of a novel and sustainable set-up for safe and economic hydrotherapy," *Proceedings of the Institution of Mechanical Engineers, Part E: Journal of Process Mechanical Engineering*, vol. 0, no. 0, pp. 1-8, 2024.
- [210] J. D. Marín, F. V. García and J. G. Cascales, "Use of a predictive control to improve the energy efficiency in indoor swimming pools using solar thermal energy," *Solar Energy*, vol. 179, pp. 380-390, 2019.
- [211] K. Bralewska and W. Rogula-Kozłowska, "Health exposure of users of indoor sports centers related to the physico-chemical properties of particulate matter," *Building and Environment*, vol. 180, no. 106935, pp. 1-22, 2020.
- [212] A. S. 55-2020, "Ashrae: Thermal Environment Conditions for Human Occupancy," 2021.
 [Online]. Available:
 https://ashrae.iwrapper.com/ASHRAE_PREVIEW_ONLY_STANDARDS/STD_55_2020.
 [Accessed 08 July 2024].
- [213] N. Kulumkanov, S. A. Memom and S. A. Khawaja, "Evaluating future building energy efficiency and environmental sustainability with PCM integration in building envelope," *Journal of Building Engineering*, vol. 93, no. 109413, pp. 1-34, 2024.
- [214] A. Khani, M. Khakzand and M. Faizi, "Multi-objective optimization for energy consumption, visual and thermal comfort performance of educational building (case study: Qeshm Island, Iran)," *Sustainable Energy Technologies and Assessments*, vol. 54, no. 102872, pp. 1-19, 2022.
- [215] D. Coakley, P. Raftery and M. Keane, "A review of methods to match building energy simulation models to measured data," *Renewable and Sustainable Energy Reviews*, vol. 37, pp. 123-141, 2014.
- [216] Y. P. P and S. A, "Effect of Sand Fines and Water/Cement Ratio on Concrete Properties," *Civil Engineering Research Journal ISSN:2575-8950*, vol. 4, no. 3, pp. 1-7, 2018.
- [217] H. Government, "Approved Document Part L, Conservation of Fuel and Power: Dwellings 2021 Edition England," *Building Regulations 2010*, vol. 1, no. 2021, (2021).
- [218] P. Wang, C. Li, R. Liang, S. Yoon, S. Mu and Y. Liu, "Fault detection and calibration for building energy system using Bayesian inference and sparse autoencoder: A case study in

- photovoltaic thermal heat pump system," *Energy and Buildings*, vol. 290, no. 113051, pp. 1-14, (2023).
- [219] A. Chakrabarty, E. Maddalena, H. Qiao and C. Laughman, "Scalable Bayesian optimization for model calibration: Case study on coupled building and HVAC dynamics," *Energy and Buildings*, vol. 253, no. 111460, pp. 1-15, (2021).
- [220] A. E. Kounni, A. Outzourhit, H. Mastouri and H. Radoine, "Building energy model automated calibration using Pymoo," *Energy and Buildings*, vol. 298, no. 113524, pp. 1-9, (2023).
- [221] M. Malagoli, S. Gallego, V. Proquez, S. Ginestet and G. Escadeillas, "A perforated heat flux plate for building measurements: calibration, in-situ performance and simulation," *Energy and Buildings*, vol. 284, no. 112843, pp. 1-14, (2023).
- [222] K. L. E.-L. c. Builidngs, "21st Century Education: Guidance from Building Bulletin 101 On Meeting the Thermal Comfort Recommendations for School Buildings," *Insulation: Technical Bulletin*, pp. 1-14, March (2019).
- [223] W. Li, M. Rahim, D. Wu, M. El Ganaoui and R. Bennacer, "Experimental study of dynamic PCM integration in building walls for enhanced thermal performance in summer conditions," *Renewable Energy*, vol. 237.Part C, no. 121891, pp. 1-12, 2024.
- [224] K. J. Kontoleon, M. Stefanidou, S. Saboor, D. Mazzeo, A. Karaoulis, D. Zegginis and D. Kraniotis, "Defensive behaviour of building envelopes in terms of mechanical and thermal responsiveness by incorporating PCMs in cement mortar layers," *Sustainable Energy Technologies and Assessments*, vol. 47, no. 101349, pp. 1-17, 2021.
- [225] M. Kazemi, A. Kianifar and H. Niazmand, "A lab-scale study on thermal performance enhancement of phase change material containing multi-wall carbon nanotubes for buildings free-cooling," *Sustainable Energy Technologies and Assessments*, vol. 50, no. 101813, pp. 1-9, 2022.
- [226] R. P. N. P. N. Talang and S. Sirivithayapakorn, "Comparing environmental burdens, economic costs and thermal resistance of different materials for exterior building walls," *Journal of Cleaner Production*, vol. 197, no. Part 1, pp. 1508-1520, (2018).
- [227] A. Habib, M. J. Hossain, M. Alam and T. Islam, "A hybrid optimized data-driven intelligent model for predicting short-term demand of distribution network," *Sustainable Energy Technologies and Assessments*, vol. 67, no. 103818, pp. 1-10, 2024.

- [228] J. Yu, Y. Yang and n. Campo, "Approximate Solution of the Nonlinear Heat Conduction Equation in a Semi-Infinite Domain," *Mathematical Problems in Engineering*, vol. 2010, no. 421657, pp. 1-24, 2010.
- [229] Ofgem, "Energy price cap," 2024. [Online]. Available: https://www.ofgem.gov.uk/energy-price-cap. [Accessed 25 January 2025].
- [230] A. T. Hammid, Y. M. Jebur, H. A. Lafta, I. W. Parwata, I. Patra and L. A. B. A. Arenas, "The arrangement of phase change materials inside a building wall and its energy performance," *Sustainable Energy Technologies and Assessments*, vol. 57, no. 103158, pp. 1-8, 2023.
- [231] S. M. R. Alavi, M. Mohammadium, H. Mohammadium, M. H. D. Bonab and G. S. Sabet, "Multi-objective optimization of free cooling potential through PCM based storage system," *Journal of Building Engineering*, vol. 86, no. 108678, pp. 1-12, 2024.
- [232] R. Desikan, D. Burger and S. W. Keckler, "Measuring Experimental Error in Microprocessor Simulation," in *Proceedings of the 28th Annual International Symposium on Computer Architecture*, Texas, Austin, 2001.
- [233] Y. Hu, D. Li, S. Shu and X. Niu, "Lattice Boltzmann simulation for three-dimensional natural convection with solid-liquid phase change," *International Journal of Heat and Mass Transfer*, vol. 113, pp. 1168-1178, 2017.
- [234] K. Yang, M. Liu, N. Du, H. Ziyu, Y. Chen, Z. Yang and P. Yan, "Performance analysis of a novel phase-change wall of wood structure coupled with sky-radiation cooling," *Energy Conversion and Management*, vol. 307, no. 118329, pp. 1-19, (2024).
- [235] Z. X. Li, A. A. Al-Rashed, M. Rostamzadeh, R. Kalbasi, A. Shahsavar and M. Afrand, "Heat transfer reduction in buildings by embedding phase change material in multi-layer walls: Effects of repositioning, thermophysical properties and thickness of PCM," *Energy Conversion and Management*, vol. 195, pp. 43-56, 2019.
- [236] G. D'Alessandro and F. de Monte, "Multi-Layer Transient Heat Conduction Involving Perfectly-Conducting Solids," *Energies*, vol. 13(24), no. 6484, pp. 1-25, 2020.
- [237] S. M. ZUBAIR and M. A. CHAUDHRY, "the transient heat conduction equation for a semi-infinite solid and Fourier's law to steady and non-steady periodic-type surface heat fluxes," International Journal of Heat Mass Transfer, vol. 38, no. 18, pp. 3393-3399, 1995.

- [238] G. Nair, L. Verde and T. Olofsson, "A Review on Technical Challenges and Possibilities on Energy Efficient Retrofit Measures in Heritage Buildings," *Energies*, vol. 15, no. 7472, pp. 1-20, 2022.
- [239] G. Gholamibozanjani and M. Farid, "A Critical Review on the Control Strategies Applied to PCM-Enhanced Buildings," *Energies*, vol. 14(7), no. 1929, pp. 1-39, 2021.
- [240] G. Gadhesaria, C. Desai, R. Bhatt and B. Salah, "Thermal Analysis and Experimental Validation of Environmental Condition Inside Greenhouse in Tropical Wet and Dry Climate," *Sustainability*, vol. 12(19), no. 8171, pp. 1-14, 2020.

PROJECT RISK MANAGEMENT

i). Risk identified: Inadequate Software Capabilities

STAR CCM+ was initially favoured for this project due to its comprehensive computational fluid dynamics (CFD) capabilities. However, during preliminary assessments, it was found that STAR CCM+ could not adequately handle the specific heat transfer problems associated with Phase Change Materials (PCMs) in building simulations. As a result, STAR CCM+ was dropped from the project.

Contingency Plan: Alternative Software Selection

TRNSYS was selected as the primary simulation tool due to its proven ability to handle dynamic thermal simulations and its specific components for modelling PCMs within building envelopes. TRNSYS has been widely used in the academic and professional sectors for building energy analysis and is well-documented for its accuracy and reliability in simulating heat transfer processes. The Type 1270a add-on in TRNSYS is particularly beneficial for this study as it provides the necessary functionality to effectively model the latent heat behaviour of PCMs.

Supporting Evidence:

TRNSYS is favoured for its flexibility in simulating complex building systems, and its component-based structure allows for detailed modelling of both conventional and advanced materials, such as PCMs. It is a widely recognised tool in the building simulation community for handling transient thermal phenomena.

Control measure: use of EnergyPlus

EnergyPlus was considered an alternative due to its robust capabilities in building energy modelling. However, the lack of an available license during the project initiation prevented its use. If a license can be secured in the future, EnergyPlus could serve as a supplementary tool, particularly for cross-verifying the results obtained from TRNSYS.

ii). Risk identified: Availability of Experimental Space

The original plan was to conduct experiments at CHASE FARM HOSPITAL, which offered an ideal space for testing the PCM-integrated building wall prototypes. However, due to space constraints or other unforeseen issues, the hospital could not provide the necessary facilities.

Contingency Plan: Alternative Experimental Location

The experiment was relocated to a laboratory at the University of Hertfordshire, which provided the necessary infrastructure and equipment for conducting the tests. The laboratory environment is suitable for controlling experimental variables and ensuring the accuracy of the data collected.

iii). Risk Identified: Delays in PCM Material Delivery

Due to Brexit, there were potential risks related to the late delivery and customs clearance of PCM materials, which could have delayed the project timeline.

Contingency Plan: Early Ordering and Reliable Couriers

To mitigate this risk, PCM materials were ordered well in advance to allow for any possible delays in shipping or customs clearance. Reputable courier agencies were used to ensure timely and secure delivery of materials. This proactive approach helped avoid disruptions to the project schedule. The supervisors constantly checked with the University's supply chain and always communicated progress; thanks for their relentless efforts.

iv). Risk Identified: Unavailability of Laboratory Equipment

Certain specialised equipment required for the experiments is not available in the primary laboratory designated for the project.

Contingency Plan: Inter-Departmental Collaboration

If specific equipment is unavailable, arrangements are made to seek support from other departmental laboratories within the University of Hertfordshire. Collaboration with other departments ensured access to the necessary tools and equipment, thereby maintaining the continuity of the experimental work.

v). Risk Identified: Project Delays

The project had a strict timeline, and any delays could have impacted the overall completion and submission of the thesis.

Contingency Plan: Strict adherence to the Project Plan, supervisory meetings

A clear and detailed project plan was developed at the outset, outlining all major milestones and deadlines. Regular supervisory meetings or progress reviews were conducted to ensure that the project remained on track. Any potential delays were identified early, and corrective actions were taken promptly to avoid cascading effects on the project timeline.

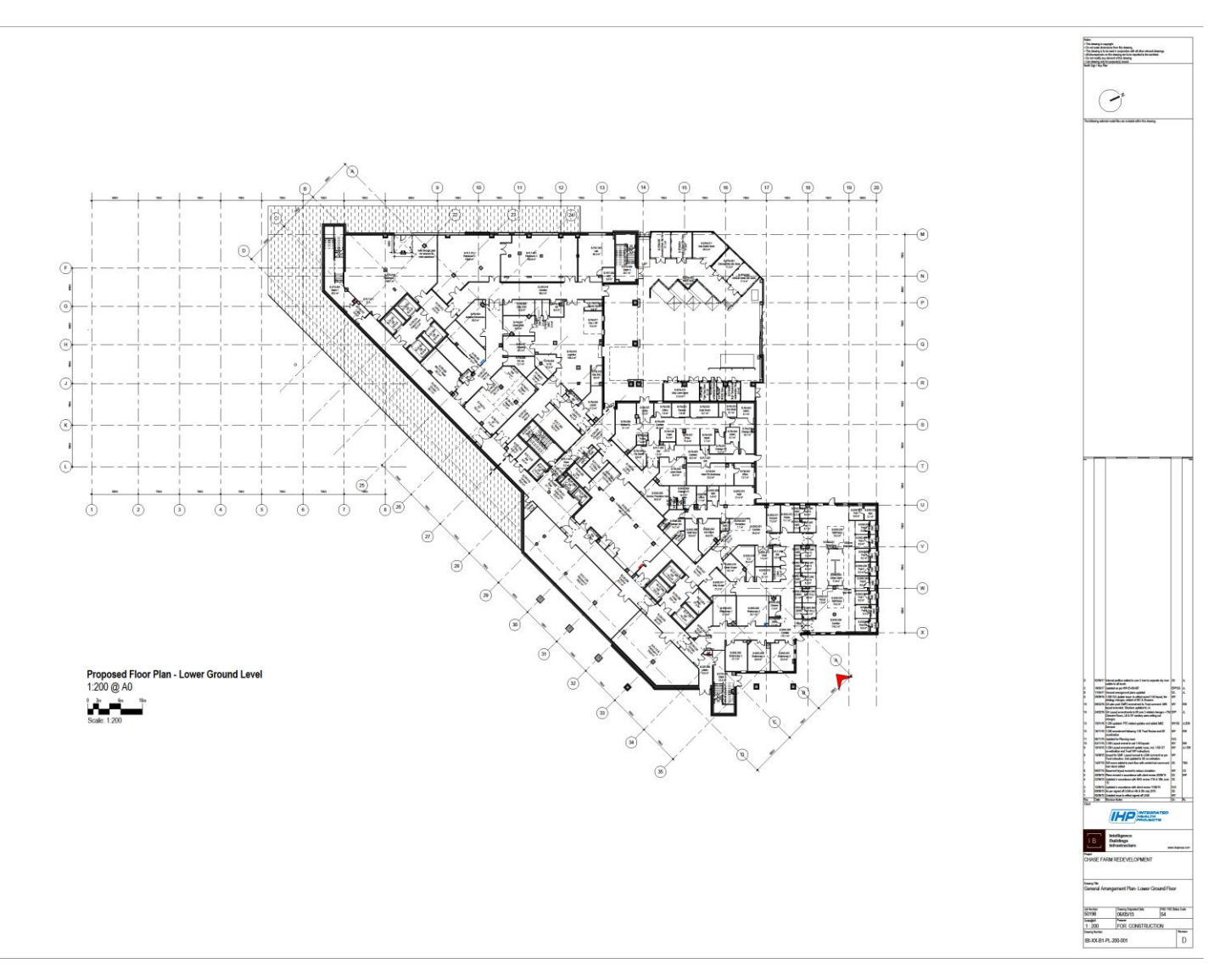
vi). Risk Identified: Resurgence of COVID-19

COVID-19 pandemic restrictions if re-imposed, limiting access to labs and physical meetings. *Contingency Plan*: Remote Work and Virtual Collaboration

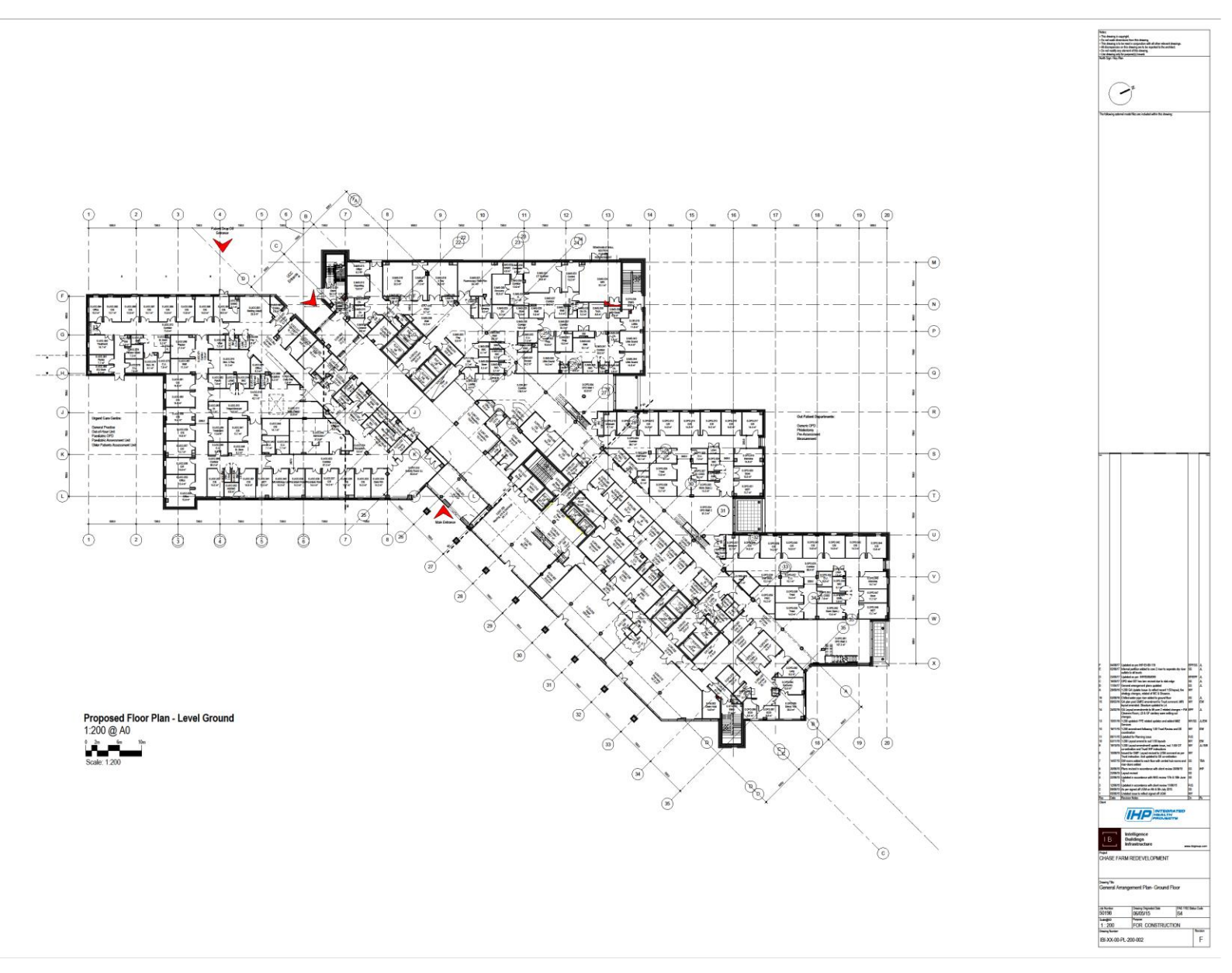
In the event of a resurgence of COVID-19, provisions are in place to continue the project remotely. Simulation work could be carried out on a work-from-home (WFH) remote access basis, and virtual collaboration tools were set up to ensure continuous communication with supervisors. Remote data analysis and report writing were also planned to ensure the project could proceed without interruption.

This contingency plan addresses the key risks identified during the project's planning phase. By proactively identifying potential issues and developing robust strategies to mitigate them, the project is well-positioned to achieve its objectives despite unforeseen challenges. Regular monitoring and flexibility in approach will be critical to the study's successful completion.

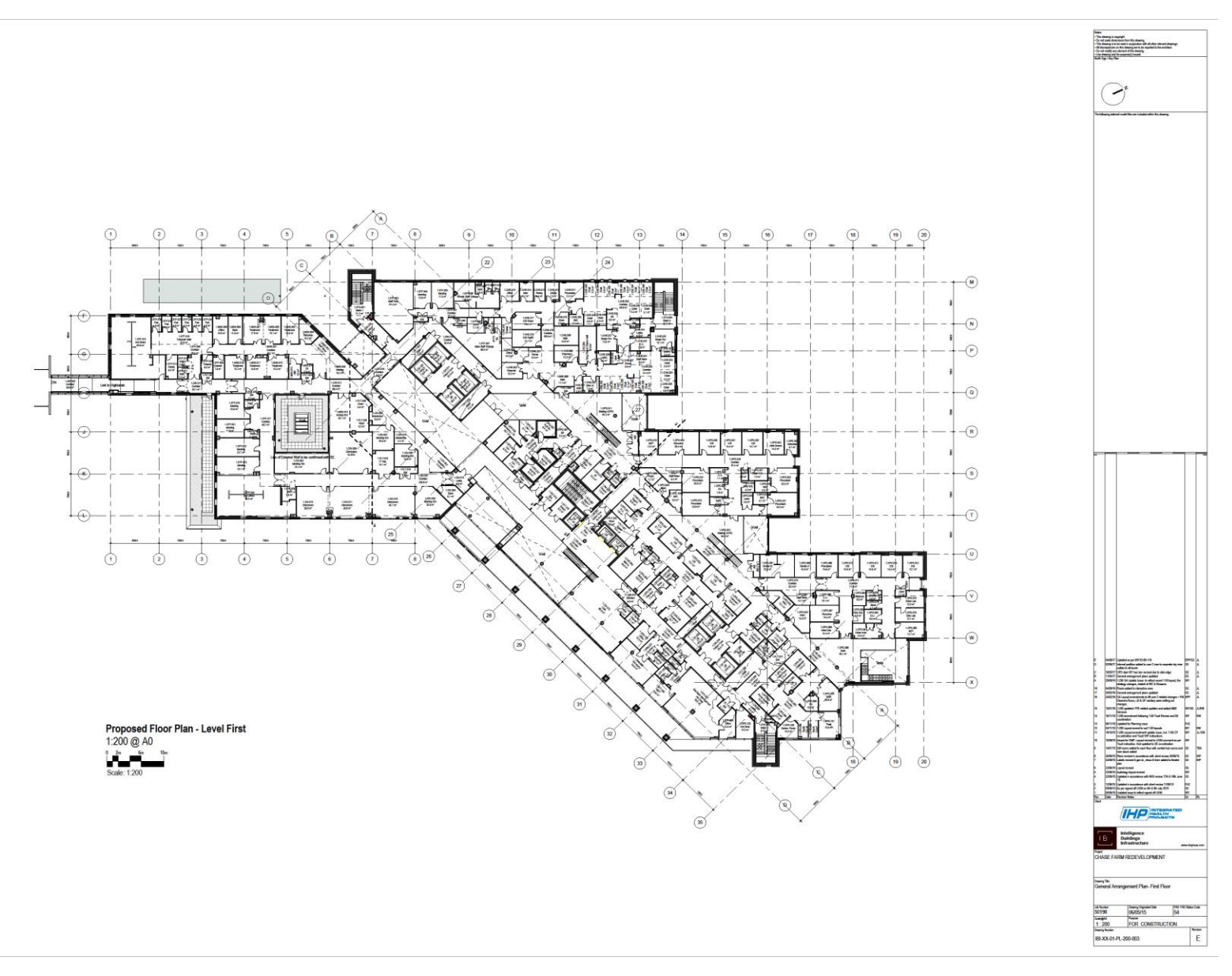
APPENDIX



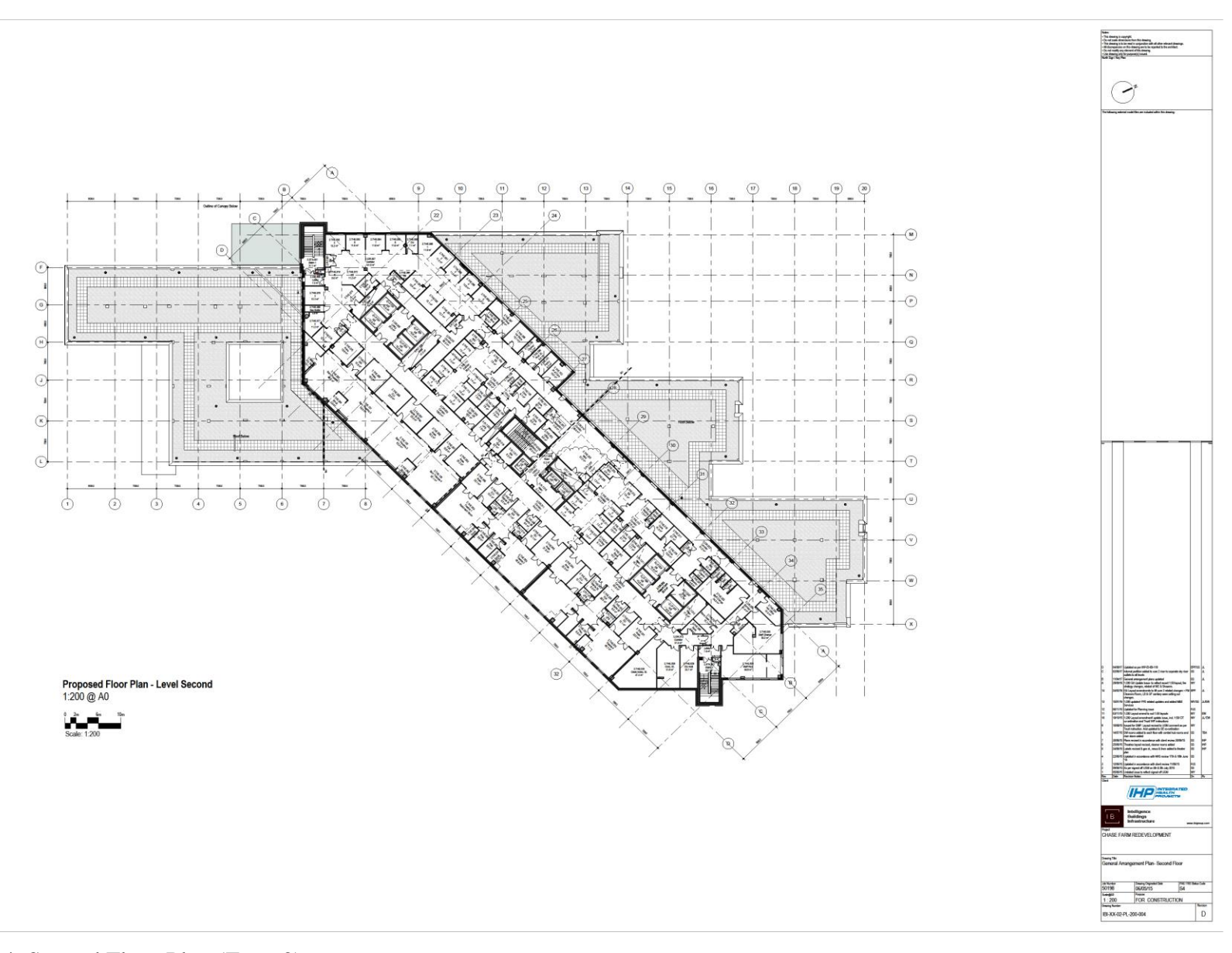
Appendix 1. Lower Ground Floor Plan (Zone LG)



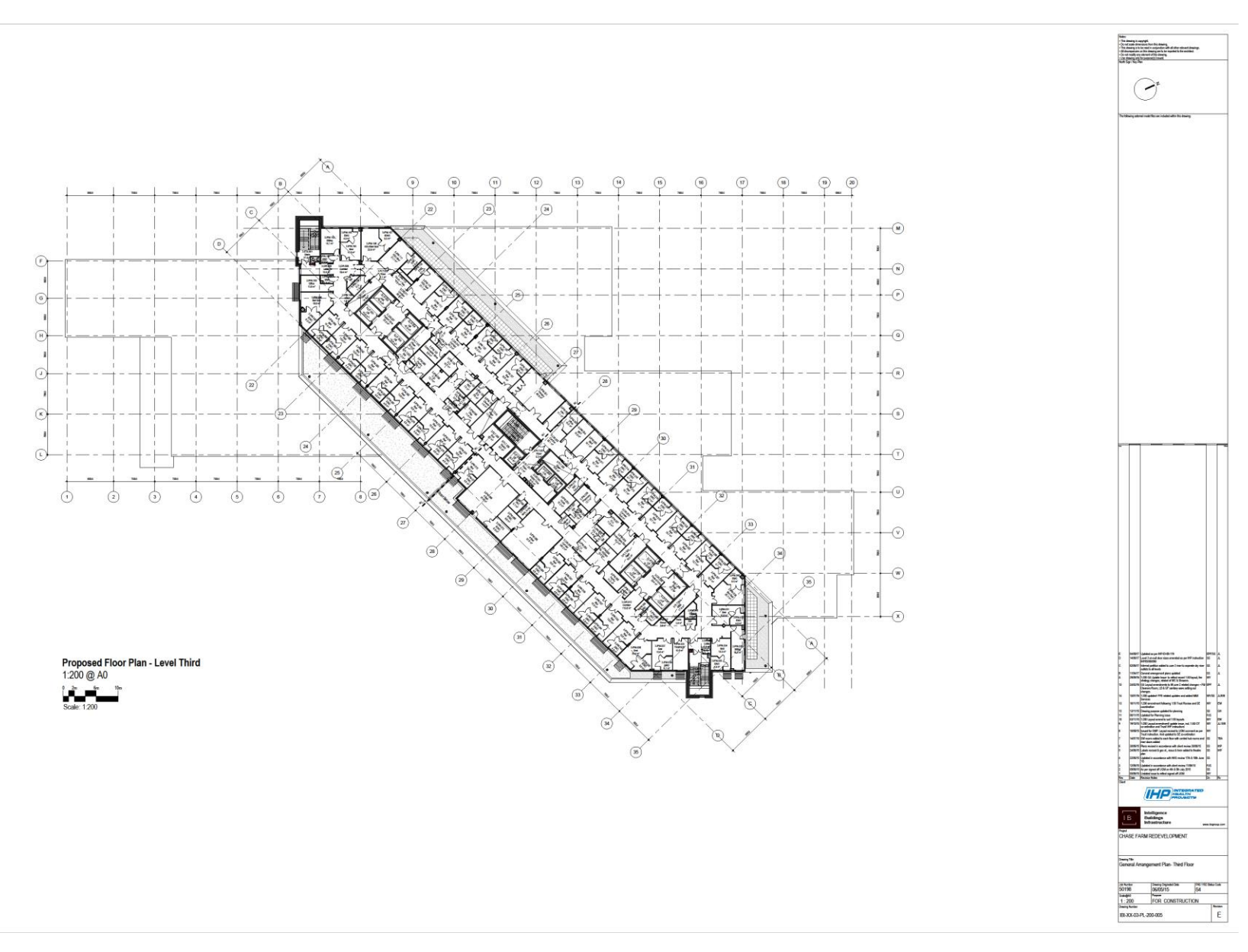
Appendix 2. Ground Floor Plan (Zone G)



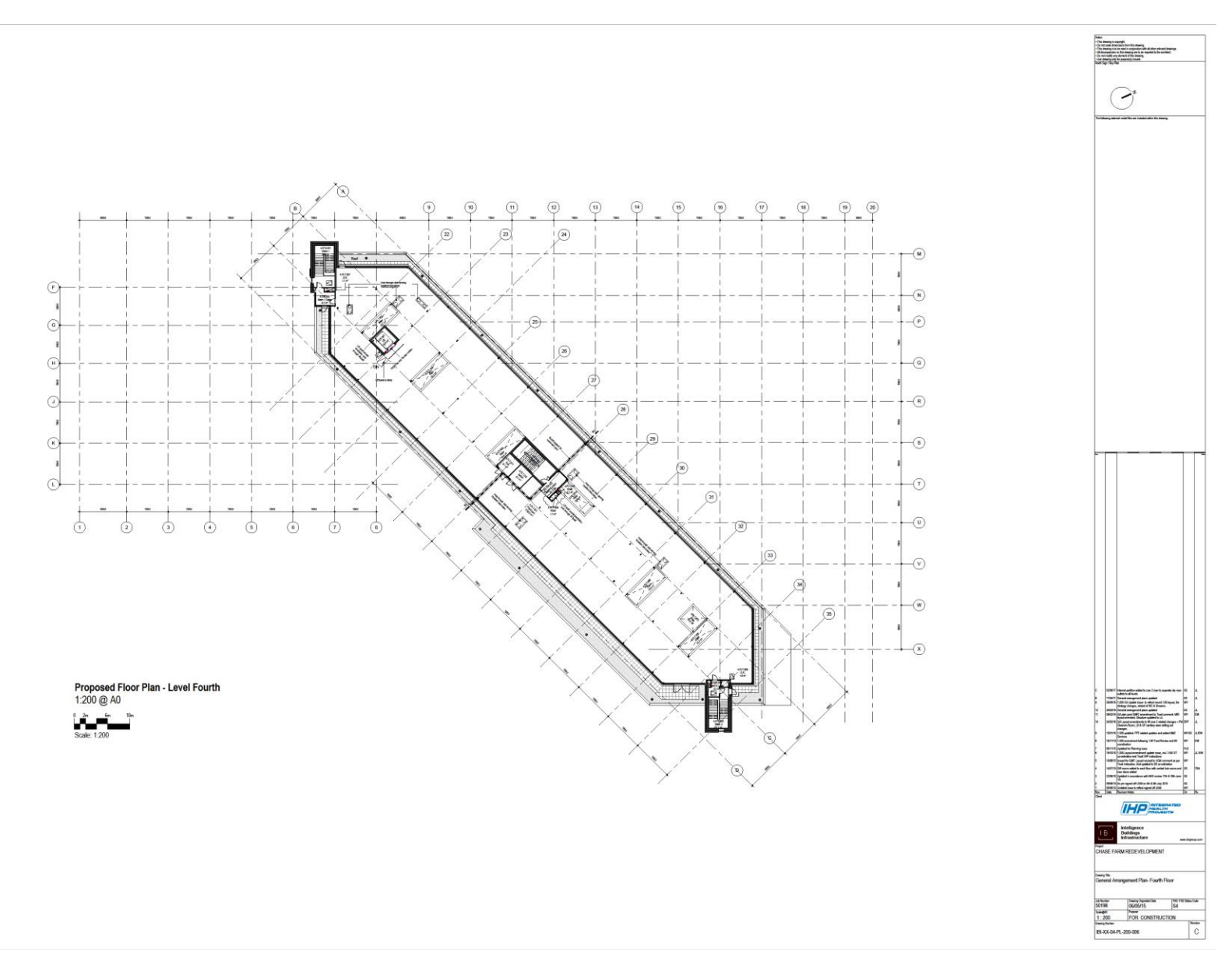
Appendix 3. First Floor Plan (Zone 1)



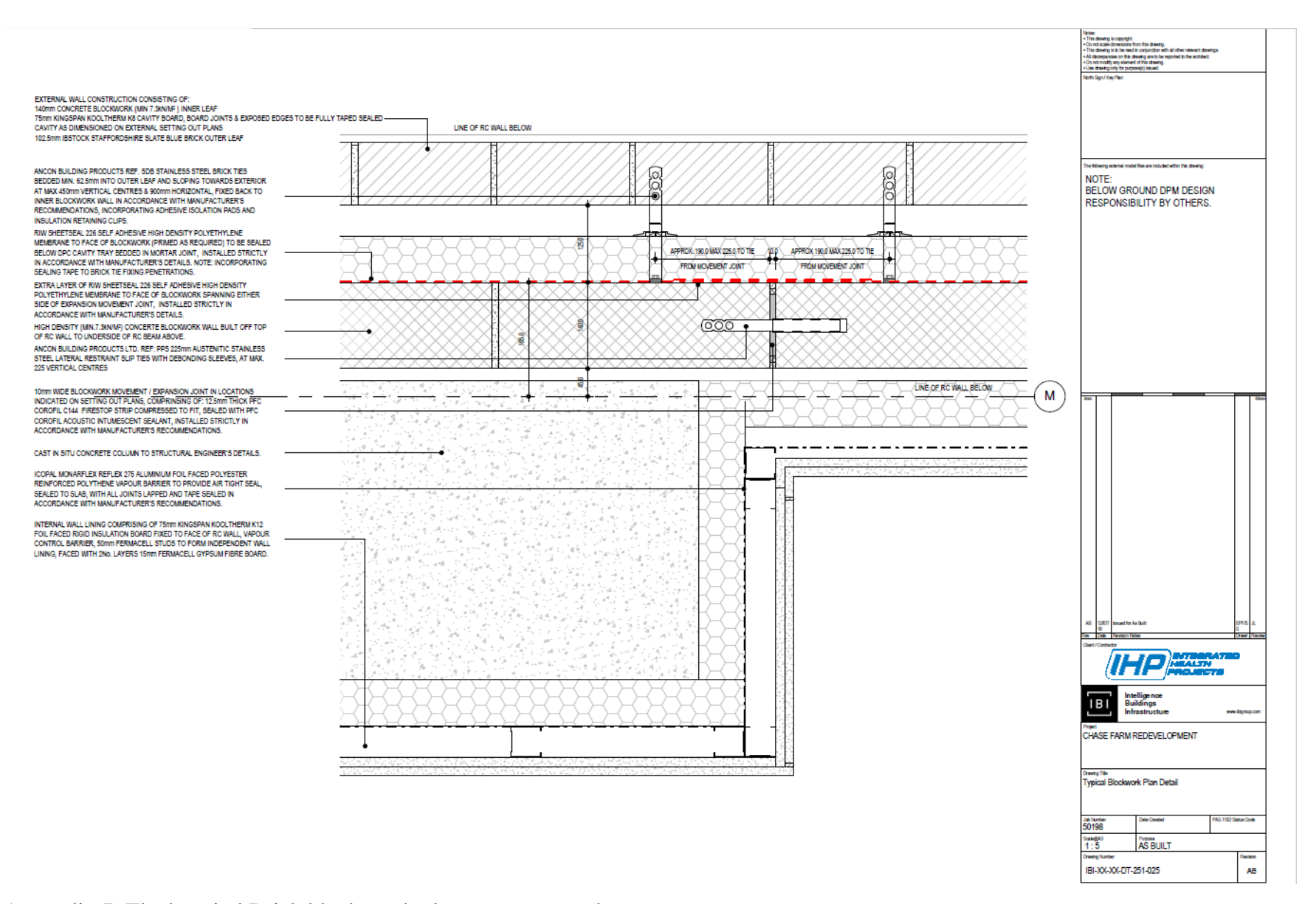
Appendix 4. Second Floor Plan (Zone 2)



Appendix 5. Third Floor Plan (Zone 3)



Appendix 6. Fourth Flow Plan (Zone 4)



Appendix 7. The hospital Brick block work plan as constructed



Rubitherm Technologies GmbH Imhoffweg 6 12307 Berlin www.rubitherm.com

Tel: +49 30 71 09 622-0 Fax: +49 30 71 09 622-22

OFFER

Number : 20230000256 Date 01.11.2023 Customer

: 92000 VAT-ID

Pos.	Part-ID / Description	Quantity	U-Price UQ	Ex-Price S			
	requested by: ronny achaku rachaku@yahoo.com Phone: 07985735734 We thank you for your interest in Rubitherm products and can offer as follows:						
1	14010015 RUBITHERM CSM 450x300x15 (10/5) HS-Code: 81499085	8 Stck	33,61	268,88 1			
2	filled with RT28 HC 96020103 minimum order surcharge	1 Stck	100,00	100,00 1			
3	96020100 cost for shipping (*)	1	10,00	10,00 1			
4	96020102 bankcharges	1	10,00	10,00 1			
5	96020100 cost for shipping (*) Offer validity:	1	180,18	180,18 1			

Validity of prices: 1 month.

University of Hertfordshire

After expiry of the validity period, this offer must be reissued. All previous offers are hereby invalid. This offer is subject to change. Our prices are in EUR, net. The goods remain the property of Rubitherm Technologies GmbH until full payment has been received. The extended and expanded retention of title applies. The offer is based exclusively on German law and the German requirements for the product. Our general terms and conditions apply exclusively.

By ordering our material you declare to accept and be bound by the conditions stated below.

Orders for less than 100 pcs of identical CSM panels carry a minimum order surcharge of 100,00EUR

Handling fee for deliveries outside Germany min. 10 € or min. 0.15 % of the invoice amount outside the EU

Delivery terms: DAP GB

If agreed Rubitherm can arrange the transportation with a third forwarder. (*)Please note, that the quoted shipping prices can differ from the shipping costs at delivery date due to surcharges that are included in the price which are subject to fluctuations on the market. Rubitherm reserves the right to charge the cost difference to the customer and the customer agrees to pay this difference.

Standard lead- time: within 4 weeks after payment

amount carried forward 569,06

Imhoffweg 6 12307 Berlin www.rubitherm.com Tel: +49 30 71 09 622-0

Fax: +49 30 71 09 622-22 Page 2

Pos. Part-ID/ Description Quantity U-Price UQ Ex-Price S

569.06

excl. shipping provided an uninterrupted production

Payment condition: prepayment via wire transfer. Credit cards are not accepted.

20230000256

If you have any queries, please do not hesitate to contact us. We assure you of conscientious execution of your order.

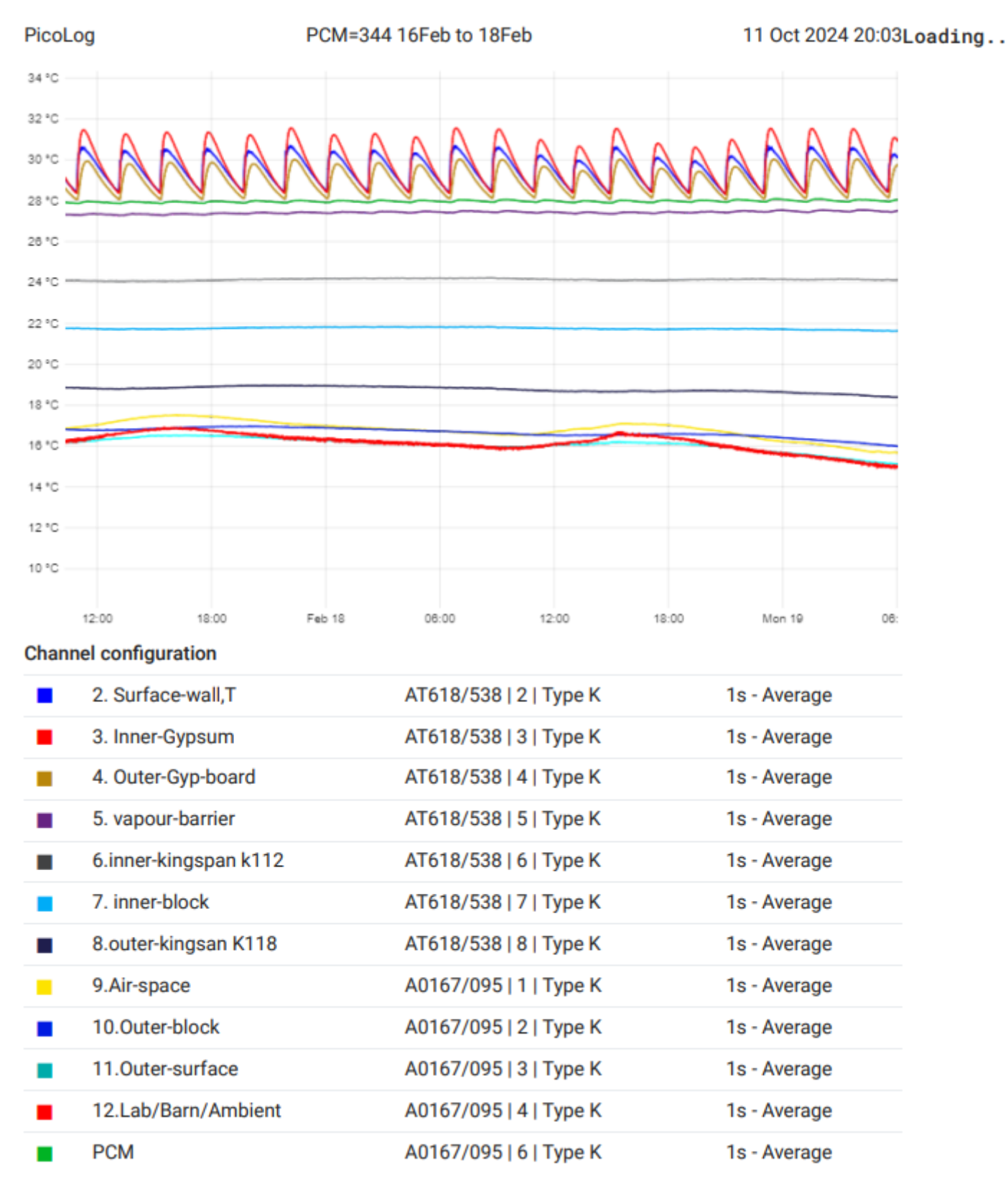
Date 01.11.2023

Netto VAT.1 VAT Netto VAT. 2 Netto VAT. 0 Total Amount 569,06 EUR

CEO: Thomas Braun, Lutz Klinkner Comm. Reg no.: Berlin-Charlottenburg, HRB 86322 B

Hypo-Vereinsbank, acc. No.: 572 64 17, bank code: 700 202 70 IBAN: DE12 7002 0270 0005 7264 17 SWIFT: HYVEDEMMXXX VAT ID: DE 230 027 919





Appendix 9. Sample Picolog data for wall with PCM activated (28°C) at the position of 344 mm.

Data sheet



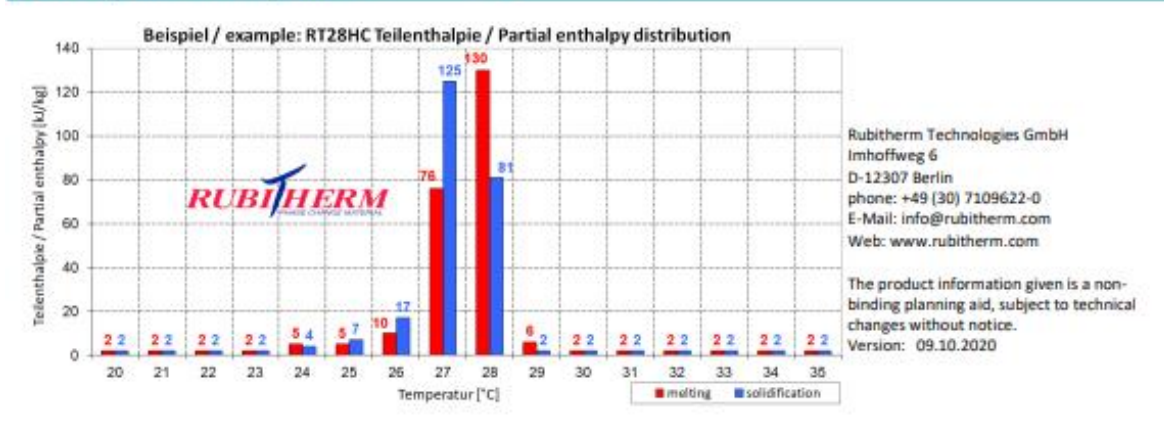
RT28HC

RUBITHERM® RT is a pure PCM, this heat storage material utilising the processes of phase change between solid and liquid (melting and congealing) to store and release large quantities of thermal energy at nearly constant temperature. The RUBITHERM® phase change materials (PCM's) provide a very effective means for storing heat and cold, even when limited volumes and low differences in operating temperature are applicable.

Properties for RT-line:

- high thermal energy storage capacity
- heat storage and release take place at relatively constant temperatures
- no supercooling effect, chemically inert
- long life product, with stable performance through the phase change cycles melting temperature range between -9 °C and 100 °C available

The most important data:	Typical Value	5	
Melting area	27-29 main peak: 28	[°C]	
Congealing area	29-27 main peak: 27	[°C]	
Heat storage capacity ± 7,5%	250	[kJ/kg]*	
Combination of latent and sensible heat in a temperatur range of 21°C to 36°C.	70	[Wh/kg]*	
Specific heat capacity	2	[kJ/kg·K]	
Density solid	0,88	[kg/l]	CHSDS
Density liquid at 40°C	0,77	[kg/l]	
Heat conductivity (both phases)	0,2	[W/(m·K)]	
Volume expansion	12,5	[%]	
Flash point	165	[*C]	
Max. operation temperature	50	[°C]	



^{*}Measured with 3-layer-calorimeter.

Appendix 10. PCM RT28HC data sheet

QUOTATION

Your Ref

Our Ref 3796Q213340

Date 28th June 2023

Customer University of Hertfordshire Your Office contact is Daniel Telling

Your Representative is Marketing/Branch Ledger Site Ref : REF PCM PROJECT RONNY ACHAKU



Quantity	Product Code and Description		Price	Per	Goods
					Amount
1 SH	105060	KINGSPAN KOOLTHERM K118 INSULATED PLASTERBOARD 1200X2400X25MM	31.23	M2	89.94
1 SH	752767	BRITISH GYPSUM GYPROC THERMALINE 2400X1200X30MM BASIC	44.45	SH	44.45
1 SH	526162	KOOLTHERM K112 FRAMING BOARD 1200X2400X50MM	95.55	SH	95.55
25 EA	334688	SOLID ULTRA LOW DENSITY BLOCK 100MM 3.6N	35.67	TN	89.18
1 BG	346656	BLUE CIRCLE HIGH STRENGTH 40N CONCRETE 20KG PLASTIC PACKED	9.73	BG	9.73
7 SH	760054	BRITISH GYPSUM GYPROC PLASTERBOARD 2400X1200X12.5MM SQUARE EDGE	10.28	SH	71.96
1 RL	521852	TYVEK AIRGUARD REFLECTIVE 1.5M X 50M	147.44	RL	147.44
1 EA	206910	C24 KILN DRIED REGULARISED TIMBER TREATED 47X100MMX4.8M	14.74	EA	14.74
2 EA	991099	C-TEC CT1 SEALANT CLEAR 290ML	11.55	EA	23.10
	-		Total		586.09
			VAT		117.22
			Grad		
		s Perkins Material quote	Total		703.31

Appendix 11. Travis Perkins Material quote